

**ASSESSMENT OF HYDROLOGICAL IMPACTS OF LAND  
COVER CHANGES AND CLIMATE VARIABILITY IN THE  
GEBA CATCHMENT, ETHIOPIA**

Thesis

Submitted in partial fulfilment of the requirements for the degree of  
**DOCTOR OF PHILOSOPHY**

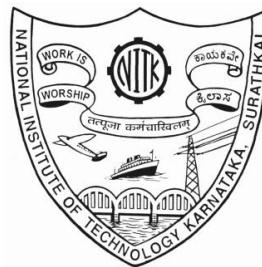
By

**GEBREMEDHIN KIROS HAILU**  
**135057AM13F02**

Under the guidance of  
**Dr. AMBA SHETTY, Associate Professor**

**Prof. LAKSHMAN NANDAGIRI**

Dept. of Applied Mechanics & Hydraulics  
NITK Surathkal



**DEPARTMENT OF APPLIED MECHANICS AND HYDRAULICS  
NATIONAL INSTITUTE OF TECHNOLOGY KARNATAKA,  
SURATHKAL, MANGALORE – 575025, INDIA  
OCTOBER – 2016**

## **DECLARATION**

*By the Ph.D. Research Scholar*

I hereby *declare* that the Research Thesis entitled “**Assessment of Hydrological Impacts of Land Cover Changes and Climate Variability in the Geba Catchment, Ethiopia**”, which is being submitted to the **National Institute of Technology, Karnataka, Surathkal** in the partial fulfilment of the requirements for the award of the degree of **Doctor of Philosophy** in the **Department of Applied Mechanics and Hydraulics (Specialization: Hydraulics and Water Resources Engineering)**, is a *bonafide report of the research work* carried out by me. The material contained in this Research Thesis has not been submitted to any University or Institute for the award of any degree.

135057AM13F02, GEBREMEDHIN KIROS HAILU

(Register Number, Name and Signature of the Research Scholar)

Department of Applied Mechanics and Hydraulics  
National Institute of Technology Karnataka Surathkal, India

Place: NITK-Surathkal

Date:

## **CERTIFICATE**

This is to *certify* that the Research Thesis entitled “**Assessment of Hydrological Impacts of Land Cover Changes and Climate Variability in the Geba Catchment, Ethiopia**”, submitted by GEBREMEDHIN KIROS HAILU (Register Number: 135057AM13F02) as the record research work carried out by him, is *accepted as the Research Thesis submission* in the partial fulfilment of the requirements for the award of the degree of **Doctor of Philosophy**.

Dr. Amba Shetty

Associate Professor

Research Guide

(Name and Signature with date and seal)

Dr. Lakshman Nandagiri

Professor

Research Guide

(Name and Signature with date and seal)

Chairman – DRPC

(Signature with date and seal)

Department of Applied Mechanics and Hydraulics  
National Institute of Technology Karnataka Surathkal, India

## **ACKNOWLEDGEMENTS**

First and above all, I am grateful to the almighty GOD, my source of strength and wisdom for providing me this opportunity and surrendering me the capability to proceed successfully. Next, I would like to express my sincere gratitude to the funding for this PhD research: Aksum University and Ministry of Education (MoE) Ethiopia. I am deeply grateful to both for giving me the opportunity of full sponsorship to pursue my PhD research work and the financial support.

Finally, the end of a journey that started with a single step and gradually developed into one massive task! My happiness and wisdom of accomplishment would not be complete without making mention of everyone who offered help and support, in one way or another during the entire period of this PhD study. The conciseness of this acknowledgement does not in any way downplay the support I have received from anyone mentioned, or not mentioned, herein. I would like to express my heartfelt thanks and gratitude to my supervisors Prof. Amba Shetty and Prof. Lakshman Nandagiri. Without their scientific advice and guidance, constructive suggestions, extraordinary patience, and support during the last three years of the research, it would have been impossible to make this PhD study come to complete. I will always remember their academic excellence, kindness and positive attitude to help in all circumstances.

My Sincere thanks goes to my Research Progress Assessment Committee (RPAC) panel members: Prof. K. Narayan Prabhu (National Institute of Technology Karnataka Department of Metallurgy) and Prof. Paresh Chandra Deka (National Institute of Technology Karnataka Department Applied Mechanics and Hydraulics) for their willingness to evaluate my work and for their valuable comments in every steps of the progress which improved the shape of the thesis.

During my study at National Institute of Technology Karnataka (NITK), Surathkal, Mangalore, I had the opportunity to work and interact with many enthusiastic and

hardworking people of the Department of Applied Mechanics and Hydraulics. Special thanks to Head of Department Prof. G.S Dwarakish for his kind help and support in every step. I would like to thank the members of the department, these people, in one way or the other, have helped to make my stay at the NITK so enjoyable.

I am thankful and acknowledged the following organizations for providing data and other related information from their Library resources and websites: Ministry of Water Resources and Energy department of hydrology, Ethiopian; National Meteorological Agency (ENMA); Tigray Region Meteorological Agency, US Geological Survey for the LANDSAT imagery (Landsat MSS, TM and ETM+), and the Food and Agriculture Organization (FAO) of the United Nations.

Thanks to all my colleagues from GIS and RS lab, especially to Vinay Doranalu C, Amit Prakesh Patil, Ram Tilak, Pradeep and Vishwanatha Bhat for the continuously and valuable help and technical support, being always willing to solve small to big technical problems which are common in such a process. Moreover, I would like to extend my deepest and humble gratitude to all my colleagues from Aksum University College of Agriculture, Shire campus especially to Seare Tajebe, Mewael Kiros, Tewelde Gebretinssae and Dr. Gizachew Yonas for their support. Special thanks to Assefa Redae Head Department of Soil Resources and Watershed management, for the continuously and valuable help and the friendly atmosphere which is giving a motivation to work. Very Special thanks to Dr. Hadush Goitom Department of Civil Engineering Mek'ele University, Ethiopia for providing necessary data, valuable support and advice, ideas and suggestions which were very important in the first stage of this PhD research work.

I would express my gratitude and thank my mother Yergalem Assefa, my father Kiros Hailu, my uncles Fikadeselassie Assefa and Shambel Menberselassie Assefa, my mother in-law Tequam Gebru, my sisters and brothers for always being there for remained very close, loving and supporting me knowing that they always held me in their thoughts and prayers gave me strength to go on. Special thanks to my brothers Kellali Tsegay and Drs Nigus Gebregiorgis for their help, advice and patience, for

every period I was away. My heartfelt thanks go to a brother-friend Dr. Riessome Weldegiorgis for his passionate support from the start to the end of this PhD work.

Most importantly, I would like to thank my kind and upright wife Abeba Adugna for her complete love, care, support, patience, understanding and all the inconvenience that she has encountered during my absence throughout my study period. Last not but least to my lovely daughters Christina and Soliana you always bring inspiration, meaning and purpose to my life, I love you all.

NITK-Surathkal, Mangalore, India

Date:

Gebremedhin Kiros Hailu

## **Dedication**

To

My respected mother and father for showing me the path to greatness and  
always dedicated for my education

My very kind and upright wife Abeba Adugna (Fikre) and my lovely daughters  
Christina and Soliana Gebremedhin for encouraging me against all odds

## **ABSTRACT**

Land use/land cover (LU/LC) and climate are the two main factors directly influencing catchment hydrological processes and consequently changes in these factors will result in significant hydrological impacts. Quantifying the magnitude and direction of these impacts is of great importance for land use planning and sustainable water resources management. The Geba catchment (5137 km<sup>2</sup>) located in the highlands of Northern Ethiopia; Africa contributes a significant portion of flow in the river Nile and forms an important source of water to a large population. In the past few decades, the catchment has experienced significant changes in LU/LC in the form of degradation due to anthropogenic activities and subsequent restoration brought about by conservation measures. Also, trend analysis of hydro-meteorological data carried out as part of this study provided evidence of changes in rainfall and temperature regimes in the catchment.

Therefore, the present study was taken up to characterize the hydrology of the Geba catchment using available hydro-meteorological data and to apply and evaluate the potential of the Soil and Water Assessment Tool (SWAT) model to simulate major hydrological processes and sediment dynamics in the catchment. The objective was to use SWAT to simulate changes in hydrological processes brought about by changes in LU/LC and climate variability within the catchment.

Accordingly, the research methodology adopted involved the following tasks: (1) Using historical (1971-2013) ground-based observations of rainfall, air temperature (7 climate stations) and streamflow (1 gauging station) statistical and trend analyses were carried out for monthly and seasonal time steps. Also, trends in several extreme climatic indices related to rainfall and temperature were analysed (2) LANDSAT satellite imagery acquired for multiple dates during the period 1971-2013 were subject to standard image processing and supervised classification procedures to derive LU/LC maps for the Geba catchment. These classified maps were used to detect changes in different LU/LC classes



during the periods 1973 – 1987, 1987 – 2000 and 2000 – 2013 (3) Using a variety of inputs (ground and satellite-based) related to topography, soils, LU/LC, rainfall and climatic variables, the ArcGIS version of the SWAT model (ArcSWAT) was applied to the Geba catchment. Given that the catchment experienced significant changes in LU/LC over the 40 year period considered, a novel model calibration/validation approach was adopted involving the use of different LU/LC maps for different time periods (4) Using observed streamflow records at the outlet of the Geba catchment, the SWAT model was subject to sensitivity analysis following which calibration and validation was carried out using both monthly and daily time steps. Model performance in simulating streamflow and sediment concentration at the outlet was evaluated using different statistical criteria (5) Using the validated SWAT model, a novel method to evaluate the separate and combined impacts of LU/LC changes and climate changes on major water balance components in the Geba catchment was implemented.

Results of trend analysis revealed that during the study period (1971-2013), rainfall and streamflow exhibited a decreasing trend, while maximum daily air temperature had an increasing trend and minimum daily air temperature showed decreasing trend at 95 % confidence level. As regards LU/LC changes, during 1973–1987 and 1987–2000 time periods about 10.83 % and 9.13 % of the catchment area was transformed largely from shrub, forest and rangeland mainly to agriculture and barren land. During 2000–2013, about 18.37 % of the total catchment area was transformed from barren land and range to agriculture, shrub, forest and urban area. SWAT model validation using observed streamflow records yielded values of coefficient of determination ( $R^2$ ) between 0.86 and 0.96 and Nash-Sutcliffe efficiencies ( $E_{NS}$ ) between 0.73 and 0.83 for different simulation periods with a monthly time step. For daily streamflow predictions,  $R^2$  values ranged between 0.77 and 0.91 and  $E_{NS}$  values were between 0.7 and 0.79. SWAT also provided reasonably accurate predictions of daily sediment concentrations during validation ( $R^2$ : 0.81-0.895,  $E_{NS}$ : 0.79-0.80). These results prove that the SWAT model is a reasonably accurate tool for simulation of hydrological processes in the Geba catchment, whereas  $R^2$

and  $E_{NS}$  for daily and monthly flow were very less (satisfactory) for the single static LU/LC (2000) map, mostly followed in many studies. Impacts of LU/LC changes and climate variability were evaluated by dividing the study period (1973-2013) into three phases based on LU/LC and climatic conditions: Phase (I) - LU/LC maps of 1973 and 1987, climate of 1974-1983 and 1984-1993 Phase (II) - LU/LC maps of 1987 and 2000, climate of 1984-1993 and 1994-2003 Phase (III) - LU/LC maps of 2000 and 2013, climate of 1994-2013 and 2004-2013. The SWAT model was run separately for four scenarios in each phase involving combinations of LU/LC and climate. Results indicated that the combined impacts of the LU/LC changes and climate variability increased streamflow and potential evapotranspiration in both Phases I and II, while available soil water contents decreased. Positive impacts in the form of reduced streamflow and increased soil moisture resulted in Phase III due to extensive conservation measures implemented after 2000. Overall, changes in LU/LC seemed to have a higher impact on hydrological processes than changes in climate.

The present study has demonstrated the applicability and efficacy of a convenient methodology integrating satellite remote sensing and modelling to characterize hydrological processes and simulate hydrological changes in a heterogeneous tropical catchment. The proposed strategy may be adopted to formulate strategies for sustainable land and water resources management in the region, and in similar hydro-climatic settings elsewhere in Africa.

***Key Words:*** *Catchment modelling, Climate variability, Geba Catchment, Hydrological impacts, LU/LC, Northern Ethiopia, Trend analysis, SWAT Model.*



# TABLE OF CONTENTS

<b>ABSTRACT .....</b>	<b>i</b>
<b>LIST OF FIGURES.....</b>	<b>xi</b>
<b>LIST OF TABLES.....</b>	<b>xv</b>
<b>LIST OF ABBREVIATIONS.....</b>	<b>xix</b>
<b>CHAPTER 1 INTRODUCTION .....</b>	<b>1</b>
1.1 Overview of Water Resources and Sustainable Development.....	1
1.2 Statement of the Problem .....	5
1.3 Research Questions .....	7
1.4 Research Objectives of the Present Study.....	8
1.5 Structure of the Thesis.....	8
<b>CHAPTER 2 REVIEW OF LITERATURE .....</b>	<b>11</b>
2.1 Introduction .....	11
2.2 Variability and Trend Analysis of Hydro-meteorological Variables .....	11
2.3 Hydrologic Modelling and Classification .....	13
2.3.1 Classification of Hydrologic Models.....	14
2.3.2 Application of Hydrologic Modelling Integrating with Remote Sensing and GIS.....	16
2.4 Applications of SWAT Model under LU/LC Change Scenario and Assessment of Hydrological Responses .....	17
2.5 Land Use/Land Cover Changes.....	19
2.5.1 Approaches and Methodologies of LU/LC Mapping .....	21
2.5.2 Land Use/Land Cover Change Studies in Ethiopia .....	22
2.6 Overview of Soil Erosion and Sediment Dynamics.....	23
2.7 Climate Variability, Change and Related Impacts .....	26

2.8 Summary of Literature .....	29
<b>CHAPTER 3 STUDY AREA AND RESEARCH METHODOLOGY.....</b>	<b>31</b>
3.1. Location of the Study Area .....	31
3.2 Topography .....	32
3.3 Climate .....	33
3.3.1 Rainfall .....	33
3.3.2 Temperature.....	34
3.4 Hydrology.....	35
3.5 Geology, Soils and land use .....	37
3.6 Data Used .....	38
3.7 Research Methodology Adopted.....	39
<b>CHAPTER 4 STATISTICAL AND TREND ANALYSIS OF HYDRO-</b>	
<b>METEOROLOGICAL DATA.....</b>	<b>41</b>
4.1 Introduction.....	41
4.2 Methodology .....	43
4.2.1 Rainfall Extreme Indices .....	44
4.2.2 Data Quality and Homogeneity Testing.....	46
4.2.3 The Mann-Kendall Trend Analysis .....	48
4.3 Results and Discussion.....	51
4.3.1 Spatial and Temporal Analysis of Meteorological Data .....	51
4.3.1.1 Patterns and Variability of Rainfall .....	51
4.3.1.2 Trend Analysis of Rainfall.....	65
4.3.1.3 Seasonal Rainfall Analysis .....	69
4.3.2 Observed Trends and Extreme Rainfall Indices .....	76
4.3.2.1 Trends in Wet-day Annual Total Rainfall (PRECTOT) and Simple Daily Rainfall Intensity (SDII) Indices.....	77
4.3.3 Changes in the Extreme Rainfall Frequency Indices.....	79
4.3.3.1 Maximum Length of Indices for the Dry and Wet Periods .....	79

4.3.3.2 Daily Rainfall of Absolute Threshold Indices .....	83
4.3.4 Changes in the Extreme Rainfall Depth and Intensity Indices .....	84
4.3.4.1 Extreme Rainfall Indices for 1-day and 5-day Event Durations .....	84
4.3.4.2 The Percentile Threshold Indices of Daily Rainfall Events .....	87
4.3.5 Temperature Data Analysis .....	89
4.3.5.1 Trend Analysis of Temperature .....	94
4.3.6 Potential Evapotranspiration Trends .....	101
4.3.7 Estimation of Evapotranspiration .....	102
4.3.8 Trend Analysis of River Discharge .....	105
4.3.8.1 Annual Streamflow Analysis .....	105
4.3.8.2 Kiremt (Rainy Season) Streamflow Analysis .....	106
4.4 Conclusion .....	108
<b>CHAPTER 5 LAND USE/LAND COVER CHANGE DETECTION .....</b>	<b>109</b>
5.1 Introduction .....	109
5.2 Methodology .....	109
5.2.1 Landsat Multispectral Scanner (MSS) .....	110
5.2.2 Landsat Thematic Mapper (TM) .....	111
5.2.3 Landsat Enhanced Thematic Mapper plus (ETM+) .....	111
5.2.4 Image Pre-processing .....	113
5.2.5 Image Processing .....	113
5.2.6 Classification Accuracy Assessment .....	114
5.2.7 Image Classification .....	115
5.2.7.1 Selection of Training Areas .....	115
5.2.7.2 Transformations and Indices .....	116
5.2.7.3 False Color Composition (FCC) .....	116
5.2.7.4 Supervised Classification .....	116
5.2.7.5 Maximum Likelihood Classification .....	117
5.2.8 Land Cover Classification System .....	118
5.3 Results and Discussion .....	119

5.3.1 Land use/land cover Changes at Watershed Level .....	119
5.3.1.1 Spatial Distribution of Land use/land cover Classes of 1973 and 1987 ..	120
5.3.1.2 Spatial Distribution of Land use/land cover Classes of 2000 and 2013 ..	126
5.3.2 Rate of Land Use/Land Cover Changes .....	128
5.3.3 Land use/land cover Changes at Sub-basin Level .....	130
5.4 Conclusion.....	133
<b>CHAPTER 6 APPLICATION OF SWAT HYDROLOGICAL MODEL .....</b>	<b>135</b>
6.1 Introduction .....	135
6.2 Methodology .....	135
6.2.1 Selection Criteria of Hydrological Model .....	135
6.2.2 Reasons for Selecting SWAT Model.....	136
6.2.3 Model Description of SWAT 2012 .....	136
6.2.4 Hydrological Component of SWAT.....	137
6.2.4.1 Surface Runoff.....	139
6.2.4.2 Sediment Component.....	140
6.2.4.3 Actual and Potential Evapotranspiration .....	140
6.2.4.4 Water Movement in Soil.....	143
6.2.4.5 Ground Water Flow Estimation.....	144
6.2.4.6 Flow Routing Phase .....	144
6.2.5 Data Acquisition and Preparation for SWAT Model .....	145
6.2.6 SWAT Model Inputs .....	145
6.2.6.1 Digital Elevation Model (DEM) .....	145
6.2.6.2 Meteorological Data.....	146
6.2.6.3 Soil Data.....	146
6.2.6.4 Land Use/Land Cover .....	147
6.2.6.5 Hydrological Data.....	147
6.2.6.6 Sediment data.....	148
6.2.7 SWAT Model Setup .....	148
6.2.7.1 Watershed Delineation.....	148

6.2.7.2 Hydrologic Response Units (HRU) .....	150
6.2.7.3 Weather Generator .....	151
6.2.7.4 Sensitivity Analysis .....	152
6.2.8 Modelling of the Geba River Catchment.....	155
6.2.8.1 Model Calibration, Validation, and Performance Evaluation.....	155
6.3 Results and Discussion.....	158
6.3.1 Sensitivity Analysis and Parameter Estimation .....	158
6.3.2 Model Calibration and Validation .....	161
6.3.2.1 Daily and Monthly Streamflow Predictions .....	163
6.3.3 Water Balance Components .....	176
6.3.4 Model Calibration and Validation for Daily Sediment Simulations.....	177
6.3.5 Demarcation of Soil Erosion Susceptibility.....	181
6.4 Conclusion.....	186

## **CHAPTER 7 HYDROLOGICAL IMPACTS TO CHANGES IN LAND**

### **USE/LAND COVER AND CLIMATE VARIABILITY ..... 189**

7.1 Introduction .....	189
7.2 Methodology .....	191
7.2.1 Land Use Land Cover Scenarios Development.....	191
7.2.1.1 Existing State (Baseline Scenario).....	192
7.2.1.2 Land Degradation Scenario.....	192
7.2.1.3 Land Restoration Scenario .....	193
7.2.2 Hydrological Impact of Changes in LU/LC and Climate Variability .....	196
7.3 Results and Discussion.....	197
7.3.1 Scenario Analysis for LU/LC Changes .....	197
7.3.1.1 Bounding Scenarios .....	198
7.3.1.2 Land Degradation Scenario.....	199
7.3.1.3 Land Restoration Scenario .....	202
7.3.2 Hydrological Impact of LU/LC Changes and Climate Variability.....	204
7.3.2.1 Impact on Runoff .....	204



7.3.2.2 Impact on Available Soil Water and Potential Evapotranspiration .....	209
7.4 Conclusions .....	213
<b>CHAPTER 8 CONCLUSIONS .....</b>	<b>215</b>
8.1 Introduction .....	215
8.2 Conclusions .....	215
8.2.1 Historical Trends of Hydro-Meteorological Analysis .....	215
8.2.2 Land Use/Land Cover Change Assessment.....	217
8.2.3 Calibration, Validation and Performance Evaluation of SWAT Model.....	218
8.2.4 LU/LC and Climate Variability Impact Assessment on the Hydrology of the Geba Catchment .....	220
8.3 Contributions from this Research.....	222
8.4 Recommendations .....	223
8.4 Perspectives for Future Studies .....	226
8.6 SWAT Model Limitation .....	226
<b>REFERENCES .....</b>	<b>227</b>
<b>APPENDIX.....</b>	<b>253</b>
<b>PUBLICATIONS.....</b>	<b>259</b>
<b>RESUME .....</b>	<b>261</b>

## LIST OF FIGURES

<b>Figure 3.1:</b> Location of the Geba Catchment .....	31
<b>Figure 3.2:</b> DEM of the Geba Catchment.....	32
<b>Figure 3.3:</b> Average monthly rainfall for the Geba basin (Ethiopian Meteorological Agency data, 1971-2013) .....	34
<b>Figure 3.4:</b> Average monthly minimum and maximum temperature for the Geba basin (Ethiopian meteorological Agency data, 1971-2013) .....	35
<b>Figure 3.5:</b> Major river basins in Ethiopia (MoWE) .....	36
<b>Figure 3.6:</b> Major Soil types of the Geba basin (FAO 1998) .....	38
<b>Figure 3.7:</b> Research Methodological Framework of the Study.....	40
<b>Figure 4.1:</b> Mean annual rainfall of rainfall stations in Geba River Basin.....	52
<b>Figure 4.2:</b> Geba River basin seasonal rainfall distributions.....	52
<b>Figure 4.3:</b> Temporal variation of average monthly Rainfall of different decades for stations (a) Abiadi (b) Adigudem (c) Adigrat (d) Hawzien (e) Mek’ele (f) Senkata and (g) Wukro of Geba River basin.....	55
<b>Figure 4.4:</b> average annual rainfalls at the Geba River basin rainfall stations.....	56
<b>Figure 4.5:</b> average monthly rainfall in the Geba River basin rainfall stations.....	57
<b>Figure 4.6:</b> Average monthly rainfall at the (a) upper stream and (b) downstream of the Geba River basin.....	58
<b>Figure 4.7:</b> Standardized anomalies of time series annual average rainfall totals of the seven stations.....	61
<b>Figure 4.8:</b> Standardized anomalies of time series of annual rainfall at the seven stations (a) Abiadi (b) Adigudem (c) Adigrat (d) Hawzien (e) Mek’ele (f) Senkata and (g) Wukro .....	64
<b>Figure 4.9:</b> Variation of annual rainfall for stations (a) Abiadi (b) Adigudem (c) Adigrat (d) Hawzien (e) Mek’ele (f) Senkata and (g) Wukro of Geba River basin .....	68

<b>Figure 4.10:</b> Variation of Rainy season rainfall for stations (a) Abiadi (b) Adigudem (c) Adigrat (d) Hawzien (e) Mek’ele (f) Senkata and (g) Wukro of Geba River basin .....	72
<b>Figure 4.11:</b> Variation of dry season rainfall for stations (a) Abiadi (b) Adigudem (c) Adigrat (d) Hawzien (e) Mek’ele (f) Senkata and (g) Wukro of Geba River basin .....	75
<b>Figure 4.12:</b> Trends in 1971-2013 for PRCPTOT (a), for CDD (b) and CWD (c) .....	81
<b>Figure 4.13:</b> Trends in 1971-2013 for the 10mm (a), for the 20mm (b) and for the 25mm (c) .....	82
<b>Figure 4.14:</b> Trends in 1971-2013 for RX1day (a), RX5day (b) and SDII (c).....	86
<b>Figure 4.15:</b> Trends in 1971-2013 for R90P (a), R95P (b) and R99P (c).....	88
<b>Figure 4.16:</b> Temporal variation of average monthly minimum Temperature of different decades for stations (a) Abiadi (b) Adigudem (c) Adigrat (d) Hawzien (e) Mek’ele (f) Senkata and (g) Wukro of Geba River basin .....	92
<b>Figure 4.17:</b> Temporal variation of average monthly minimum Temperature of different decades for stations (a) Abiadi (b) Adigudem (c) Adigrat (d) Hawzien (e) Mek’ele (f) Senkata and (g) Wukro of Geba River basin .....	94
<b>Figure 4.18:</b> Linear trend line corresponding to average monthly maximum temperature at the seven stations (a) Abiadi (b) Adigudem (c) Adigrat (d) Hawzien (e) Mek’ele (f) Senkata and (g) Wukro .....	97
<b>Figure 4.19:</b> Linear trend line corresponding to average monthly minimum temperature at the seven stations (a) Abiadi (b) Adigudem (c) Adigrat (d) Hawzien (e) Mek’ele (f) Senkata and (g) Wukro .....	100
<b>Figure 4.20:</b> Variations of average monthly PET for the stations in the Geba Catchment.....	102
<b>Figure 4.21:</b> Temporal variation of average monthly ET of different decades for Geba River basin.....	103

<b>Figure 4.22:</b> Time series plots for the annual River discharge at the outlet gauge station. The straight line shows the trend line .....	106
<b>Figure 4.23:</b> Time series plots for the rainy season River discharge at the outlet gauge station. The straight line shows the trend line .....	107
<b>Figure 5.1:</b> Methodology adopted for LU/LC change analysis and detection.....	119
<b>Figure 5.2:</b> Land use/land cover map of Geba River basin in 1973.....	124
<b>Figure 5.3:</b> Land use/land cover map of Geba River basin in 1987 .....	125
<b>Figure 5.4:</b> Land use/land cover map of Geba River basin in 2000 .....	126
<b>Figure 5.5:</b> Land use/land cover map of Geba River basin in 2013 .....	127
<b>Figure 5.6:</b> Changes in LU/LC in the Geba River basin from1973 to 2013.....	128
<b>Figure 5.7:</b> Annual rate of change in LU/LC at Geba River basin .....	130
<b>Figure 6.1:</b> Input and Output Components of the SWAT Model.....	138
<b>Figure 6.2:</b> Soil map of the Geba basin (FAO 1998) .....	146
<b>Figure 6.3:</b> Geba catchment area sub-basins.....	149
<b>Figure 6.4:</b> Time series plots of catchment streamflow and rainfall .....	159
<b>Figure 6.5:</b> Sensitivity ranking for hydrology in the Geba River basin for SWAT Model .....	162
<b>Figure 6.6:</b> Time series of the observed and simulated average monthly streamflow for calibration and validation period for 1973, 1987, 2000 and 2013 land use land cover map .....	167
<b>Figure 6.7:</b> Scatter plots of simulated and observed flow for calibration period (a) 1973, (b) 1987, (c) 2000 and (d) 2013 land use land cove map .....	169
<b>Figure 6.8:</b> Scatter plots of simulated and observed flow for validation period (a) 1973, (b) 1987, (c) 2000 and (d) 2013 land use land cove map .....	171
<b>Figure 6.9:</b> Scatter plot of observed and simulated sediment for calibration and validation period for 2000 and 2013 land use/land cove map .....	177

<b>Figure 6.10:</b> Time series of the observed and simulated daily sediment for Calibration and validation period for (a) 2000 and (b) 2013 land use land cover map .....	179
<b>Figure 6.11:</b> Predicted annual net soil loss for the 1973, 1987, 2000 and 2013 LU/LC maps in the Geba catchment .....	183

## LIST OF TABLES

<b>Table 4.1:</b> Meteorological stations selected for analysis with details of coordinates, elevation, observation period and observed mean annual rainfall values .....	44
<b>Table 4.2:</b> Definition of the rainfall indices used in this study .....	45
<b>Table 4.3:</b> Showing the stations with their ID and Missing data (%).....	46
<b>Table 4.4:</b> Annual and seasonal rainfall (mm) and their coefficient of variation estimated over the period 1971–2013 .....	59
<b>Table 4.5:</b> Average contribution of the three seasons (in Percent) and the highest monthly and peak rainfall contribution to the annual totals (mm) .....	60
<b>Table 4.6:</b> The driest and wettest years and seasons by station during the period 1971–2013 .....	62
<b>Table 4.7:</b> Annual rainfall trend detection for the stations in the Geba River basin .....	66
<b>Table 4.8:</b> Rainy seasonal rainfall trend detection for the stations in the Geba River basin for the period (1971-2013).....	70
<b>Table 4.9:</b> Dry seasonal rainfall trend detection for the stations in the Geba River basin for the period (1971-2013).....	73
<b>Table 4.10:</b> The occurrence of the lowest and highest Simple Daily Intensity Index (SDII) .....	78
<b>Table 4.11:</b> Mann-Kendall Statistic (P) and Sen's slope for PRCPTOT, CDD, CWD, R10mm, R20mm and R25mm for all stations .....	79
<b>Table 4.12:</b> Mann-Kendall Statistic (P) and Sen's slope for R95, R95, R99P, SDII, R1x day and R5x day for all stations .....	78
<b>Table 4.13:</b> Decadal CV of minimum temperature for the stations in the Geba River .....	89
<b>Table 4.14:</b> Decadal CV of maximum temperature for the stations in the Geba	

River basin.....	90
<b>Table 4.15:</b> Results of the Mann-Kendall test for the average monthly maximum daily temperature data.....	95
<b>Table 4.16:</b> Results of the Mann-Kendall test for the average monthly minimum temperature data.....	98
<b>Table 4.17</b> Temporal Variation of monthly ET of different decades for Geba River basin.....	103
<b>Table 4.18</b> Temporal Variation of monthly PET of different stations for Geba River basin .....	104
<b>Table 4.19</b> Results of the Mann-Kendall test for the annual streamflow data .....	106
<b>Table 4.20</b> Results of the Mann-Kendall test for the seasonal (rainy and dry) streamflow data .....	107
<b>Table 5.1:</b> Description of Landsat Multispectral Scanner (MSS) .....	111
<b>Table 5.2:</b> Description of Landsat Thematic mapper (TM) .....	111
<b>Table 5.3:</b> Description of Landsat Thematic Mapper Plus (ETM+) .....	112
<b>Table 5.4:</b> Spatial distribution land use/land cover classes during 1973 to 2013 time period of the Geba River basin .....	120
<b>Table 5.5:</b> Land use/land cover Change detection matrix .....	121
<b>Table 5.6:</b> Land use/land cover types and changes from1973-2013 at Geba River basin .....	129
<b>Table 5.7:</b> Major land use/land cover changes from 1973 to 1987 in sub-basins (Percentage of change is computed with respect to the area of the sub-basin) ....	131
<b>Table 5.8:</b> Major land use/land cover changes from 1987 to 2000 in sub-basins (Percentage of change is computed with respect to the area of the sub-basin) ....	131
<b>Table 5.9:</b> Major land use/land cover changes from 2000 to 2013 in sub-basins. (Percentage of change is computed with respect to the area of the sub-basin) ....	132
<b>Table 6.1:</b> Soil Available Water and Hydraulic Conductivity.....	146
<b>Table 6.2:</b> The slope classes of the Geba Catchment .....	150

<b>Table 6.3:</b> HRU distribution across the sub-basins .....	151
<b>Table 6.4:</b> SWAT parameters Sensitivity class .....	153
<b>Table 6.5:</b> Parameters and their ranges in sensitivity analysis of SWAT model .....	154
<b>Table 6.6:</b> SWAT most sensitive parameters and their MRS values .....	159
<b>Table 6.7:</b> SWAT flow sensitive parameters and fitted values after calibration .....	162
<b>Table 6.8:</b> SWAT model performance evaluation for daily and monthly streamflow predictions using static LU/LC (2000) map.....	163
<b>Table 6.9:</b> SWAT model performance evaluation for daily streamflow predictions.....	166
<b>Table 6.10:</b> SWAT model performance evaluation for monthly streamflow predictions.....	166
<b>Table 6.11:</b> Average annual water balance components derived from the SWAT model (all values are in mm of water) .....	178
<b>Table 6.12:</b> Model Performance values for sediment during calibration and validation periods for 2000 and 1987 LU/LC maps.....	179
<b>Table 6.13:</b> Identification of soil erosion susceptible area .....	183
<b>Table 6.14:</b> Sub-basin sediment yield of the simulation period.....	184
<b>Table 7.1:</b> Characteristics of 2013 LU/LC data and deforestation scenarios .....	191
<b>Table 7.2:</b> Characteristics of simulated LU/LC afforestation scenarios .....	192
<b>Table 7.3:</b> Simulation results from bounding cases scenarios .....	196
<b>Table 7.4:</b> Simulation results from land degradation scenarios .....	197
<b>Table 7.5:</b> Simulation results obtained from land restoration scenarios .....	200
<b>Table 7.6:</b> Simulated surface runoff volumes for the 1973-2013 land use/land cover scenarios .....	202
<b>Table 7.7:</b> Simulated baseflow from 1973 to 2013 land use/land cover conditions.....	204



<b>Table 7.8:</b> Predicted average annual runoff volume under various LU/LC and climatic conditions .....	207
<b>Table 7.9:</b> Predicted average annual soil water and PET under different LU/LC and climatic conditions .....	208

## LIST OF ABBREVIATIONS

---

<b>Abbreviations</b>	<b>Description</b>
ARMA	Auto-Regressive Moving Average
ARIMA	Auto-Regressive Integrated Moving Average
ARS	Agricultural Research Service
ASTER	Advanced Space borne Thermal Emission and Reflection Radiometer
CDD	Consecutive dry days
CN	Curve Number
CSA	Central Statistical Agency of Ethiopia
CV	Coefficient of Variation
CWD	Consecutive wet days
DEM	Digital Elevation Model
ENMA	Ethiopian National Meteorological Agency
ENVI	ENvironment for Visualizing Images
ETCCDMI	Expert Team Climate Change Detection and Monitoring Indices
ET	Actual Evapotranspiration
ETM+	Enhanced Thematic Mapper Plus
FAO	Food and Agricultural Organization
FCC	False color composition
GIS	Geographic Information System
GLCF	Global Land Cover Facility
HRU	Hydrological Response unit
IPCC	Intergovernmental Panel on Climate Change
ITCZ	Inter-tropical Convergence Zone
IWRM	Integrated Water Resources Management
JJAS	June, July, August and September

LU/LC	Land use/land cover
LH-OAT	Latin Hypercube and ‘One-factor-At-a Time’
LCCS	Land Cover Classification System
MCE	Multi-Criteria Evaluation
MoWE	Ministry of Water and Energy
MoWIE	Ministry Water, Irrigation and Energy
MoWR	Ministry of Water Resources
MRS	Mean Relative Sensitivity
MSS	Multispectral Scanner
MUSLE	Modified Universal Soil Loss Equation
NASA	National Aeronautics and Space Administration
NCC	Natural Color Composite
NDVI	Normalized Difference Vegetation Index
NRCS	Natural Resource Conservation Service
NSE	Nash and Sutcliffe simulation efficiency
PBIAS	Percent bias
PEST	Parameter ESTimation
PET	Potential Evapotranspiration
$R^2$	Coefficient of determination
RGB	Red, Green and Blue
RMSE	Root Mean Square Error
ROI	Regions of Interest
RS	Remote Sensing
RSR	Ratio of root mean square error to measured Standard deviation
SAM	Spectral Angle Mapper
SCS	Soil Conservation Service
SD	Standard Deviation
SDII	Simple daily intensity index
SPOT	Systeme Polyvalent pour Observation de la Terre

SSY	Specific Sediment Yield
SUFI-2	Sequential Uncertainty Fitting
SWAT	Soil and Water Assessment Tool
SWAT-CUP	Soil and Water Assessment Tool – Calibration and Uncertainty Program
TM	Thematic Mapper
UNECA	United Nations Economic Commission for Africa
USA	United States of America
USDA	United States Department of Agriculture
USGS	United States Geological Survey
USLE	Universal Soil Loss Equation
UTM	Universal Transverse Mercator



# CHAPTER 1

## INTRODUCTION

### 1.1 Overview of Water Resources and Sustainable Development

The availability of water in the right quality and quantity for human and ecological uses is being threatened by pollution, droughts and floods. Various bio-physical factors that modify the earth's environment as well as socio-economic factors have led to mismanagement of natural resources (IPCC, 2001). Among the factors that have direct impact on water resources; climate changes due to global warming and land use/land cover (LU/LC) changes due to anthropogenic activities, play central roles. Increased stress on available water resources is being caused due to population growth, rainfall variability and increased consumption across various sectors. This is especially true in the context of Africa, where non-availability of desired levels of water supply and environmental degradation are posing severe constraints on human welfare and economic growth.

Efforts to provide adequate water resources for Africans have been confronted with several challenges, including population pressure, erosion/siltation and likely environmental consequences of LU/LC changes on the hydrological cycle (IPCC, 2007; Conway and Schipper, 2011). An integrated approach is required for the assessment of management issues and strategies relating to use and distribution of water resources. Integrated water resources management is not only required for analysing consequences of the adverse natural conditions such as floods or droughts but also to evaluate and assess promising strategies to reduce vulnerability to environmental constraints and changing climate (IPCC, 2007). In addition, the concept of water resources management requires matching of water availability and water use in a river basin (Tilahun, 2006; Lin et al., 2007; Guo et al., 2008). River basins are the preferred land surface units for water

related studies because their drainage areas represent natural spatial integrators or accumulators of water and associated material transport and thus allow for the investigation of cumulative effects of climate and human activities on the water cycle and environment (Vanmaercke et al., 2010; Zenebe et al., 2013).

Water availability in the form of surface water or groundwater is determined by a large number of factors/variables related to soil-vegetation-atmosphere continuum. An aspect often forgotten in this respect is the impact of new patterns of LU/LC on availability of water. There are many connections between land surface characteristics and water cycle. Primarily, LU/LC can affect the partitioning incident rainfall into infiltration and surface runoff components thereby affecting surface and sub-surface hydrological processes (Belay, 2002; Lambin et al., 2003; Bewket and Sterk, 2005; Lin et al., 2007; Tewelde, 2009). Any changes in LU/LC will have effects not only on hydrological regimes, but also on ecological communities (Hadgu, 2008; Nyssen et al., 2010; Girmay et al., 2010; Taye et al., 2013; Mahmoud and Alazba, 2015; Babar and Ramesh, 2015).

Within the African continent, Ethiopia faces a large number of water-related problems enumerated earlier. Located in the horn of East Africa, Ethiopia has a geographical area of about 1.13 million km<sup>2</sup>. The population of the country is more than 90 million, increasing by 2.7 % each year, and as such is the second populous country in Africa next to Nigeria (CSA, 2008). The annual rainfall in the country varies from less than 100 mm in the low lands along the border with Somalia and Djibouti to 2,400 mm in the southwest highlands, with a national average of 744 mm (Awulachew et al., 2007). Ethiopia is known for its substantial water resources potential, hence, known as the water tower of Africa, contributing more than 85 % of the flow to the Nile River in addition to contributions to many trans-boundary rivers. The total annual runoff is estimated to be about  $122 \times 10^9$  m<sup>3</sup>; however only less than 20 % is naturally contained within the country with the remaining leaving the country as trans-boundary river flow (MoWE, 2010). There is ample water resource in central, western and south western parts, while most of the North Eastern and Eastern parts of the country are relatively dry. The distribution and

availability of water is erratic both in space and time. Hence, despite abundance in some parts, the country is highly water-scarce due to paucity of water control and storage infrastructure.

Recent studies in the Eastern African region have revealed that changes in LU/LC and variability of climate pose challenges to the integrity of quality and availability of water, and agricultural productivity (Nyssen et al., 2005; 2007; Setegn et al., 2011). Moreover, there are several indicators of water stress and scarcity in the region, including the amount of water available per person and the volume ratio of water withdrawn and potentially available (IPCC, 2001; IPCC, 2007b). This situation has been attributed to the increasing population, which translates into increased demand for water supply (for domestic and agricultural productivity), as well as to climate change. Global warming would induce changes in precipitation and wind patterns, changes in the frequency and intensity of storms, ecosystem stress, reduce availability of fresh water, and a rising global mean sea level (Hurni et al., 2005; Legesse et al., 2010; UNECA, 2011). Although the impacts may not be easily predicted, changes in weather patterns may lead to the prevalence of severe drought conditions or extreme flood events in the region. The existence of prolonged drought periods regarding water scarcity has seriously affecting agricultural production and the socio-economic activities in the region. Ethiopia is one of the eastern African countries likely to experience continuous land, water and ecological degradation as a result of global and local climate anomalies, which is a challenge for water resources management to sustain economic development in the country (Nyssen et al., 2004; Zenebe et al., 2013).

To balance supply and demand for water resources and to reduce undesirable effects for the environment and society, changes in actual LU/LC have to be studied at all spatial scales. The land surface provides a critical role in the water cycle as it is the level at which precipitation is redistributed into evaporation, runoff or soil moisture storage (Setegn et al., 2008, 2009). Thus, Land use/land cover studies should be viewed as responding to the complex interactions and responses linking social and biophysical processes that



occur on the land (Chow et al., 1988; Maidment, 1993; Nyssen et al., 2009). With increasing human activities concerning water conflicts, it is important to understand the interactions between hydrological processes and associated LU/LC and climate changes in catchments (Nyssen et al., 2010; Friedrich et al., 2012; Wubishet et al., 2015). Such an understanding can be achieved by integrating land use planning and water resources management. Land use/land cover change data represents a key variable in the management and understanding of the environment, as well as driving many environmental models such as hydrological models within large river basins or even for particular smaller to medium catchments. There is a need to develop proper planning and management approaches within the context of Integrated Water Resource Management (IWRM). IWRM is defined as a process that considers the co-ordinated development and management of water, land and related resources to enhance economic and social welfare without jeopardising the sustainability of the ecosystems (Global Water Partnership, 2005). Thus, sustainable development of water resources is a key to the maintenance of the natural ecosystem that supports the well-being of human populations.

A crucial first step towards implementing IWRM is to assess the temporal and spatial variability of available water resources at catchment-scale. Typically, this requires analysis of long-term observations of river flows and groundwater levels at multiple locations within a catchment. However, spatio-temporal analyses of water resources are usually rendered difficult, if not impossible, in developing countries such as Ethiopia due to sparse ground-based data networks. Even with availability of surface and groundwater observations, characterizing the working of the hydrological cycle and understanding the linkages between hydro-climate and LU/LC is not possible unless additional observations on soil moisture, evapotranspiration, surface runoff, baseflow, sediment concentrations and groundwater recharge are available. To circumvent this problem, the use of mathematical models which seek to represent the working of the hydrological cycle within a catchment have been proposed as solution. Once an appropriate hydrological model has been applied, calibrated and validated for a given catchment using available observations of streamflow, it can be used not only to provide estimates of available

water resources but also to evaluate the impacts of likely changes in LU/LC and climate. A large number of hydrological models of different types – empirical, conceptual or mechanistic; lumped, semi-distributed or distributed; deterministic or probabilistic; event-based or continuous, have been developed over the past several decades. Different types of hydrological models vary with respect to process representation, input data requirement, complexity of use and nature of output provided. A state-of-the-art review of currently available hydrologic models can be found in Daniel et al. (2011).

The Soil and Water Assessment Tool (SWAT) hydrological model (Arnold et al., 1998) has been widely recognized as a powerful tool for carrying out such studies. The free availability, good modelling capability, GIS interface, incorporation of key features of catchment properties, including links between LU/LC and hydrological responses makes it an attractive and most sought after hydrological model. The ArcSWAT2012 version of the model is integrated within a Geographical Information System (GIS) platform and also derives certain inputs from satellite remote sensing. SWAT has been widely used in various regions of the world and in different climatic zones at daily, monthly and annual time steps. It has been successfully implemented at spatial scales ranging from small watersheds to large River basins in different parts of the world (Fohrer et al., 2005; Li et al., 2009; Mango et al., 2011; Van Griensven et al., 2012; Arnold et al., 2012). In some parts of Ethiopia, SWAT has been effectively implemented to predict water yield, sediment yield and water quality of different catchments (Setegn et al., 2008; Easton et al., 2010; Betrie et al., 2011; Setegn et al., 2011; Mengistu and Sorteberg, 2012; Van Griensven et al., 2012).

## **1.2 Statement of the Problem**

The Geba River is a tributary of the Tekeze River which in turn is a major tributary of the Nile River. The Geba basin is endowed with terrestrial diversity ranging from forests and wildlife. However, the basin and its natural resources are under great pressure due to rapid rural and urban population growth, poor agricultural practices, and deforestation.

These practices have resulted in land degradation, soil erosion, loss of biodiversity, poverty and unemployment.

Inappropriate water resources management, poor land use practices, deforestation, lack of appropriate water harvesting and soil conservation measures are major problems in the basin. Also, undulating topography, intense rainfall and sparse vegetation cover have played a major role in causing severe soil erosion and land degradation problems in the Northern highlands of Ethiopia. The effect of degradation arising from poor land use practices are accelerating runoff and sheet erosion within the catchment area, leading to severe rill, gully, and stream bank erosion and sedimentation. Increased sediment loads cause deposition in the lower reaches of rivers. Consequently, highlands of the country are losing soil at a rate of 1.3 billion tons per year (Hurni, 1988). As a result the country is facing severe erosion causing a decline in land productivity (Nyssen et al., 2005). The average rate of soil erosion from croplands in the highlands is estimated at  $42 \text{ t ha}^{-1}$  per year (Hurni, 1988) and is by far greater than an average agricultural soil formation rate of approximately  $1 \text{ t ha}^{-1}$  per year (Lal, 2000). Soil erosion is even more severe in the barren hillsides in Northern highlands of the country.

The Northern highlands of Ethiopia represent a complex environment with a long history of human occupation, deforestation and severe problems of land degradation and soil erosion (Nyssen et al., 2004; 2005). This continuous change in LU/LC has impacted the water balance of the catchment by changing the magnitude and pattern of runoff. Consequently, crop and livestock production and energy supply situations are at risk with a negative impact on the socio-economic situation of the country. Moreover, there is a clear general lack of quantification of the impact of LU/LC changes and climate variability on hydrological responses and lack of erosion and sediment yield estimates due to data scarcity. In addition, knowledge of the interactions between LU/LC, climate and runoff processes is lacking in the area. Therefore, the question as to when, where and to what extent these changes can occur and how these can affect hydrological processes

and sediment dynamics is still open and needs to be answered before meaningful adaptation strategies can be adopted.

In light of the above mentioned problems, it is imperative to understand the hydrological processes occurring within the Geba river basin using appropriate modelling tools and techniques. There is an urgent need to use hydrologic modelling techniques that can assess the impacts of LU/LC changes and climate variability on the hydrologic responses relating to runoff and sediment yields from the sub-basins of the Geba river basin. This would help to estimate the catchment's water budget, runoff/sediment timing and magnitudes and the impacts of anthropogenic activities and climate changes on the hydrology of the river basin. These estimates will support decision makers and planners to optimize water supply and demand, and to advocate sound land use practices, while ensuring environmental sustainability.

### **1.3 Research Questions**

The following questions need to be answered with respect to hydrological characteristics of the Geba catchment.

- a) Are there changes in runoff, rainfall and temperature in the Geba river basin? If there are changes, what are the pattern of the changes i.e. are the changes increasing or decreasing? Are the changes gradual or abrupt? If there are changes, in which months/season do they occur? Do extreme climate events show a trend?
- b) How has LU/LC changed over the past four decades in the Geba catchment? Can analysis of land cover dynamics and change detection be carried out using satellite data available in the public domain?
- c) Is there a potential to use a readily available hydrological model to simulate the hydrology of the Geba basin in the presence of spatial heterogeneity in physical characteristics and hydro-climatic conditions? How can data from a variety of ground-based measurements be used as input to the model? Is there a potential to use satellite data in the modelling exercise?

- d) What should be the most appropriate hydrological modelling strategy to be adopted in a situation where rapid changes in LU/LC take place?
- e) Can a distributed hydrologic model provide information on the temporal and spatial variability of major hydrologic components of runoff, evapotranspiration, soil moisture and sediment concentrations? What will be the level of accuracy of such simulations?
- f) How can the combined and separate hydrological impacts of likely LU/LC changes and climate changes be simulated using a hydrological model?

#### **1.4 Research Objectives of the Present Study**

In an effort to provide answers to the research questions posed in Article (1.3), the present study was taken up with the following specific research objectives:

1. To statistically analyse historical records of relevant hydro-meteorological variables in the Geba catchment and investigate changes and trends over time;
2. To explore the feasibility of using satellite imagery to analyse land cover dynamics and detection of changes in LU/LC in the Geba basin over the past four decades;
3. To understand the overall hydrological processes using available hydro-meteorological data, and to apply and evaluate the potential of the SWAT model to simulate major hydrological processes and sediment dynamics in the Geba catchment;
4. To quantify, assess and analyse the impacts of LU/LC changes and climate variability on streamflow and sediment dynamics in the Geba catchment.

#### **1.5 Structure of the Thesis**

**Chapter One** provides an introduction to problems related to sustainable water resources management specifically in the context of Africa and Ethiopia. Challenges with regard to characterization of available water resources, LU/LC changes and climate

variability in the Geba catchment are discussed. Based on critical questions which need to be answered for sustainable water resources management in the catchment, research objectives of the present study are presented. A brief, chapter-wise description of the present thesis is presented.

**Chapter Two** reviews literature relating to LU/LC change detection, climate variability, sediment transport, hydrologic modelling and hydrologic impact assessment. Previous studies elaborating advances made in hydrologic models and their use investigating the impacts of climate and LU/LC changes are reviewed.

**Chapter Three** provides a description of the physiographical features, location, soil types, topography, LU/LC and overall climatic conditions in the Geba catchment. A description of the different datasets used in the present study and the overall research methodology adopted in the present study are discussed.

**Chapter Four** discusses the statistical and trend analysis of historical hydro-meteorological data obtained for the Geba catchment. Monthly and seasonal averages of rainfall, air temperature and streamflow are subjected to trend analysis. Also, trends in extreme climate indices relating to rainfall and temperature are detected.

**Chapter Five** discusses LU/LC dynamics and change assessment within the Geba River catchment based on a supervised Maximum Likelihood classification of Landsat imagery MSS and TM for 1973 and 1987, and Landsat imagery ETM+ for 2000 and 2013. The variability in spatial LU/LC extents for each classified LU/LC class between the four periods has been examined. The results are used in chapter six. Moreover, this chapter investigated the LU/LC changes within the upper Geba River catchment. The implemented change detection methods quantitatively reveal the major changes that have occurred in the catchment between 1973 and 2013.

**Chapter Six** focuses on methods adopted for application, calibration, validation and performance evaluation of the SWAT model to the Geba catchment. Integration of input

data from a variety of ground and satellite-based sources to implement the model and the accuracy of the model simulated streamflow and sediment concentrations are described.

**Chapter Seven** presents the strategy adopted for application of the SWAT model to assess the impacts of LU/LC and climate variability on hydrological processes in the Geba catchment. Results with regard to catchment responses; especially streamflow, sediment, soil moisture and evapotranspiration, to changes in LU/LC and climate variability are discussed.

**Chapter Eight** is devoted to presentation of the conclusions arising out of the present research. Important recommendations based on findings are also listed. Moreover, limitations of the study and scope for future studies are presented.

## CHAPTER 2

### REVIEW OF LITERATURE

#### 2.1 Introduction

This review of literature provides an overview of application of hydrologic modelling for assessment of hydrological responses to changes in land use/land cover and climate variability. Hydrologic models are increasingly used in hydrology and to simulate changes in river basin management, to explore the effects of external influences (such as land use/land cover changes and climate) and also to outspread data sets. This chapter reviews five topics that are core to this research, namely:

- ™ Variability and trend analysis of hydro-meteorological variables, Ethiopian Scenario;
- ™ Hydrologic modelling and classification and integration with Remote sensing and GIS;
- ™ Land use / land cover (LU/LC) changes, methodologies and Ethiopian Context;
- ™ Erosion and sediment dynamics;
- ™ Climate variability, change and relater impacts.

#### 2.2 Variability and Trend Analysis of Hydro-meteorological Variables

Opiyo et al. (2014) investigated the temporal trends such as monthly, seasonal and annual rainfall and temperature variability for the period 1979 to 2012 in Turkana, Kenya. Results showed that except for the months August and November which showed statistically significant increasing trends for maximum temperature in the entire study, there is a mix of positive and negative trends, though they are not statistically significant at 90 % and 95 % significance level. Schreck and Semazzi (2004) and Omendi et al. (2013) highlighted that there is a general increase in warm extremes particularly at night while cloud extremes are decreasing in the horn of Africa. Kinh Uyu et al. (2000), Schrech and Semazzi (2004) studied the climate variability across the Eastern Africa



region; results revealed that there has been temperature variability in the region, especially within the arid and semi-arid environments. In addition, by the end of 21<sup>st</sup> century, roughly 1.5 times the global mean response as a region of climate models suggest that median temperature increases between 3 °C and 4 °C in Africa (IPCC, 2007; Bryan et al., 2013).

Collier et al. (2008) investigated that many semi-arid parts of the developing world are likely to become hotter and dryer with time as changes in temperature patterns are widely experienced. Compared to the global average, the average temperature rise in Africa is faster and is likely to continue in the future (Hulme, 2001). Collier et al. (2008) suggested that this warming occurred at the rate of about 0.5 °C per decade with a slightly larger warming where crops are grown close to the thermal acceptance limits.

Several previous studies carried out are at different spatial scales (Nicholson 2000; Hulme et al. 2001; Schreck and Semazzi 2004; Nyong and Niang-Diop, 2006; Mwangi and Desanker 2007; Tesemma et al., 2010; Mondal et al., 2012; Moyo et al., 2012; Omondi et al., 2013; Wagesho et al., 2013; Opiyo et al., 2014) have revealed high inter-annual rainfall variability within arid and semi-arid environments. This assumes significance given the importance of rain-fed agriculture in such environments and the associated impacts on agricultural productivity.

Ethiopia is a typical example where 85 % of the population is involved in subsistence agricultural and majority of the gross domestic product is dependent on the low productivity of rain-fed agriculture (Shang et al., 2011). In some parts of the country, such as Northern Ethiopia, high historical variability of rainfall and frequent drought conditions have been identified (Meze-Hausken, 2004; Hadgu et al., 2013). However, few studies previously carried out in this region have reported inconsistent conclusions with regard to historical rainfall trends. For example, Conway (2000) found no trends in long-term annual rainfall in the highlands of north eastern Ethiopia. Seleshi and Zanke (2004) reported no trend in annual and seasonal rainfall totals or number of rainy days over the period of 1965 to 2002 for the central, Northern and north western parts of the

country, but found a decline in rainfall totals in the eastern, south-western and southern parts of the nation. Cheung et al. (2008) detected a substantial decreasing rainfall trend in the central and south-western parts of Ethiopia for the rainy season (June September). However, no significant trend for extreme rainfall events was detected at climate stations located in the north western highlands parts of Ethiopia (Shang et al., 2011). On the other hand, Seleshi and Camberlin (2006) showed decreasing trends in extreme rainfall intensity in the eastern, south-western and southern parts of Ethiopia, while no trends were found in other parts of the country. Over the past decades Deressa et al. (2011) observed a complex rainfall pattern characterized by irregular trends for the past 50 years in Southern Ethiopia. Afewerki (2012) reported decreasing trends in mean annual rainfall at all stations in Northern Ethiopia, except one where an increasing trend was found. Furthermore, Angassa and Oba (2007) revealed decreasing trends in the mean annual rainfall at Borana in the southern Ethiopia. Hadgu et al. (2013) investigated rainfall trends during the period 1980-2009 in Northern Ethiopia and found high spatial variability in annual and seasonal totals but insignificant trend for all stations. The reasons for such contradicting results being reported for the same geographical region may be associated with (i) differences in the historical period analysed, (ii) spatial scale adopted, (iii) quality of data used, (iv) presence or absence of extreme values in the time series, (v) differing definitions of seasons, and (vi) differences in the methods adopted for trend testing. The present study was taken up to analyze trends in annual and seasonal rainfall in the Geba River basin located in Northern Ethiopia during the most recent historical period by implementing standard and well-accepted statistical procedures.

### **2.3 Hydrologic Modelling and Classification**

The fundamental objective of modelling has been defined as a means of gaining an understanding of the hydrological system in order to provide reliable information for managing water resources in a sustained manner to increase human welfare and protect the environment (Schulze, 1998; 2000). Hydrological models are mathematical representations of processes involved in the transformation of climatic inputs such as

precipitation through surface and subsurface transfers of water and energy into hydrological outputs, typically flow in rivers, soil moisture or water level in aquifers (Hughes, 2004). The objective of modelling is also part of the requirements of Integrated Water Resources Management (IWRM), and goes beyond meeting the traditional input requirements for engineers designing water related structures to addressing a range of diverse issues that include human impacts and other hydrological related phenomena which needs integration.

Over the past decades, the application of hydrologic modelling has passionately developed. Hydrologic modelling is linked to spatial processes of the hydrologic cycle and is frequently applied to calculate basin water resources as well as for impact assessment or more precisely water resources management. Several hydrologic models have been developed in the past. Moreover, the models are being advanced and applied to determine the performance of watersheds under predictable land use/land cover changes, climate change, and increased climate variability. This is done in the form of sensitivity analysis where baseline conditions of climate, land use/land cover and streamflow are established, and then used to compare the effect on streamflow due to changes in precipitation, temperature, land use/land cover and other climate variables. These investigations bring about evidence on the magnitude and direction of streamflow changes and understanding into which variables are most important in forecasting these variations. Such information would be very imperative for decision makers to assess management alternatives or the effects of different land use and climate scenarios, as well as to help policies regarding water allocations between various sectors such as agriculture, ecosystems, domestic and industry.

### **2.3.1 Classification of Hydrologic Models**

i. Hydrologic models can be either lumped or spatially distributed. Across the modelling domain, lumped models only simulate a spatially averaged hydrologic system, not considering spatial heterogeneity. Spatially distributed hydrologic models permit for spatially fluctuating climatic variables like precipitation, temperature, and the spatial

incidence of watershed characteristics such as soils, land use/land cover types and slope (Chow et al., 1988). Therefore, across the catchment hydrologic properties and processes are represented in the models. In the hydrologic system there are also semi-distributed models which have both lumped and distributed representation. Usually the semi- and fully-distributed models require large amounts of data, which are not always readily available especially in the developing countries. Among these models SWAT is a semi distributed model (Arnold et al., 1998). Although better representation of the natural hydrologic processes given by these two types of distributed models than the lumped models, data gathering, processing, and preparation of input files require enormous effort and time and are a big challenge to the hydrologist, especially when such data are not readily available. Furthermore, the large number of model parameters that make calibration quite difficult. In such condition, most of the time not likely to find one distinctive parameter set and this leads to the same result (Beven and Freer, 2001). Therefore, the simplicity with which model parameters are identified is reduced; this indicated that associations between model parameters and catchment characteristics are not identified directly.

ii. Hydrologic models can be either single-event (e.g. a rainstorm) or continuous simulation models. To simulate water quantity and quality characteristics in the catchment over a stretched period of time, continuous simulation models are designed and provide output representing longer-term average conditions.

iii. Hydrologic models can also be distinguished on a theoretical basis as being empirical or physically-based. Laterally the range of procedures applied in hydrological modelling categorised at one extreme, the empirical, black-box techniques and at the other extreme, the physically-based techniques. The black box models only match the input and output of the catchment system, not take into account the inner assembly and response of the catchment. Hence, the models do not simulate the hydrologic processes that are involved in the input-output relationship. Based on theoretical concepts and physical laws that govern hydrological processes the physically-based techniques involve complex systems

of equations. The conceptual models remain between the purely empirical and physically based models. These models characterize a reasonable thought of simple conceptual basics that simulate processes happening in the catchment. Within a watershed there are, however, inherent limitations in representing all hydrologic processes, for example, physically-based models may comprise some empirical relationships that need a convinced quantity of appropriate or lumping of features at some scale across the landscape.

iv. Hydrological Modelling occasionally comprises stochastic modelling, where the importance is on mimicking the statistical features of hydro-climatic time-series. No trial at all is made to model input-output relationships (Singh and Woolhiser, 2002). A set of mathematical expressions with parameters assessed in stochastic modelling from the data, designates the procedures in nature as closely to their true characteristics as the data. For planning and management of water resource systems stochastic models are applied to produce synthetic arrangements of hydrologic time series. Stochastic models in hydrology simulate variables such as precipitation time series among others, which can serve as inputs to hydrological models. Typical models that have been used in the past and are still being used are the autoregressive moving average (ARMA) type models, with variations such as autoregressive integrated moving average (ARIMA), to generate synthetic sequences. In hydrological time series of nonlinear climate dynamics, more complex stochastic models are being used to simulate long-term hydrological data such as the hidden state Markov models due to some variability (Sveinsson, et al., 2003; Fortin et al., 2004; Akintug and Rasmussen, 2005).

### **2.3.2 Application of Hydrologic Modelling Integrating with Remote Sensing and GIS**

Advancements in computer technology, remote sensing and geographical information system (GIS) applications have provided a more effective and less costly way to study hydrologic systems. Remote sensing and GIS provide input for hydrological models in various applications (Baumgartner and Apel, 1996). In several hydrological models land

use/land cover is required that is produced by remote sensing. For earth observation, the sensors on board satellites have provided a means to describe past and current land use/land cover characteristics and dynamics. Remote sensing provides rapid and reasonably low-cost evidence about land-cover changes over large areas. To improve the quality of land use/land cover data for use in application, combining ground-based and remote sensing data collection systems is very crucial. In remote sensing variations in time over large areas are measured to provide data input into various hydrological models. The advantage of remote sensing is delivering of long term spatio-temporal data sets over relatively large regions and, therefore, of monitoring the (temporal, spectral and spatial) variations of objects at the earth's surface.

In addition to remote sensing, GIS has contributed considerably to applied hydrology in monitoring and predicting projects. Analysis of spatial information is becoming an emerging approach which is capable of acquiring, managing and analyzing complex problems of river basins. In recent years, GIS has shown to be a good alternative to serve as a better decision support tool in the planning, management and implementation of soil and water resources. GIS technology is a very useful tool and provides for effective and efficient storing, processing, manipulating and visualization of remotely sensed information, and other spatial databases and non-spatial information (Chang, 2008). One of the typical applications of GIS is use of a digital elevation model (DEM) for the extraction of hydrologic catchment properties such as the delineation of the catchment boundary, elevation, slope, flow accumulation and direction. The interaction between GIS and remote sensing has qualified hydrologists to model spatio-temporal variations of hydrological processes efficiently, and especially for the distributed hydrological models.

#### **2.4 Applications of SWAT Model under LU/LC Change Scenario and Assessment of Hydrological Responses**

Recent development of spatially distributed hydrologic models utilizing remote sensing technology and GIS has made it possible to simulate river flows by capturing a vast amount of spatial parameters and variables. Linkage with GIS and distributed

hydrological models have made models such as SWAT (Soil and Water Assessment Tool) more capable for runoff and flood predictions, land use change analysis, soil erosion and sediment transport estimation, and of course a tool for hydrologists and water resources engineers to make decision for planning and management of watershed resources.

Numerous studies have been conducted in the past two decades that point to the application of SWAT model. Examples of studies carried out include those of Fontaine et al. (2001); Van Liew and Garbrecht (2001); Varanou et al. (2002); Jha et al. (2004), Gosain et al. (2006); who studied and predicted the potential impacts of climate change on water resources and yields. To predict various impacts of land management on water quantity (Srinivasan and Arnold, 1994); assess the watershed response impact to land use/cover changes on the annual water balance and temporal runoff dynamics (Fohrer et al., 2001; Pikounis et al., 2003; Kepner et al., 2004; Fohrer et al., 2005), to predict streamflow which were compared favourably with measured data for a variety of watershed scales (Saleh et al., 2000; Santhi et al., 2001; Govender and Everson, 2005; Mao et al., 2009).

Similarly, in Ethiopian watersheds the SWAT model has been successfully applied. For instance the model was used in the Northern Highlands of Ethiopia (Setegn, 2008; Setegn et al., 2009; Abteu et al., 2009; Setegn et al., 2010; Easton et al., 2010; Betrie et al., 2011; Van Griensven et al., 2012) among many others and other part of the country to model the hydrological process, sediment yield and estimate water balance. The overall performance of the model in most cases appears to be reasonable. All these studies have shown varied results due to different regions considered, and also have employed different methodologies to construct land use/land cover change and scenarios on the impacts of the hydrological responses. However, most of these studies concluded that SWAT is suitable for long-term simulations (monthly, seasonal and yearly) have been preferred for use in impact assessment and that daily flows are simulated with lower efficiencies (Shawul et al., 2013; Kiros et al., 2015).

## **2.5 Land Use/Land Cover Changes**

LU/LC can be classified into land use/land cover conversions, and land use/land cover modification. Conversion refers to change from one cover or use type to another, as is the case in agricultural expansion, deforestation, or change in urban extent. Land use/land cover modification, on the other hand, involves the maintenance of broad cover or use type in the face of change in its attributes. Both conversion and modifications of land use/land cover have significant environmental consequences through their impacts on soil and water, biodiversity, and microclimate, hence, contribute to watershed degradation (Lambin et al., 2003; Nyssen et al., 2004; Nyssen et al., 2009; Li et al., 2013b).

LU/LC is always caused by multiple interacting factors originating from different levels of organization of the coupled human environment systems. It is the result of complex interactions between several biophysical and socio-economic conditions which may occur at various temporal and spatial scales. The mix of driving forces of LU/LC varies in time and space, according to specific human-environment conditions (Girmay, 2003; Elfert and Bormann, 2010). Understanding the underlying LU/LC drivers is an important input for planning and decision making. As a result, information on LU/LC has an important role to play at local and regional planning and management of natural resources. Quite often the study of LU/LC is necessitated by the need to know, in quantitative terms, the nature, extent and rate at which these changes advance and the problems or impacts they cause. Furthermore, some studies tried to comprehend the effect of changes in upstream land use/land cover, resulting alterations in the movement of water and its availability at the downstream. Increased consciousness of these impacts enhanced their estimating, forecasting and modelling at the regional scales. However, quantifying impacts of LU/LC and management practices at a watershed scale is still complex because of the inherent variability and complex interactions among different factors (Guo et al., 2008). Thus, in order to provide foundations for effective management of natural resources particularly the land water resources, an understanding



must be built on the variability in time and space of the resources and role of human cultures and institutions in bringing those variations (Agarwal et al., 2002).

The need to provide food, water and shelter to people worldwide has led to changes in land cover such as forests, agricultural lands etc. (Guo et al., 2008). Researchers in the past decades have recognized the need to understand how LU/LC processes link to broader changes in the global environment and how environmental sustainability can be achieved. Enormous efforts have been made to understand the driving forces of land-use change and to develop regionally and globally integrated models of land cover change (Fohrer et al., 2002; Lambin et al., 2003). The great interest in land use and cover results from their direct relationship to many of the earth's fundamental characteristics and processes, such as land productivity, water resources management, diversity of plant and animal species, and the biochemical and hydrological cycles (de Sherbinin, 2002). Land cover is transformed by land use changes, for example, when a forest is converted to agricultural land or pasture. Overgrazing and other agricultural practices lead to land degradation and desertification. Lambin et al. (2003), have recognized that a systematic analysis of local scale land use change studies, conducted over a range of timescales, helps to uncover general principles to provide an explanation and prediction of new land use changes.

Comprehensive knowledge of LU/LC is useful for restructuring past land use/land cover changes and for predicting future changes, and thus may help in elaborating sustainable management practices aimed at preserving essential landscape functions (Li et al., 2009). The primary drivers of LU/LC and their interrelationship with the hydrological regimes has to be identified to develop projections of future land use and management decision outcomes under a range of economic, environmental, and social scenarios. Currently, improved understanding of processes of LU/LC has led to a shift from a view condemning human impact on the environment as leading mostly to a deterioration of earth system processes to emphasis on the potential for effective utilization of resources and ecological restoration through watershed management. This change reflects an

evolution of the research questions, methods, and scientific paradigm (Victor and Ausubel, 2000). As a result, general statements about impacts of LU/LC and land–water interactions need to be continuously questioned to determine whether they represent the best available information and whose interests they support in decision-making processes (FAO, 2002; Bewket and Sterk, 2005; FAO, 2005).

### **2.5.1 Approaches and Methodologies of LU/LC Mapping**

There are a number of methodologies and approaches to LUCC analysis. These include obtaining information from historical records and statistics; use of questionnaires to national governments, other institutions and indigenous communities, normalized difference vegetation index (NDVI), photogrammetry, satellite imagery etc. Patterns of LUCC and land management are determined by the interaction of socio-economic, environmental, political and industrialization factors among others. Therefore, the ability to forecast land use/cover change in order to quantify the effects of change would depend on our understanding of the past, current and future drivers of land use/cover changes.

Satellite information has been acquired since 1972, and used extensively worldwide in the measurement of land cover changes. Many satellite sensors, e.g. Multispectral Scanner (MSS) with a spatial resolution of 79 meters, Thematic Mapper (TM) Scanner having a spatial resolution of 30 meters and seven spectral bands, Enhanced Thematic Mapper Plus (ETM+), SPOT (Systeme Polyvalent pour Observation de la Terre), ASTER where the only high spatial resolution instrument of 15 meters etc., have been used extensively in collecting land cover information and change detection (Chang, 2008). One such satellite whose imagery has been used in this study is Landsat/ASTER, which provides a local to global perspective that helps researchers to understand the landscape's interaction with human activities, and how this interaction leads to changes in land use. Remote sensing, in addition to GIS, have contributed significantly to applied hydrology in mapping, monitoring and forecasting of landscape changes within catchments.

### **2.5.2 Land Use/Land Cover Change Studies in Ethiopia**

Studies carried out at different parts of Ethiopia indicated that agricultural lands have been expanded at the expense of natural vegetation, including forests and shrub lands; for instance Gete and Hurni, 2001 (North-Western Ethiopia); Belay, 2002 (North Ethiopia); Girmay, 2003 (North-Eastern Ethiopia); Gregor et al. 2004 (South Ethiopia); Bewket and Sterk, 2005 (North Ethiopia); and Solomon, 2005 (North Ethiopia). Shibru et al. (2003) reported that the effect of LU/LC in causing major gullies and quantified the rate of expansion and their effects on the people's livelihood in eastern and central highlands of Ethiopia. Hadgu (2008) identified that natural vegetation depletion and agricultural land expansion and intensification over a period of 41 years in Tigray, Northern Ethiopia. He concluded that population pressure was an important driving factors for expansion and intensification of agricultural land in recent periods.

In many parts of highlands of Ethiopia, agriculture has gradually expanded from gently sloping land into the steeper slopes of the neighbouring mountains. According to many literatures, population that has been steadily increased at a growth rate of 2 to 3% per year during the past five decades is the major cause of this expansion. The impact of population growth on the environment and poverty is not simple and one directional. Basically, the complex relationship between human development and the environment is what causes land degradation, in which the use and management of the natural resources is a central issue. Hence, most of the empirical evidences indicated that land use/land cover changes and socioeconomic dynamics have a strong relationship; as population increases the need for cultivated land, grazing land, fuel wood; settlement areas also increase to meet the growing demand for food and energy, and livestock population. Thus, population pressure, lack of awareness and fragile management are considered as the major causes for the deforestation and degradation of natural resources in Ethiopia (Nyssen et al, 2004; 2007).

## 2.6 Overview of Soil Erosion and Sediment Dynamics

Modelling of sediment transport began long before the days of computers. DuBoys is one of the earlier researchers in sediment transport modelling with his theory of tractive force for bed load transport in 1879. The studies by Lacy (1930) laid the foundation of basic fluvial hydraulics. Efforts for mathematically predicting soil erosion started only about seventy years ago. Number of equations available in literature, by considering rainfall energy, soil properties, slope and land cover as variables (Smith and Whitt, 1948; Van Doren and Bartelli, 1956). Information on soil erosion, sediment, nutrient and contaminant export from catchments as well as information on the processes that cause erosion is needed for integrated watershed management. On-site effects of soil erosion in a catchment include soil, nutrient and crop yield loss; off-site effects are muddy floods, reservoir sedimentation and so on. The Universal Soil Loss Equation (USLE) formulated by Wischmeier and Smith (1965) expresses the rate of soil loss per unit area due to sheet and rill erosion. The average annual soil loss,  $A$  ( $\text{tons}\cdot\text{ha}^{-1}\cdot\text{yr}^{-1}$ ) is a function of rainfall erosivity  $R$ , soil erodibility  $K$ , field slope  $S$  and slope length  $L$ , crop management  $C$  and conservation practice  $P$ .

USLE has widely been used for planning purposes and major step towards predicting the impact of land use change on soil loss caused by erosion. Since 1965, there have been studies done to improve USLE to suit additional types of land use, climatic conditions and management practices (Renard et al., 1974; Hadda and Sandhu, 2001; Mikos et al., 2006). From the perspectives of land use and environmental management accurate prediction of soil erosion and sediment yield is important from sub catchments and the whole catchment as well. To aid in this prediction Williams (1975) developed the Modified Universal Soil Loss Equation (MUSLE), by replacing the rainfall energy factor of the USLE (Wischmeier and Smith 1965) with a runoff energy factor. The energy factor in MUSLE is a function of the product of the runoff volume and the peak runoff rate and predicting sediment yield for an individual storm. As noted by Williams (1989), MUSLE has certain advantages over USLE, especially in simulating sediment yield from

a watershed. The advantages include (1) application to individual storms, (2) elimination of the need for sediment delivery ratios because the runoff factor reflects energy used in sediment transport as well as sediment detachment, and (3) greater accuracy because runoff generally accounts for more sediment yield variation than does rainfall.

Recently around the world particularly in the east African regions, hydrological and soil erosion models have been developed in order to estimate, analyze and predict runoff, soil erosion and sediment yield and to relate the spatial variability of land characteristics to runoff generation and erosion processes (e.g., Haregeweyn et al., 2005; Nyssen et al., 2005; Tamene et al., 2006; Setegn et al., 2008; Setegn et al., 2009; Abteu et al., 2009; Setegn et al., 2010). These models are generally meant to describe the physical processes monitoring the transformation of precipitation to runoff and detachment and transport of sediments (Haregeweyn and Yohannes, 2003; Mohamed et al., 2004; Hengsdijk et al., 2005; Steenhuis et al., 2009; Setegn et al., 2010).

In Ethiopia there are almost not any adaptable methodologies for sediment yield and soil erosion prediction assessment. In some cases, the past studies for the estimation of sediment yield and soil erosion have been mainly based on plot level or empirical model such as Universal Soil Loss Equation (Wischmeier and Smith, 1965). Although such studies provided good insight into the relationships between soil loss under different cover, soils and slopes (Tamene and Vlek, 2008; Setegn et al., 2009), however, this model was not designed for soil loss estimation at catchment level (Hudson, 1995). Hence, the results cannot be extrapolated for an entire catchment directly; as such approaches possess many limitations in terms of representation, and reliability of the resulting data (Lal, 2000). In other cases, a range of specific sediment yield (SSY) values between 800 and 1200 t km<sup>-2</sup> year<sup>-1</sup> has been adopted across the region, but no exact source is provided.

Integrated watershed management strategies are critical to efficiently utilize the natural resources base in general and the water resources in particular while maintaining sound environmental quality in any climatic conditions. Approximately 80 % of the Ethiopian

Highlands population depends on subsistence agriculture in which the most critical risk that impedes the agricultural productivity in this area are soil and water out of many other different resources potential. The processes that threaten the water and land resources are land degradation, desertification and soil erosion (Hurni, 1990; Nyssen et al., 2005; Easton et al., 2010). The Ethiopian Highlands provide just about 85 % of flow in the main stem of Nile in Egypt, and support 80 % of the Ethiopian population (Swain, 1997). Thus it is very crucial to understand the processes and sources impacting the potential of water resources in its quantity, quality and most importantly erosive losses and sedimentation mechanisms that threaten both agricultural productivity and considerable infrastructure.

Ethiopia has plentiful water resources potential yet underutilized, and more than 3.7 million hectare of potentially irrigable land can be used to improve agricultural production and productivity (MoWR, 2002; Awulachew et al., 2007). However, agricultural productivity in Ethiopia lags other, similar, regions, which is attributed to unsustainable environmental degradation mainly from erosion and loss of soil fertility (Grunwald and Norton, 2000). Therefore, understanding the hydrological processes of different parts of the basin is very important to water and land resources management. Soil erosion by water represents a major threat to the long-term productivity of agriculture in the Northern Highlands of Ethiopia. In this region the estimated soil erosion rates range from as low as  $16 \text{ t ha}^{-1} \text{ y}^{-1}$  (Gizawchew, 1995) to as much as  $300 \text{ t ha}^{-1} \text{ y}^{-1}$  (Hurni, 1993; Herweg and Stillhardt, 1999). Therefore, as both reliable data and prediction methods are lacking, different designers follow different approaches to take account of loss of storage due to sedimentation. This means that the risk of siltation is usually poorly addressed at the planning stage of the water storage structures. Hence, sediment yield data and appropriate prediction tools are essential requirements for planning and managing water resource development schemes in the country.

## **2.7 Climate Variability, Change and Related Impacts**

Any modification in climate over a period of time, whether due to natural causes or as a result of anthropogenic activities is called climate change (IPCC, 2007). In the recent past the subject of climate change has received attention of researchers in various fields ranging from engineering, physical science, to social science and politics. Most of the warming detected over the last 50 years is attributed evidence to anthropogenic activities (IPCC, 2012). Anthropogenic activities such as the usage of fossil fuels, changes in land use/land cover (e.g. deforestation), agriculture and industrial activities contribute to the releases of greenhouse gasses in so doing increasing the concentration of greenhouse gases in the atmosphere. Increase in surface temperature, sea-level rise, changes in precipitation and snow cover (IPCC, 2007) are the impacts of climate change observed around the world. These impacts could result influence on other concerns such as human health, shortage of water supply, biodiversity, ecosystem and industry. There has been a lot of literature on climate and land cover change impacts on water resources (e.g. Fontaine et al., 2001; Fohrer, et al., 2001; Legesse et al., 2003; Setegn et al., 2011; Taye et al., 2011; Taye and Willems, 2013; Li et al., 2013a). Changes in climate affects all characteristics of the hydrologic cycle namely rainfall, runoff, soil water and evapotranspiration and others. Consequently, availability and variability of water resources potential worldwide also get affected. Hence, a change in climate is likely to distress supplies and demands of water and the ecosystems, migration of population which would pose significant socio-economic and political problems.

The subject of climate change and variability made full of uncertainties concerning the assessment of the forthcoming water resource availability and supply (Taye et al., 2011; Setegn et al., 2011). Hydrologic models are methods usually used to assess the impacts of climate variability on water resources and such models ought to consider for soil moisture. Plant growth and evapotranspiration are also estimated by these models which are responsive to changes in soil moisture and climatic variables (for instance, rainfall

and temperature). Amongst different models the SWAT was the model choice in this study.

Water resource management systems impacts assessment as a result of changes in climate is sophisticated by the coarse spatial resolution of climate change predictions. In the East Africa region, with regard to potential impacts of climate change on water resource management systems, comparatively a few studies have been carried out. In the subsequent half century water resources in Africa is anticipated to be under extreme pressure even in the absence of climate change impacts. Global warming adds further pressure on the variation of water accessibility and adaptability of the water systems. Recently, the challenge for water managers is how water resource management systems will manage with increased variability and demand, and decreased availability over time, comprising the influences of climate change.

Catchment behaviour may be affected by climate change through several ways, such as variations in rainfall totals, intensity, seasonality and locations, effects on temperatures, radiation and evapotranspiration (Roberts, 1998), and effects on drainage density (Moglen et al., 1998). There are signals that the frequency of heavy rainfall events is prospectively to increase (IPCC, 2007), and studies have revealed that inconsistency is anticipated to increase with variations in monthly totals greater than annual variation (Arnell and Reynard, 1996). Nevertheless, overall, it is challenging to enumerate these effects as they happen at higher resolutions in space and time than can be foreseen by different models (Arnell and Reynard, 1996; Sefton and Boorman, 1997). Some of the influences of changes in climate on water resources (IPCC, 2012) comprise;

i) Spatial patterns, seasonality and variability of precipitation and changes in temperature may have the consequence of altering the runoff dynamics, soil moisture, groundwater recharge, peak runoff and catchment hydrology. These subsequently cause changes in predictable yield of agricultural productivity, water quality and quantity, reservoir systems, water supply infrastructure, requirement of storage in water supply systems. (ii) Fluctuations in sea level rise results loss of land due to saline interruption into coastal



aquifers and movement of salt-front estuaries distressing freshwater abstraction points. This indicates decreased water quality and ground water abstractions. (iii) Decreased transpiration due to CO<sub>2</sub> enhancement, increased photosynthesis, resulting to increased water use efficiency. (iv) Factors affecting alteration in water yields and high pressure on water conveyance schemes comprise; increased evaporation from lakes and reservoirs, faster plant growth, decreased runoff groundwater recharge, higher irrigation water demand, bathing and cooling because of increased temperatures. (v) Variations in extreme events such as drought and flood hazards can cause changes in seasonal water renewal, risk in flood plains and alter risks for water resource potentials and reservoir operations.

Global warming resulting in climate changes across various spatial and temporal scales of the Earth varies is a cause for major concern in recent times. Air temperature is rising on the African land mass and the surrounding oceans (Bryan et al., 2013). During the period 1901-2005 the earth's averaged surface temperature has increased by 0.74 °C and among regions the rates of climate change is significantly different as reported by the latest estimates by IPCC (2007). Furthermore, the globally averaged surface temperature show a warming of 0.85 °C, over the period 1880 to 2012, when multiple independently produced datasets exist whereas, the total increase between the average of the 1850–1900 period and the 2003–2012 period is 0.78 °C, based on the single longest dataset available (IPCC, 2013). This is likely to lead to a more dynamic hydrological cycle, with changes in precipitation and evapotranspiration rates that are regionally variable. These changes in turn affect water availability and runoff dynamics and therefore may affect the overall catchment hydrology.

Land use/land cover and climate change affect each other. It is Obvious that climate change influences on the changes in LU/LC and the ecosystem as a whole, similarly it is true that land use/land cover activities contribute to climate change and variability. Changes in LU/LC such as deforestation may perhaps disturb regional climate change, ecosystems and water resources to a comparable or more extent than would global

climate change (Hadgu, 2008). Land use/land cover effects on climate could be as a result of changes in rainfall, temperature, and humidity etc., attributed to changes in vegetation characteristics.

Studies indicated that local climate may change due to variations in flora and leaf area index related with land use/land cover practices e.g. deforestation, agricultural intensification and free grazing (Hadgu, 2008). The effects of changes in LU/LC on climate and how LU/LC patterns can directly influence mass and energy fluxes e.g. when large areas of forest coverage are cleared to intensify agriculture and some other purposes, evapotranspiration is reduced this results in less cloud formation, less rainfall and increased drying (Setegn et al., 2011). On the other hand, LU/LC characteristics impact surface temperature and latent heat flux, and contrasting characteristics of nearby LU/LC types can tempt convection that improves cloud formation and precipitation.

## **2.8 Summary of Literature**

From the review of previous studies on changes in LU/LC and climate variability on hydrological processes and water resources found that river basin studies are most important for sustainable water resources development and management. The water balance method is extensively used to estimate the hydrological components in a river basin. Due to the availability of streamflow data at the gauging station, a model can be calibrated and validated with respect to time and space. There are several studies carried out across the world based on water balance, numerical and spatial models in a river basin.

Although a few studies have carried out on variability and trend analysis of hydro-meteorological observations in a river basin. These studies revealed that the extreme rainfall analysis play a vital role in design, implementation and operation of flood measures. It also focused to assess the changes in rainfall pattern for extreme rainfall intensity and frequency. Hence, these have been applied at coarser spatio-temporal scales. Given the importance of possible climate change imposing constrains on further water

resources development in the river basin, there is a need to carry out extreme trend analysis and variability at finer spatio-temporal scales.

The SWAT model has ascertained to be very popular in simulating the hydrology of catchments over various sizes, possessing a variety of LU/LC types and located in diverse hydro-climatic regions of the world. However, there appears to be further scope for comprehensive performance evaluation of the model in semi-arid watersheds in Northern Ethiopia at different time steps under changed LU/LC and climate scenarios.

Since the Northern highlands of Ethiopia particularly the Geba river basin has been facing deforestation, severe problems of land degradation, soil erosion and water scarcity on account of anthropogenic activities, assessing the hydrological impacts of further changes in LU/LC and climate variability in the basin is very crucial. Moreover, there need to be studies for establishing land use planning and sustainable water resources management linkage in a quantitative manner.

The next chapter explain about the study area, data used and overall methodology of the research work.

## CHAPTER 3

### STUDY AREA AND RESEARCH METHODOLOGY

#### 3.1. Location of the Study Area

The Geba River basin surrounded by the Danakil basin in the east, by the Tekeze River basin in the south and the Werie River basin in the west is located in Northern Ethiopia between 38°38'E and 39°48'E and 13°18'N and 14°15'N. The Geba River is a major tributary of the Tekeze River (called Atbara River in Sudan) which is the uppermost tributary of the Nile River (Figure 3.1). The basin has a total drainage area of 5137 km<sup>2</sup>.

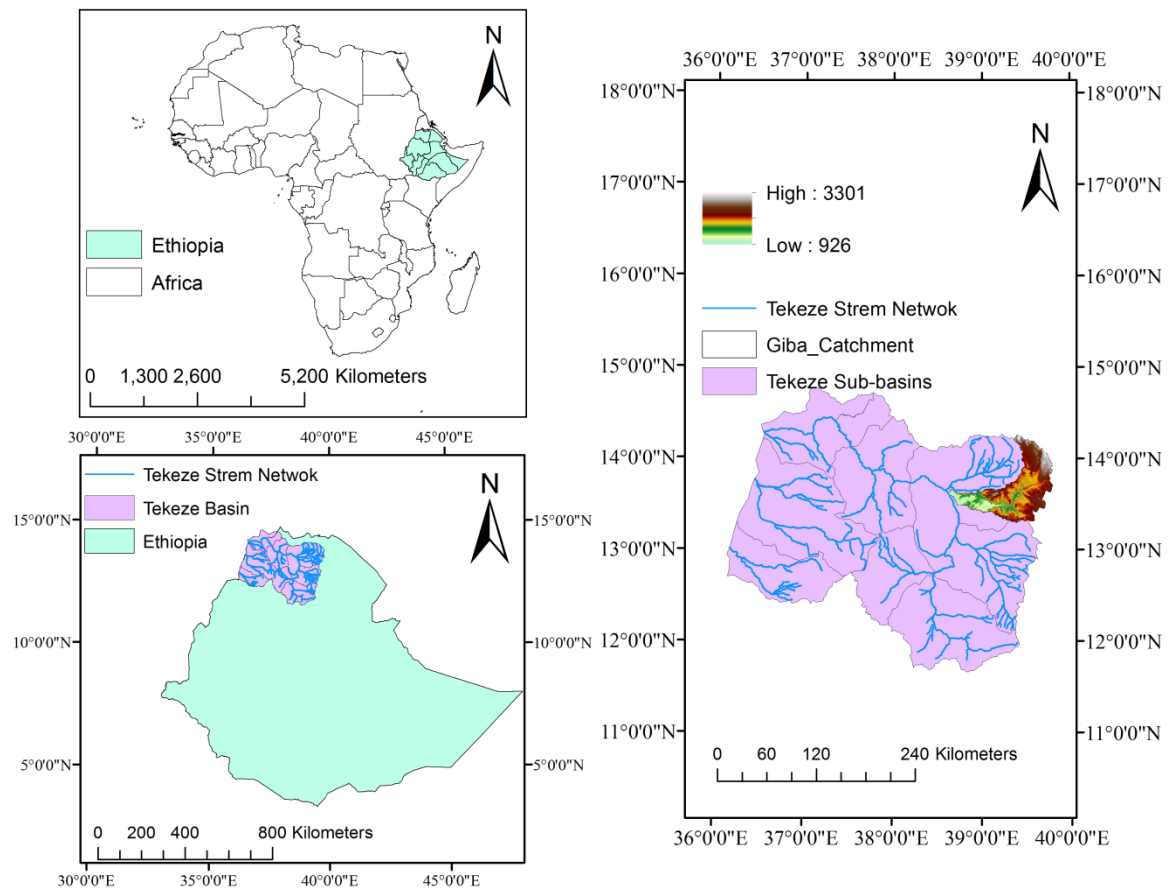
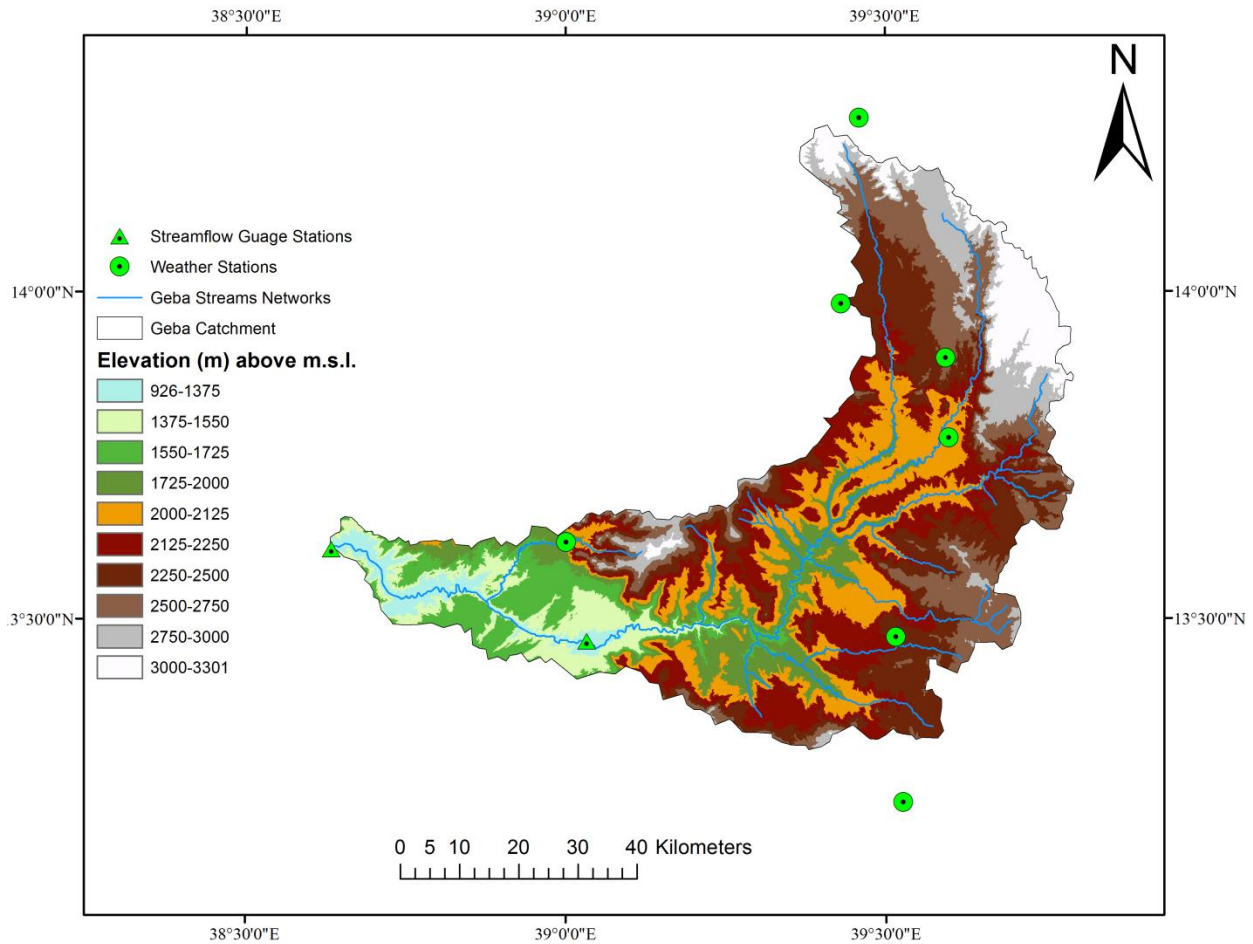


Figure 3.1 location of the Geba Catchment.



**Figure 3.2 DEM of the Geba Catchment.**

### **3.2 Topography**

The Geba basin is mountainous with undulating topography and is characterized by steep volcanic mountains with sharp cliffs and plateaus in the north, deep gorges and cliffs in the centre and ragged terrain in the southwest. The elevation ranges from 926 m above mean seal level at Chemoy valley at the last outlet point where it joins the Tekeze River to 3301 m at the Mugulat Mountains near Adigrat. The mean elevation of the basin is 2146 m, and the mean slope is 14.4%. DEM of the basin in shown in Figure 3.2.

### **3.3 Climate**

Climate conditions in Ethiopia are controlled by both global atmospheric circulations and variability due to local topography. The climate pattern of the country is primarily controlled by the latitudinal migration and interchanges of the Inter-tropical Convergence Zone (ITCZ) across the equator and the influence of the Indian Monsoon throughout the year (Camberlin and Philippon 2002). The ITCZ is a zone of low-pressure near the equator, where two easterly winds originating from the Northern and southern hemispheres converge. Those two major air streams cause dry and rainy seasons: from late June to early September, when the ITCZ is Northernmost, the equator dominant air stream direction is south-east in southern Ethiopia and south-west in central to Northern Ethiopia. These warm and moist winds are the result of high evaporation and water vapour saturation of the air mass both above the Indian Ocean and the Atlantic Ocean and Congo Basin, respectively.

Climatic conditions in the study area are quite diverse due to considerable differences in the altitude and relief. The climate of the region has been classified as Sub Saharan semi-arid. In most parts of the country, annual precipitation follows a bimodal distribution and the annual pattern is commonly distinguished as: main rainy season (*Kiremt*) from June to September where it accounts for 50-80 % of the annual total precipitation of the country (Korecha and Barnston, 2007); dry season from October to February (*Bega*); and small rainy season from March to May (*Belg*) (Legesse et al., 2003).

#### **3.3.1 Rainfall**

Rainfall in the basin occurs in three distinct seasons: Kiremt season is the main rainy season and starts from the first June to mid of September, Bega season are the dry season usually from October to February and *Belg* ('small rains' season, March–May). About 80 % of the annual rainfall in the Geba basin occurs in the Kiremt period from June to September and 63 % of the annual rainfall is the peak which is recorded in the months of July and August (Figure 3.3). The average annual rainfall of the catchment based on 43

years rainfall data recorded at 7 stations within and nearby the basin is about 633 mm. The average annual rainfall varies from about 513 mm around Adigudem to more than 935 mm around Abiadi. The rainfall is highly variable and unpredictable with no correlation to elevation (Nyssen et al., 2005; Zenebe et al., 2013).

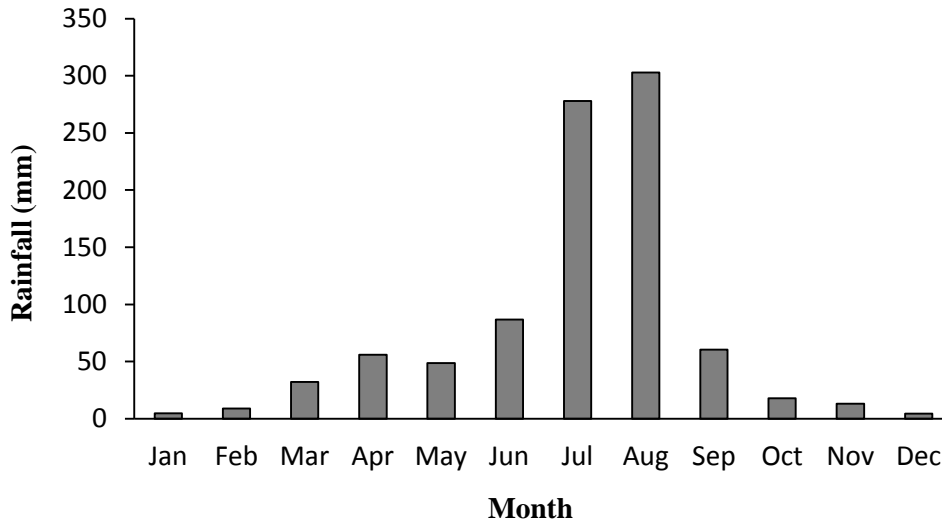


**Figure 3.3 Average monthly rainfall for the Geba basin (Ethiopian Meteorological Agency data, 1971-2013).**

### 3.3.2 Temperature

Depending on topography and geographic location, three climatic zones are recognized in Ethiopia: the cool zone (locally called Dega) 2,400 meters above mean sea level where temperatures range from near freezing to 16°C; the temperate zone (Weyna Dega) at elevations of 1,500 to 2,400 meters above mean sea level with temperature from 16 to 30°C and the hot zone (Kola) below 1,500 meters above mean sea level with both tropical and arid conditions and daytime temperatures ranging from 27 to 50°C (Figure 3.3). Mean annual potential evapotranspiration varies between 1,700 and 2,600 mm in arid and semi-arid areas, and 1,600 to 2,100 mm in dry sub-humid areas (MoWE, 2001). All the climatic zones are found in the study area where hot season mean temperatures range from between 22°C in the high plateaus to about 30°C in the area close to Abiadi on the low land areas. The temperature of the coldest month average about 6°C on the

high plateau and reaches 15°C near the Abiadi area (Figure 3.4). The highest mean monthly temperatures are reached just prior to the onset of the rainy season in April and May.

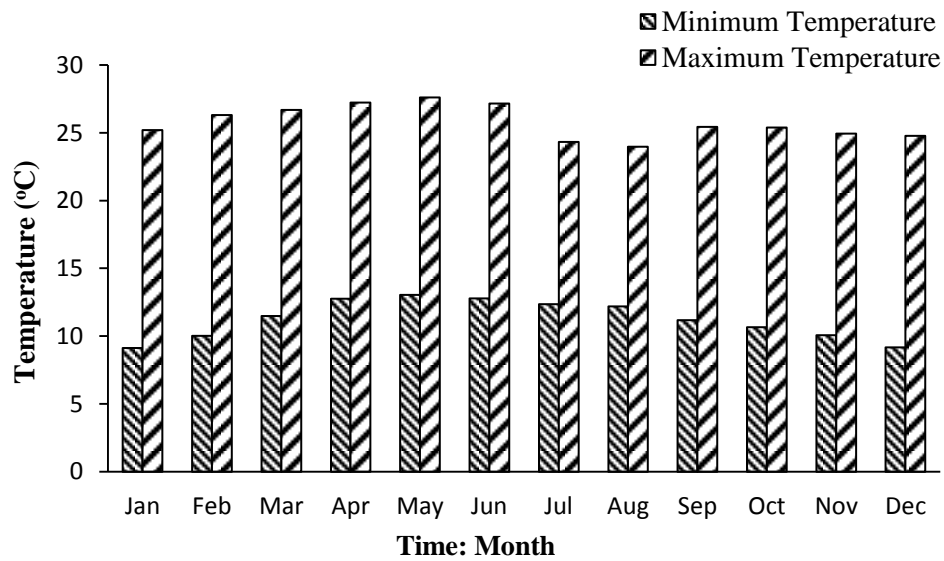


**Figure 3.4 Average monthly minimum and maximum temperature for the Geba basin (Ethiopian meteorological Agency data, 1971-2013).**

### 3.4 Hydrology

Ethiopia is known for its enormous surface water resources potential, hence, known as the water tower of Africa, a major source of the Nile River and for its many trans-boundary rivers. The country's river basins have been divided into 12 major river basins (MoWE, 2010). The basins generally fall into three major drainage systems (Figure 3.5). The first and largest is the western system, which includes the river basins of the Abbay (Blue Nile), Tekeze (Atbara), and Baro-Akobo and Mereb rivers, which are part of Nile River System flowing usually in the western to the White Nile in Sudan eventually terminating in the Mediterranean Sea. The second system is the Rift Valley internal drainage system, composed of the Awash River, the Rift-valley Lakes Region which is a self-contained drainage basin, Omo River (flows south into Lake Rudolf on the border with Kenya), Denakil and Aysha as all of them drain their water in the Great East African



Rift-valley. The Awash flows and dissipates into a series of swamps in the northeast to the Denakil Plain and Lake Abe at the border with Djibouti. The remaining are Wabi Shebelle, Genale-Dawa and Ogaden which are part of the Eastern Highlands and flows southeast direction towards Somali and then to the Indian Ocean. Only the Genale (known as the Jubba in Somalia) makes it to the sea, while the Wabi Shebele disappears just before the coastline.

The total annual surface runoff is estimated to be about  $122 \times 10^9 \text{ m}^3$ ; however only less than 20 % is naturally contained within the country, the remaining drains into neighbouring countries of Eastern Africa as trans-boundary river flow (MoWE, 2010).

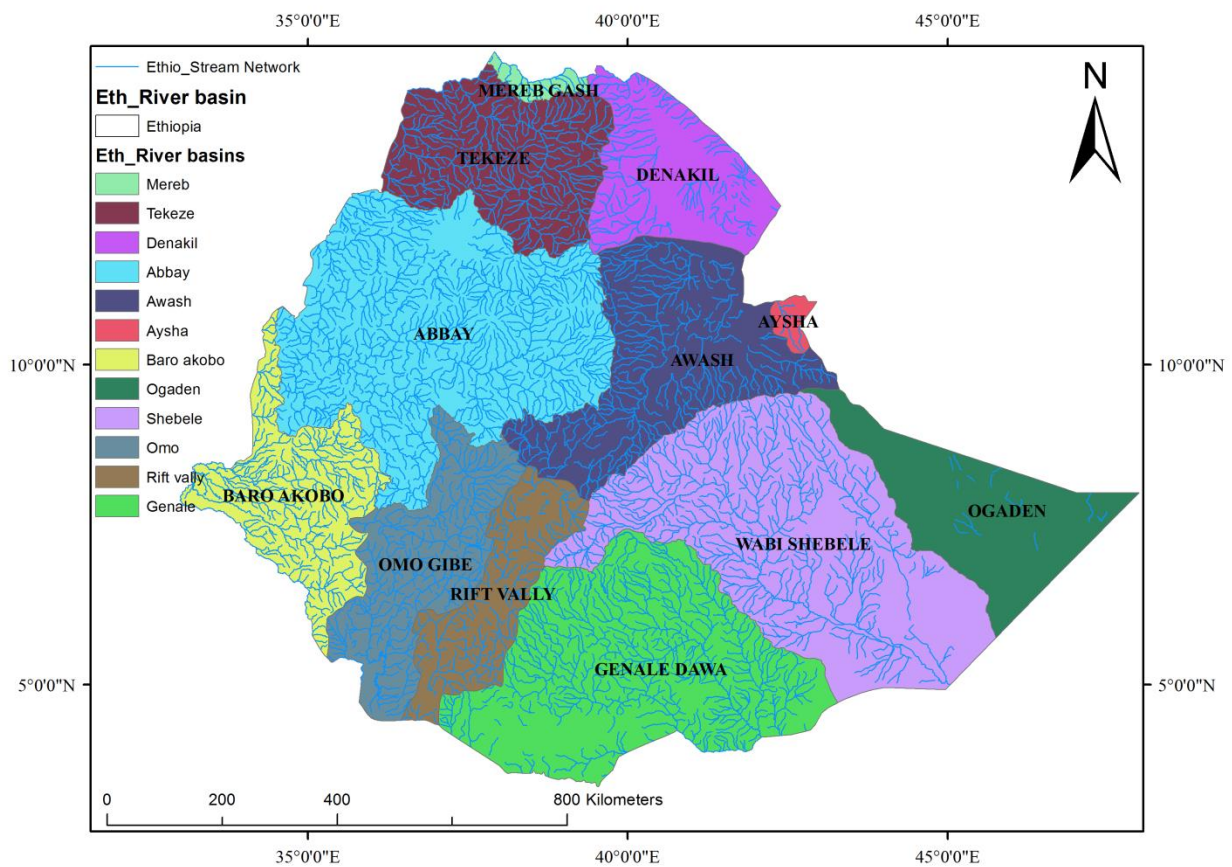


**Figure 3.5 Major river basins in Ethiopia (MoWE).**

### 3.5 Geology, Soils and land use

The Geba basin's geology is characterized by steep volcanic mountains with sharp cliffs and plateaus and consists of sedimentary rock layer such as sandstones in the north, deep gorges and cliffs of limestone in the centre, and subterranean vault complex plateau having ragged metamorphic terrain in the southwest (Zenebe, 2009). The fault-controlled Mek'ele, Wukro and Senkata areas, and the Atsbi horst are the major plains of the Geba basin (Tewolde, 2009). Alluvium occurs along narrow incised River valleys. Based on 1:50,000 maps, seven major soil types were identified in the catchment: Leptosols, Vertisols, Cambisols, Luvisols, Calcisols, Arenosols and Alisols (Figure 3.6). The predominant soil textural classes are: clay loam (40 %), sandy clay loam (31 %), loam (18 %) and clay (11 %). The dominant soil group in Geba catchment is the (lithic) Leptosols. These soils are a widespread soil type and very shallow where the unweathered rock is reached within 10 cm below the surface in the Geba basin (Zenebe, 2009; Tewelde, 2009; Zenebe et al., 2013). They occur on all rock types and, thus, include all textures; they are most common on steep landscapes however, their distribution increases as soil erosion results in the depletion of soil depth. These soils are not suitable for the production of crop; nevertheless farmers use it for cultivation due to shortage of arable land. The land use generally includes seven types these are agricultural, shrub, range, barren, forest, urban areas and water bodies where agricultural land is the dominant one accounting about 40 % of the total area. The dominant cereal crops grown are mainly wheat (*Triticum aestivum*), barley (*Hordeum vulgare*), tef (*Eragrostis tef*), Sorghum (*Sorghum bicolor*) and pea (*Pisum sativum*).

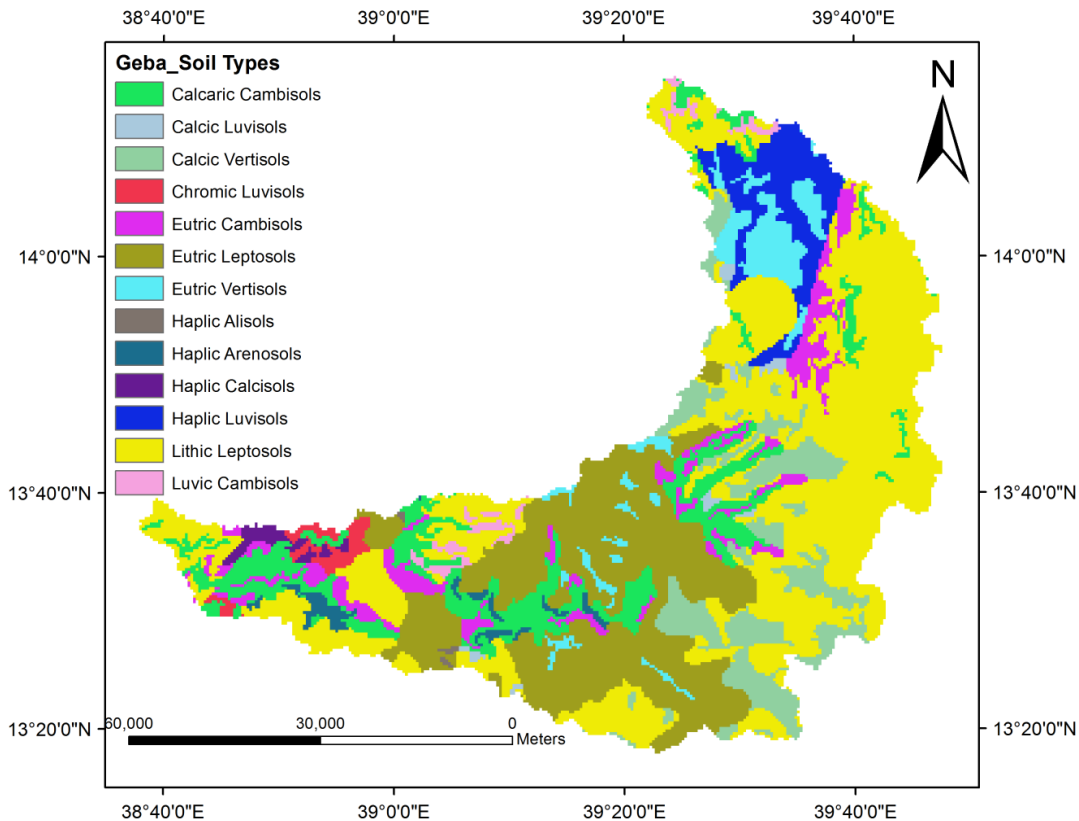


**Figure 3.6 Major Soil types of the Geba basin (FAO, 1998).**

### 3.6 Data Used

Digital Elevation Model (DEM) defines the topography which illustrates the altitude of any position in a given area at a particular spatial resolution. A 90 m by 90 m resolution DEM were obtained from USGS website. The DEM was used to demarcate the catchment and investigate the stream network pattern of the landscape. Parameters of sub-basins such as slope length of the terrain, slope gradient, and the stream network features such as channel length, width and slope were extracted from DEM. SWAT model needs various soil textural and physicochemical properties such as soil texture, hydraulic conductivity, available water content, organic carbon content and bulk density for various layers of individual soil type. These data were acquired from the Soil and Terrain Database for North-Eastern Africa Food and Agriculture Organization of the United Nations, FAO (1998). Based on the geomorphology of Ethiopia at the scale of

1:50,000 topographic maps, major seven soil types were identified in the catchment: Leptosols, Vertisols, Cambisols, Luvisols, Calcisols, Arenosols and Alisols. Satellite imagery, LANDSAT imagery (Landsat MSS, TM and ETM+) was obtained from US Geological Survey. The MSS, TM and ETM+ images for 1973, 1987, 2000 and 2013, respectively were pre-processed, band composite, image classification and LU/LC maps were produced using most commonly supervised Maximum Likelihood classifier. The discharge data of the Geba River was acquired from the Ministry of Water Resources and Energy (MoWE) department of hydrology, Ethiopia which included daily and monthly data for the 1973-2013 time periods. During this time the weather information was also obtained from the Ethiopian National Meteorological Agency (ENMA), which comprised daily data for rainfall, temperature (minimum and maximum), solar radiation, wind speed and direction and relative humidity for the meteorological stations in and in close proximity to the Geba catchment. Hydro-meteorological measurement of data was initiated in the late 1960s; however, all stations share 40 years records in common from 1973 to 2013. Therefore, considering the common availability of all data were taken the study period.

Complete details of the various data used in the present study are provided in relevant chapters of this thesis.

### **3.7 Research Methodology Adopted**

To achieve the objectives of this study, a broad research methodology was formulated. This involved trend analysis of hydro-climatic variables, analysis of LU/LC changes in the Geba basin, application of the SWAT hydrological model through integration of various input data within a GIS framework and finally simulating the hydrologic impacts of likely changes in LU/LC and climate in the basin. Figure 3.7 depicts the flow of tasks performed in the study.

Subsequent chapters of this thesis provide a detailed description of each of these tasks and discussion of results obtained thereof. Using multiple LU/LC images in a dynamic

environment the model has calibrated and validated specifically using streamflow and sediment for all the respective LU/LC images unlike other studies.

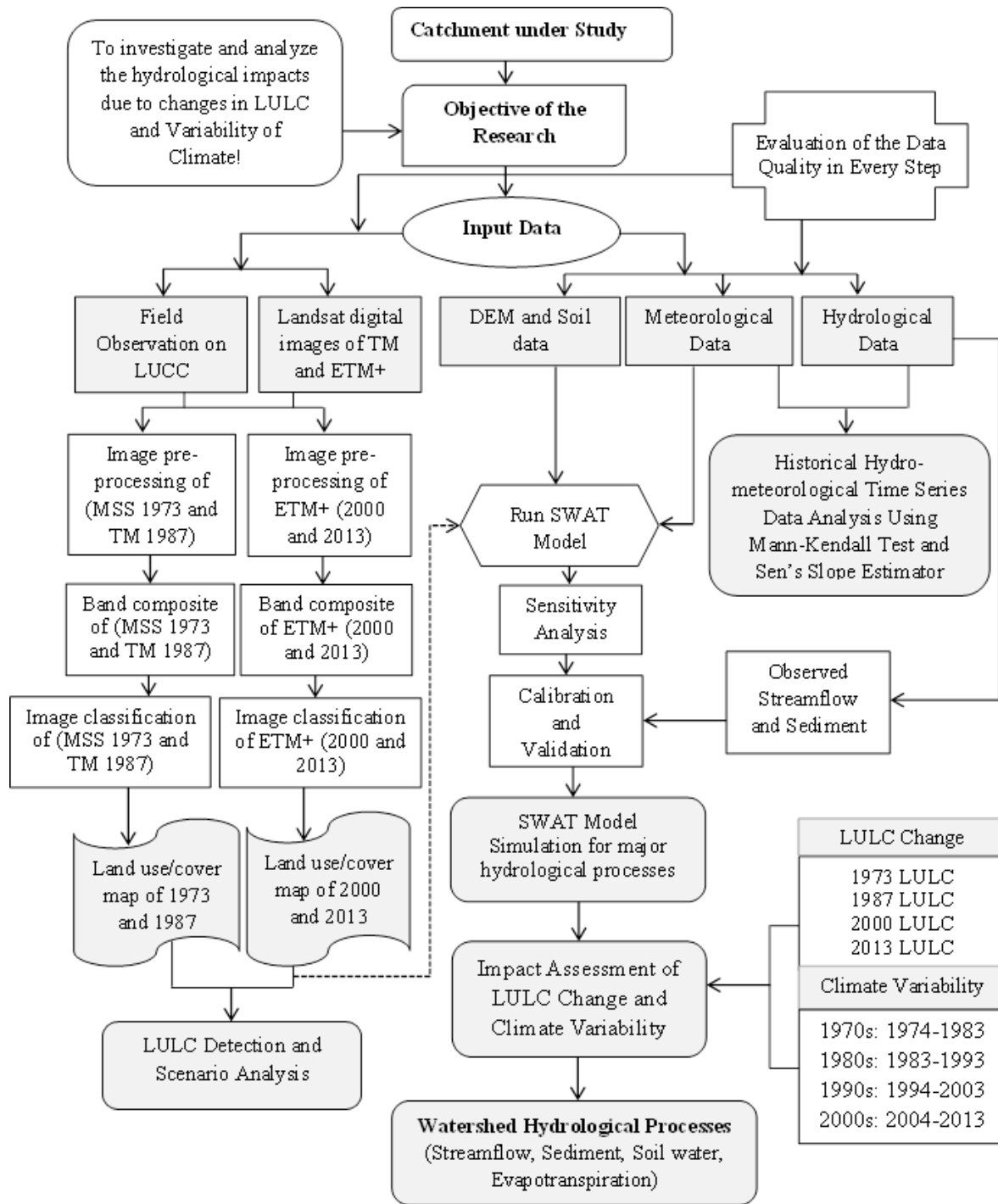


**Figure 3.7 Research Methodological Framework of the Study.**

## CHAPTER 4

# STATISTICAL AND TREND ANALYSIS OF HYDRO-METEOROLOGICAL DATA

### 4.1 Introduction

Hydro-meteorological time series almost always exhibit seasonality due to the periodicity of the weather. In the study region, this arises greatly from seasonal variations in precipitation volume, temperature as well as the rate of evapotranspiration. For observed data that exhibit high seasonality, methods to analyze trends should be those that incorporate the seasonal component. River discharge is known to reflect an integrated response of the river basin while rainfall serves as one of the major input into the runoff processes. This chapter examines the hydro-meteorological trend changes in space and time that have taken place and whether or not they are significant.

Rainfall events in the arid and semi-arid tropics exhibit spatial and temporal variability depending on the movement, intensity and size of storm and this gives rise to large variations at local scales. Convective rainfall is an important element of the tropical and sub-tropical weather system and it contributes to spatial and seasonal variability of rainfall (Conway 2000; Tabari et al., 2015). The dynamic behaviour of convective rainfall affects streamflow response, in terms of volume, intensity and time to peak (Tesemma ZK et al., 2010). Presently, an effort to forecast the spatial and temporal variability of rainfall is gaining significance due to global changes in climate (Tabari et al., 2011). Studies on climate change-induced rainfall variability at various spatial and temporal scales have attracted attention from the research community (Babar and Ramesh 2013; Wagesho et al., 2013; Opiyo et al., 2014). Global warming resulting in climate change across various spatial and temporal scales of the Earth varies is a cause for major concern in recent times. Air temperature is rising on the African land mass and the surrounding oceans (Bryan et al., 2013). During the period 1901-2005 the earth's

averaged surface temperature has increased by 0.74 °C and among regions the rates of climate change is significantly different as reported by the latest estimates by IPCC (2007). Furthermore, the globally averaged surface temperature show a warming of 0.85 °C, over the period 1880 to 2012, when multiple independently produced datasets exist. Whereas, the total increase between the average of 1850–1900 period and the 2003–2012 period is 0.78 °C, based on the single longest dataset available (IPCC, 2013). Collier et al. (2008) investigated that many semi-arid parts of the developing world that are likely to become hotter and dryer with time as changes in temperature patterns are widely experienced. Compared to the global average, the average temperature rise in Africa is faster and is likely to continue (Hulme, 2001). Collier et al. (2008) suggested that this warming occurred at the rate of about 0.5 °C per decade with a slightly larger warming where crops are grown close to the thermal acceptance limits.

Ethiopia is likely to be highly susceptible to future climate change like other African countries (Conway and Schipper, 2011). Some studies have indicated that warming has occurred across much of Ethiopia, particularly since the 1970s, at a variable rate (Conway, 2000; Conway et al., 2004; IPCC, 2007; Gebrehiwot and van der Veen, 2013). A study made by Ethiopian National Meteorological Services Agency (ENMA) also reveals that there has been a warming trend in temperature over the past 50 years in the country. The average annual minimum temperature over the country has been increasing by about 0.25 °C every ten years while average annual maximum temperature has been increasing by about 0.10°C every decade (ENMA, 2007).

A number of techniques have been developed for the analysis of the hydro-climatic data. Trend detection and analysis is performed through parametric and non-parametric tests only for consistent data. The parametric test assesses whether the slope coefficient of the fitted linear regression is significantly different from zero, indicating the presence of a linear trend. The slope coefficient sign would then indicate whether there is a positive or a negative trend. The non-parametric Mann–Kendall test, which is used in this study, establishes the presence of a positive or negative trend for a given confidence level.

Trends may be analysed at a variety of time steps such as daily, weekly, seasonal or annual and spatial scales ranging from a single station to a River basin. The past studies on extreme rainfall analysis revealed that the extreme rainfall analysis plays a major role in design, implementation and operation of flood measures. It also focused to assess the changes in rainfall patterns for extreme rainfall intensity and frequency. These have been applied at coarser spatio-temporal scales. Hence, there is a need to carry out extreme trend analysis and variability at finer spatio-temporal scales.

## **4.2 Methodology**

Daily meteorological data series for 18 stations located within and close to the Geba River basin were obtained from the Ethiopia National Meteorological Agency (NMA). Only seven stations were taken for analysis after quality control these are Abiadi, Adigudem, Adigrat, Hawzien, Mek'ele, Senkata and Wukro. All the seven stations share 43 years records in common from 1971 to 2013. In this study rainfall, temperature for selected stations, discharge for the gauge station were collected, ET is estimated and were analyzed for the trend. Table 4.1 summarizes the climate stations used in this study with their coordinates, elevations, and the observed mean rainfall values for the period 1971-2013 for the stations in the basin.



**Table 4.1: Meteorological stations selected for analysis with details of coordinates, elevation, observation period and observed mean annual rainfall values.**

Station ID	Station name	Longitude	latitude	Elevation (m)	Mean rainfall (mm/y)
Abd1361	Abiadi	39 <sup>0</sup> .00'E	13 <sup>0</sup> .61'N	1337	879.86
Adm1325	Adigudem	39 <sup>0</sup> .51'E	13 <sup>0</sup> .25'N	2107	508.62
Adt1428	Adigrat	39 <sup>0</sup> .45'E	14 <sup>0</sup> .28'N	2509	573.26
Hwn1397	Hawzien	39 <sup>0</sup> .43'E	13 <sup>0</sup> .97'N	2243	555.46
Mkl1347	Mek'ele	39 <sup>0</sup> .53'E	13 <sup>0</sup> .47'N	2256	630.92
Snt1407	Senkata	39 <sup>0</sup> .57'E	14 <sup>0</sup> .07'N	2269	671.05
Wkr1379	Wukro	39 <sup>0</sup> .6'E	13 <sup>0</sup> .79'N	1783	610.78

#### 4.2.1 Rainfall Extreme Indices

For investigating changes in the frequency, intensity and proportion of extremes in total rainfall 12 extreme rainfall indices were selected in this study. These indices were proposed by the joint the Expert Team Climate Change Detection and Monitoring Indices (ETCCDMI) (Peterson et al., 2001; Alexander et al., 2006) and are reviewed by Zhan et al. (2011).

Definitions and description of the indices selected for the present study are summarized in Table 4.2. The extreme indices were calculated at the monthly and annual time steps for each individual station in the Geba catchment.

**Table 4.2: Definition of the rainfall indices used in this study.**

<b>S.N</b>	<b>Rainfall indices</b>	<b>Description</b>	<b>Definition</b>	<b>Units</b>
1	PRCPTOT	Annual total wet-day rainfall	Annual total rainfall in wet days ( $\geq 1.0\text{mm}$ )	Mm
2	Rx1day	Highest rainfall amount in one-day period	Monthly maximum 1-day rainfall	Mm
3	Rx5day	Highest rainfall amount in 5 consecutive days	Monthly maximum consecutive 5-day rainfall	Mm
4	R90p	Rainfall on wet days	Annual total rainfall when daily rainfall $>90\text{p}$	Mm
5	R95p	Rainfall on very wet days	Annual total rainfall when daily rainfall $>95\text{p}$	Mm
6	R99p	Rainfall on extremely wet days	Annual total rainfall when daily rainfall $>99\text{p}$	Mm
7	SDII	Simple daily intensity index	Simple rainfall intensity index  (Annual total rainfall/number of wet days)	Mm/day
8	R10mm	Heavy rainfall days	Annual count of days when daily rainfall $\geq 10\text{mm}$	days
9	R20mm	Very heavy rainfall days	Annual count of days when daily rainfall $\geq 20\text{mm}$	days
10	R25mm	Extremely heavy rainfall days	Annual count of days when daily rainfall $\geq 25\text{mm}$	days
11	CDD	Consecutive dry days	Max. number of consecutive day days with $P < 1.0\text{mm}$	days
12	CWD	Consecutive wet days	Max. number of consecutive day days with $P \geq 1.0\text{mm}$	days

#### 4.2.2 Data Quality and Homogeneity Testing

The essential preliminary step in trend detection analysis is data quality assessment. In this study special emphasis was given to quality control and data set selection. Given that robust trend analysis needs comparatively long records (Kundzewicz and Robson, 2004); a first selection was made among all available stations prior to further control of data quality and homogeneity for the sake of consistency across the station networks. The daily climatic data collected from the Ethiopian Meteorological Agency from seven meteorological stations for the period of 1971 to 2013 were subject to homogeneity test. The list of the stations name and their missing data (%) is given in Table 4.3.

**Table 4.3: Showing the stations with their ID and Missing data (%).**

Station name	Missing data (%)
Abiadi	0.06
Adigudem	0.01
Adigrat	0.01
Hawzien	0.03
Mek'ele	0.01
Senkata	2.13
Wukro	0.05

The data were selected from seven weather stations, the selection was based on important combination of criteria related to the spatial distribution of the series over Geba River basin and data length, completeness, quality and homogeneity: Only stations with less than 3 % of missing values were used; any given month was considered complete if no more than 3 days were missing from the records; a year was considered complete if no more than 15 days were missing. Basic quality controls have been applied to all the series with the purpose to identify errors in the data; the daily data were searched for anomalous values (“outliers”). The missing data (%) ranges from 0.01 to 2.13 for the selected stations.

The daily climatic data was arranged and sorted in Excel sheet and checked the homogeneity using standard normal homogeneity test the RAINBOW a software package for hydro-meteorological frequency analysis and testing the homogeneity of the historical data series (Raes et al., 2006). It is required that the frequency analysis of data to be homogeneous and independent. The restriction of homogeneity assures that the observations are from the same population. The RAINBOW offers a test of homogeneity which is based on the cumulative deviations from the mean and deals also statistical tests for investigating whether data follow a certain distribution. The homogeneity of the data of a time series is tested, by evaluating maximum and the range of the cumulative deviations from the mean (Raes et al., 2006). RAINBOW allows also to analyse time-series with zero or near zero events (the so called nil values) by separating temporarily the nil values from the non-nil values. The data series from these seven stations in the Geba basin are used in this study were found to be homogeneous. A thorough checking of the data revealed that average missing data of all the stations is about 0.33% for the period of 1971 to 2013. Weighing method was adopted such as correlation and inverse distance was used to estimate the missing data during this analysis. To analyze the trends in precipitation and temperature for all the seven stations using the monthly and annual data for the period 1971 to 2013, the Mann-Kendall test using XLSTAT was employed. The test is to identify whether or not a statistically significant decreasing or increasing trends or none could be found in a data set. Mann-Kendall test is a nonparametric test for identifying trends in a series of data. To classify the significance of the trends confidence level of 95% were taken as thresholds, before the trend test was concluded to be significant p-values smaller than 0.05 must to be fulfilled.

In and around a particular rain gauge station sometimes a significant change may occur. Being reported from that particular station such a change occurring in a particular year will start affecting rain gauge data. After a number of years, it may be felt that the data of that station is not giving consistent rainfall values. In order to detect any such inconsistency, a technique, called double mass curve method is generally adopted to correct and adjust the reported rainfall values (Garg, 2005; Wang, 2013). In the

surrounding area of the doubtful station a group of 5 to 10 neighboring stations are chosen in this method. The mean yearly values are worked out for each consecutive year of available record of the yearly rainfall values reported from the serial of this group of stations. These mean yearly rainfall values (of the chosen group of stations) are serially arranged in a reverse chronological order (i.e. the latest year getting the first entry). The recorded yearly rainfall values of the doubtful station are also serial for each year against these values. The cumulative values are then worked out for both the columns.

#### **4.2.3 The Mann-Kendall Trend Analysis**

Non-parametric Mann-Kendall test a statistical procedure that is used for analyzing trends in data over time. Assumptions like statistical normally distribution of the data is not required for the Mann-Kendall test (e.g., normal, lognormal, etc.,) and can be used with data sets which include missing data and irregular sampling intervals (Mann, 1945; Gilbert, 1987, Kendall, 1975). This method was applied for the temporally distributed hydro-meteorological data trends at 95 % level of significance. Though the performance of the test can be adversely affected, the Mann-Kendall test can be computed if there are missing values and values below the one or more limits of detection. The assumption of independence requires that the time between samples be sufficiently large so that there is no correlation between measurements collected at different times (Hirsch et al., 1982).

The procedure to compute for the Mann Kendall test considers the time series of  $n$  data points and  $X_k$  and  $X_j$  as two subsets of data where  $k = 1, 2, 3, \dots, n-1$  and  $j = k+1, k+2, k+3, \dots, n$ . The data values as an ordered time series are evaluated. Each data value is compared with all subsequent data values. The statistic  $S$  is incremented by one, if a data value from a later time period is higher than a data value from an earlier time period. On the other hand,  $S$  is decremented by 1, if the data value from a later time period is lower than a data value sampled earlier. The net result of all such increase and decrease yields the final value of  $S$  (Drapela and Drapelova, 2011).

Therefore, the Mann–Kendall S Statistic trend test for a time series is computed as follows:

$$S = \sum_{k=1}^{n-1} \sum_{j=k+1}^n \text{sign}(X_j - X_k) \quad (4.1)$$

$$\text{Sign}(X_j - X_k) = \begin{cases} +1 & \text{if } (X_j - X_k) > 0 \\ 0 & \text{if } (X_j - X_k) = 0 \\ -1 & \text{if } (X_j - X_k) < 0 \end{cases} \quad (4.2)$$

Where  $X_j$  and  $X_k$  are the annual values in years  $j$  and  $k$ ,  $j > k$ , respectively (Motiee and McBean, 2009) as can be seen from the equation (4.2). The test statistic depends not on their actual values resulting in a distribution free test statistic rather on the ranks of the observations, because for any distribution, the ranks remain the same.

If  $n < 10$ , the value of  $|S|$  is compared directly to the theoretical distribution of  $S$  which is derived by the Mann and Kendall. The two tailed test is used. At certain probability level  $H_0$  is rejected in favour of  $H_1$  if the absolute value of  $S$  equals or exceeds a specified value  $S_{\alpha/2}$ , where  $S_{\alpha/2}$  is the smallest  $S$  which has the probability less than  $\alpha/2$  to appear in case of no trend. A positive (negative) value of  $S$  indicates an upward (downward) trend. (Drapela and Drapelova, 2011)

For  $n \geq 10$ , the statistic  $S$  is approximately normally distributed with the mean and variance as follows (Kendall 1975):

$$E(S) = 0 \quad (4.3)$$

$$\text{Var}(S) = \frac{n(n-1)(2n+5)}{18} \quad (4.4)$$

Where  $n$  is the number of observations. The existence of tied ranks (equal observations) in the data results in a reduction of the variance  $\text{Var}(S)$  for the  $S$ -statistic is defined by:

$$Var(S) = \frac{n(n-1) - 2n \sum_{p=1}^q t_p(t_p-1)}{18} \quad (4.5)$$

Where  $t_p$  is the number of ties for the  $p^{\text{th}}$  value and  $q$  is the number of tied values this means the summation term in the numerator is used only if the data series contains tied values. The standardized test statistic  $Z_s$  is calculated as follows (Gilbert, 1987).

$$Z = \begin{cases} \frac{S-1}{\sqrt{\text{var}(S)}} & \text{if } S > 0 \\ 0 & \text{if } S = 0 \\ \frac{S+1}{\sqrt{\text{var}(S)}} & \text{if } S < 0 \end{cases} \quad (4.6)$$

The test statistic  $Z_s$  is used a measure of significance of trend. In fact, this test statistic is used to test the null hypothesis,  $H_0$ . If  $|Z_s|$  is greater than  $Z_{\alpha/2}$ , where  $\alpha$  represents the chosen significance level (e.g. 5 % with  $Z_{0.025} = 1.96$ ) then the null hypothesis is invalid implying that the trend is significant (Motiee and McBean, 2009).

The linear slopes where the magnitudes of trends are calculated using the Thiel–Sen approach (TSA) (Sen, 1968; Thiel, 1950). The TSA slope  $\beta$  is given by:

$$\beta = \text{median} \left[ \frac{X_j - X_k}{j - k} \right] \text{ for all } k < j \quad (4.7)$$

Where  $X_k$  and  $X_j$  are data at time points  $k$  and  $j$ , respectively. If the total number of data points in the series is  $n$ , then there will be  $\frac{n(n-1)}{2}$  slope estimates and the test statistic  $\beta$  Sen is the median of all slope estimates. Positive and negative sign of test statistics indicate increasing and decreasing trends respectively. For performing the statistical

Mann-Kendall test software Addinsoft's XLSTAT 2015 is applied. For rainfall, streamflow and temperature data for the seven stations in the Geba River basin, the null hypothesis is tested at 95 % confidence level. Besides, to compare the results obtained from the Mann-Kendall test, linear trend lines are plotted for each station using Microsoft Excel<sup>®</sup>.

## **4.3 Results and Discussion**

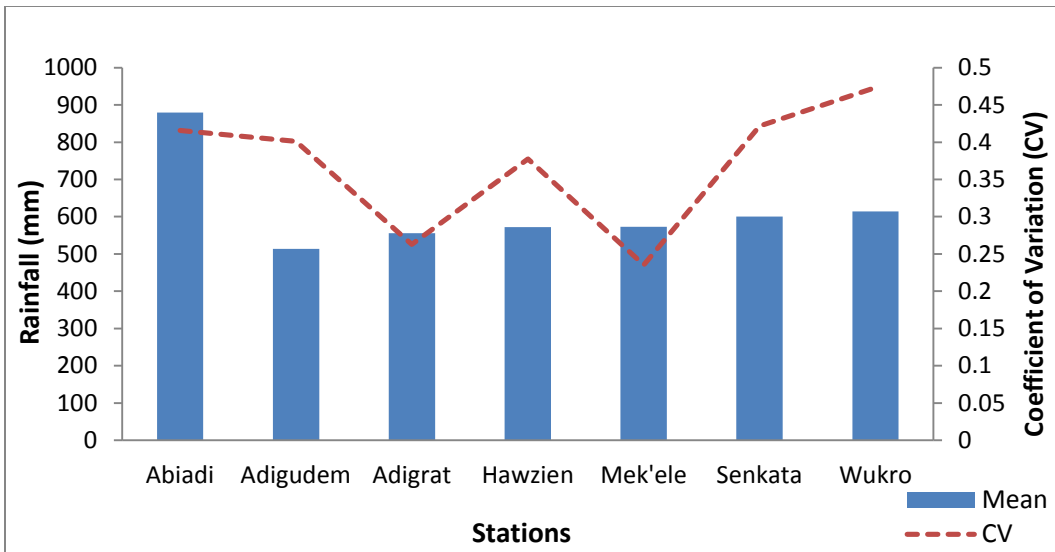
### **4.3.1 Spatial and Temporal Analysis of Meteorological Data**

To study the temporal variation of hydro-meteorological variables, analysis has been carried out at decadal intervals for monthly average values. The spatio-temporal variability analyses of hydro-meteorological factors are important for further understanding of hydrological process and hydro-meteorological modelling. Traditionally temporal variability was quantitatively described using coefficient of variation based on statistics. The spatio-temporal variability of rainfall and evapotranspiration of the Geba River basin is relatively higher and the spatio-temporal variability of temperature is relatively small.

#### **4.3.1.1 Patterns and Variability of Rainfall**

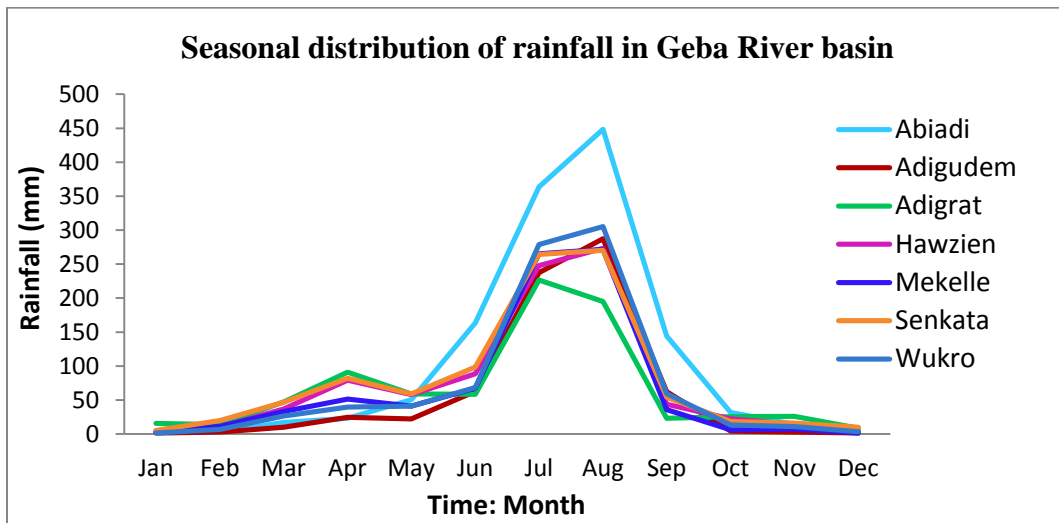
The Geba River basin is one of the tributaries of the Tekeze basins exhibiting high spatial and temporal rainfall variability (annual and seasonal). Spatially, annual rainfall varies from as low as 300 mm towards the eastern end of the basin to greater than 900 mm in the downstream part around Abiadi. Mean annual rainfall distribution around Abiadi is about 880 mm. Generally, the coefficient of variation (CV) of rainfall is high in Geba River basin with annual CV ranges from 0.23 to about 0.5. The CV is highly correlated with elevation profile of the basin. It is very high for lower elevation stations and relatively lower for highland stations located in upper part of the basin. Figure 4.1 presents the annual variation of rainfall over the basin using climate stations distributed over the basin.





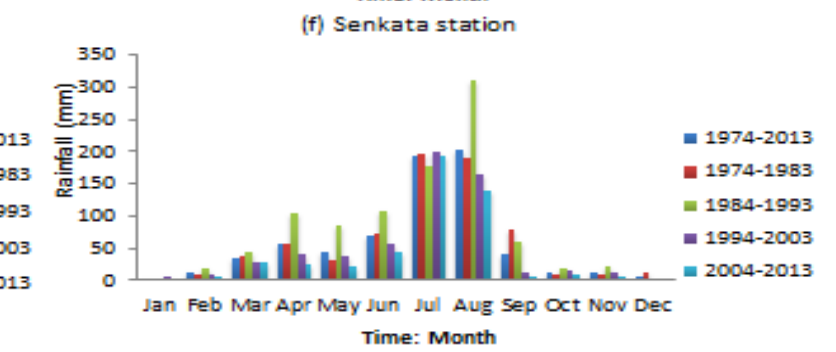
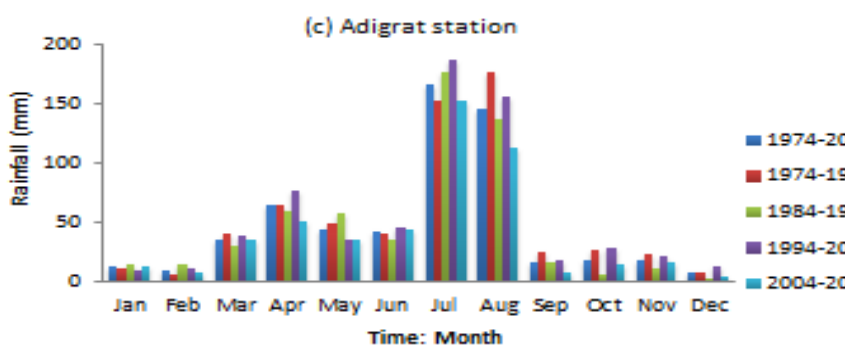
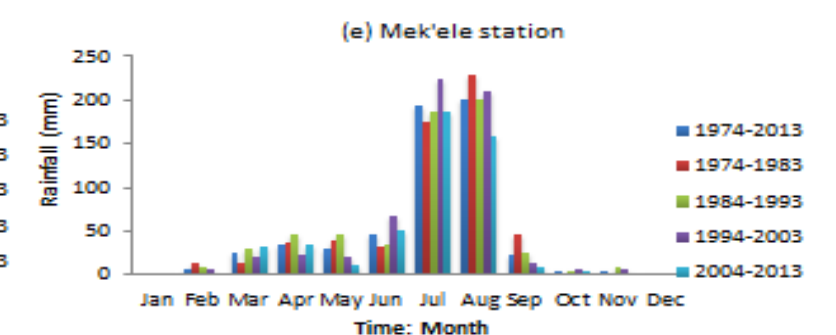
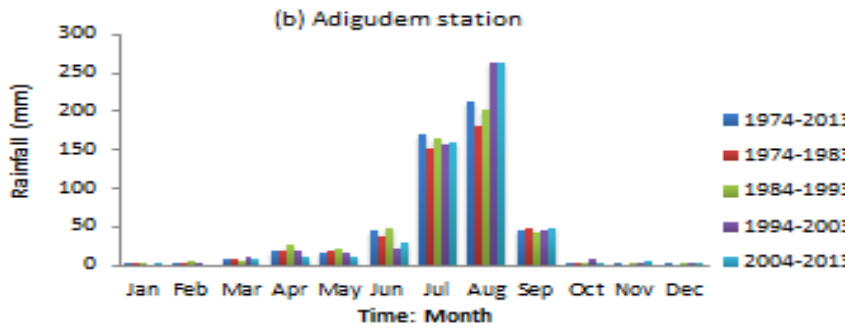
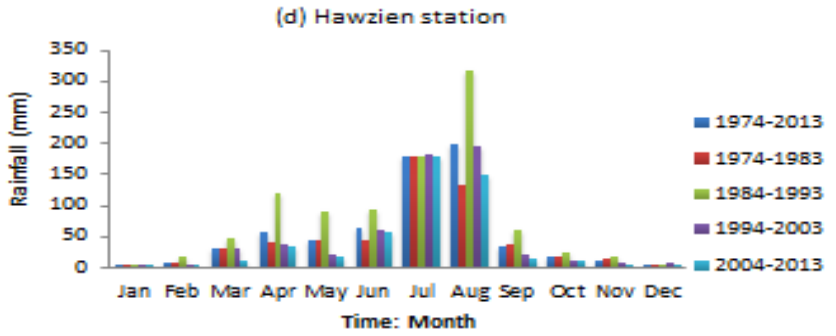
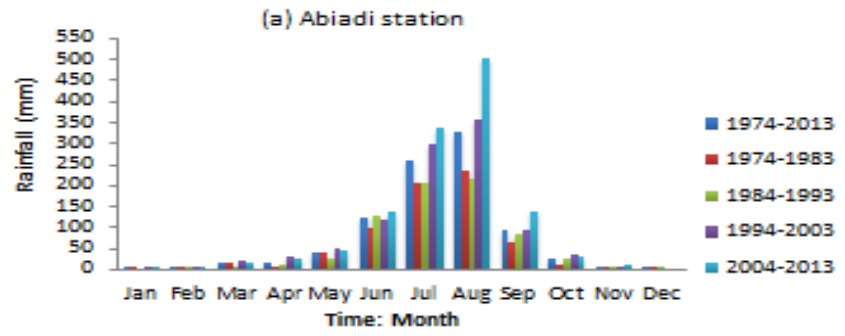
**Figure 4.1 Mean Annual rainfall of rainfall stations in Geba River Basin.**

The Geba River basin is usually divided into altitude ranges as upper, middle and lower. This subdivision, however, doesn't necessarily reflect the hydrological regimes of the basin. The basin has mono-modal rainfall characteristics with the peak rainfall occurring in July-August although there are small rains in the Belg season (March-May-April) where the high variability of rainfall in this season highly affects the agricultural production of the area (Figure 4.2).



**Figure 4.2: Geba River basin seasonal rainfall distribution.**

Upon analysis of the overall rainfall regime dynamics, the decadal time step results revealed a general decrease in rainfall amounts, especially after the second decade, all the weather stations except at stations Abiadi and Wukro showing slightly increasing change as shown in the bar charts of rainfall for the seven climate stations (Figure 4.3 a to g). Thus, especially during the periods of rainy season (June-September) of the first and second decade a general increase has been noticed, and decrease in the third and fourth decade which caused, for this climatic parameter as well, an acceleration of climatic stress on natural components.



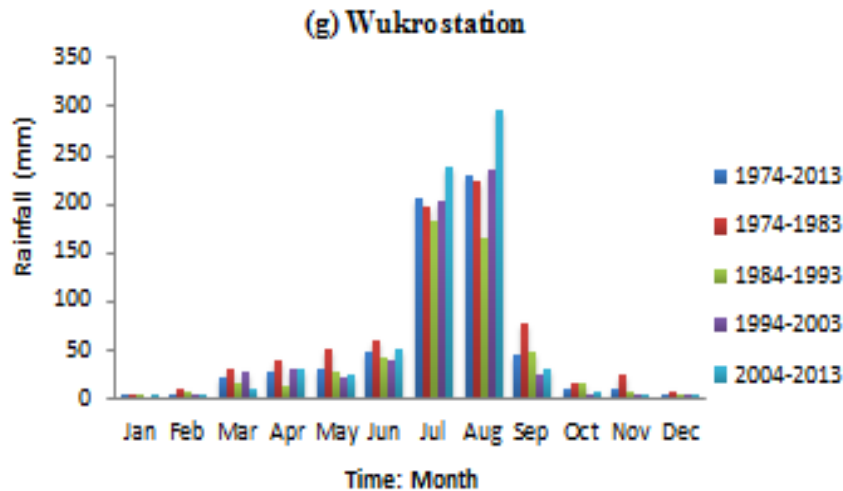


**Figure 4.3 Temporal variation of average monthly Rainfall of different decades for stations (a) Abiadi (b) Adigudem (c) Adigrat (d) Hawzien (e) Mek’ele (f) Senkata and (g) Wukro in Geba River basin.**

Station-wise comparison of annual rainfall totals indicated considerable spatial variability in the study area. Rainfall varied from about 945 mm per year in some areas in the downstream part to less than 300 mm per year in the upstream part of the study area. The average annual rainfall estimates from the historical records indicate that the rainfall of the study area is 633 mm. For the period 1971-2013, the mean annual rainfall averaged over all the rain gauges showed a decline of 8.3 % over this period (Figure 4.4). Rainfall exhibited significant variability over seasons, with the mean rainfall during the Kiremt (rainy) season being 79.62 % of the annual rainfall and the remaining 20.38 % occurring in the Bega (dry season). Seasonal rainfall appeared to vary inversely with elevation. During the Kiremt season (June to September), the upstream parts of the study area received low rainfall as compared to downstream parts which are at a lower elevation. The variation (161.6 mm) in rainfall was greatest mainly in the rainy season, when the rainfall mean (200 mm) was the highest. In contrast, the Bega season had a rainfall variation of (12.53 mm) and the lowest mean rainfall (6.1 mm) indicated in the annual time series of the stations. Additionally, the large values of the variance or standard deviation for Kiremt and the annual series indicate a significant fluctuation in rainfall

during these periods. Climatologically drought shows insufficiency of rainfall compared to normal rainfall in a given region and the major impact of drought is felt in semi-arid regions where the occurrence of drought years is fairly high. Within this context the temporal fluctuations of annual rainfall in the study area were analyzed in terms of the normalized rainfall difference. Rainfall pattern in the study area exhibited a very high variability over time as indicated by the temporal analysis and is frequently highlighted with more negative and less positive anomalies.

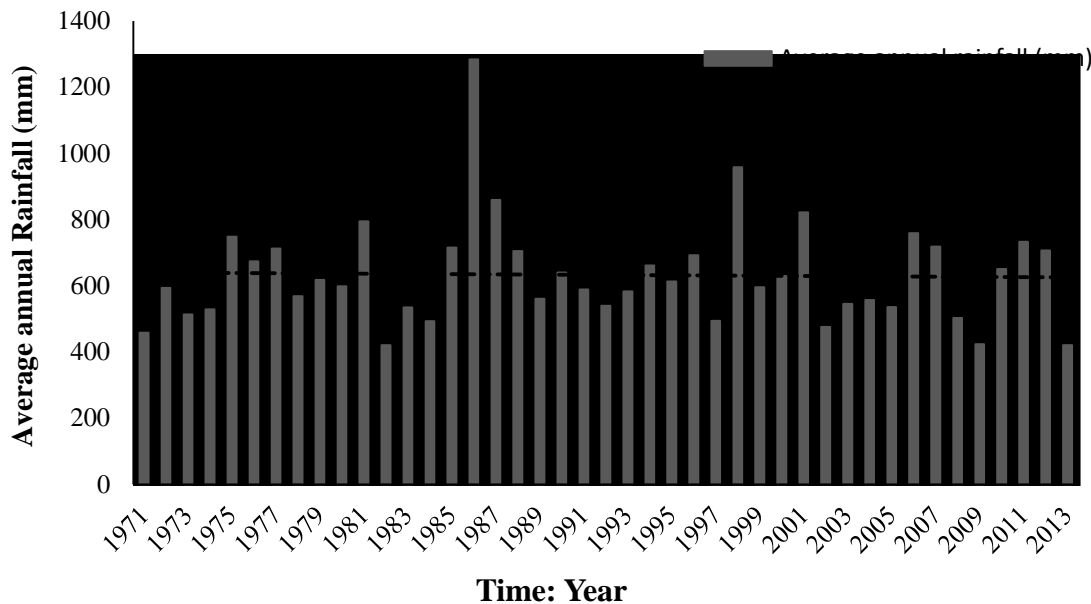


**Figure 4.4 Average annual rainfall in the Geba River basin rainfall stations.**

The monthly distribution of the average rainfall data for the 1971-2013 time periods shown that a rainfall is peaking in July and August whereas in the dry season the basin receiving less than 60 mm rainfall (Figure 4.5).

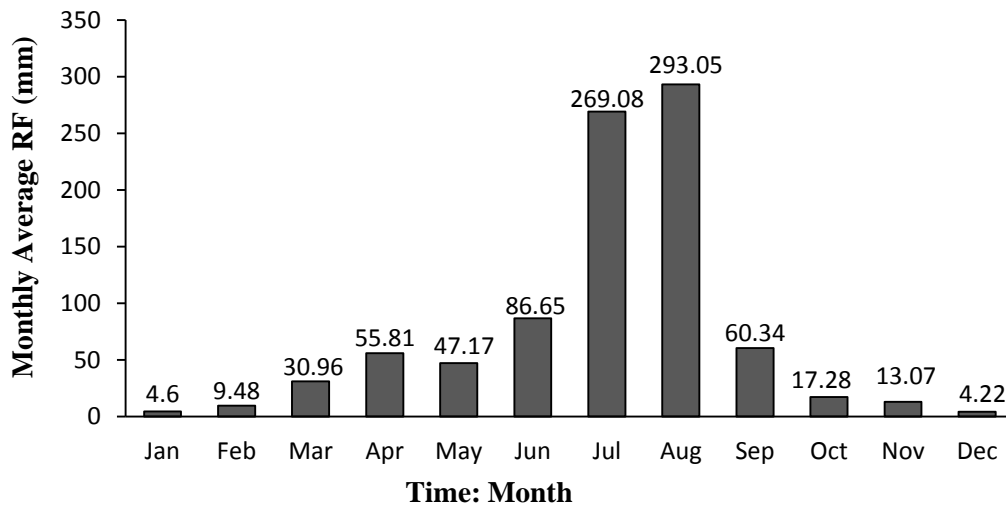


**Figure 4.5 Average monthly rainfall in the Geba River basin rainfall stations.**

The monthly average rainfall volumes for the lower and upper streams of the catchment stations are shown in (Figure 4.6). At the downstream of the Geba basin rainfall stations have shown the monthly rainfall volume with high variation ( $SD = 109.64$  mm) than the upper streams of the Geba basin ( $SD = 86.11$  mm) but for the recorded period of analysis it was also shown that the average annual total rainfall on both landscape positions did not show a significant change. The upstream watershed which are mountainous and high elevation areas receive lesser rainfall than the downstream portion of the basin as it shown from the comparison of the rainfall volumes for the downstream and upstream parts of the Geba River basin. The study also found that the rainfall record within the same area showed inter-stations variability.

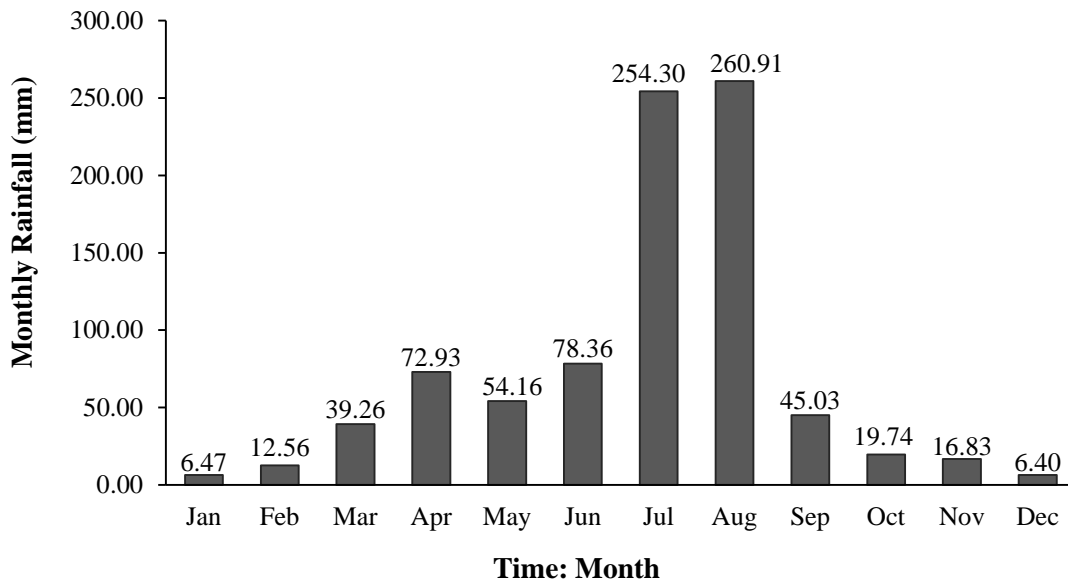


**Figure 4.6 (a) Average monthly rainfall at the upper stream in the Geba River basin.**

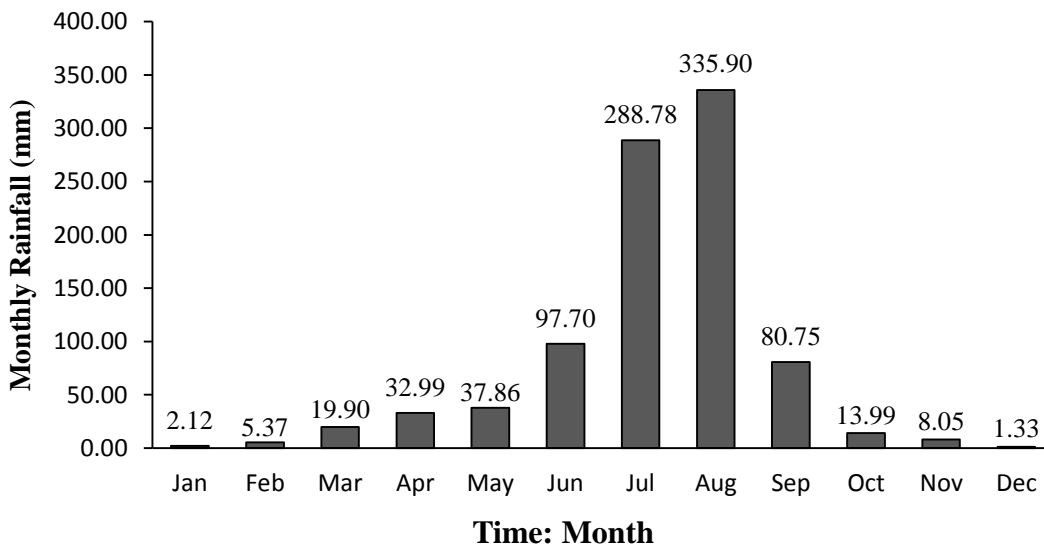


**Figure 4.6 (b) Average monthly rainfall at the downstream in the Geba River basin.**

Furthermore, the average annual Kiremt (rainy) season rainfall is more than 80 % of the annual rainfall with a peak in July and August and 70 % of the total annual rainfall were recorded in these peak months whereas remarkable contribution of the total annual rainfall has occurred in the Belg season (15 %). Most of the area receive less rainfall

annually indicating the existence of spatial variations in rainfall consistent with topographic and elevation differences in addition to the late start of rainfall in June in the early end in September. Temporally, during the Kiremt season (June – September); the upper stream parts of the study area receive low rainfall as compared to the downstream. Climatologically drought shows the insufficiency of rainfall compared to normal rainfall in a given region and the major impact of drought is felt in semi-arid regions where the occurrence of drought years is fairly high.

**Table 4.4: Annual and seasonal rainfall (mm) and their coefficient of variation estimated over the period 1971–2013.**

Stations Name	Annual		Kiremt		Bega		Belg	
	Mean	CV (%)	Mean	CV (%)	Mean	CV (%)	Mean	CV (%)
Abiadi	879.86	41.57	799.96	45.67	36.72	163.75	64.56	100.93
Adigudem	513.27	40.09	465.46	46.65	8.33	131.95	40.08	76.27
Adigrat	555.46	26.28	360.81	37.38	62.55	91.1	139.93	59.81
Hawzien	571.89	37.74	467.78	58.9	38.48	133.2	123.43	135.01
Mek'ele	573.25	23.52	459.13	29.34	20.02	109.16	89.34	71.97
Senkata	600.54	42.16	491.6	62.81	48.31	124.73	132.99	126.6
Wukro	614.27	47.3	515.79	42.96	24.34	176.94	76.55	103.64

Ethiopian rainfall is characterized by high inter-annual variability as the rainfall over the tropical semi-arid and arid areas exhibits such variability. The annual rainfall coefficient of variation (CV) of the stations in the Geba River basin ranging from relatively a minimum of 23.52 % to a maximum of 47.3 % this indicating that the variability in rainfall totals between the rainfall gauge stations is very high (Table 4.4). While considering the analysis of variability of Kiremt season rainfall, which is directly affecting agricultural production over most parts of the country, all of the seven stations



showed evidence of a coefficient of variation (CV) above 25 %. The Kiremt season which is the long rainy duration (June – September) bring about 509 mm more than (80 %) and the Belg season where the short rains (March – May) bring about 95mm (15 %) of the total annual rainfall in the study area. Therefore, about 95 % of the total annual rainfall of the Geba River basin occurs in the Kiremt and Belg seasons. The coefficient of variation for the analysis of rainfall for the Kiremt and Belg seasons rainfall over the stations of the Geba River basin is highly variable ranging from 29 to 63 % and 60 to 135 % respectively (Table 4.4), this further indicated that the mean CV of the long rainfall season is found to be 46 %, which is smaller than that of the short rainfall season, CV = 96 %.

**Table 4.5: Average contribution of the three seasons (in Percent) and the highest monthly and peak rainfall contribution to the annual totals (mm).**

Stations Name	Kiremt	Bega	Belg	Highest monthly	Peak Rainfall Months (mm)
Abiadi	88.49	4.17	7.34	323.21	585.51
Adigudem	90.57	1.62	7.81	207.19	387.33
Adigrat	63.55	11.26	25.19	163.45	304.02
Hawzien	71.69	6.73	21.58	196.89	375.38
Mek'ele	80.93	3.49	15.58	196.07	378.2
Senkata	69.81	8.05	22.14	194.87	385.27
Wukro	83.58	3.96	12.46	220.06	421.05

Generally, the Belg (March to May) and the Bega (dry season: October to February) rainfalls are much more variable than the Kiremt rainfall. This study results is consistent with (Mersha, 1999), in his study analyzed rainfall data from 419 stations throughout the country draw similar conclusion where the Belg and Bega rainfalls are more variable than Kiremt rainfall. Furthermore this study corroborates and similar to other previous studies conclusion (Bewket and Conway, 2007) in their study analyzed variability of rainfall data

from 12 stations of Amhara region of Ethiopia. Mersha (1999, 2003) also reported that in areas of low annual rainfall there is higher variability in rainfall.

The Kiremt rainfall contribution to the annual total of the study area ranges from 63.55 % in Senkata in the upper part of the River basin to just about 90.6 % in Adigudem in the middle part of the catchment (Table 4.5). The contribution of the Belg rainfall is significant to the annual total in the upper stream stations of Adigrat, Hawzien and Senkata. Because of the south-easterly winds from the Indian Ocean blowing towards a thermal low (cyclone) which develops over the south of Sudan during this season these stations record rainfall during the Belg season (Seleshi and Zanke, 2004).

In a given region the deviation of the rainfall from the standard or normal rainfall indicated that there is meteorological drought. In semi-arid regions, the occurrence of drought years is comparatively high compared to other climatic regions. Consequently, within this circumstance the temporal and inter-annual variations of annual rainfall in the Geba River basin were analyzed in terms of standardized rainfall anomaly.

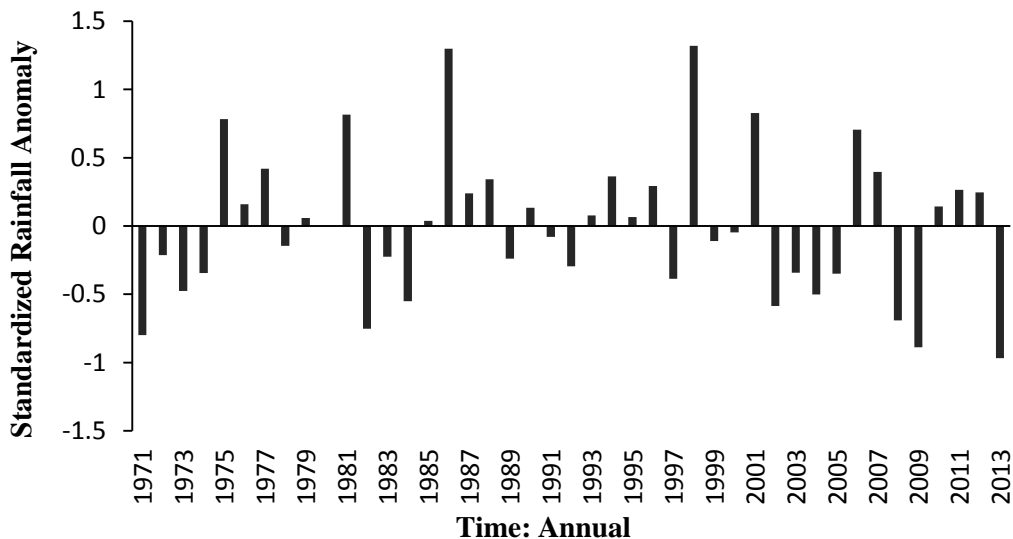


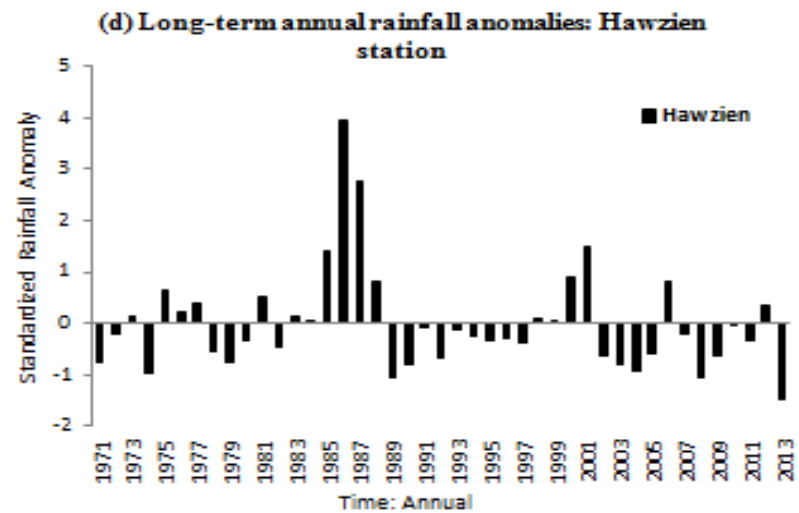
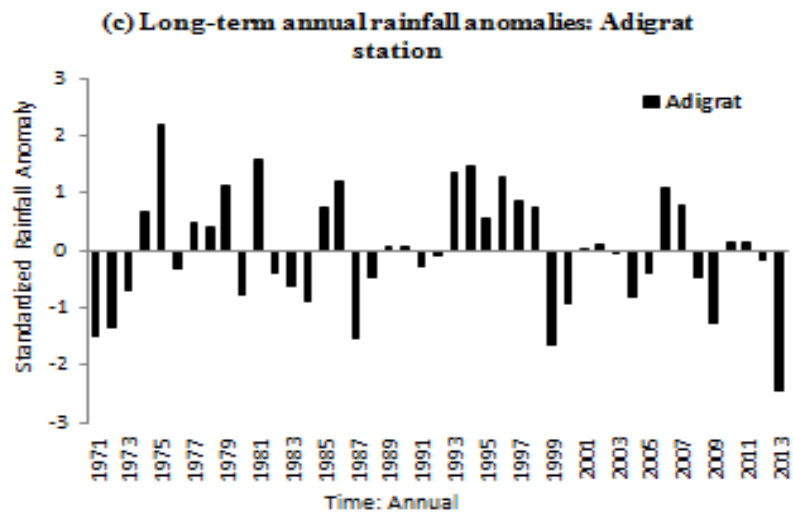
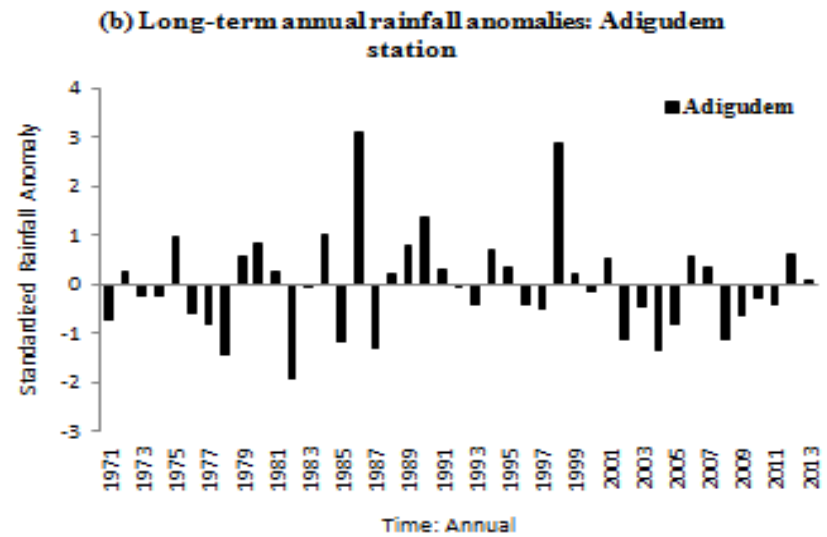
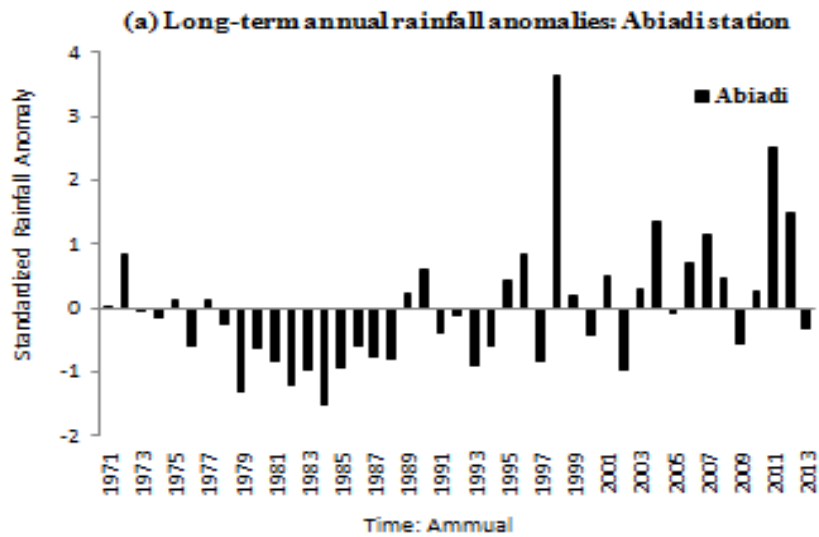
**Figure 4.7 Standardized anomalies of time series annual average rainfall totals in the seven stations.**

The temporal analysis indicated that the pattern of rainfall in the study area revealed fairly often a very high variability over time and is highlighted with positive and negative anomalies (Figure 4.7). As a result, in statistical point of view years like, 1971, 1972, 1973, 1974, 1978, 1982, 1983, 1984, 1989, 1991, 1992, 1997, 1999, 2000, 2002, 2003, 2004, 2005, 2008, 2009 and 2013 can be represented as meteorological drought years with respect to long-term annual mean of rainfall, where a period of negative rainfall anomalies is viewed, and the rest of the other rainfall periods are described as normal years (Table 4.6).

**Table 4.6: The driest and wettest years and seasons by station during the period 1971–2013.**

Stations Name	Driest years			Wettest years		
	Annual	Kiremt	Belg	Annual	Kiremt	Belg
Abiadi	1984	1984	1997	1998	1998	1996
Adigudem	1982	1987	1999	1986	1986	1993
Adigrat	2013	1992	1983	1975	1975	1993
Hawzien	2013	1982	1988	1986	1986	1987
Mek'ele	2008	2013	1999	1988	1988	1993
Senkata	2009	1982	1988	1978	1986	1987
Wukro	1978	1992	1973	1981	1976	1981

The standardized anomalies of annual rainfall at the seven stations are shown in Figure 4.8. From the total number of observations the percentage of negative standardized anomalies varied from about 49 % (in Adigudem) to 72 % (in Wukro) in the 1971 – 2013 span of time. Rainfall in the region shows considerable variability where a year with a negative anomaly tends to be followed by another year with a negative anomaly as do years with positive anomalies and in some years it is observed that a negative anomaly is followed by a positive one.



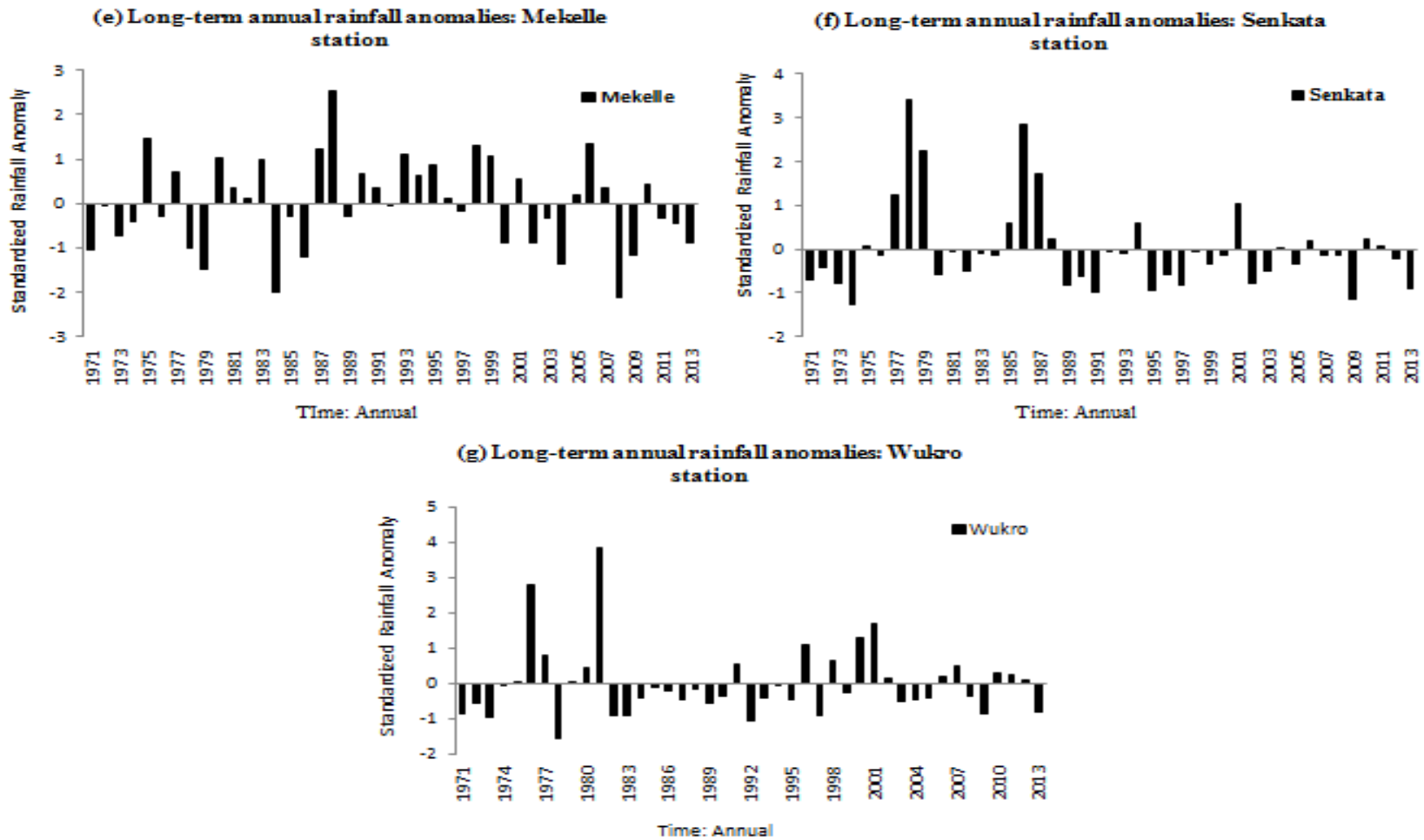


Figure 4.8 Standardized anomalies of time series of annual rainfall at the seven stations (a) Abiadi (b) Adigudem (c) Adigrat (d) Hawzien (e) Mek'ele (f) Senkata and (g) Wukro.

In all the stations there is an alternative negative and positive anomalies is observed in the study period. Throughout the driest and wettest years of the long-term (1971–2013) 0.99 and 4.66 (for Abiadi), 1.31 and 3.52 (for Adigudem), 1.67 and 3.03 (for Adigrat), 0.74 and 4.69 (for Hawzien), 1.22 and 3.25 (for Mek'ele), 0.73 and 4.59 (for Senkata) and 0.96 and 3.68 (for Wukro) times the standard deviation below and above average respectively. Further analysis indicated that 65 %, 55 %, 67 %, 63 % and 67 % negative anomalies were observed for stations Abiadi, Adigrat, Hawzien, Mek'ele and Senkata respectively.

#### **4.3.1.2 Trend Analysis of Rainfall**

In the Mann-Kendall test all the rainfall time series data are analyzed. For the annual, Kiremt i.e., the rainy season (June to September) and Bega i.e., the dry season (October to May) the test was performed independently. The test results of the statistical analysis at 95 % confidence level for the annual rainfall trend detection presented in Table 4.7 revealed that negative trends dominated the annual series. Five (71 %) of the 7 stations showed a negative trend. Even though, there is a decreasing trend in all of these 5 stations Adigudem (-0.767 mm/y), Adigrat (-0.818 mm/y), Hawzien (-2.094 mm/y) Mek'ele (-0.692 mm/y) and Senkata (-0.794 mm/y) the trends showed not statistically significant at the 95 % significance level (Table 4.7 and Figure 4.9) with linear trends ranging from -0.692 to -2.094 mm/year.

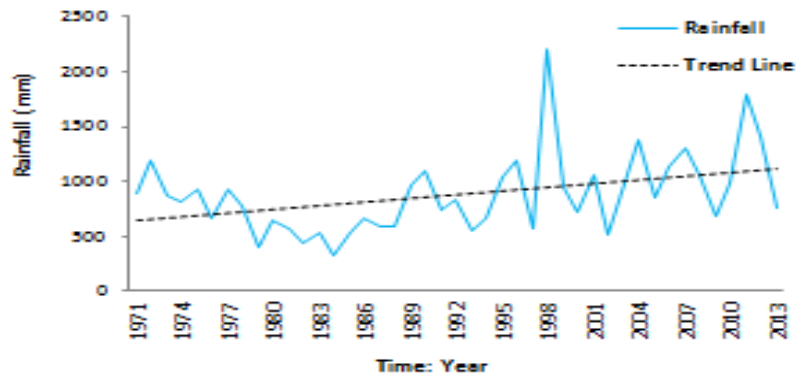
The trend of the spatial distribution was in a pattern where one station positive trend confined to the downstream part of the basin and the middle as well as the upper stream part had all negative trends, mixed with one positive trend in the upper stream. On the other hand, only two stations Abiadi and Wukro showed an increasing trend in rainfall and only Abiadi revealed statistically significant trend with a Sen's magnitude of 10.091 mm/year. However, all negative trends were statistically insignificant at 95 % confidence level. The study results of annual rainfall is consistent with other annual analysis of rainfall conducted in some other parts of the country (Afewerki, 2012; Bewket and Conway, 2007; Seleshi and Zanke, 2004) found decreasing trends in annual rainfall series

in some stations of their study area. In the upper stream part, the annual average rate of change was -1.235 mm/year, in the middle it was 0.948 mm/year, whilst the downstream experienced an increase with an average annual rate of change of 10.091 mm/year. Therefore, the pattern of change is clearly seen in the downstream than the upper stream and the middle landscape position of the study area. From results shown above it can be concluded that there is a mixed trend of rainfall experienced in the last decades in the Geba River basin.

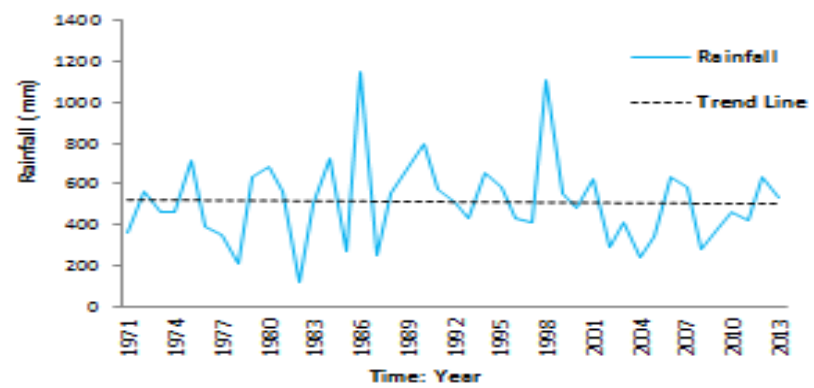
**Table 4.7: Annual rainfall trend detection for the stations in the Geba River basin for the period (1971 to 2013).**

Station name	p for $\alpha=0.05$	Sen's slope mm/y	Trend nature
Abiadi	0.014	10.091	Positive
Adigudem	0.739	-0.767	Negative
Adigrat	0.746	-0.818	Negative
Hawzien	0.307	-2.094	Negative
Mek'ele	0.677	-0.692	Negative
Senkata	0.724	-0.794	Negative
Wukro	0.405	1.678	Positive

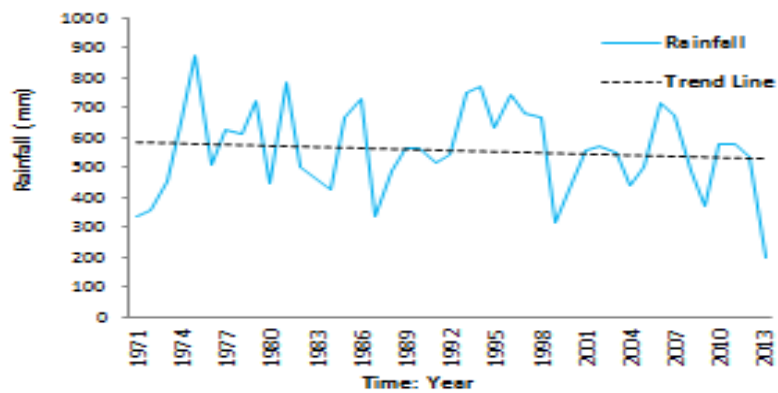
(a) Annual Rainfall Abiadi station



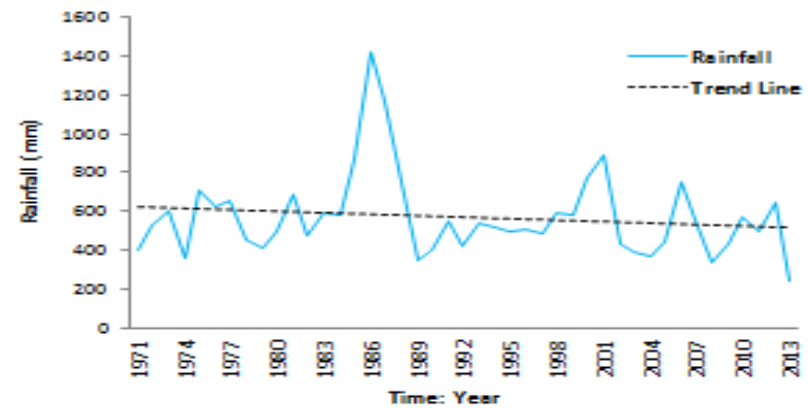
(b) Annual Rainfall for Adigudem station



(c) Annual Rainfall for Adigrat station



(d) Annual Rainfall for Hawzien station





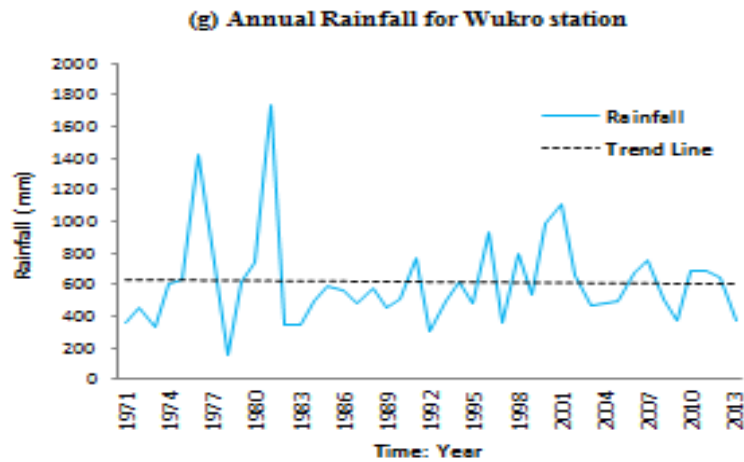
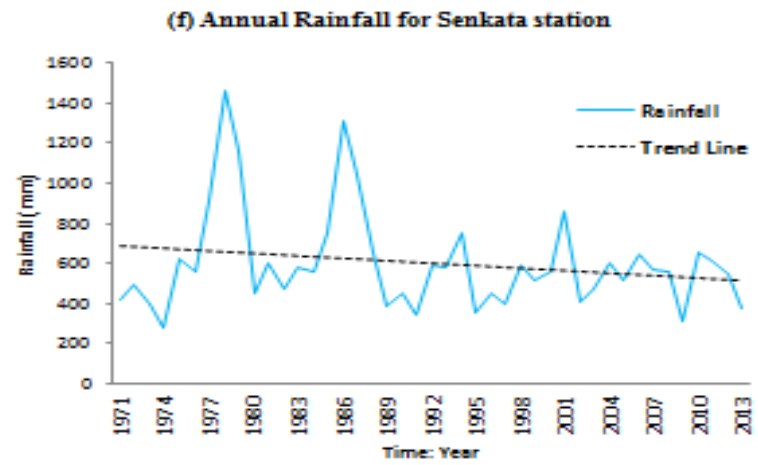
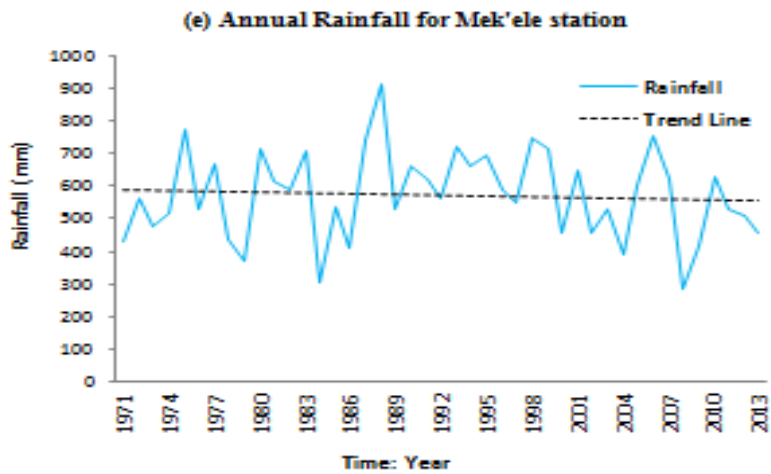


**Figure 4.9** Variation of annual rainfall for stations (a) Abiadi (b) Adigudem (c) Adigrat (d) Hawzien (e) Mek'ele (f) Senkata and (g) Wukro in Geba River basin.

#### **4.3.1.3 Seasonal Rainfall Analysis**

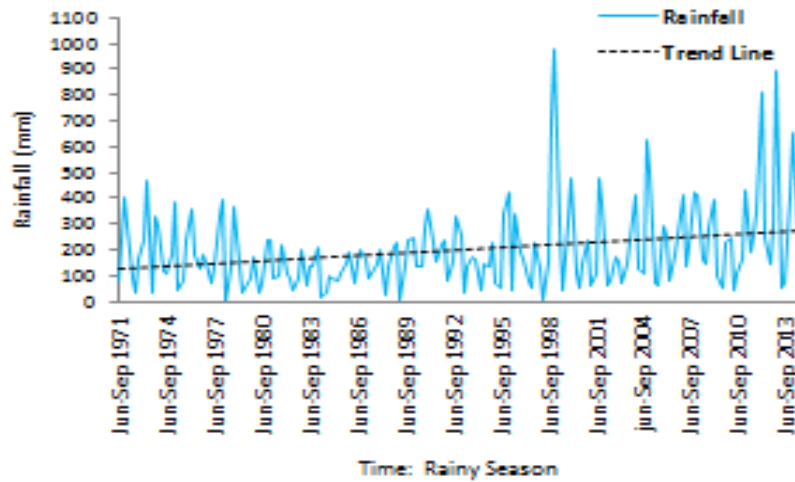
According to the analysis performed, the test results for the Kiremt (rainy season) rainfall trend detection are given in Table 4.8 for the time period 1971 to 2013. The Kiremt season total rainfall showed similar trends to the annual trends pattern. Four stations (Adigrat, Hawzien, Mek'ele, and Senkata) which are about 57.14 % of the total stations showed negative trends and spatially the negative trends dominate in the upper stream part of the River basin. Furthermore, the negative trends were statistically insignificant at 95% confidence level. Positive trends were found at two of the stations, Wukro in the upper stream and Abiadi in the downstream part which, however, both stations showed statistically insignificant positive trend at 95% level of significance (Table 4.8 and Figure 4.10). One station that is Adigudem in the middle of the River basin showed no trends at all. The downstream of the Geba River basin experienced rate of change of + 0.521 mm/year. On the other hand, the Kiremt average seasonal rates of change in the middle and upper stream position of the basin were  $- 0.025$  and  $- 0.055$  mm/year, respectively.

The findings of this study agree with other studies previously applied in other parts of the country (Seleshi and Zanke, 2004; Seleshi and Camberlin, 2006; Bewket and Conway, 2007; Cheung et al., 2008; Afewerki, 2012) found a decline of annual and rainy season rainfall in Northern, Eastern, Southern, North western, and South western Ethiopia. Furthermore, the study results are in line with studies undertaken in the East Africa regions (Schreck and Semazzi, 2004; Opiyo et al., 2014) observed that there is a downward trend in the rainy season rainfall.

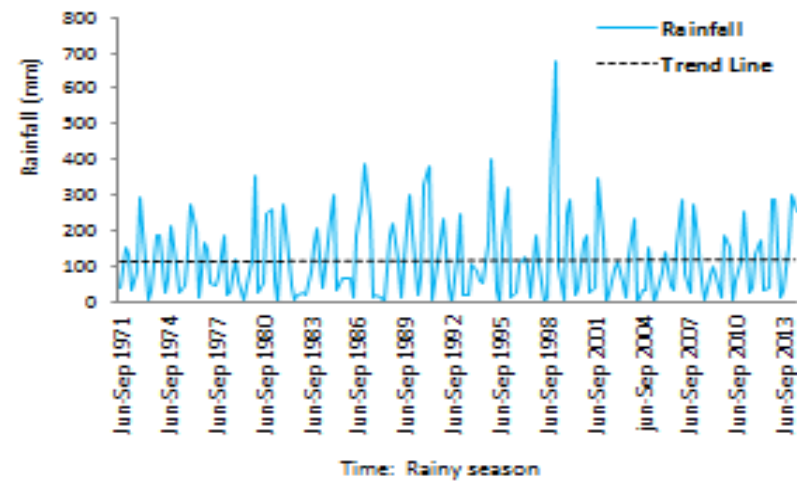
**Table 4.8: Rainy seasonal rainfall trend detection for the stations in the Geba River basin for the period (1971 to 2013).**

Station name	p for $\alpha=0.05$	Sen's slope (mm/y)	Trend nature
Abiadi	0.08	0.521	Positive
Adigudem	0.984	0	Zero
Adigrat	0.880	-0.014	Negative
Hawzien	0.897	-0.026	Negative
Mek'ele	0.7799	-0.05	Negative
Senkata	0.480	-0.125	Negative
Wukro	0.704	0.056	Positive

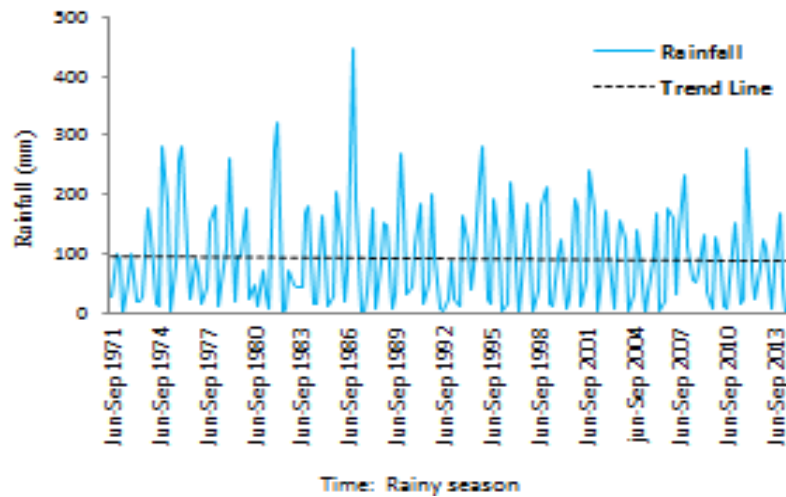
(a) Rainy season for Abiadi station



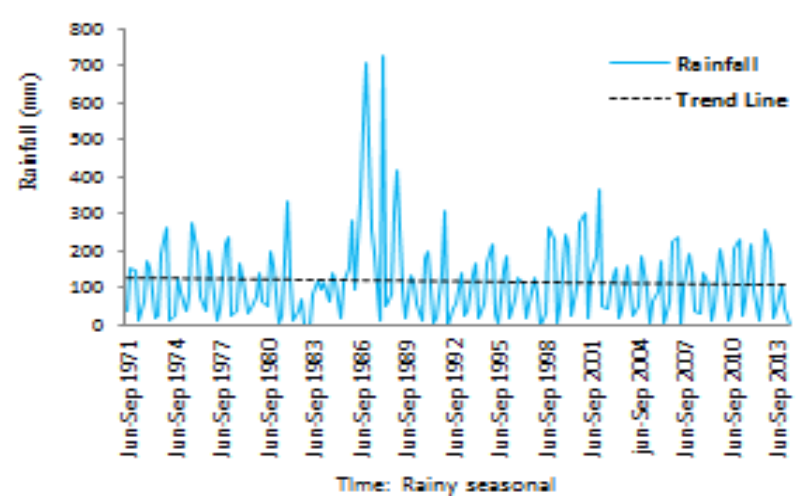
(b) Rainy season for Adigudem station



(c) Rainy season for Adigrat station



(d) Rainy season for Hawzen station



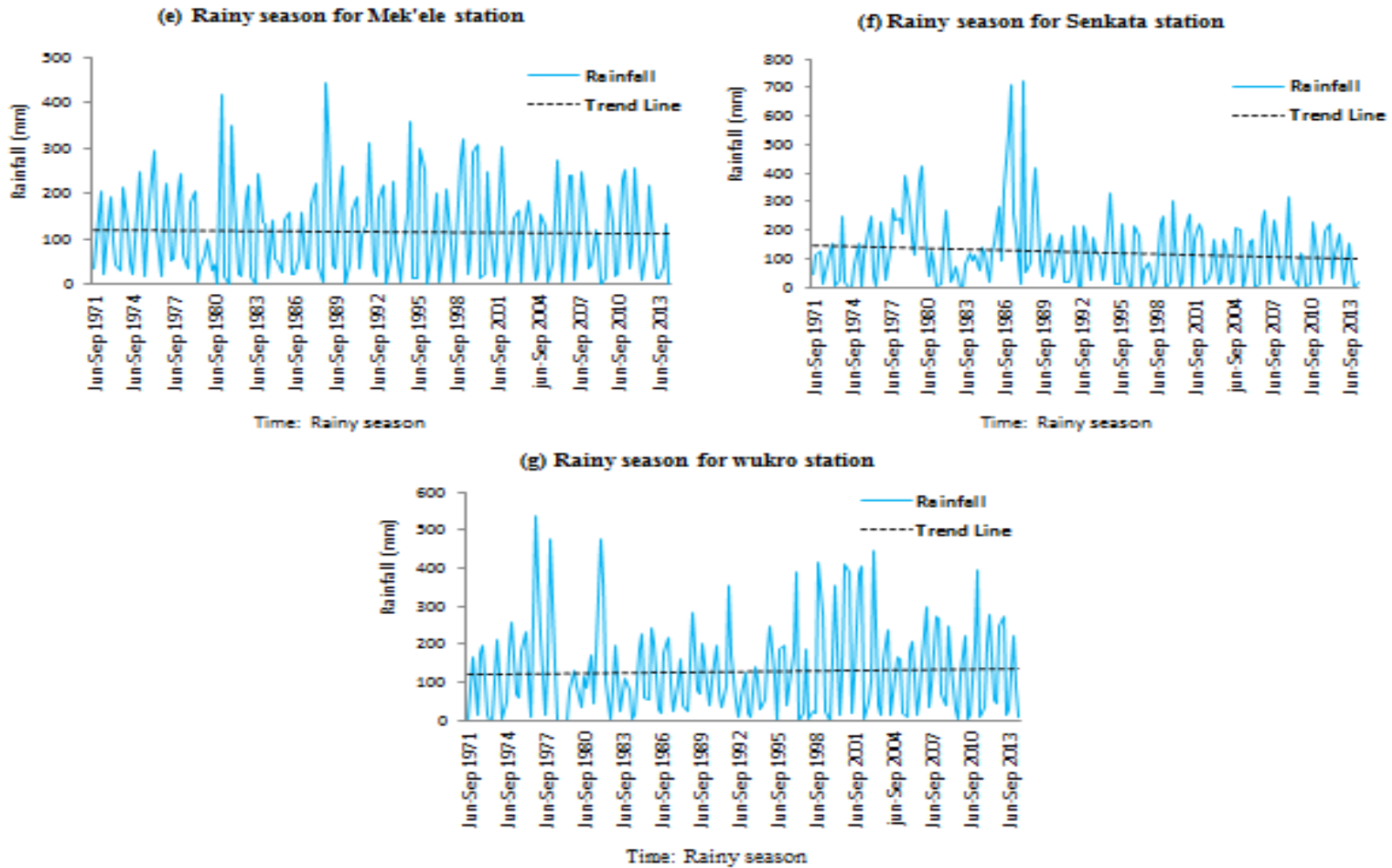


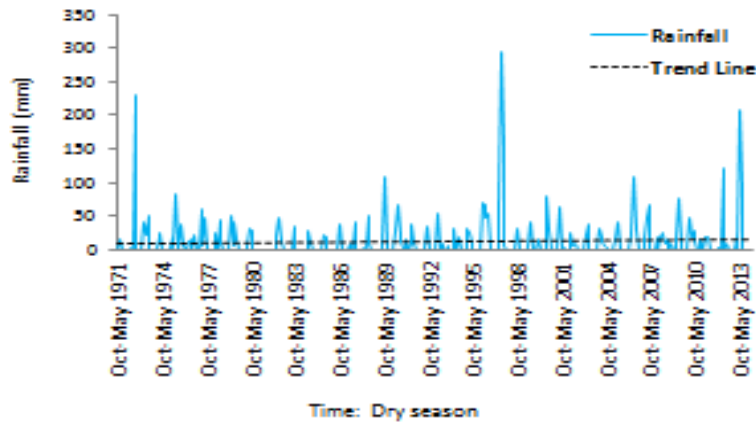
Figure 4.10 Variation of Rainy season rainfall for stations (a) Abiadi (b) Adigudem (c) Adigrat (d) Hawzien (e) Mek'ele (f) Senkata and (g) Wukro in Geba River basin.

**Table 4.9: Dry seasonal rainfall trend detection for the stations in the Geba River basin for the period (1971 to 2013).**

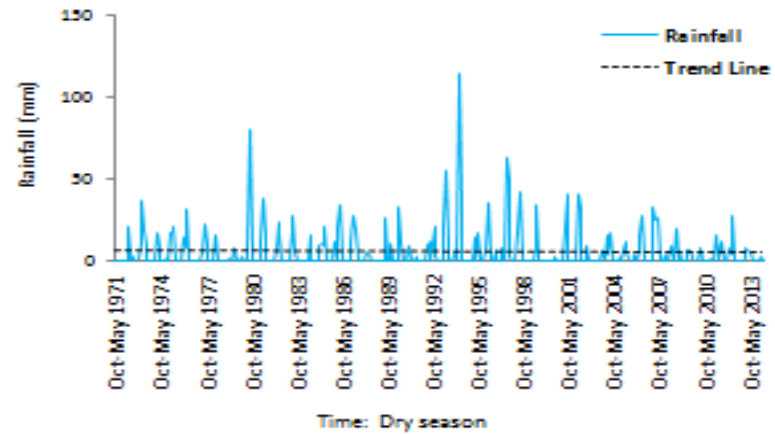
Station name	p for $\alpha=0.05$	Sen's slope mm/y	Trend nature
Abiadi	0.560	1.563	Positive
Adigudem	0.793	-0.504	Negative
Adigrat	0.462	0.032	Positive
Hawzien	0.386	-1.048	Negative
Mek'ele	0.711	-1.985	Negative
Senkata	0.875	-2.443	Negative
Wukro	0.454	-1.267	Negative

The test results for the Bega (dry season) rainfall trend detection are given in Table 4.9 and Figure 4.11. For the Bega season totals, similar to the annual rainfall trend analysis five (71.43 %) out of the seven stations in the basin showed a decreasing trend in the Bega seasonal rainfall totals in which none of these stations are statistically significant. In the Bega season variability series stations Abiadi in the downstream and Adigrat in the upper stream position of River basin showed positive trend and accounts 28.57 %. Negative trends are more dominated in the upper stream part of the study area and the basin wide average rate linear trend of change was  $-5.65$  mm/year.

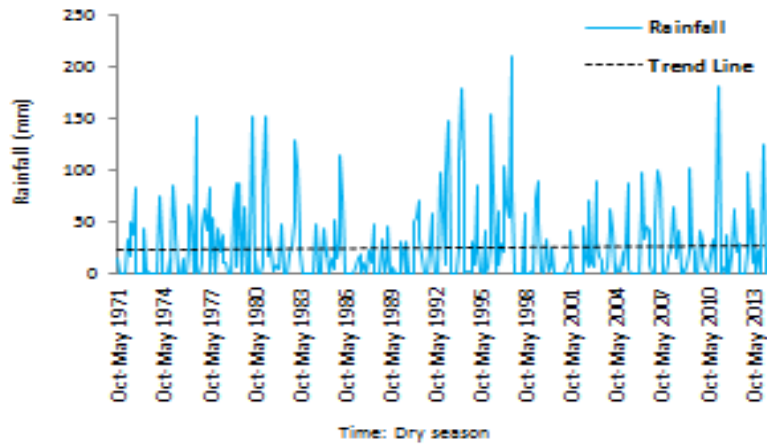
(a) Dry season for Abiadi station



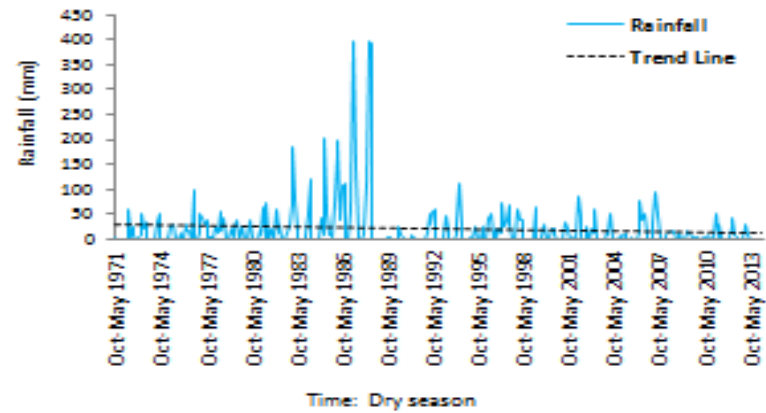
(b) Dry season for Adigudem station



(c) Dry season for Adigrat station



(d) Dry season for Hawzien station



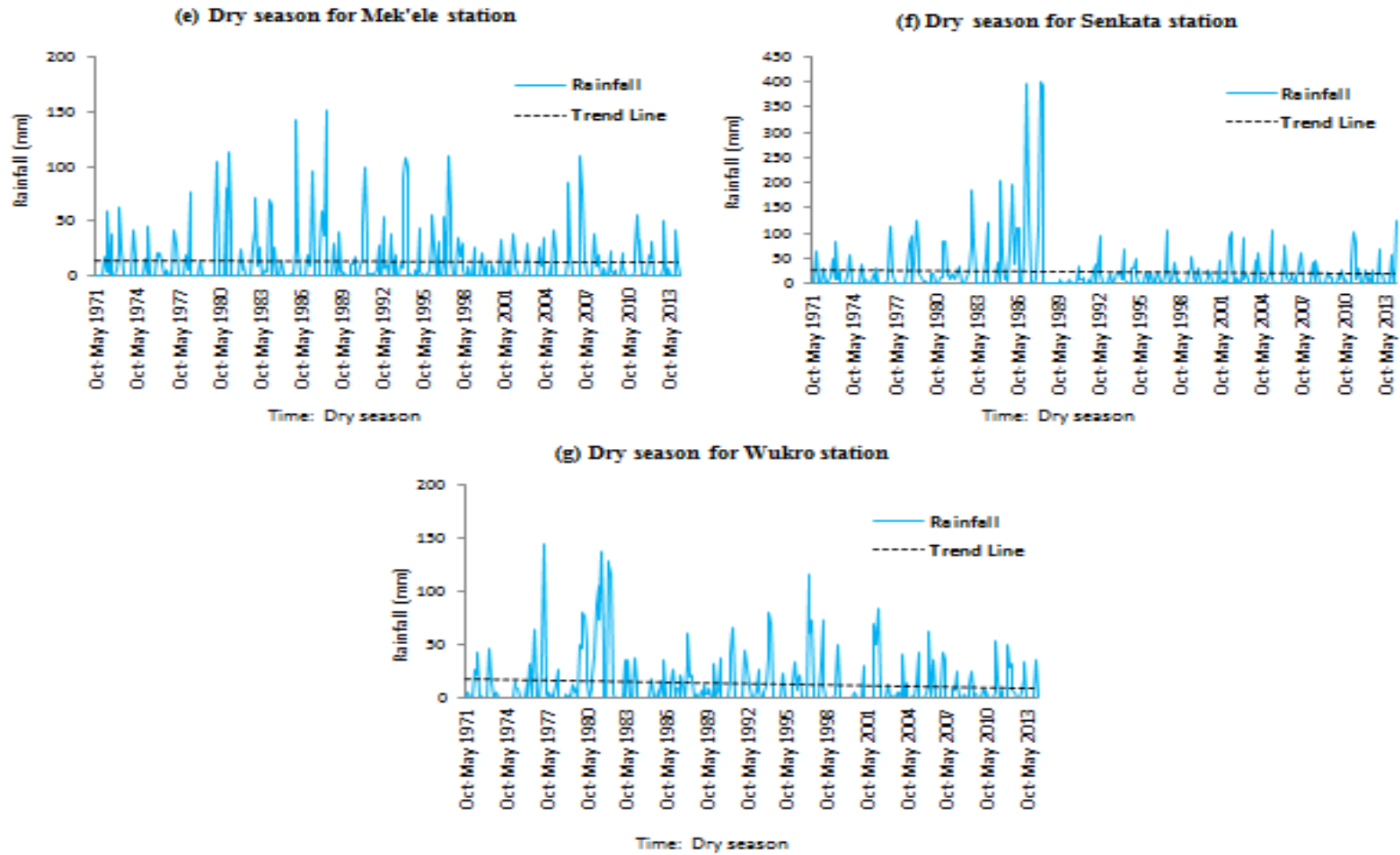


Figure 4.11 Variation of dry season rainfall for stations (a) Abiadi (b) Adigudem (c) Adigrat (d) Hawzien (e) Mek'ele (f) Senkata and (g) Wukro in Geba River basin.



Comparison of seasonal rainfall trend analysis results showed that the Kiremt or rainy season (June to September) rainfall is decreasing in most of the stations in the Geba River basin, except for Abiadi and Wukro though these stations felt to show statistically significant increasing trend at 95 % level of significance. Furthermore, the Bega or dry season (October to May) rainfall has showed a decreasing trend in most of the stations in the entire basin except for the stations Abiadi and Adigrat revealed positive nature of trend significance. From this it can be concluded that the Kiremt rainfall, most important for rain-fed agriculture in the basin, is experiencing slightly decreasing changes in rainfall in most of the stations though there are increasing trends in very few stations.

#### **4.3.2 Observed Trends and Extreme Rainfall Indices**

Information regarding extreme rainfall indices, such as rainfall type, frequency, intensity and extremes, etc., is specified in the Expert Team for Climate Change Detection Monitoring and Indices (ETCCDMI) (Alexander et al., 2006). The extreme rainfall indices can be categorized into two groups: one group calculates the frequency (number of cases) of the index exceeding or not exceeding its defined threshold (CDD, CWD, R10 mm, R20 mm and 25 mm), while the second one measures the rainfall depth (mm) or intensity (mm per day) (RX1day, RX5day, PRCPTOT, SDII, R90P, R95P and R99P). The partition of magnitude and frequency is expected that can give an additional insight into the often slight differences of the climatic regions across the Northern highlands of Ethiopia. In addition, it is likely obvious that these indices are also important for the probable impact assessment of climate changes on semi-arid and arid environments related to agriculture, water resources, sustainable development, and other sectors.

The time series trend analyses results of 12 extreme rainfall indices are summarized in (Tables 4.11 and 4.12) estimated over the period 1971–2013. Table 4.11 gives the frequency (number of cases) of the index exceeding or not exceeding its defined threshold in rainfall indices calculated individually for the 7 stations' data and the corresponding statistically significant results at the 95 % significance level and the Sen's

magnitude. Moreover, Table 4.12 shows the trends in the rainfall depth (mm) or intensity (mm per day) of the extreme rainfall indices and their corresponding Sen's magnitude.

#### **4.3.2.1 Trends in Wet-day Annual Total Rainfall (PRECTOT) and Simple Daily Rainfall Intensity (SDII) Indices**

Generally any discussion on changes to extremes of rainfall begins with changes of PRCPTOT index at local and regional levels. This is probably the most important parameter reflecting rainfall variations over the entire year which is one of the twelve rainfall indices analysed in this study. Positive trends in PRCPTOT occurred on stations Abiadi, Adigrat and Wukro which is ranging the Sen's magnitude from 0.21 to 14.14 mm per year (Table 4.11, Figure 4.12). However, there is only Abiadi that shows statistically significant increasing trend at 95 % significance level. The remaining four stations that show decreasing trends and none of them showed statistically significant rainfall totals in the 1971 to 2013 period which decreases on average 1.2 mm per year (Table 4.11)

Further analysis indicated that one index that considers not only the total amount of rainfall throughout the year but also reflects a change in daily rainfall is the Simple Daily Intensity Index (SDII). This index combines the amount of annual rainfall totals and the number of days when rainfall (greater than or equal to 1 mm) actually occurs. The results for the SDII and PRCPTOT indices show the considerable inter-annual variability in these indices where the lowest SDII rainfall indices (< 8.0 mm) occurred in different years (Table 4.10) for their respective stations which were the driest periods on record, and these incidences coincide temporally with the lowest PRCPTOT of the rainfall indices (< 500 mm).

**Table 4.10: The occurrence of the lowest and highest Simple Daily Intensity Index (SDII).**

Stations	Occurrence of lowest SDII	Occurrence of highest SDII
Abiadi	1979, 1984, 1993	1995, 1998, 2001, 2004, 2007, 2008, 2011, 2012
Adigudem	1971, 1978, 1982, 1987, 1993, 1996, 1997, 2000, 2004, 2005, 2008, 2009, 2010, 2011	1981, 1986, 1987, 1988, 2000
Adigrat	1971, 1973, 1987, 1991, 1999, 2012	1975, 1979, 1981, 1986
Hawzien	1971, 1974, 1989, 1993, 1996, 2004	1981, 1986, 1987, 1988, 2000
Mek'ele	1971, 1978, 1979, 1984, 2008, 2013	1980, 1981, 1982, 1983, 1987, 1988
Senkata	1974, 1980, 1993, 1997, 2009, 2013	1986, 1987, 1988
Wukro	1983, 1985, 1989, 1992, 2013	1981, 1996, 1998, 1999, 2000, 2001, 2002

The highest values of SDII (> 16 mm for Abiadi), (> 12 mm for Adigudem), (> 11mm for Adigrat and Mek'ele), (> 13 mm for Hawzien and Wukro) and (> 15 mm for Senkata) were also determined (Table 4.10) with the highest PRCPTOT (> 900 mm for Abiadi, Senkata and Wukro, and > 700 mm for rest of the other stations) happened in the corresponding years. Most climate stations located in the Geba River basin experienced a decreasing trend magnitude ranging from -0.02 to 0.05 mm per day per year except two stations (Abiadi and Adigrat which range from 0.14 to 0.21mm per day/year) located in the down and upper stream part of the River basin, respectively and all these stations result statistically insignificant at 95 % significance level. Only Abiadi station showed statistically significant increasing trend in the 1971– 2013 period (Table 4.12). These results are relevant to the variation in rainfall based on the SDII index will have significant inference to the future reliability of water resources for the purpose of different activities, agricultural strengthening, and ecological sustainability and possibly increase of flood risk.

### 4.3.3 Changes in the Extreme Rainfall Frequency Indices

#### 4.3.3.1 Maximum Length of Indices for the Dry and Wet Periods

Values of rainfall indices for R10 mm, R20 mm, R25 mm, CDD and CWD are shown in Table 4.11.

**Table 4.11: Mann-Kendall Statistic (P) and Sen's slope for PRCPTOT, CDD, CWD, R10mm, R20mm and R25mm for all stations**

Stations Name	PRCPTOT (mm/y)		R10mm (days/y)		R20mm (days/y)		R25mm (days/y)		CDD (days/y)		CWD (days/y)	
	p for $\alpha=0.05$	Sen's slope	p for $\alpha=0.05$	Sen's slope	p for $\alpha=0.05$	Sen's slope	p for $\alpha=0.05$	Sen's slope	p for $\alpha=0.05$	Sen's slope	p for $\alpha=0.05$	Sen's slope
Abiadi	<b>0.001</b>	14.14	<b>0.001</b>	0.6	<b>0.001</b>	0.308	<b>0.008</b>	0.20	0.45	-0.19	0.211	0.083
Adigudem	0.875	-0.42	0.159	-0.14	0.893	0.00	0.739	0.00	0.294	-0.09	<b>0.012</b>	0.143
Adigrat	0.942	0.219	0.695	0.00	<b>0.043</b>	-0.08	0.092	-0.04	0.426	-0.27	0.386	0.00
Hawzien	0.278	-2.35	0.896	0.00	0.261	-0.05	0.135	-0.04	0.637	0.1	0.165	0.036
Mek'ele	0.594	-1.15	0.249	-0.08	0.643	0.00	0.98	0.00	<b>0.023</b>	-0.9	0.491	0.00
Senkata	0.739	-0.82	0.291	-0.09	0.17	-0.08	0.483	-0.03	0.992	0	0.841	0.00
Wukro	0.603	1.028	0.507	0.074	0.42	0.034	0.276	0.06	0.261	0.533	0.941	0.00

A measure of change to drier conditions amongst the indices is the Consecutive Dry Days (CDD) Index. Results of trend magnitudes (days per year) for stations with increasing and decreasing trends to CDD and CWD at  $\alpha = 0.05$  significant level are shown in (Table 4.11, Figure 4.12). For the period 1971-2013, annual rainfall shows decreasing trends of the Consecutive Dry Days Index (CDD) detected for Abiadi, Adigudem, Adigrat and Mek'ele stations examined in this study with a trend magnitudes ranging from -0.09 to -0.9 days per year. The negative trends at Mek'ele (-0.9 days per year) is the only stations statistically significant at 0.05 level of significance in CDD. The negative trends in annual rainfall at Abiadi, Adigudem and Adigrat are also somehow moderate to high, though not statistically significant due to large inter-annual fluctuations. The positive trends in annual rainfall at stations Hawzien and Wukro showed are moderate to high though not statistically significant and the Senkata station showed no trend at all. Provided that, CDD is a measure of dryness; then the Consecutive Wet Days (CWD) index, on the contrary, reveals the time-series variations that can direct to wetter conditions. For the study period the CWD shows positive trend in three out of seven stations over the Geba River basin (Table 4.11).

The positive trend at Adigudem (0.143 days per year) is statistically significant at 0.05 levels of significance. Though there not statistically significant there is increasing trends at stations Abiadi and Hawzien with trend magnitudes are ranged between 0.036 to 0.083 days per year and the other four stations Adigrat, Mek'ele, Senkata and Wukro showed no trend at all (Table 4.11). Further analysis indicated that annual rainfall indices for CWD take the lowest values ( $< 5$  mm) in 1971 for Wukro, 1971, 1980 and 1982 for Senkata, 1985 for Adigudem and Mek'ele, 1990 for Hawzien, 2001 for Abiadi and 2009 for Adigrat. Most of climate stations analyzed for study area showed decreasing trends in the number of consecutive dry days (CDD) index. In contrast, increasing and no trends were detected for the number of consecutive wet days (CWD) over majority of the climate stations analyzed in this study.

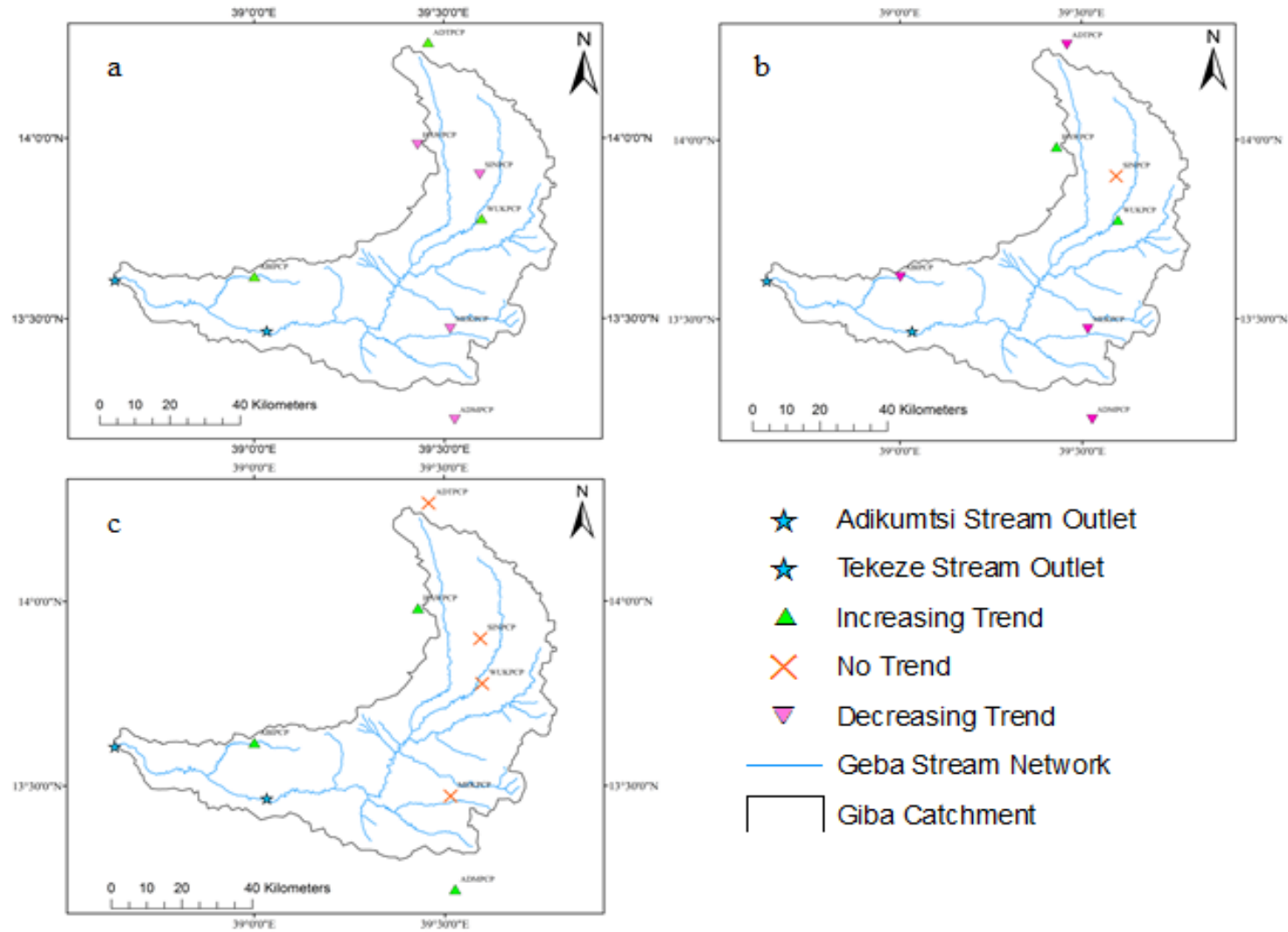


Figure 4.12 Trends in 1971-2013 for PRCPTOT (a), for CDD (b) and CWD (c).

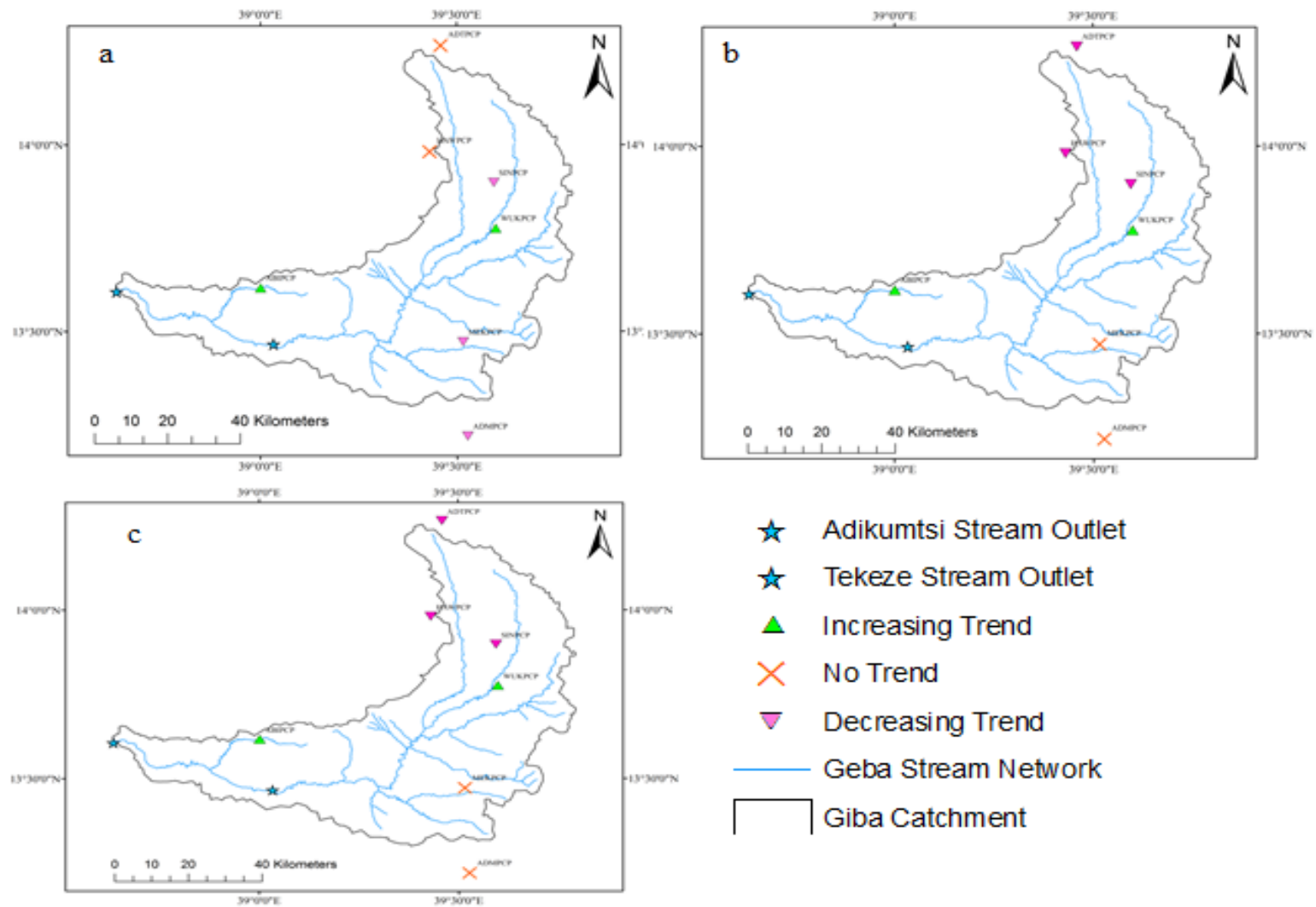


Figure 4.13 Trends in 1971-2013 for the 10mm (a), for the 20mm (b) and for the 25mm (c).

#### 4.3.3.2 Daily Rainfall of Absolute Threshold Indices

Results of trend magnitudes (days per year) for stations with statistically significant changes to R10 mm and R20 mm at  $\alpha = 0.05$  significant level are shown in (Table 4.11, Figure 4.13). The number of cases (annual count number of days ) with daily rainfall equal or exceeding the 10 mm, 20 mm and 25 mm limits is the measure of persistence of intense rainfall, defined as the R10 mm, R20 mm and R25 mm indices. The R10 mm had showing a decreased changes in the stations Adigudem, Mek'ele and Senkata with a trends magnitude ranging from -0.08 to -0.14 days per year, but the trend is not statistically significant. In addition, in stations Abiadi and Wukro the R10 mm index had shown increasing trends having a trends magnitude 0.6 and 0.074 days per year, respectively, however only Abiadi revealed statistically significant and the other two Adigrat and Hawzien stations showed no trend at all.

Further analysis revealed that there are more stations with a significant change to R20 mm than to R10 mm and 25 mm. Only two stations Abiadi and Adigrat showed a statistically significant trends to R20 mm with an increasing (0.308 days per year ) and a decreasing (-0.05 days per year) trends, respectively at the 95 % confidence level (Table 4.11). Over the Geba River basin increasing trends for stations Abiadi and Wukro and only Abiadi showed statistically significant trend. There are three stations Adigrat, Hawzien and Senkata which are located in the upper stream of the catchment revealed a decreasing trend, all are located at high elevations for the 20 mm this is mainly explained by the altitude gradients observed for rainfall. This is in consistent with the decreasing and increasing trends detected for the 25 mm index where three stations; Adigrat, Hawzien and Senkata showed decreasing, two stations Abiadi and Wukro showed increasing and stations Adigudem and Mek'ele with no trend at all. Decreasing trends have been found in the extreme rainfall indices, R10 mm and R20 mm and 25 mm, in most of the stations except Abiadi and Wukro, which respectively represent the number of days when rainfall equal or exceed 10 mm or 20 mm or 25 mm (R10 mm/R20 mm/25 mm).



#### **4.3.4 Changes in the Extreme Rainfall Depth and Intensity Indices**

##### **4.3.4.1 Extreme Rainfall Indices for 1-day and 5-day Event Durations**

On the basis of results obtained for the Rx1day index (Table 4.12; Figure 4.14); the monthly maximum 1-day rainfall of four stations located in the Geba River basin had decreased with the magnitudes of change ranging from -0.001 to -0.013 mm per year. Some positive change had also occurred for stations Abiadi and Wukro. Only Abiadi and Mek'ele showed statistically significant increasing and decreasing trends respectively and one station showed no trend. The trend magnitudes for stations with increasing changes are ranging from 0.024 to 4.81E-04 mm per year. For the RX5day index which corresponds to the maximum consecutive 5-day rainfall amount (a potential indicator of flood producing events), four out of the seven stations in the study area show positive changes (Table 4.12). Two of them are experiencing statistically significant at 95 % significance level. Three stations (Adigudem, Adigrat and Mek'ele) also show negative change, but none of them showed statistically significant. The trend magnitudes for stations experiencing decreasing and increasing changes range from about -0.02 to -0.037 and 0.012 to 0.202 mm per year, respectively. Therefore, a mix of decreasing and increasing trends were detected in the stations of the River basin where a decreasing trend is seen Adigudem, Adigrat and Mek'ele and an increasing trends for Abiadi and Wukro stations.

**Table 4.12: Mann-Kendall Statistic (P) and Sen's slope for R95, R95, R99P, SDII, R1x day and R5x day for all stations.**

Stations Name	R90p (days/y)		R95p (days/y)		R99p (days/y)		SDII (mm/y)		RX1day (mm/y)		RX5day (mm/y)	
	p for $\alpha=0.05$	Sen's slope	p for $\alpha=0.05$	Sen's slope	p for $\alpha=0.05$	Sen's slope	p for $\alpha=0.05$	Sen's slope	p for $\alpha=0.05$	Sen's slope	p for $\alpha=0.05$	Sen's slope
Abiadi	<b>0.004</b>	3.481	<b>0.020</b>	2.29	0.126	0.35	<b>0.002</b>	0.136	<b>0.034</b>	0.024	<b>0.003</b>	0.202
Adigudem	1.00	0.046	0.950	0.03	0.771	0.037	0.196	-0.044	0.404	-0.004	0.771	-0.037
Adigrat	0.603	0.369	0.868	0.075	0.367	0.12	0.942	0.209	0.267	-0.006	0.589	-0.02
Hawzien	0.429	-0.715	0.205	-0.71	0.515	-0.149	0.603	-0.015	0.964	0.00	0.162	0.101
Mek'ele	0.901	0.176	0.884	-0.047	0.234	-0.195	0.218	-0.026	<b>0.012</b>	-0.013	0.63	-0.025
Senkata	0.950	0.055	0.967	0.037	0.769	0.103	0.405	-0.015	0.819	-0.001	0.847	0.012
Wukro	0.708	0.378	0.917	-0.10	0.884	0.056	0.338	0.045	0.926	4.81E-04	<b>0.026</b>	0.201

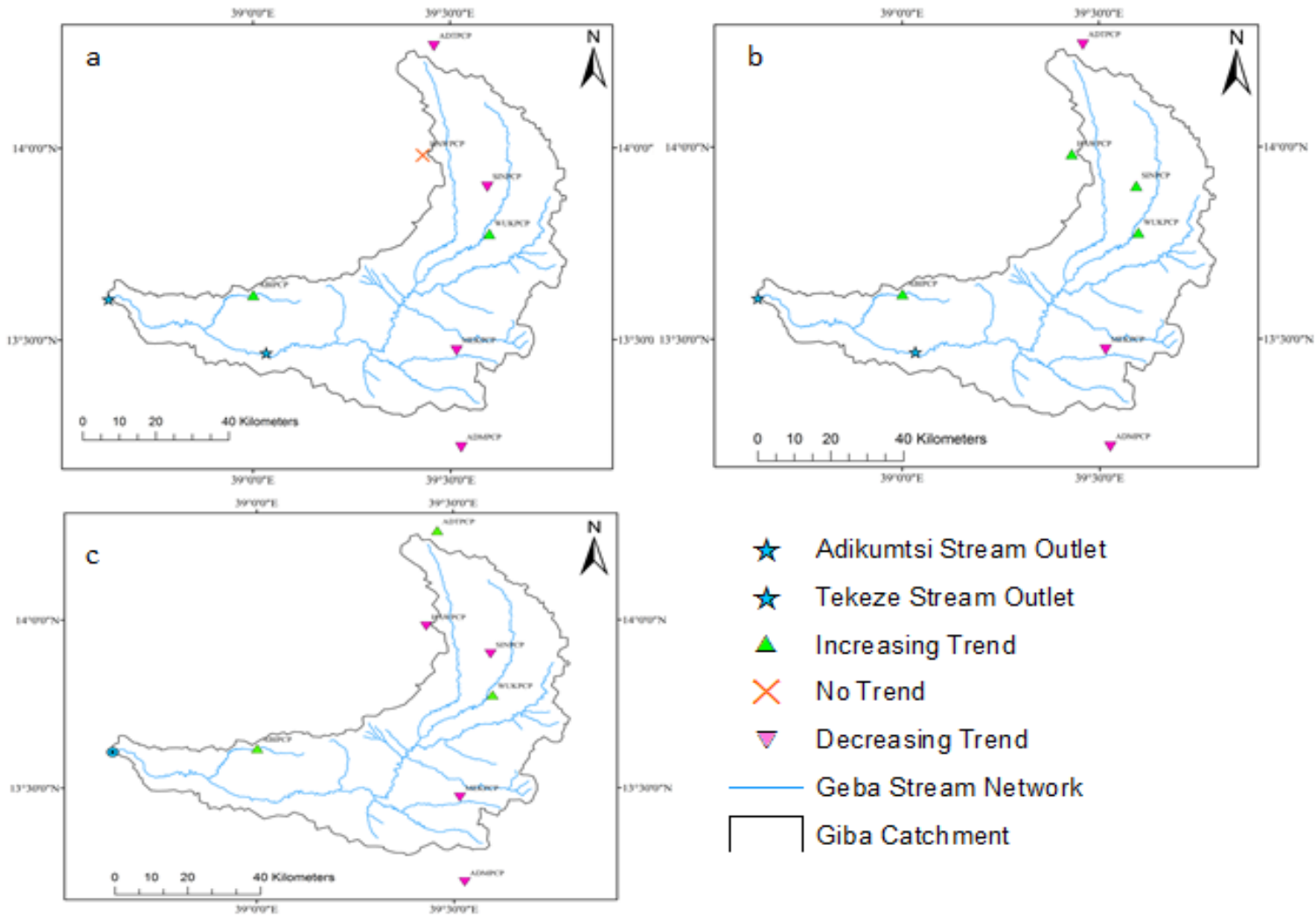


**Figure 4.14 Trends in 1971-2013 for RX1day (a), RX5day (b) and SDII (c).**

#### 4.3.4.2 The Percentile Threshold Indices of Daily Rainfall Events

The heavy rainfall that exceeds the 90, 95 and 99 percentile thresholds are measured by R90P, R95P and R99P indices (Table 4.12; Figure 4.15). For extreme rainfall events that exceeded the 90 % (R90P), 95 % (R95p) and the 99 % (R99P) thresholds generally showed increasing trends in most of the stations, but only Abiadi showed statistically significant positive trend at 95 % significance level in the 1971–2013 period that accompanies the annual total rainfall. The trend in the R99P index is positive with a trend magnitude ranging from (0.037 to 0.35 mm per year) in the 1971–2013 period; the contribution of the rainfall on extremely wet days to the total rainfall amount is between 42 and 65.62 mm. The R95P index exhibits slightly increases in all the station (0.031 to 2.29 mm per year) in the full 43-year record period, while the contribution of the rainfall due to very wet days (above the 95<sup>th</sup> percentile) to the total rainfall varies between 101.46 and 167.65 mm. In this index, however only Abiadi showed statistically significant trend. The R90p index has a trend pattern similar to R95p, although more pronounced with an increase (0.046 to 3.481 mm per year).

On an average, the contribution of rainfall on wet days (above the 90<sup>th</sup> percentile) to the total annual rainfall varies between 160.24 and 262.42 mm in the in 1971– 2013 period. Across all the indices Hawzien stations showed a decreasing pattern with a trend magnitude of -0.715, -0.71 and -0.149mm per year for R90P, R95P and R99P respectively (Table 3.6). The annual total rainfall when daily rainfall exceeds 90, 95 or 99 % threshold index, R90p/R95p/R99p, an increasing trends seen in most of the stations and mostly positive trends were observed for R90p. However, a decreasing trend were detected for R90p/R95p/R99p in Hawzien, Mek'ele and Wukro stations

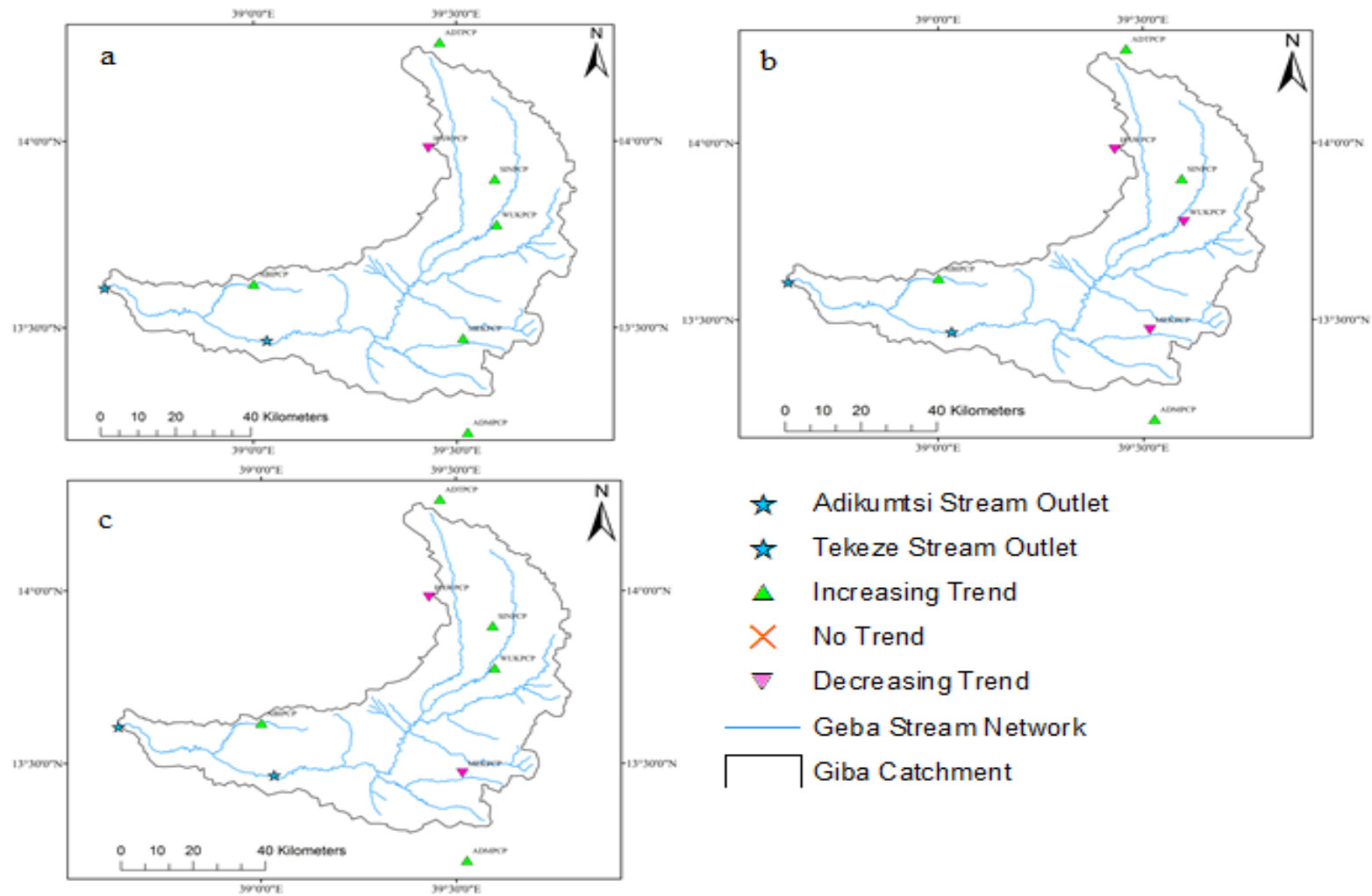


Figure 4.15 Trends in 1971-2013 for R90P (a), R95P (b) and R99P (c).

### 4.3.5 Temperature Data Analysis

Temperature generally increases towards the downstream part of the basin where there is low elevation. The spatial variability of temperature is explained as functional relationship between monthly minimum and maximum temperatures with elevation. The coefficient of variation (CV) of minimum temperature varies between 0.12 and 0.42 in the middle and upper steam part of the basin, respectively. The temporal variation of minimum temperature in Geba River basin is slightly significant as shown in Table 4.13. CV of minimum temperature in the highland stations (as in the case of Adigrat) is higher during the first and second decades which is greater than 0.5 and lower during the first decade for Abiadi, and second and fourth decade for Mek'ele and the temporal variation in terms of CV is less than 0.1.

**Table 4.13: Decadal CV of minimum temperature for the stations in the Geba River basin.**

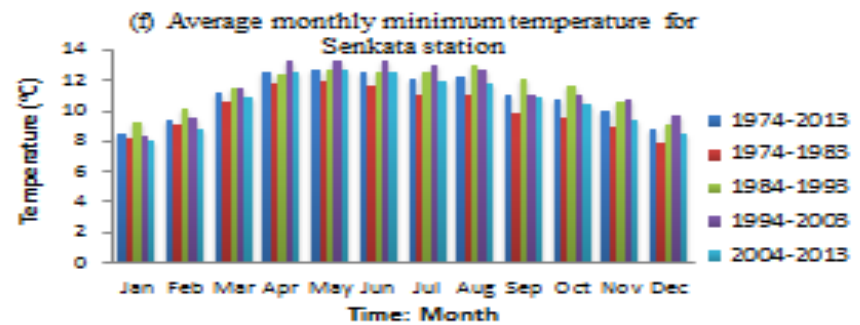
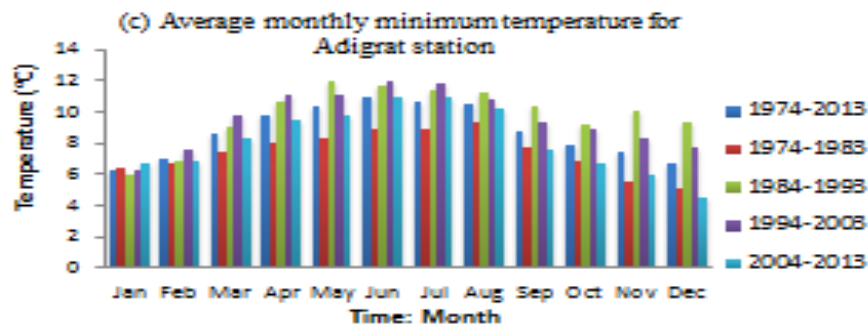
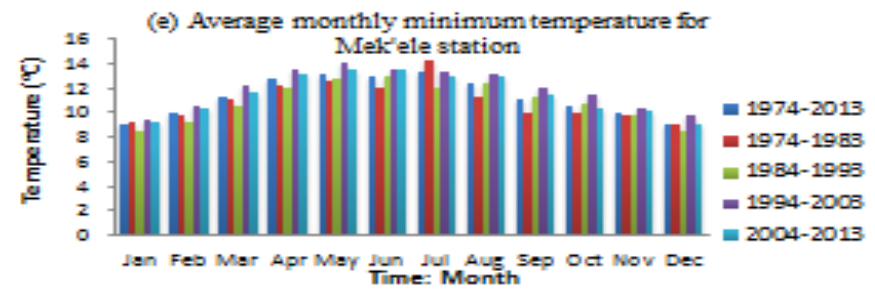
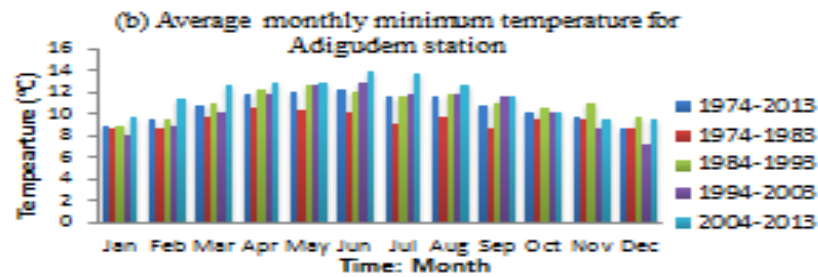
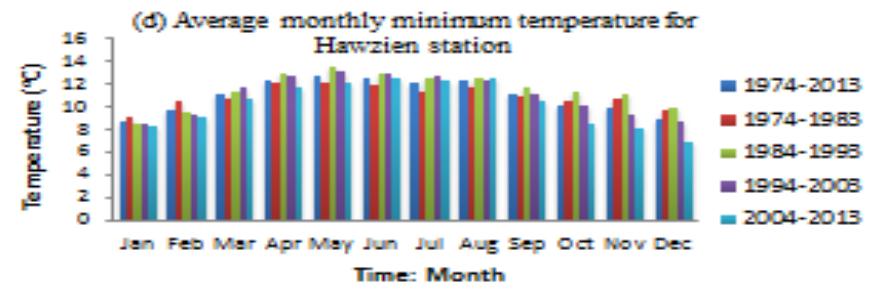
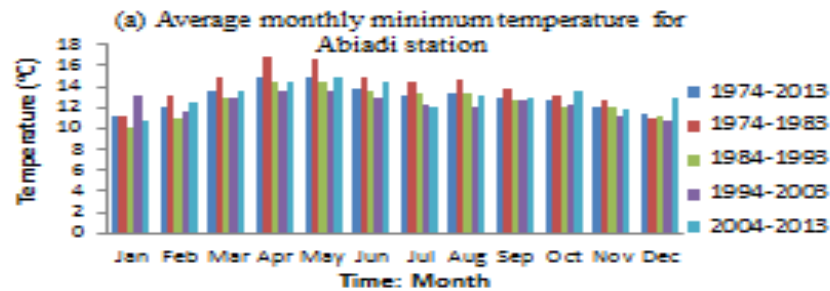
Stations	Decade 1 (1974-1983)	Decade 2 (1984-1993)	Decade 3 (1994-2003)	Decade 4 (2004-2013)	Average CV of station
Abiadi	0.08	0.23	0.20	0.16	0.16
Adigudem	0.42	0.21	0.19	0.21	0.26
Adigrat	0.69	0.52	0.21	0.26	0.42
Hawzien	0.17	0.22	0.11	0.14	0.16
Mek'ele	0.19	0.18	0.05	0.06	0.12
Senkata	0.21	0.21	0.18	0.20	0.20
Wukro	0.23	0.24	0.20	0.15	0.20

Maximum temperature variation is very less and not as such significant compared to the minimum temperature in the basin. The coefficient of variation (CV) of maximum temperature is almost less than or equal to 0.1 within a very narrow range (Table 4.14).

**Table 4.14: Decadal CV of maximum temperature for the stations in the Geba River basin.**

<b>Stations</b>	<b>Decade 1 (1974-1983)</b>	<b>Decade 2 (1984-1993)</b>	<b>Decade 3 (1994-2003)</b>	<b>Decade 4 (2004-2013)</b>	<b>Average CV of station</b>
Abiadi	0.08	0.09	0.10	0.07	0.08
Adigudem	0.08	0.12	0.13	0.04	0.09
Adigrat	0.10	0.09	0.06	0.03	0.07
Hawzien	0.20	0.07	0.08	0.08	0.11
Mek'ele	0.05	0.11	0.10	0.04	0.07
Senkata	0.07	0.09	0.05	0.04	0.06
Wukro	0.09	0.08	0.05	0.04	0.06

To study the changes in temporal variation of temperature, analysis has been carried out at decadal intervals for monthly average values. Figure 4.16 and 4.17 show the bar charts of minimum and maximum temperature at seven climate stations of the Geba River basin, respectively. It can be observed that there is a decrease in minimum temperature in most of the stations except Abiadi in the downstream part of the basin in the fourth decade. Moreover, there is an increase in maximum temperature in the third decade and decrease in the fourth decade in most of the stations. The probable reasons for this as discussed in Chapter 5.





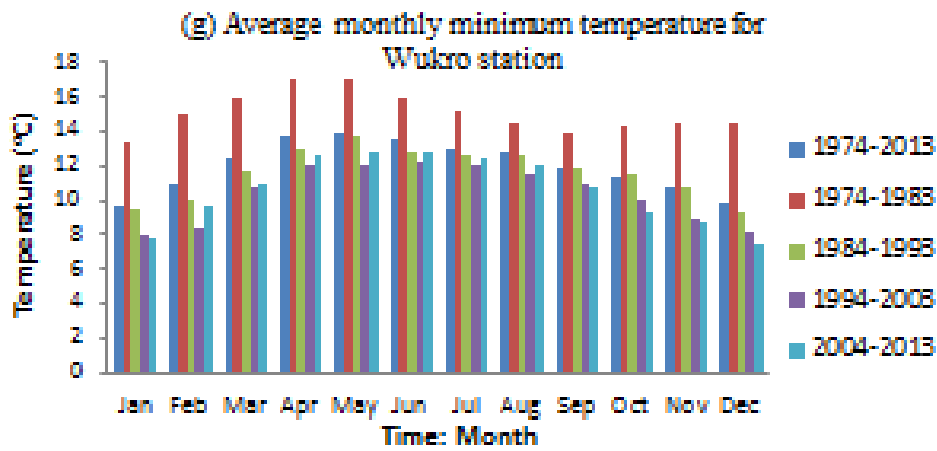
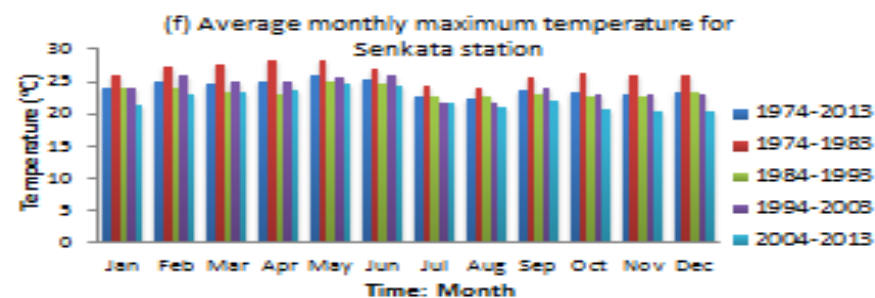
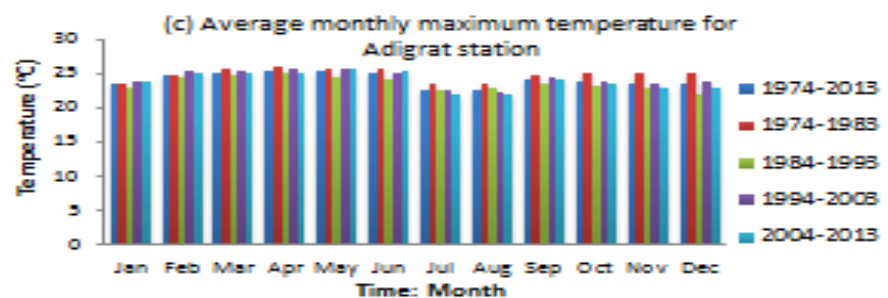
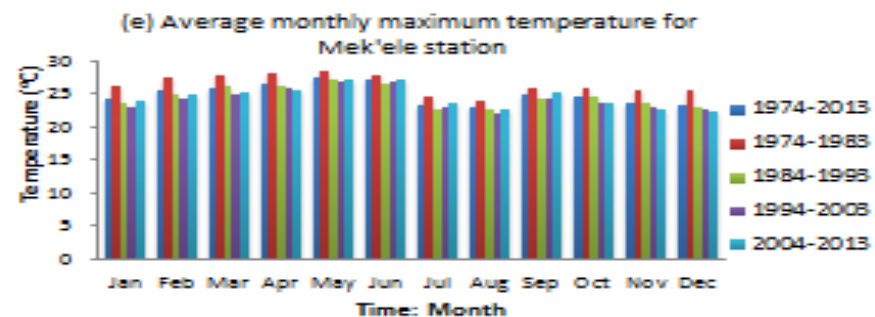
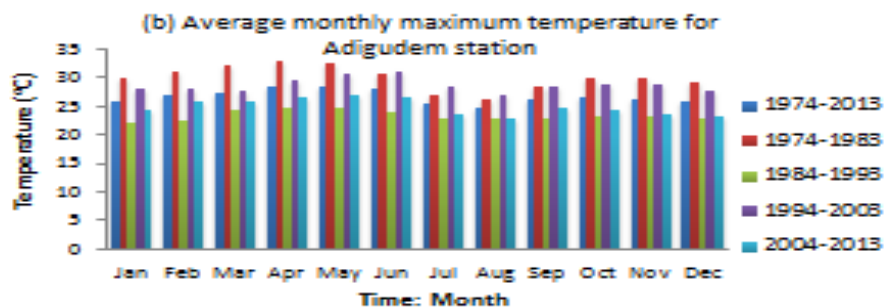
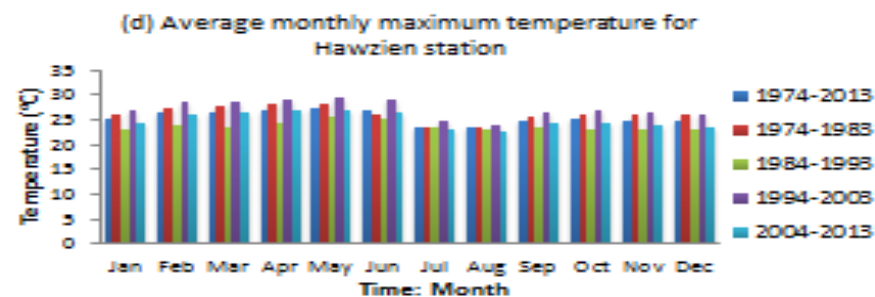
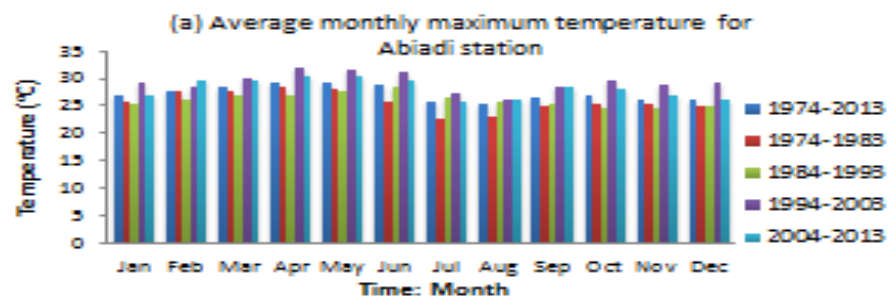
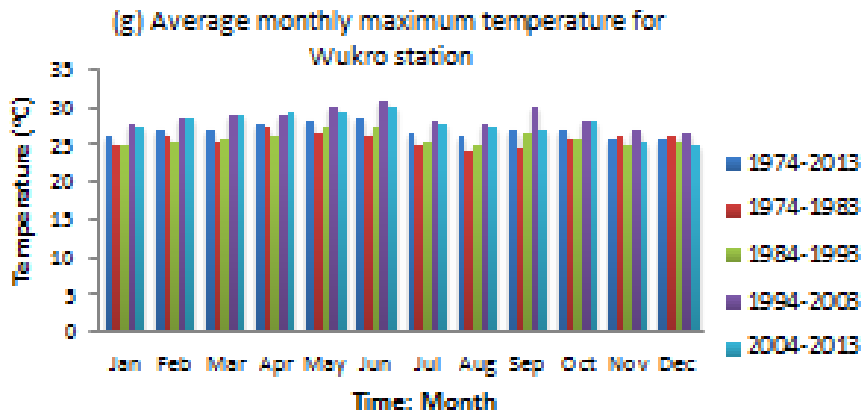


Figure 4.16 Temporal variation of average monthly minimum Temperature of different decades for stations (a) Abiadi (b) Adigudem (c) Adigrat (d) Hawzien (e) Mek’ele (f) Senkata and (g) Wukro in Geba River basin.





**Figure 4.17 Temporal variation of average monthly maximum Temperature of different decades for stations (a) Abiadi (b) Adigudem (c) Adigrat (d) Hawzien (e) Mek’ele (f) Senkata and (g) Wukro in Geba River basin.**

#### 4.3.5.1 Trend Analysis of Temperature

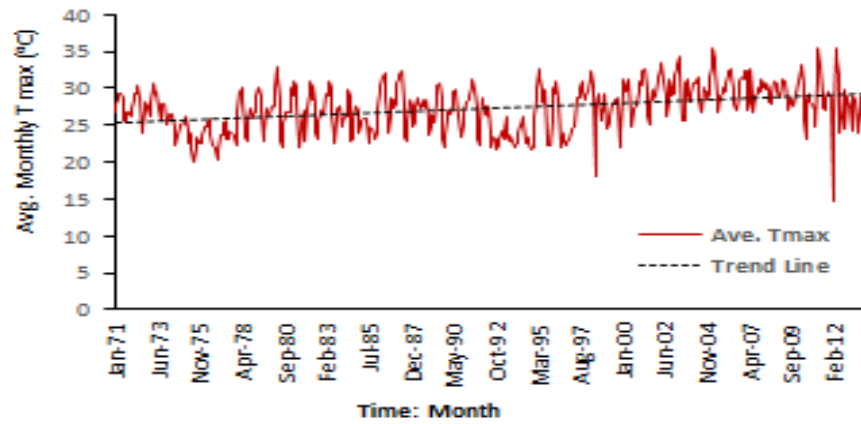
Results obtained by application of the Mann-Kendall test on monthly average daily minimum and monthly average daily maximum and annual average daily minimum and maximum temperature data for all the seven stations in the Geba river basin are analyzed. If the p value is less than the significance level  $\alpha$  (alpha) = 0.05, H0 is rejected. Rejecting H0 indicates that there is a trend in the time series, while accepting H0 indicates no trend was detected in the time series. On rejecting the null hypothesis, the result is said to be statistically significant.

Table 4.15 indicates that the null hypothesis was rejected for all the stations except Hawzien. The monthly maximum temperature shows a greater number of decreasing trends than increasing trends. Decreasing trends were observed at five stations with four stations showing statistically significant trends (Figure 4.18). Hawzien showed a decreasing trend in monthly maximum temperature but it is not statistically significant at 95 % significance level ( $p = 0.264$ ). A statistically significant increasing trend in the monthly maximum temperature was, however, observed at Abiadi and Wukro stations ( $p \leq 0.0001$ ) though the magnitude of the Sen's slope is slightly small 0.008 and 0.009 degree Celsius per year respectively.

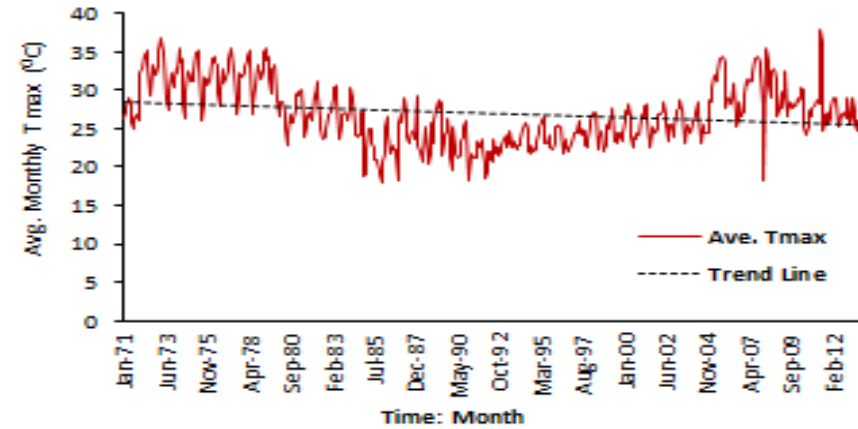
**Table 4.15: Results of the Mann-Kendall test for the average monthly maximum daily temperature data.**

Station name	Mean	Std. deviation	p for $\alpha=0.05$	Sen's slope, $\beta$ ( $^{\circ}\text{C}/\text{y}$ )	Trend nature	Trend significance
Abiadi	27.321	3.083	< 0.0001	0.008	Positive	Yes
Adigudem	26.935	4.024	0.002	-0.004	Negative	Yes
Adigrat	24.221	2.226	< 0.0001	-0.002	Negative	Yes
Hawzien	25.346	3.578	0.264	-0.001	Negative	No
Mek'ele	25.287	2.553	< 0.0001	-0.007	Negative	Yes
Senkata	24.273	2.917	< 0.0001	-0.008	Negative	Yes
Wukro	26.974	3.365	< 0.0001	0.009	Positive	Yes

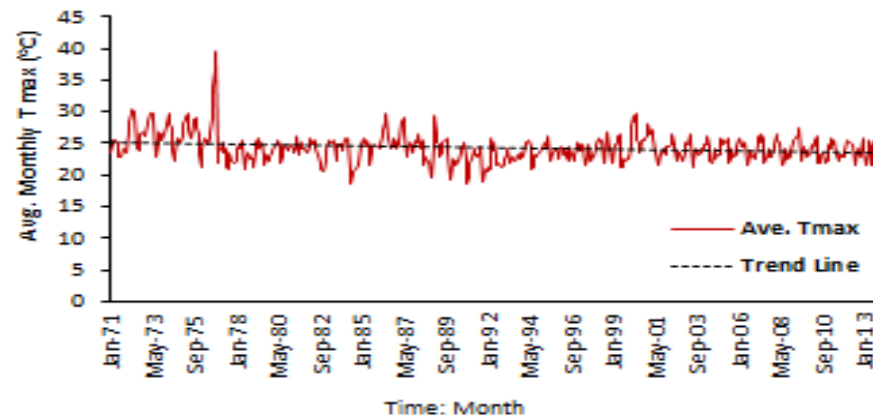
**(a) Average Monthly maximum temperature:  
Abiadi station**



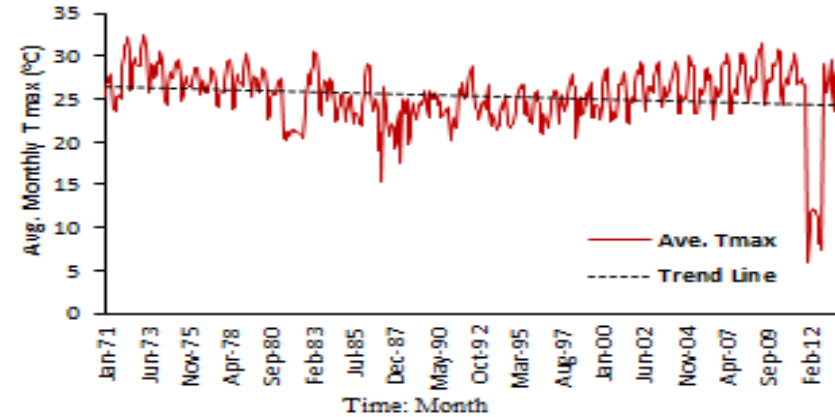
**(b) Average monthly maximum temperature:  
Adigudem station**



**(c) Average monthly maximum temperature:  
Adigrat station**



**(d) Average monthly maximum temperature:  
Hawzien station**



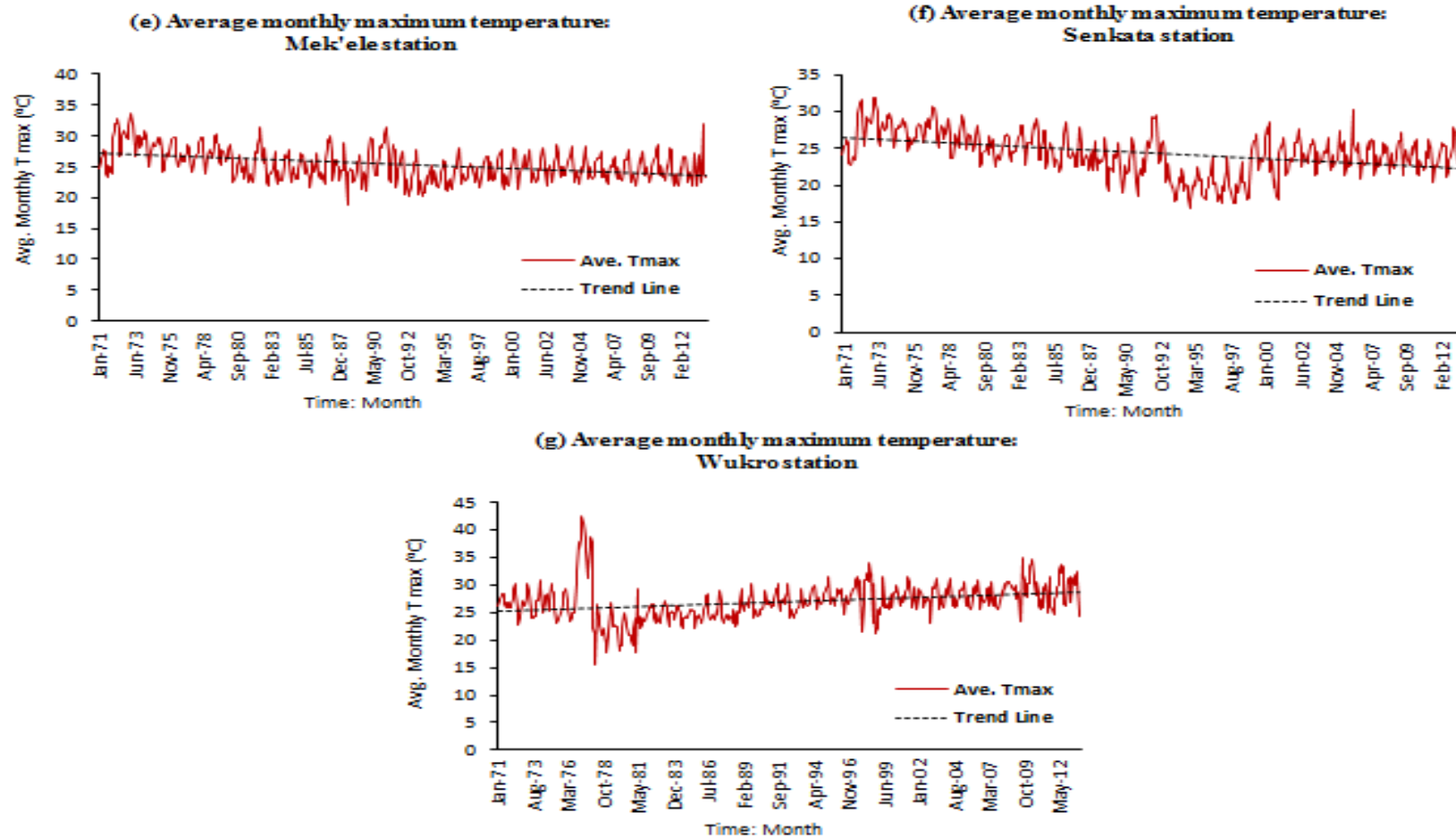
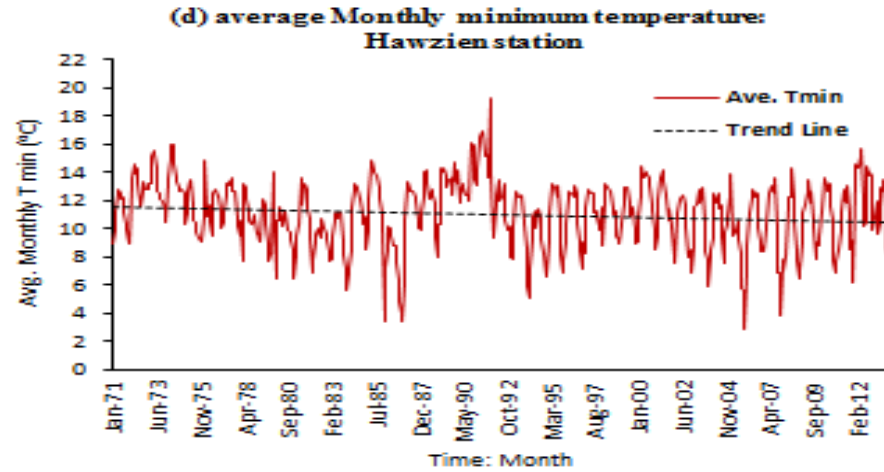
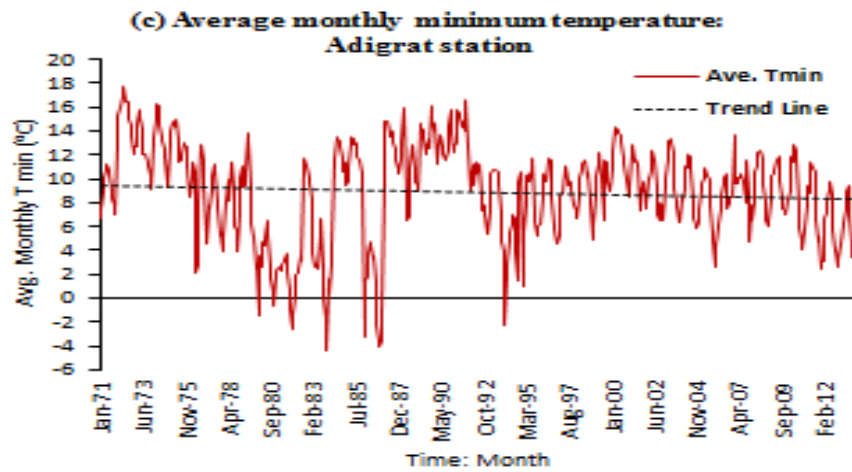
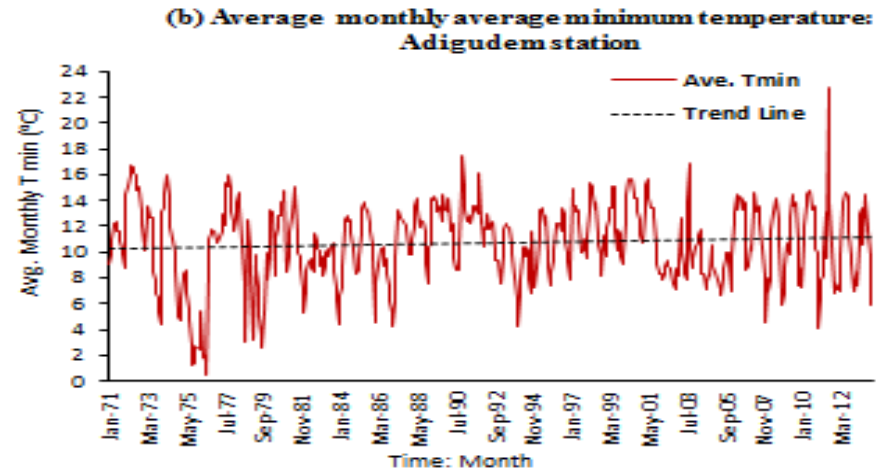
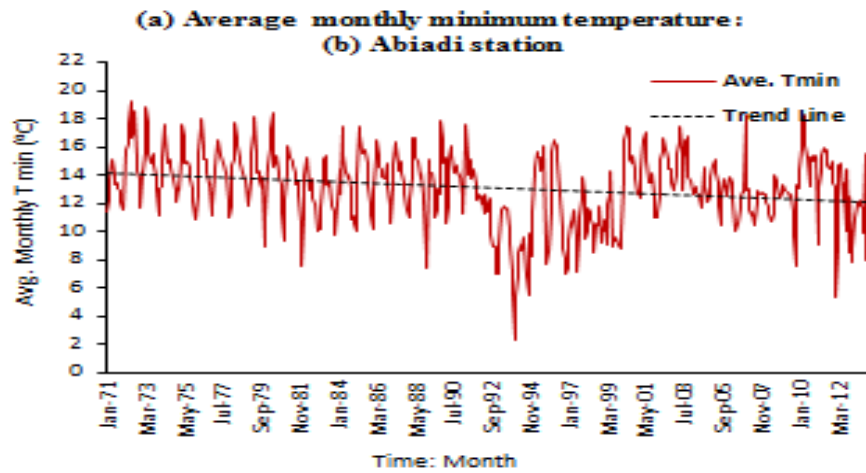


Figure 4.18 Linear trend line corresponding to average monthly maximum temperature at the seven stations (a) Abiadi (b) Adigudem (c) Adigrat (d) Hawzien (e) Mek'ele (f) Senkata and (g) Wukro.

The trends in the time series of average monthly minimum temperature were also investigated. Except Adigudem, all the six stations exhibited a decreasing trend out of which four (Abiadi, Adigrat, Hawzien and Wukro) were statistically significant (Table 4.16). The variable average monthly minimum temperature exhibited a decreasing trend at two stations, but none of these were statistically significant ( $p = 0.069$ ) and ( $p = 0.803$ ) respectively. The increasing trends in average monthly minimum temperature (Figure 4.19) were observed at one station in which it was not statistically significant (Adigudem,  $p = 0.448$ ).

**Table 4.16: Results of the Mann-Kendall test for the average monthly minimum temperature data.**

Station name	Mean	Std. deviation	p for $\alpha=0.05$	Sen's slope ( $^{\circ}\text{C}/\text{y}$ )	Trend nature	Trend significance
Abiadi	13.11	2.56	< 0.0001	-0.004	Negative	Yes
Adigudem	10.65	3.08	0.448	7.07E-4	Positive	No
Adigrat	8.861	4.11	0.000	-0.005	Negative	Yes
Hawzien	11.06	2.38	0.002	-0.002	Negative	Yes
Mek'ele	11.36	2.14	0.069	0.001	Negative	No
Senkata	11.00	2.61	0.803	-1.96E-4	Negative	No
Wukro	12.08	3.41	< 0.0001	-0.009	Negative	Yes





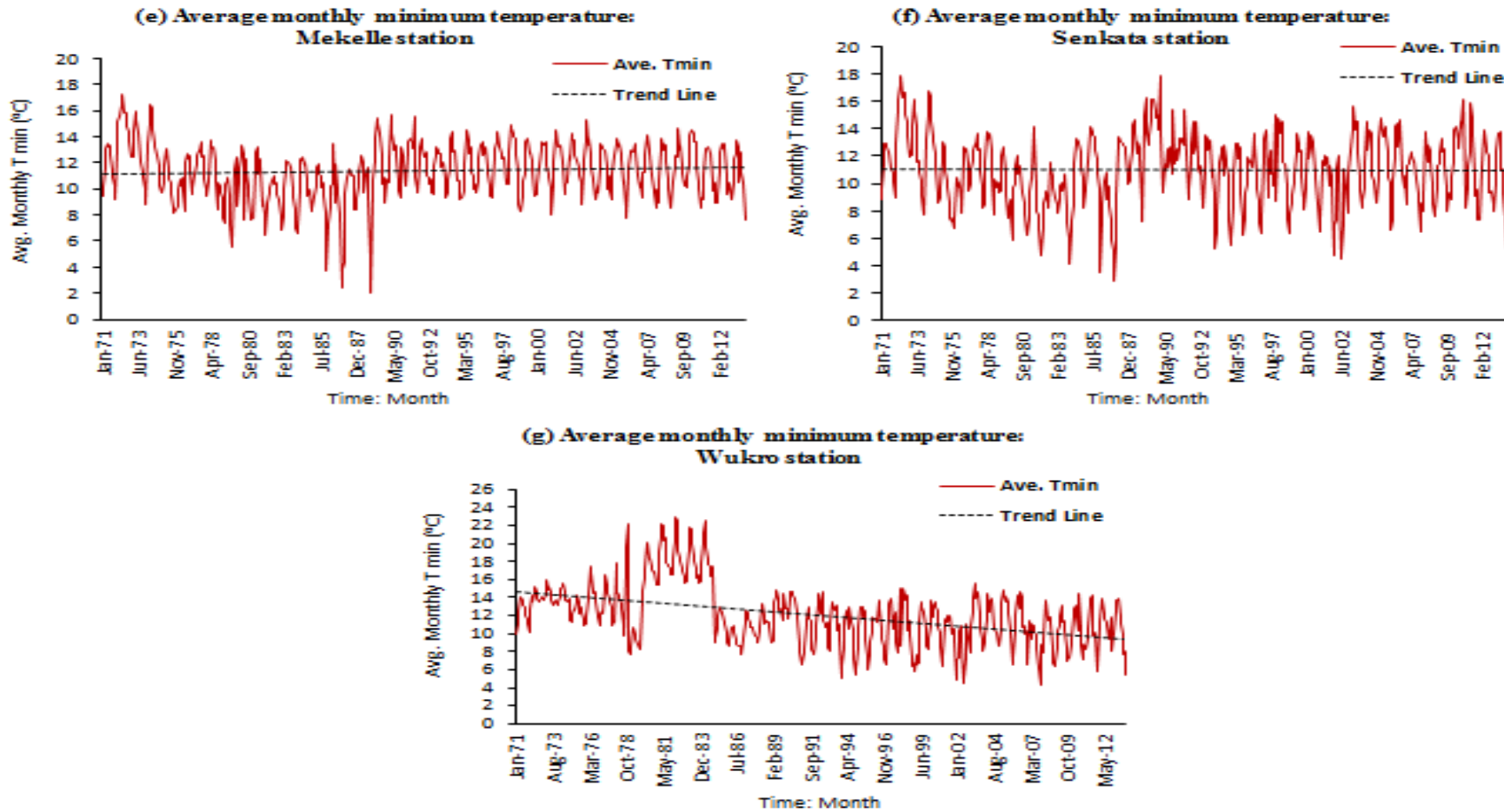
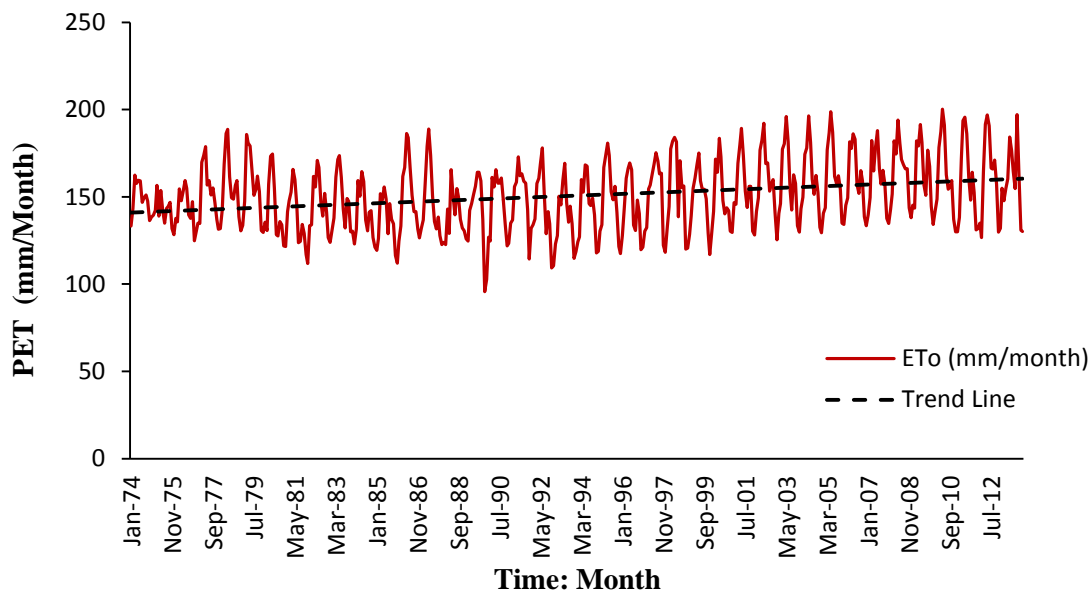


Figure 4.19 Linear trend line corresponding to average monthly minimum temperature at the seven stations (a) Abiadi (b) Adigudem (c) Adigrat (d) Hawzien (e) Mek'ele (f) Senkata and (g) Wukro.

#### **4.3.6 Potential Evapotranspiration Trends**

Mean monthly evapotranspiration (1971-2013) values determined through FAO Penman-Monteith equation for three selected locations and Hargreaves Method for another four stations are shown in Table 4.18. For the sake of continuity trend analysis of ET are presented following which ET estimated is presented and discussed. The results of the application of the MK tests for trend identification of monthly  $ET_0$  are analysed. The overall assessment of the temporal dynamics of the study's monthly trends of PET revealed a value increased roughly after the mid of the third decade of the study period, especially in the warm season indicated higher PET values mainly in March, April and May. The trend tests revealed statistically significant trends at Abiadi, Adigrat, Mek'ele and Wukro stations especially from December to May at 95 % level of confidence. This is largely influenced by temperature dynamics, given the methodology for computing potential evapotranspiration.

The results for the slope magnitude of significant trends (in monthly scales) indicated that the observed trends in Abiadi, Adigrat, Mek'ele and Wukro stations were more rapid in comparison with other stations. The average values of increasing (0.01 mm/month) and slopes of the significant trends in the monthly PET data were observed in the span of study period. Analysis of the impact of climatic variables on the significant increasing trend in monthly PET shows that the increasing trend is mainly caused by a significant increase in maximum air temperature and wind speed during the study period. Figure 4.20 shows the temporal analysis of monthly PET trends for each month in Geba catchment during the period of 1971–2013. Therefore, the highest numbers of significant trends were found in the months of March to April and December to February, respectively.



**Figure 4.20 Variations of average monthly PET for the stations in the Geba Catchment.**

#### 4.3.7 Estimation of Evapotranspiration

The SWAT model result comprises several annual, seasonal and daily hydrologic outputs. Evapotranspiration is among the most important climate parameters of the hydrological cycle following precipitation and temperature, and plays an essential role in mass and energy flows between the atmospheric and terrestrial systems (Allen et al., 1998). The model calculates total evapotranspiration as a sum of evaporation of water intercepted by vegetation, transpiration of the vegetative cover and evaporation from bare soil and open water bodies. Evapotranspiration turns out to be the main and complex component in the water balance of the Geba catchment. Out of the total rainfall, about 54 %, 54 %, 55 % and 53 % (or 556, 582, 633 and 527 mm) water leaves the basin annually through evapotranspiration from the basin in 1973, 1987, 2000 and 2013 LU/LC conditions, respectively (Table 4.17 and Figure 4.21). About 55 % of this evapotranspiration takes place during the rainy (Kiremt) season while the rest 45 % takes place during the dry season. This is mainly due to the fact that there is little rain during the dry season and the vegetation cover is less. The average monthly evapotranspiration varies from minimum of about 19.6 mm in October to maximum of 115 mm in August and is primarily related to the obtainability of rainfall and availability seasonal vegetation cover

**Table 4.17: Temporal Variation of monthly ET of different decades for Geba River basin.**

Month	Decade 1 (1974-1983)	Decade 2 (1984-1993)	Decade 3 (1994-2003)	Decade 4 (2004-2013)
Jan	29.7	32.4	33.46	30.88
Feb	31.33	32.74	35.76	31.92
Mar	33.57	34.60	36.73	32.57
Apr	39.11	39.43	43.12	33.91
May	47.27	44.66	48.19	38.41
Jun	54.01	53.99	58.89	47.94
Jul	98.46	102.84	112.80	91.98
Aug	97.63	103.15	115.10	93.22
Sep	50.55	53.73	59.95	48.40
Oct	19.60	20.69	24.13	18.76
Nov	26.58	31.55	32.51	29.38
Dec	28.20	31.92	32.79	29.56

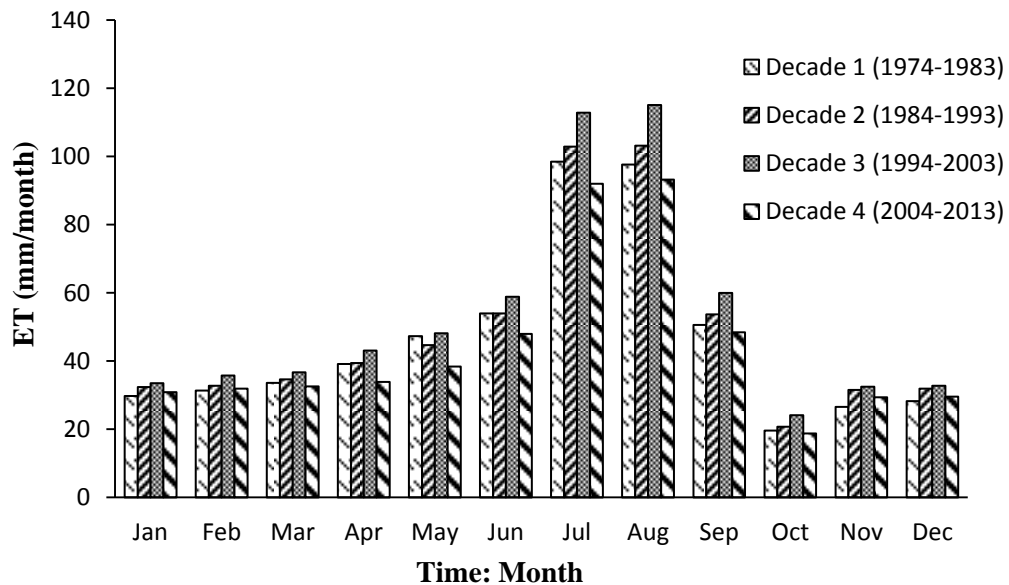


**Figure 4.21 Temporal variation of average monthly ET of different decades in Geba River basin.**

Potential Evapotranspiration (PET) is the most important parameter for agricultural water use planning and water resource management. Historical analysis of monthly PET in the Geba River basin was carried out using Hargreaves and Penman Monteith equation (Hargreaves and Samani, 1985; Allen et al., 1998) for the stations distributed in the basin. The daily PET data for each of the studied stations were calculated for the study period. Then the data is summarized on monthly basis to find the average values per month for the whole basin.

**Table 4.18: Temporal Variation of monthly PET of different stations in the Geba River basin**

Month	Hargreaves Method				Penman Monteith		
	Stations in the Geba River Basin						
	Abiadi	Adigudem	Hawzien	Wukro	Adigrat	Mek'ele	Senkata
Jan	186.45	165.62	191.81	182.92	178.19	181.33	169.87
Feb	188.14	187.72	192.70	188.56	178.76	193.28	168.01
Mar	216.95	194.36	208.69	209.25	186.99	196.63	173.28
Apr	215.21	213.57	211.71	210.42	185.39	201.91	180.77
May	229.81	216.76	217.82	227.08	198.85	209.65	184.38
Jun	205.05	193.64	191.09	205.56	175.61	167.31	169.39
Jul	156.63	144.96	156.47	155.11	149.22	150.99	155.74
Aug	155.75	146.47	159.8	151.21	142.98	148.22	151.28
Sep	166.94	176.12	162.62	163.77	146.6	169.05	160.09
Oct	162.99	165.41	173.45	166.27	155.01	170.24	163.83
Nov	179.48	152.78	182.22	169.80	172.46	177.33	164.83
Dec	182.77	154.73	183.12	178.91	172.15	178.74	166.65

The changes in PET with time was examined by calculating the average monthly evapotranspiration (mm per month) for the whole study period of the stations and plotting monthly time series PET variation for the study period. The highest average monthly PET occurred in the dry season (October to May) and the lowest in the rainy season especially in the months of July and August (Table 4.18). Taking into account the average precipitation in this period equal to 633 mm, water deficit can be expected in the semi-arid region of the Geba River basin, on average. The close relationship between PET and rainfall is a characteristic feature of a transitory semi-arid climate. PET had rather high temporal variability in the multi-year period.

#### **4.3.8 Trend Analysis of River Discharge**

Historical streamflow data are the most essential factors in planning and designing water resource projects. These data are affected by many factors such as natural climate variability and change and anthropogenic activities because of their time-dependent characteristics. To identify the trends in observed river discharge and their occurrence in space and time is one of the main steps in water resources work. The decisions on water resources management and policies could be impacted by the detection of a significant trend in streamflow. As a contribution to assess streamflow in mountain basins in semi-arid areas, seasonal and annual discharge linear trends were estimated for one station in the downstream parts of the studied catchment (i.e., in the outlet). Homogenous data were tested over a 43-year period (1971–2013) for this station.

##### **4.3.8.1 Annual Streamflow Analysis**

In order to analyze the annual streamflow trend significance the Mann-Kendall test was conducted for the streamflow trend analysis as the test results are shown in (Table 4.19). A significance level of  $\alpha = 0.05$  was set as a standard to test trend significance. The trend analysis results show that the Adikumtsi gauge station in the Geba River basin was exhibiting downward streamflow trend, with a test value of 0.677 for the annual streamflow (Table 4.19). Even though, it is not statistically significant at 95 % level of confidence. The Theil-Sen estimator was used to perform the trend slope calculation, where a trend slopes greater or less than zero indicates an upward or

downward streamflow trend (Figure 4.22). To calculate the annual streamflow the trend slope values were also used to create a trend line. Therefore, the result showed that there is a decreasing trend having a Sen's slope magnitude -0.341 mm per year.

**Table 4.19: Results of the Mann-Kendall test for the annual streamflow data.**

Gauging Station	Variable	Period	p for $\alpha=0.05$	Sen's slope	Trend nature	Trend significance
Adikumtsi	River discharge	1971-2013	0.677	-0.341	Negative	No

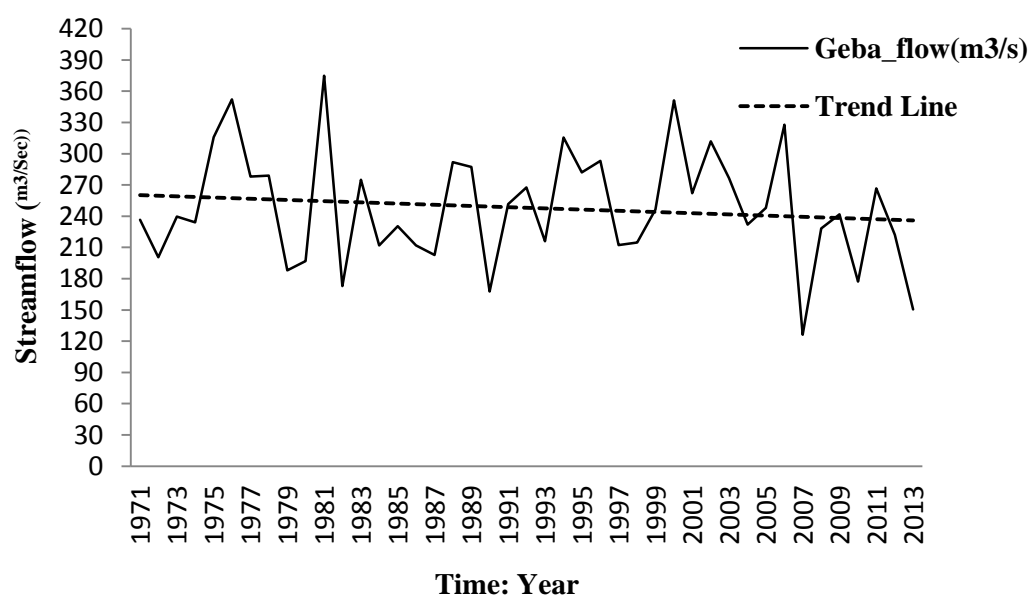


**Figure 4.22 Time series plots for the annual River discharge at the outlet gauge station. The straight line shows the trend line.**

#### 4.3.8.2 Kiremt (Rainy Season) Streamflow Analysis

Prior to studying the analysis results, the year was divided into three seasons: *Kiremt* ('main rains' season, June–September), *Bega* (the dry season, October–February) and *Belg* ('small rains' season, March–May). However, due to different obstructions in the upper stream part of the River basin, the analysis for the *Bega* (the dry season, October– February) and *Belg* ('small rains' season, March–May) were not undertaken for analysis. Using the gauging station data, long-term Kiremt season (June –





#### **4.4 Conclusion**

The purpose of analyzing the extreme rainfall, temperature, evapotranspiration and streamflow data in this study is to determine whether or not the observed time trend in hydrologic/climatic variables during the last 43 years in the Geba River basin is statistically significant. In general, the findings in this study are in agreement with other studies that examined changes in rainfall in East Africa, where slight existence of statistically significant trend in some stations in the frequency and intensity of rainfall over the last 43 years. Even though, there is an increase or decrease trend in the extreme rainfall trend test analysis, the majority of stations did not show statistically significant change over time in the 1971–2013 span of time, except Abiadi station which showed statistically significant increasing trend for most of the extreme rainfall indices (PRCPTOT, R10 mm, R20 mm, R25 mm, P90p, P95p, P99p, SDII, RX1D and RX5D) at the 95 % confidence level. Moreover, the analysis of monthly minimum and maximum temperature records has shown a mix of decreasing and increasing trend for the study period. The monthly maximum temperature exhibits a statistically significant increasing trend in the Abiadi and Wukro stations, and at Adigudem station monthly minimum temperature exhibit positive trend though it is statistically insignificant at 95 % confidence level. Monthly average minimum temperature also showed a decreasing trend at six stations of which four are significant and two are not and one station showed an increasing trends and statistically insignificant trend at the 95 % confidence level. In general, the findings showed that a slightly decrease in the monthly temperature occurred in the 1971 to 2013 span of time. Analysis indicated that there is a decreasing trend in the annual and rainy season streamflow, but not statistically significant. Moreover, there are local factors for the variability of rainfall in the region that can be attributed to local topography (orographic processes) and proximity to sources of moist air and seasonal air mass movements. Therefore, temporal variability of seasonal and annual rainfall may affect the agricultural crop production and future water availability in the undulating topography of the region. Finally results of this study contribute to climate change research in the region and provide inputs for better planning in adapting to changing climate.

## CHAPTER 5

# LAND USE/LAND COVER CHANGE DETECTION

### 5.1 Introduction

As highlighted in Chapter 1 of this thesis, the Geba catchment has undergone significant changes in LU/LC during the past 40 years on account of anthropogenic activities and subsequent conservation efforts towards restoration of degraded land. The primary objective of the present study is to develop a modelling strategy to evaluate the impacts of such changes on the hydrology of the catchment. In an effort towards achieving this objective, detailed analysis of the nature and magnitude of changes in LU/LC within the catchment was carried out using Landsat satellite imagery for multiple dates during the period 1973-2013. The present chapter provides a detailed description of the methodology adopted to map the areal extents of major LU/LC classes and procedures implemented to detect changes in the spatial location and areal extents of these classes over the past 4 decades. While the derived LU/LC maps were used as input to the SWAT model (Chapter 6), results of change detection provided the basis for developing possible future scenarios of LU/LC within the Geba catchment for hydrological impacts assessment (Chapter 7).

### 5.2 Methodology

Multi-temporal, high resolution satellite remote sensing imagery level 1 from Landsat MSS (1973), TM (1987) and ETM (2000/2013) were acquired from the USGS Global Land Cover Facility (GLCF), University of Maryland, USA website. The Landsat MSS imagery is in four channels (2 visible, 2 near-infrared) at 57- meter resolution. Landsat Thematic Mapper (TM) imagery provides seven multispectral channels (3 visible, 1 near-infrared, 2 mid-infrared, 1 thermal-infrared) at 30-meter resolution (120-meter resolution for the thermal-infrared band). Enhanced Thematic Mapper Plus (ETM+) enhances an extra 15-meter resolution panchromatic band and upgraded resolution for the thermal-infrared band (60-meters). All these imageries were acquired within the same season between 27<sup>th</sup> January and 7<sup>th</sup> February during

different years. In the Geba River catchment, these images were utilized for mapping LU/LC dynamics and change assessment. Detailed features of the land surfaces were achieved from the high spectral Landsat with 30 m resolution. This is the scale of the features required for this study. Moreover, Landsat has provided a continuous time series of such data since 1972 to present (Global Land Cover Facility, 2013) that is critical for understanding and recording LU/LC dynamics within the Geba River catchment. Supplementary digital mapping data sets were obtained from the Regional state of Tigray environmental protection, land use and administration Agency, and Ethiopian mapping agency to complement the satellite information.

### 5.2.1 Landsat Multispectral Scanner (MSS)

The Multispectral Scanner (MSS), the world's first Earth observation satellite sensor was launched on-board Landsat 1 in July 1972. Two of the bands are in the visible range while 2 of them are in the reflective near-infrared. These bands have a spatial resolution of 79 m x 79 m. Band 8 (thermal infrared) was only present on the Landsat 3 satellite and had a spatial resolution of 240 m x 240 m (Table 5.1). To study specific resources on Earth the band sensitivities were selected. To identify green reflectance from healthy vegetation MSS band 1 can be used, and band 2 is considered for detecting chlorophyll absorption in vegetation. MSS bands 3 and 4 are ideal for recording near-infrared reflectance peaks in healthy green vegetation and for detecting water-land interfaces.

**Table 5.1: Description of Landsat Multispectral Scanner (MSS).**

Satellite	Date of acquisition	Band	Wavelength (um)	Spectral location	Spectral resolution
MSS	January 27, 1973	1	0.5-0.6	Green	79
		2	0.6-0.7	Red	79
		3	0.7-0.8	Near IR	79
		4	0.8-1.1	Near IR	79
		5	10.4-12.6	Thermal IR	240

### 5.2.2 Landsat Thematic Mapper (TM)

Landsat TM is a multispectral scanning system was launched as a sun-synchronous with a 16-day repetitive cycle. The satellite records reflected/emitted electromagnetic energy in the visible, reflective-infrared, middle-infrared and thermal infrared regions of the spectrum. It crosses the equator on the north-south portion of each orbit at 9:45 a.m. local time. It has a radiometric resolution of 8 bits, a spatial resolution of 28.5 x 28.5 metres for all bands except band 6, which has 120 metres resolution. The seven spectral bands of the TM along with a brief summary of the intended principal applications of each are shown below (Table 5.2).

**Table 5.2: Description of Landsat Thematic mapper (TM).**

Satellite	Date of acquisition	Band	Wavelength (um)	Spectral location	Spectral resolution (m)
Landsat TM	February 12, 1987	1	0.45-0.52	Blue	30
		2	0.52-0.60	Green	30
		3	0.63-0.69	Red	30
		4	0.76-0.90	Near IR	30
		5	1.55-1.75	Mid IR	30
		6	10.4-12.5	Thermal IR	120
		7	2.08-2.35	Mid IR	30

### 5.2.3 Landsat Enhanced Thematic Mapper plus (ETM+)

Landsat 7 uses the Enhanced Thematic Mapper Plus (ETM+) to observe the Earth was launched in 1999. Similar orbits and repeat patterns are used but with major improvements that include an additional band, the panchromatic, which have a resolution of 15 m and a 60 m spatial resolution thermal channel (Table 5.3).

**Table 5.3: Description of Landsat Enhanced Thematic Mapper plus (ETM+).**

Satellite	Date of acquisition	Band	Wavelength (um)	Spectral location	Spectral resolution (m)
Landsat 7 ETM+	February 07, 2000 and January 23, 2013	1	0.45-0.515	Blue	30
		2	0.525-0.605	Green	30
		3	0.63-0.690	Red	30
		4	0.75-0.90	Reflective IR	30
		5	1.55-1.75	Mid IR	30
		6	10.40-12.50	Thermal IR	60
		7	2.09-2.35	Mid IR	30
		Pan	0.52-0.9		15

The software ENvironment for Visualizing Images (ENVI<sup>®</sup>, 2005), was used to accomplish image analysis and classification. The images were processed using supervised classification methods, and incorporating ground surveys information obtained from the Regional state of Tigray environmental protection, land use and administration Agency, and Ethiopian mapping agency. A total of seven land cover classes were considered namely; agriculture, shrub, range, barren land, forest, urban, and water bodies. To check the accuracy of the classification results obtained different approaches were established. These included i) measures of separability of the Regions of Interest (ROIs) (ROIs are used as training classes in the supervised classification); ii) the Confusion Matrix which shows the accuracy of a classification result by comparing a classification result with ground truth information; iii) the overall accuracy, producer and user accuracies, and kappa coefficient. Details of these measures of accuracy can be obtained from the ENVI manual as well as from other remote sensing and image analysis literature.

An important aspect of the present study was the acquisition of multi-temporal Landsat imagery. A distinct temporal path of LU/LC dynamics and change assessment can be identified using multi-temporal remote sensing data, and this information provides increased LU/LC identification competence. Considering the

present scale of spatio- temporal changes in LU/LC in the area, a 40 years period offers a comprehensive LU/LC mapping and change monitoring zone.

However, a major challenge to acquiring satellite imagery in tropical regions is the presence of cloud cover. Climate of the study area is mainly sub-tropical with 80 % of rainfall occurring during the monsoon season from June to September (JJAS) and a marked dry winter season. Therefore, cloud free satellite images are mainly available during the dry period from January to March. Clouds introduce significant noise to an image by obscuring reflectance of radiation from Earth surface materials.

#### **5.2.4 Image Pre-processing**

Reflectance characterizes the ratio of exitance to irradiance, and thus provides a standardized measure which is directly comparable between images where the image bands were calibrated to reflectance values. Reflectance is unit less and hence is measured on a scale from 0 to 1 (or 0-100%). It is important to transform the images into a common base value for simplicity of comparison between different dates. In calibration, the digital numbers were converted into reflectance and the calibrated images were then subjected to the classification process. To qualify image interpretation different colour composites and band ratios were resulted.

The spectral bands 7,4,2 and 5,4,1 which provide a “natural-like” color; 3,2,1 which makes ground features appear in colors similar to their appearance to the human eye; 4,3,2 which is the standard false color composite and 5,4,3 which also gives a lot of information and color contrasts. The effects of environment on the image, such as shading or lighting were reduced by the band ratios. Ratios make available distinctive evidence and spectral reflectance or color differences between surface materials that are often difficult to detect in a standard image. The following ratios were used: 2/3 which differentiates cultivated lands well from bare surfaces; 3/2 and 7/2 separate forests and cultivated lands well; and 5/7 which splits land and water adequately.

#### **5.2.5 Image Processing**

Land use/land cover mapping and subsequent quantitative change detection required geometric registration among MSS, TM and ETM+ scenes, and

radiometric rectification to adjust for differences in atmospheric conditions, viewing geometry and sensor noise and response (Lillesand et al., 2004; Jensen, 2005).

### 5.2.6 Classification Accuracy Assessment

In the process of investigating remote sensing data, accuracy assessment of land use/land cover mapping is an important stage. It provides evidence about errors in the data, for improvement of the mapping procedure, and allows for future users of the classification to assess the suitability of data for particular applications. This may be done by using different approaches. The most common one is by expressing overall and category accuracies (Lillesand et al., 2004). Overall classification accuracy provides a general picture of how a specific classifier is performing while the user and producer accuracies help to ascertain whether the classified pixel actually represents the relevant information class on the ground (Lillesand et al., 2004).

Overall classification accuracy is the ratio of number of correct classifications to total number of samples evaluated (Congalton and Green, 1999). The overall accuracy constitutes the percentages of correctly classified classes lying along the diagonal and is determined as in Eq. 5.1.

$$\text{Overall accuracy} = \frac{\sum(\text{correctly classified classes along diagonal})}{\sum(\text{row total or column total})} \quad (5.1)$$

Producer's accuracy is a measure of how accurately the analyst classified the image data by category (columns). Producer accuracy details the errors of omission. An error of omission results when a pixel is incorrectly classified into another category. It is an important measure because the producers of spatial data are interested in knowing how well a particular area on the Earth surface can be mapped. Producer accuracies result from dividing the number of correctly classified pixels in each category (on the major diagonal) by the number of reference pixels used for that category (the column total). Producer accuracy is calculated as in Eq. 5.2.

$$\text{Producer accuracy} = \frac{\text{number of correctly classified item in a column}}{\text{total number of items verified in a row}} \quad (5.2)$$

User accuracy represents the probability that a sample from the classified image actually represents that category on the ground. User accuracy details errors of commission. An error of commission indicates the probability that a pixel classified into a given category actually represents that category on the ground. User accuracy is important for users of spatial data because users are principally interested in knowing how well the spatial data actually represents what can be found on the ground (Lillesand et al., 2004). The user accuracy is computed by dividing the number of correctly classified samples of the relevant class by the total number of samples that were verified as belonging to that class. User accuracy is determined as in Eq. 5.3.

$$\text{User accuracy} = \frac{\text{number of correctly classified item in a row}}{\text{total number of items verified in a row}} \quad (5.3)$$

The results were then tabulated in the form of an error matrix. The columns of the error matrix table define the final stage data and the rows define the initial image classes. The values in the cells of the table indicate how well the classified data agrees with the reference data. The diagonal elements of the matrix indicate correct classifications. The higher the proportion of the pixels within the user and producer accuracies for the individual class in question, the more accurate the classified maps are.

## **5.2.7 Image Classification**

### **5.2.7.1 Selection of Training Areas**

The location of training sample is normally done by fieldwork or the use of aerial photographs and map interpretation (Mather, 1993). On the other hand, in the lack of consistent ground data, the choice of training data has to be considered to some extent subjective. For the Geba River catchment, no reliable supplementary data are available; hence, signatures were chosen visually through combining spectral and contextual information. It was then necessary to determine appropriate band sets as



input for land use/land cover classification. Various conversions were carried out on the original bands to achieve the condition.

#### **5.2.7.2 Transformations and Indices**

To enhance certain characteristics of the land surface, Landsat image bands were combined in transformations and indices with physical meaning. To achieve image enhancement several techniques can be used. The process of visually interpreting digitally enhanced imagery endeavours to improve the harmonizing capabilities of the human mind and the computer. To emphasize different land use/land cover areas, different bands of a multi-spectral image were combined to specify the nature of the landscape involved. This was compulsory for the collection of training data for successive classification of the images. In this study, the following types of transformations and indices were applied.

#### **5.2.7.3 False Color Composition (FCC)**

Jensen (2005) and Lillesand et al. (2004) investigated that digital images are typically presented as additive colour composites that are commonly composed of three bands, each assigned to one of the basic colours: Red, Green and Blue (RGB). The RGB displays are applied comprehensively in digital processing to display normal colour, false colour infrared and arbitrary colour composites (Lillesand et al., 2004; Jensen, 2005). Two types of colour composites i.e. a false colour composite (FCC) and a natural colour composite (NCC) are distinguished here. It was essential to identify the reflection features of the fundamental cover types of the earth surface to generate a clear feature on the Landsat images. The best FCC depends on the purpose of the study. For the Geba River catchment, from several FCC combinations of the Landsat bands (Table 5.1 to 5.3) created for visual interpretation, the best combinations were: (bands 7, 4, and 2); and (bands 4, 3 and 2) in red, green and blue respectively.

#### **5.2.7.4 Supervised Classification**

Corresponding to user defined regions of interest (ROIs) or training classes which are selected as representative areas to be mapped in the output the supervised

classification technique is applied to cluster pixels in a dataset into classes. Supervised classification techniques include Parallelepiped, Minimum Distance, Mahalanobis Distance, Maximum Likelihood, Spectral Angle Mapper (SAM), and Binary Encoding. Training classes were defined prior to performing supervised classification. Hence, in this study the Maximum Likelihood classification has been used among others.

#### 5.2.7.5 Maximum Likelihood Classification

In this study, the Maximum Likelihood algorithm was used for the classification. Maximum Likelihood is a supervised classifier, i.e. the researcher oversees the classification by identifying illustrative or training areas. These areas are then described mathematically and accessible to the computer algorithm, which classifies the pixels of the whole scene into the corresponding spectral class that performs to be most identical. The distribution of the response configuration of each class is supposed to be normal (Gaussian) in the Maximum Likelihood classification. Within each class the records ought to comprise all spectral variation. In principle, a statistically based algorithm needs a minimum of  $n+1$  pixel for exercise in each class, where  $n$  is the number of wavelength bands. Nevertheless, in practice, the use of a minimum of  $10n$  to  $100n$  is recommended (Lillesand et al., 2004).

#### The Maximum Likelihood Algorithm Consists of Two Steps:

Model parameters assessment which defines the a posteriori probability a given pixel be appropriate to class  $i$ , given that the pixel has feature  $f$ . This probability is calculated using Bayes Rule of conditional probability Eq. 5.4.

$$p(i / f) = \frac{p(f / i)p(i)}{\sum_j p(f / i)p(i)} \quad (\text{Eq 5.4})$$

Where  $p(f/i)$  is the probability of a pixel having feature  $f$ , given that it fits to class  $i$ , and  $p(i)$  is the probability that class  $i$  occurs on the image of interest (also referred to as the a priori probability). For optimal results the discriminant functions, establish the decision rule to classify a pixel is regularly set to be equal to the a posteriori probability. It is specified as follows (Eq. 5.5): if a pixel satisfies the equation, then it is allocated to

class  $i$ .

$$D_i(f) = D_k(f) \epsilon \quad (\text{Eq.5.5})$$

### 5.2.8 Land Cover Classification System

The FAO/LCCS legend structure land cover classification (LCCS) (Food and Agricultural Organization, 2005) was used to accomplish land cover synchronization within Africa and on a global scale. All amendments in the classifications were carried out keeping in view the area under study and application of the divided land cover maps i.e. hydrological modelling. Figure 5.1 provides an overview of the methodology adopted for LU/LC change analysis and detection. Landsat MSS, TM and ETM+ Satellite images; field observation and collection of information on LU/LC were verified and corrected for their inconsistencies, e.g., temporal inconsistencies of historical land use/land cover maps.

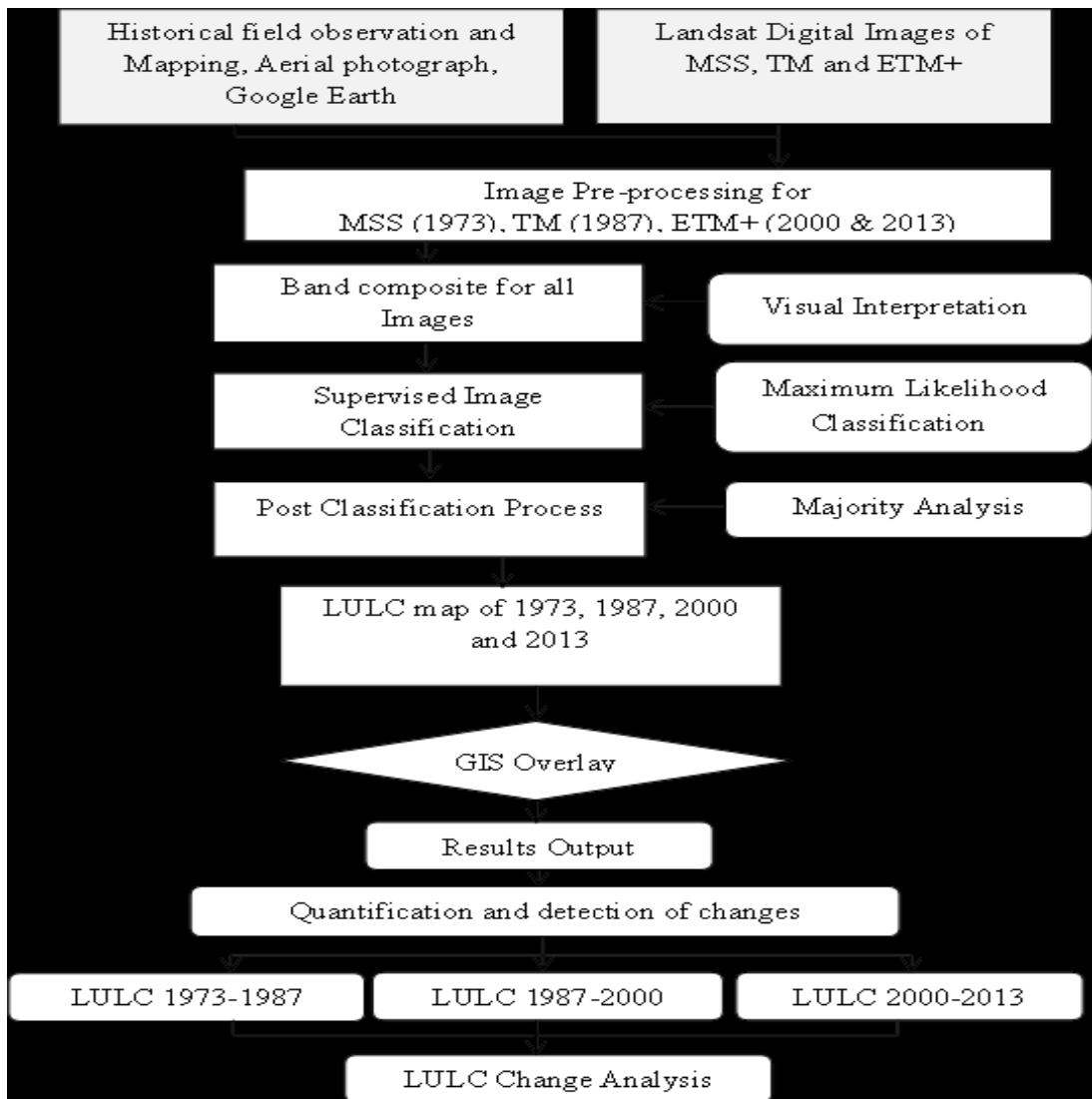


**Figure 5.1 Methodology adopted for LU/LC change analysis and detection.**

## 5.3 Results and Discussion

### 5.3.1 Land use/land cover Changes at Watershed Level

The spatial extent of each land use/land cover type for 1973, 1987, 2000 and 2013 are shown in Table 5.4. The geographical representation of spatial distribution of land use/land cover classes for 1973, 1987, 2000 and 2013 are respectively shown in Figures 5.2 to 5.5.

### 5.3.1.1 Spatial Distribution of Land use/land cover Classes of 1973 and 1987

The 1973 and 1987 land use/land cover map classification as shown in Figure 5.2 and 5.3 have been produced from the Landsat MSS and TM imagery, respectively. The 1973 land use/land cover classification indicates large areas of shrubs mainly scattered in all landscape escarpments occupying 1951.79 Km<sup>2</sup> (38 %). Shrub lands are associated with scattered trees and bush thickets (short height) as well as open grasslands. Agricultural/cultivated land, which is concurrently used as grazing areas after crop harvest, formed the next dominant covering 1406.71 Km<sup>2</sup> of the total study area representing 27.39 %. Rangeland formed another class accounted to 1124 Km<sup>2</sup> indicating 21.88 % of the study area. Barren land coverage is 389.56 Km<sup>2</sup> of the total area representing 7.58 %. The forest areas covering 215.19 Km<sup>2</sup> (4.19 %) form mostly tall and branched trees and less shrubs or no undergrowth being the dominant vegetation. The fresh water body and urban areas formed another class occupied very small area of the land surface demonstrating an extent of less than 1 % in the Geba catchment.

**Table 5.4: Spatial distribution land use/land cover classes during 1973 to 2013 time period in the Geba River basin.**

LU/LC Type	1973		1987		2000		2013	
	Area		Area		Area		Area	
	(km <sup>2</sup> )	(%)	(km <sup>2</sup> )	(%)	(km <sup>2</sup> )	(%)	(km <sup>2</sup> )	(%)
BARR	389.56	7.58	573.29	11.16	923.08	17.97	449.73	8.76
RNGE	1124.00	21.88	919.84	17.91	849.64	16.54	605.78	11.79
AGRL	1406.71	27.39	1696.50	33.03	2023.04	39.39	2196.10	42.75
RNGB	1951.79	38.00	1714.89	33.39	1201.06	23.38	1537.67	29.94
FRST	215.19	4.19	190.67	3.71	82.77	1.61	180.22	3.51
URBN	24.58	0.48	27.52	0.54	37.87	0.74	144.35	2.81
WATR	24.75	0.48	13.88	0.27	19.13	0.37	22.73	0.44
Total	5136.58	100	5136.58	100	5136.58	100	5136.58	100

Description: BARR-Barren land; RNGE-Rangeland; AGRL-Agricultural land; RNGB-Shrub land; FRST-Forest; URBN-Urban area; WATR-Water bodies

**Table 5.5: Land use/land cover change detection matrix.**  
**(a) 1973 to 1987**

		Initial State							Class Total
		BARR	RNGE	AGRL	RNGB	FRST	URBN	WATR	
Final State	LU/LC Type	Area (Km <sup>2</sup> )	Area (Km <sup>2</sup> )	Area (Km <sup>2</sup> )	Area (Km <sup>2</sup> )	Area (Km <sup>2</sup> )	Area (Km <sup>2</sup> )	Area (Km <sup>2</sup> )	Area (Km <sup>2</sup> )
		BARR	<b>352.2</b>	25.28	50.49	145.32	0	0	0
	RNGE	0	<b>892.51</b>	0	27.33	0	0	0	919.84
	AGRL	37.38	158.74	<b>1353.26</b>	136.24	0	0	10.87	1696.49
	RNGB	0	38.25	0	<b>1619.48</b>	57.16	0	0	1714.89
	FRST	0	9.22	0	23.42	<b>158.03</b>	0	0	190.67
	URBN	0	0	2.96	0	0	<b>24.56</b>	0	27.52
	WATR	0	0	0	0	0	0	<b>13.88</b>	13.88
	Class Total	389.58	1124	1406.71	1951.79	215.19	24.56	24.75	<b>5136.58</b>
	Class change	45.18	107.9	105.5	206.88	4.73	0	0	
	Image difference	183.73	-204.16	289.79	-236.9	-24.52	2.94	-10.87	
<b>Producer's Accuracy</b>					<b>User's Accuracy</b>				
	BARR	= 352.2/389.58 = 90.41%			BARR = 352.2/573.29 = 61.4%				
	RNGE	= 892.51/1124 = 79.4%			RNGE = 892.51/919.84 = 98.03%				
	AGRL	= 1353.26/1406.71 = 96.2%			AGRL = 1353.26/1696.49 = 79.77%				
	RNGB	= 1619.48/1951.79 = 82.97%			RNGB = 1619.48/1714.89 = 94.44%				
	FRST	= 158.03/215.19 = 73.44%			FRST = 158.03/190.67 = 82.88%				
	URBN	= 24.56/24.56 = 100%			URBN = 24.56/27.52 = 89.24%				
	WATR	= 24.75/24.75 = 100%			WATR = 24.75/24.75 = 100%				
Overall accuracy = (352.2+892.51+1353.26+1619.48+158.03+24.56+24.75)/5136.58 = <b>87.07%</b>									

**(b) 1987 to 2000**

		Initial State							Class Total
Final State	LU/LC Type	BARR	RNGE	AGRL	RNGB	FRST	URBN	WATR	Area (Km <sup>2</sup> )
		Area (Km <sup>2</sup> )	Area (Km <sup>2</sup> )	Area (Km <sup>2</sup> )	Area (Km <sup>2</sup> )	Area (Km <sup>2</sup> )	Area (Km <sup>2</sup> )	Area (Km <sup>2</sup> )	Area (Km <sup>2</sup> )
	BARR	<b>528.25</b>	20.80	60.90	313.12	0	0	0	923.08
	RNGE	0	<b>730.35</b>	<b>0</b>	119.29	0	0	0	849.64
	AGRL	45.04	129.88	<b>1632.03</b>	130.71	85	0	0	2023.04
	RNGB	0	19.23	0	<b>1131.19</b>	50.64	0	0	1201.06
	FRST	0	7.54	0	20.58	<b>54.65</b>	0	0	82.77
	URBN	0	7	3.56	0	0	<b>27.52</b>	0	37.87
	WATR	0	0	0	0	0	0	<b>13.88</b>	13.88
	Class Total	573.29	919.84	1696.5	1714.889	190.672	27.52	13.88	<b>5136.58</b>
	Class change	45	189.75	64.46	583.7	135.64	0	0	
	Image difference	<b>349.79</b>	<b>-70.2</b>	<b>326.54</b>	<b>-513.83</b>	<b>-107.9</b>	<b>10.35</b>	<b>5.25</b>	

**Producer's Accuracy**

BARR = 528.25/573.29 = 92.14%

RNGE = 730.35/919.84 = 73.4%

AGRL = 1632.03/1696.5 = 96.2%

RNGB = 1131.19/1714.89 = 66%

FRST = 54.65/190.67 = 28.66%

URBN = 27.52/27.52 = 100%

WATR = **13.88/13.88** = 100%

**User's Accuracy**

BARR = 528.25/923.08 = 57.23%

RNGE = 730.35/849.64 = 86%

AGRL = 1632.03/2023.04 = 80.67%

RNGB = 1131.19/1201.06 = 94.18%

FRST = 54.65/82.77 = 66.03%

URBN = 27.52/37.87 = 72.67%

WATR = 13.88/13.88 = 100%

Overall accuracy = (528.25+730.35+1632.03+1131.19+54.65+27.52+13.88)/5136.58 = **80.17%**

**(c) 2000 to 2013**

		<b>Initial State</b>							
		BARR	RNGE	AGRL	RNGB	FRST	URBN	WATR	Class Total
	LU/LC Type	Area (Km <sup>2</sup> )	Area (Km <sup>2</sup> )	Area (Km <sup>2</sup> )	Area (Km <sup>2</sup> )	Area (Km <sup>2</sup> )	Area (Km <sup>2</sup> )	Area (Km <sup>2</sup> )	Area (Km <sup>2</sup> )
	<b>Final State</b>	BARR	<b>368.49</b>	19.13	62.11	0	0	0	0
RNGE		0	<b>674.68</b>	0	0	0	0	0	674.68
AGRL		46.14	119.97	<b>1953.08</b>	76.91	0	0	0	2196.1
RNGB		428	28.89	0	<b>1107.20</b>	3.81	0	0	1537.67
FRST		80	6.98	0	13.83	<b>78.96</b>	0	0	180.22
URBN		0	0	4.25	10.23	0	<b>107.87</b>	0	144.35
WATR		0	0	3.60	0	0	0	<b>19.13</b>	22.73
Class Total		923.08	849.64	2023.04	1201.06	82.77	107.87	19.13	<b>5136.58</b>
Class change	554.14	174.97	69.96	192.97	3.81	0	0		
Image difference	-	-	173.06	336.61	97.45	106.48	3.6		

**Producer's Accuracy**

BARR = 368.49/923.08 = 39.92%  
 RNGE = 674.68/849.64 = 76.23%  
 AGRL = 1953.08/2023.04 = 96.54%  
 RNGB = 1107.20/1201.06 = 92.19%  
 FRST = 78.96/82.77 = 95.40%  
 URBN = 107.87/107.87 = 100%  
 WATR = 19.13/19.13 = 100%

**User's Accuracy**

BARR = 368.49/449.73 = 81.94%  
 RNGE = 674.68/674.68 = 100%  
 AGRL = 1953.08/2196.1 = 88.93%  
 RNGB = 1107.20/1537.67 = 72.01%  
 FRST = 78.96/180.22 = 43.81%  
 URBN = 107.87/144.35 = 100%  
 WATR = 19.13/19.13 = 74.73%

Overall accuracy = (368.49+674.68+1953.08+1107.2+78.96+37.87+19.13)/5136.58 = **82.53%**



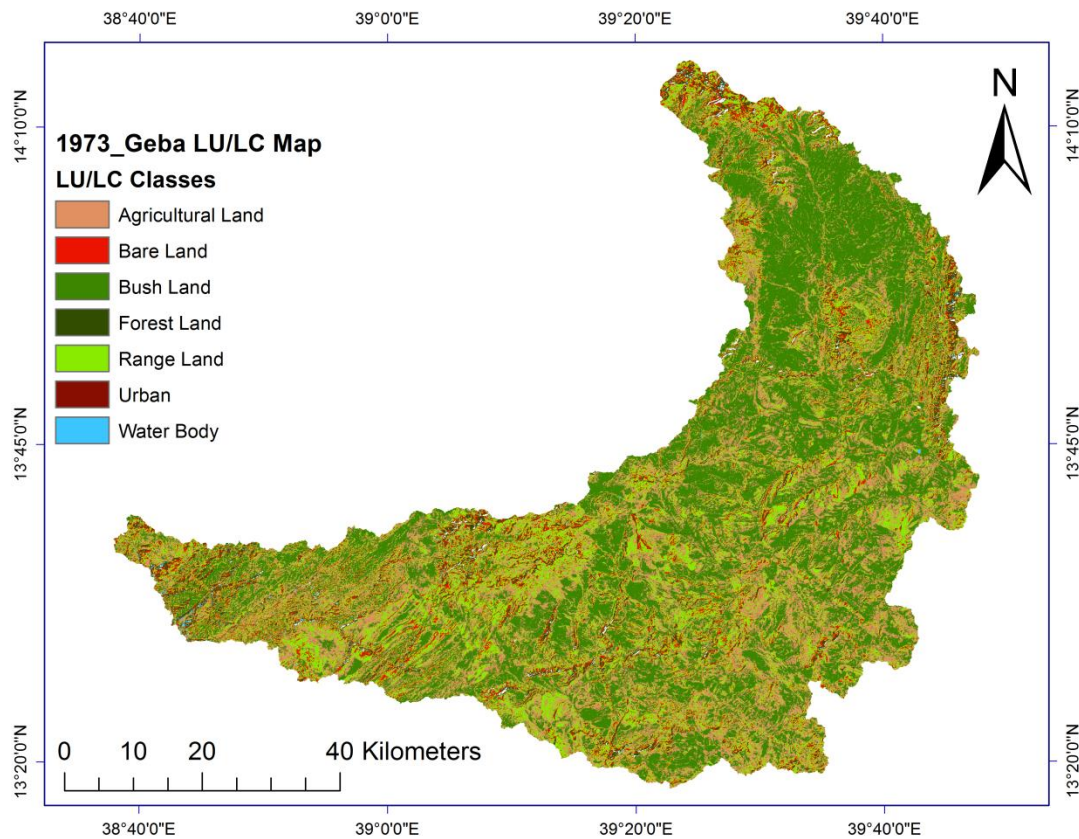


**Figure 5.2 Land use/land cover map in Geba River basin in 1973.**

The magnitude of coverage of land surface features for 1987 was slightly similar with the 1973 land use/land cover map as graphically represented in Figure 5.3. Among all the land cover classes, shrub, agriculture and rangeland areas had the largest extents covering about 1714.89, 1696.5 and 919.84 Km<sup>2</sup> (33.39, 33.03 and 17.91 %) of the land surface, respectively. The next large categories included barren land 573.29 Km<sup>2</sup> (11.16 %). The smallest category was occupied by forest, water bodies and urban areas with 4.52 % of the study area representation.

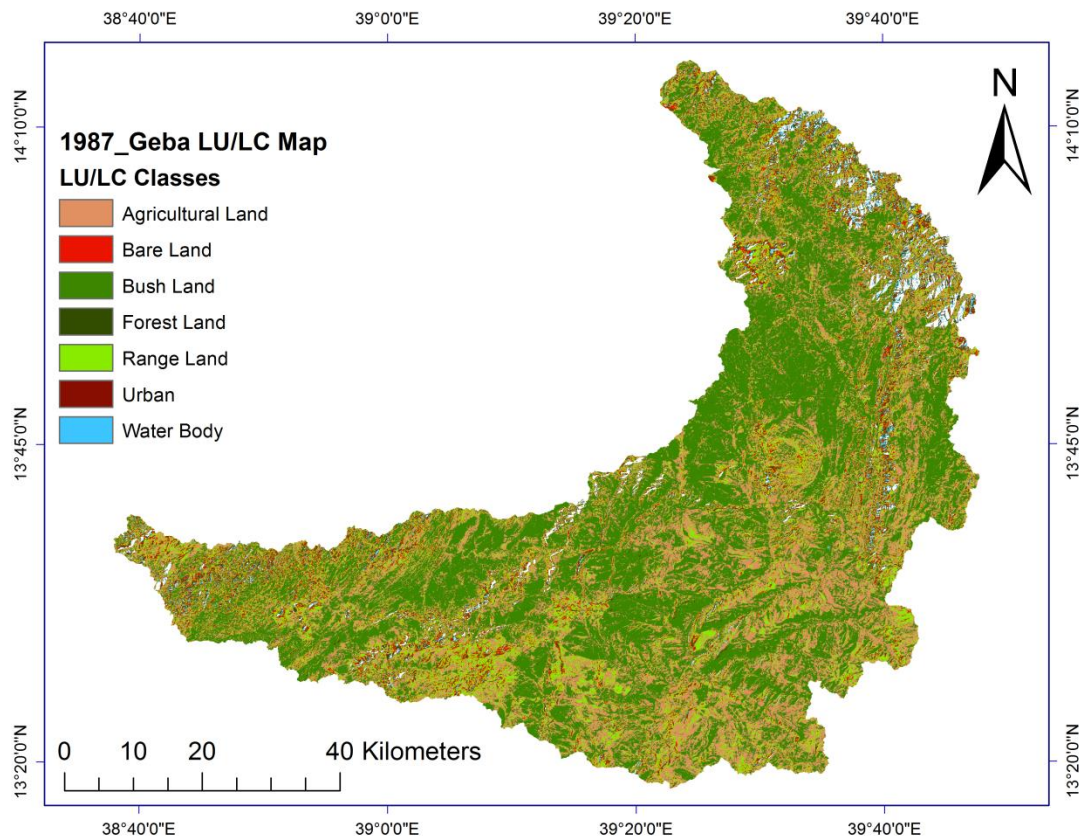


**Figure 5.3 Land use/land cover map in Geba River basin in 1987.**

It is revealed that there is increased of agricultural land and decline in shrub land, forest, rangeland, and water bodies over the last 14 years period from 1973 to 1987 land use/land cover condition. This scenario is primarily happened because of the growing rate of population that triggered the intensification demand for new agricultural land, fuel wood and as a source of economy which in turn brought about reduction on other land use/land cover types of the study area. For example, the forest and shrub land coverage during the 1973 LU/LC map was 4.19 % and 38 % of the total area of the catchment while this value were declined to 3.71 % and 33.39 % on the 1987 LU/LC map, respectively. This is perhaps because of the human intervention towards deforestation activities that has taken place for the determination of agriculture strengthening and fuel wood by clearing forests.

### 5.3.1.2 Spatial Distribution of Land use/land cover Classes of 2000 and 2013

The 2000 and 2013 land use/land cover map classification as shown in Figure 5.4 and 5.5 have been produced from the Landsat ETM+ imagery. The 2000 land use/land cover map classification in Geba River basin, resulted the agricultural land constituting the highest share with 39.39 %, followed by shrub, barren, and rangeland with 23.38 %, 17.97 % and 16.54 %, respectively. Forest area covered 1.61 % and of the total area. While urban area and water bodies took the minimum area coverage which is about 1 % as shown in Table 5.4.

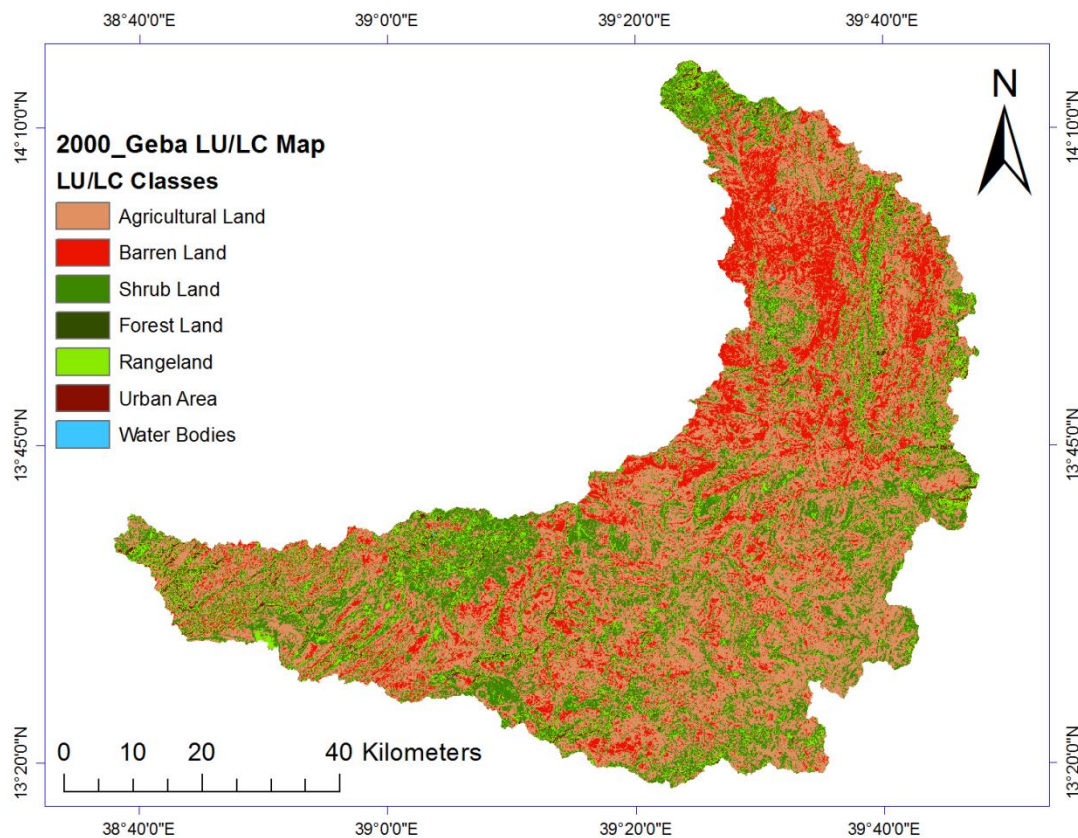


**Figure 5.4 Land use/land cover map in Geba River basin in 2000.**

The classification for 2013 land use/land cover map of Geba basin resulted with seven classes. Agricultural land took the highest portion covering 44.58 % of the total area, followed by shrub, range and barren land with 29.94 % and 11.79 %, and 8.76 %, respectively. Forest land and urban area constituted 3.51 % and 2.81 %, respectively. Water bodies took the smallest share with less than 1 % (Table 5.4 and Figure 5.5).

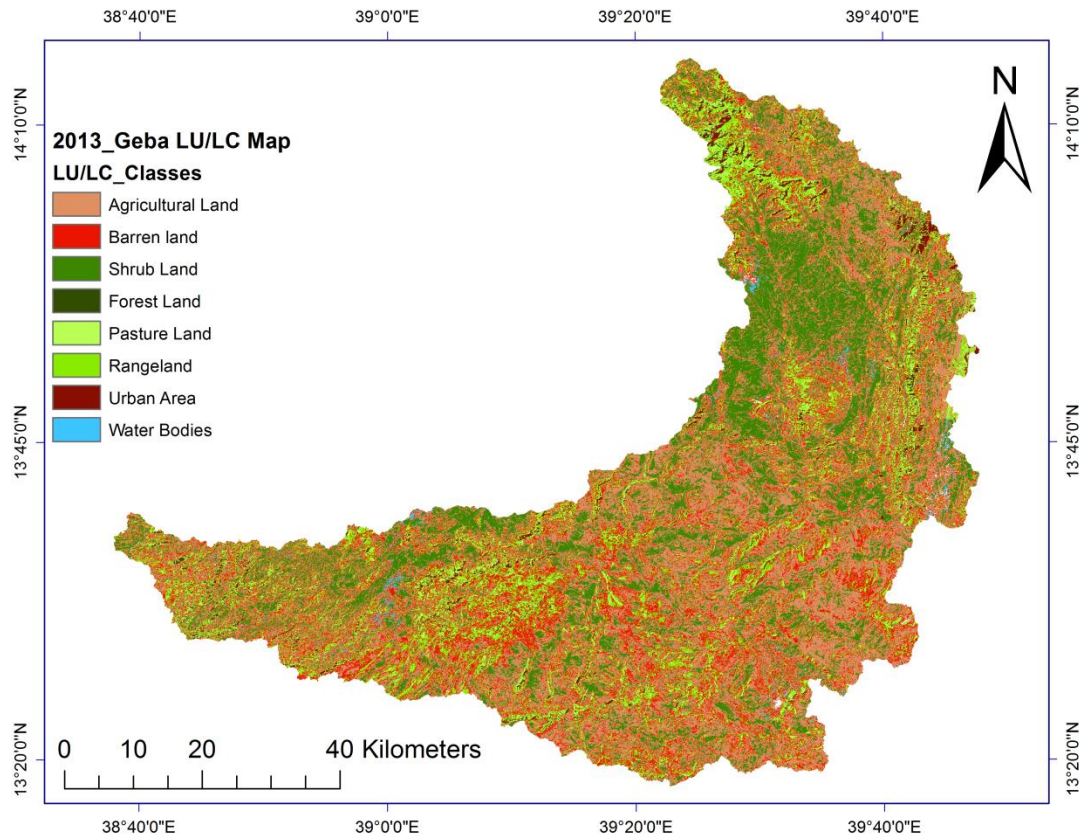


**Figure 5.5 Land use/land cover map in Geba River basin in 2013.**

The variations in LU/LC maps of the study area for the corresponding years are shown in Figures 5.2 to 5.5. The general result recommend that there has been a decrease in vegetation cover especially the shrub and forest land from 1973 to 2000, while areas like agriculture and barren land have increased over this time span. The land use/land cover in Geba catchment for the corresponding years confirm a significant transformation, in 1973 shrub land, rangeland and forest covered 38 %, 21.88 % and 4.19 % of the total area, respectively. Agricultural land shared 27.39 % and urban area constituted less than 1 % of the total area. However, in 1987 after fourteen years bush land declined to 33.39 % while agricultural land and barren land increased to 33.03 %, 11.16 %, respectively (Figure 5.6). As it is shown in these conditions in 1973 the density of the population in the area was low. However, during the 1973 to 1987 time period, the LU/LC of the area had transformed due to major socioeconomic changes that had taken place.



In 2000, after three decades, agricultural land and barren land constitute 39.39 %, 17.97 % of the total area, respectively. While shrub land and forest decreased to 23.38 % and 1.61 %, respectively. The urban area and water body in this land cover map has not been relatively changed progressively as compared to other land cover classes. The progressive expansions in agricultural land by clearing forests and shrub lands turn signals of a constant growth in population density (Bewket and Sterk, 2005).

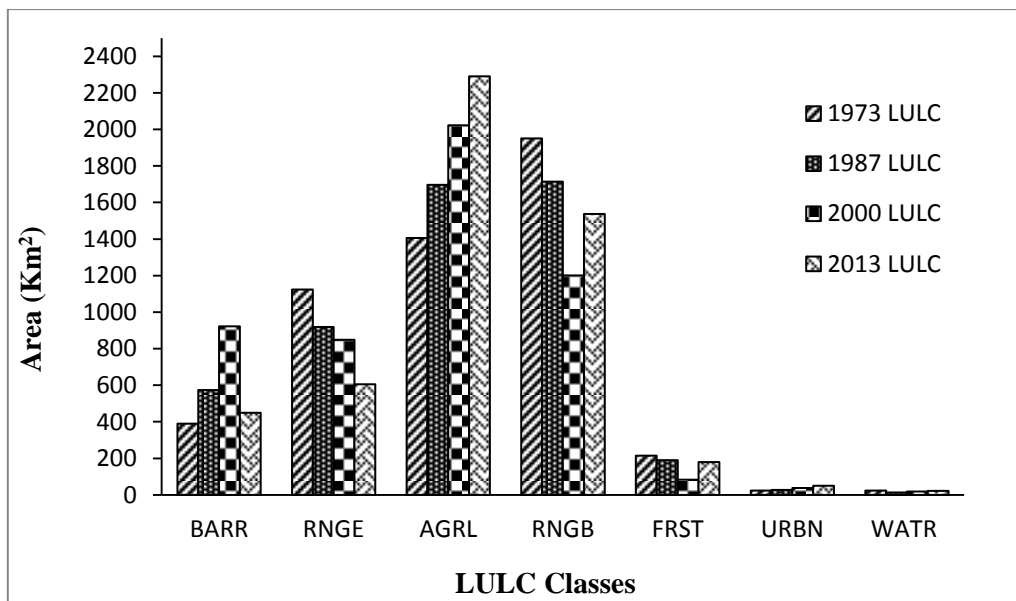


**Figure 5.6 Changes in LULC in the Geba River basin from 1973 to 2013.**

In 2013, the agriculture, shrub land, forest and urban area coverage in Geba river basin increased to 42.75 %, 29.94 %, 3.51 % and 2.81 %, respectively from 39.39 %, 23.38 %, 1.61 % and 0.74 %, respectively in 2000 land cover map. On the contrary, barren land and rangeland decreased to 8.76 % and 11.79 %, respectively from 17.97 % and 16.54 % in 2000 land cover map. Water bodies in the area increased insignificantly from 0.37 % to 0.44 % in the specified period.

### 5.3.2 Rate of Land Use/Land Cover Changes

Comparing the four land use/land cover maps, it was able to determine changes in land cover from 1973 to 2013 with respect to the total area of the watershed.

**Table 5.6: Land use/land cover types and changes from 1973-2013 in the Geba River basin.**

LU/LC Type	% change with respect to total area (1973-1987)		% change with respect to total area (1987-2000)		% change with respect to total area (2000-2013)	
	(%)	Rate (km <sup>2</sup> /yr)	(%)	Rate (km <sup>2</sup> /yr)	(%)	Rate (km <sup>2</sup> /yr)
BARR	3.58	13.12	6.81	26.91	-9.22	-36.41
RNGE	-3.97	-14.58	-1.37	-5.40	-4.75	-18.76
AGRL	5.64	20.70	6.36	25.12	3.37	13.31
RNGB	-4.61	-16.92	-10.00	-39.53	6.55	25.89
FRST	-0.48	-1.75	-2.10	-8.30	1.90	7.50
URBN	0.06	0.21	0.20	0.80	2.07	8.19
WATR	-0.21	-0.78	0.10	0.40	0.07	0.28

As shown in Table 5.6 and Figure 5.7, there was an increase in agricultural land while shrub, rangeland and forest decreased between 1973 and 1987 in the study area. The rate of increment in agricultural land was 5.64 km<sup>2</sup>/yr in the interim, and the rate of decrease for shrub, rangeland and forest land were 16.92 km<sup>2</sup>/yr, 14.58 km<sup>2</sup>/yr, and 1.75 km<sup>2</sup>/yr respectively. Moreover, the rate of increment in agricultural land and barren area between 1973 and 1987 became 20.7 km<sup>2</sup>/yr and 13.12 km<sup>2</sup>/yr, respectively. However, between 1987 and 2000 the rate of decline for shrub land and forest were highly significant which is 39.53 and 8.3 km<sup>2</sup>/yr, respectively, whereas the rate of increase in barren and agricultural land shared 26.91 km<sup>2</sup>/yr, 25.12 km<sup>2</sup>/yr respectively. These conditions showed the shift from shrub land and forest land to agricultural and barren land. On the other hand, between 2000 and 2013 agricultural land, shrub land and forest increased at the rate of 13.31 km<sup>2</sup>/yr, 25.89 km<sup>2</sup>/yr and 7.5 km<sup>2</sup>/yr, respectively. While, the rate of decrease in barren and rangeland were 36.41 km<sup>2</sup>/yr and 18.76 km<sup>2</sup>/yr in the order for the mentioned respective periods. This mainly due to some integrated physical and biological conservation practices of natural resources at the basin in the context of integrated watershed management programs as a result some areas are treated as area enclosures where there is no

contact with anything else (i.e. zero grazing) so that the area is becoming regenerating itself to attain its normal condition.

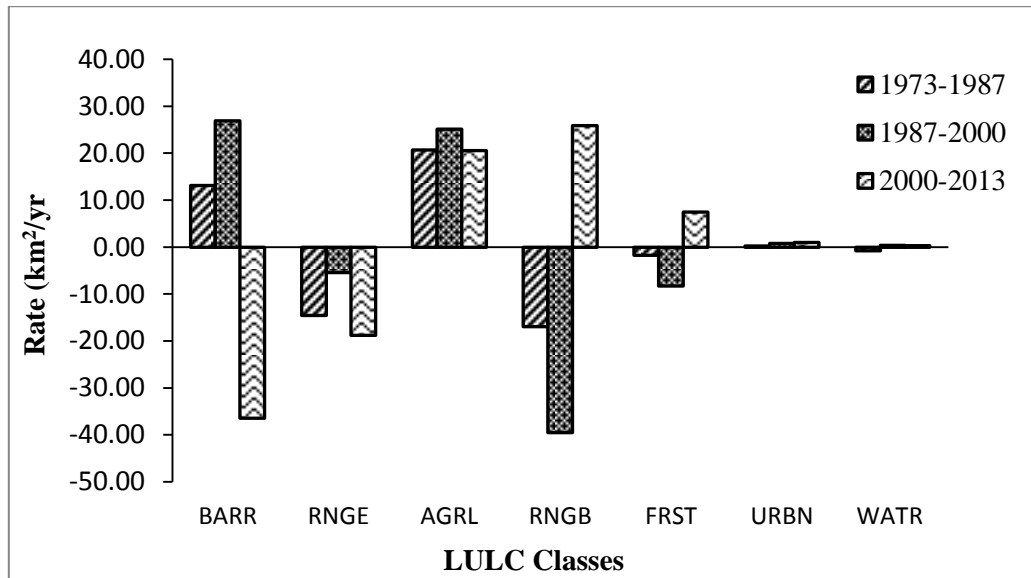


**Figure 5.7 Annual rate of change in LU/LC in the Geba River basin.**

The rapid growing population along with less awareness toward natural resources remain the major cause of sequence of environmental and ecological problems in the area. Population growth has also been the most important growing encroachment of farming activity into marginal areas and the high occurrence of conflicts on natural resources specifically over land. Population increased significantly in the region for the reason of both likely natural growth and resettlements. This rapid growing rate of population has declined the per capita land accessibility and increased population density, and has concentrated to the agricultural land intensification. Between 1973 and 2000 time periods the agricultural land increased at the expense of shrub, rangeland and forest while from 2000 to 2013 the expansion is from barren and rangeland in the study area.

### 5.3.3 Land use/land cover Changes at Sub-basin Level

To acquire better understandings of land use/land cover conversion at a finer spatial scale discussing the land use/land cover that occurred at each sub-basin is very crucial. Table 5.7 to 5.9 demonstrate the pattern of land use/land cover changes in each sub- basin during the study periods of the four LU/LC maps.

**Table 5.7: Major land use/land cover changes from 1973 to 1987 in sub-basins  
(Percentage of change is computed with respect to the area of the sub-basin).**

Sub-basin	1973 -1987					
	Area (km <sup>2</sup> )	% change in BARR	% change in RNGE	% change in AGRL	% change in RNGB	% change in FRST
1	967.95	4.62	-3.95	2.71	-3.31	0.00
2	730.03	4.32	-0.21	5.15	-8.57	-0.23
3	7.90	3.94	-1.21	21.46	-21.19	0.00
4	693.26	2.20	-4.53	4.85	-1.76	-0.24
5	45.63	0.11	0.14	0.32	0.12	0.00
6	326.13	1.91	-0.12	2.64	-3.88	-0.42
7	237.21	2.83	-3.53	12.22	-11.22	-0.31
8	342.20	2.91	-6.17	5.24	-1.67	-0.66
9	252.80	1.05	-14.46	7.97	6.24	-0.78
10	881.64	6.08	-5.28	6.20	-6.31	-0.66
11	181.21	1.69	-4.78	11.29	-5.90	-2.22
12	171.08	2.85	-2.57	5.10	-5.39	0.00
13	299.54	1.60	-2.34	10.33	-7.94	-1.64

**Table 5.8: Major land use/land cover changes from 1987 to 2000 in sub-basins  
(Percentage of change is computed with respect to the area of the sub-basin).**

Sub-basin	1987-2000					
	Area (km <sup>2</sup> )	% change in BARR	% change in RNGE	% change in AGRL	% change in RNGB	% change in FRST
1	967.95	1.80	-0.46	6.90	-8.37	0.00
2	730.03	6.27	-1.88	6.53	-8.28	-3.00
3	7.90	15.97	-4.43	9.47	-23.66	0.00
4	693.26	11.07	-0.28	5.78	-13.29	-3.51
5	45.63	3.96	-0.73	18.44	-22.22	0.00
6	326.13	7.60	-2.77	9.46	-4.73	-10.68
7	237.21	2.20	-0.89	9.88	-7.10	-4.77
8	342.20	8.98	-1.93	5.47	-11.47	-1.86
9	252.80	16.20	-0.33	5.60	-21.27	-0.21
10	881.64	4.52	-1.23	3.90	-6.52	-0.69
11	181.21	8.48	-1.76	5.27	-10.86	-1.19
12	171.08	9.81	-6.19	11.73	-16.11	0.00
13	299.54	11.02	-2.05	3.92	-12.76	-0.14



**Table 5.9: Major land use/land cover changes from 2000 to 2013 in sub-basins.  
(Percentage of change is computed with respect to the area of the sub-basin).**

Sub-basin	2000-2013					
	Area (km <sup>2</sup> )	% change in BARR	% change in RNGE	% change in AGRL	% change in RNGB	% change in FRST
1	967.95	-5.01	-2.29	5.95	1.17	0.00
2	730.03	-5.51	-8.54	10.88	1.52	1.19
3	7.90	-12.70	-2.28	0.86	9.65	0.00
4	693.26	-10.06	-2.81	1.94	4.87	5.84
5	45.63	-3.33	-17.94	7.04	14.16	0.00
6	326.13	-11.45	-3.00	3.00	11.02	0.00
7	237.21	-12.55	-5.67	3.25	8.38	5.29
8	342.20	-12.84	-6.45	6.40	9.09	2.77
9	252.80	-16.15	0.38	7.94	6.35	1.45
10	881.64	-9.24	-5.61	3.61	9.77	1.47
11	181.21	-8.67	-5.27	0.70	10.12	3.11
12	171.08	-13.21	-9.69	7.64	14.65	0.00
13	299.54	-13.61	-3.86	2.55	13.58	1.34

The percentage increase in agriculture and barren land during the 1973 to 2000 time period has almost occurred in all sub-basins especially in the 1987-2000 periods with a higher percentage than the 1973-1987, while decrease in rangeland, shrub land and forest (Table 5.7 and 5.8). In contrast, in all the sub-basins there was an increase of in agricultural land, shrub land and to some extent forests during the 2000-2013 time periods (Table 5.9). Generally, from 1973 to 2000 the land use/land cover was changed mostly to agricultural and barren land at the cost of shrub land, rangeland and forest. While, from 2000 to 2013 the land use/land cover has shown a positive scenario on the shrub land and forest though there is still increasing trend in agricultural land. This is due to a series of soil and water conservation activities have been applied to control land degradation and soil erosion to maintaining agricultural productivity and environmental rehabilitation in the study area.

Study results from earlier researches reveal the same consensus about the LU/LC dynamics. For instance, Gete and Hurni (2001) acknowledged that about 99 % of the forest covers was changed to agricultural land at Dembecha area between 1957 and 1995 in the Northern highlands of the country. They also detected that cultivation

expanded to marginal areas as steep as greater than 30 % slope. Within the Blue Nile basin in about 40 years (1957-1998) agricultural conversion of 79 % of the Riverine forests of the Chemoga watershed (Bewket, 2003). Mekuria (2005) reported 75 % of at Shomba catchment, in the south western part of Ethiopia, was transformed to farmlands and settlements from other LU/LC between the years 1967 to 2001. Another study by Mengistu (2009) reported expansion of farmlands and settlements (84 %) and reduction of other LU/LC in the period (1975 2004), during this time almost 41 % of the vegetation at the beginning of that period was lost to farmlands and reduced to 22.4 %.

#### **5.4 Conclusion**

The purpose of this chapter was multi-temporal classification of Landsat satellite imagery to provide a recent perspective of land use/land cover types, and evaluate land use/land cover dynamics and change assessment within the Geba River catchment during the past four decades. An insight of varied land use/land cover classes dominant in the study area was got by incorporating appropriate information and additional data. Seven land use/land cover classes were mapped for the Geba river catchment, with an overall accuracy of 87%. Thus, the classification procedure not only separated land use/land cover in to various classes, but also demonstrated the patterns that exist across the landscape. Furthermore, this study has produced land cover maps for the Geba River catchment, covering 5137 km<sup>2</sup>. These maps were prepared using Landsat satellite data, acquired in 1973, 1987, 2000 and 2013 as the key data source and therefore represent the land use/land cover existing at that time. The land use/land cover maps have well-matched the digital formats hence can simply be applied to a variety of future GIS applications. Further themes can be combined as more resource information becomes accessible, or as new management needs are identified.

With a population growth rate estimated at approximately 3 % per year and high population density, the study area is found to be under high anthropogenic pressure. The extremely low income and small agricultural area per household much of the population result in over-exploitation of natural resources in the basin that can

seriously affect the sustainable development of the area. From this investigation, it can be concluded that there is a significant change in land use/land cover in the Geba catchment over the past four decades.

Rapid LU/LC change occurred from 1973 to 2000, especially dramatically decreased shrub, rangeland, and forest from 38 %, 21.88 % and 4.19 % to 23.38 %, 16.54 % and 1.61 %, respectively. However, increase in cultivated land was observed from 27.39 % to 44.58 % until 2013. This indicated that deforestation and increase in cultivated land that was manifested by the rapid increase in population has transformed the Geba catchment. It is identified that land use/land cover changes has a remarkable trend during the three periods (1973-1987, 1987-2000 and 2000-2013). Forest, shrub and grasslands were changed to agricultural and barren land in the 1973 to 2000 time period, however, in the 2000 to 2013 time period decreased rate of barren land and rangeland has shown while increased rate of Forests, shrub land and agricultural land in the study area. The possible reasons for the decrease of forest, shrub and rangelands in the 1973 to 2000 time period could be the increased demand of farmlands due to population increase the Geba catchment as well as in the region.

On the other hand, the positive change in 2000 to 2013 period the possible reason could be the integrated environmental rehabilitation taking place in the area for the last decade. Nevertheless, the predominant change in land use/land cover during the whole period is increased in agricultural land, in most of the sub-basins, and the overall decrease in rangelands. Meanwhile, sub-watersheds that are close to small towns are highly affected than the other ones. Considerable conversions of other land use/land cover to agricultural land were also evident.

## CHAPTER 6

# APPLICATION OF SWAT HYDROLOGICAL MODEL

### 6.1 Introduction

The main emphasis of the present study was to understand the overall hydrological processes under study through an integrated approach. SWAT hydrological model was used to simulate major hydrological processes and sediment dynamics in the Geba catchment Northern Highlands of Ethiopia using available hydro-meteorological data and other data related to topography, LU/LC and soils. SWAT model is extensively used in different hydro-climatic conditions (Section 2.4) to an acceptable level of accuracy. Unlike other studies (Setegn et al., 2008; Setegn et al., 2010; Mango et al., 2011; Mengistu and Sorteberg, 2012; Shawul et al., 2013; Babar and Ramesh, 2015), a novel way of calibration and validation were performed using multiple land cover data sets.

This chapter is dedicated to a detailed description of the SWAT hydrological model used, data inputs, methodology implemented in applying the model and detail discussion of results obtained.

### 6.2 Methodology

#### 6.2.1 Selection Criteria of Hydrological Model

There are several standards for choosing the right hydrological model which can be used for solving a specific problem. These criteria are always dependent on the field of interest, since every field has its own specific requirements. Furthermore, some criteria are also user dependent and therefore, subjective. Among the various field dependent selection measures, there are four common and fundamental ones that must be always answered (Cunderlik, 2003):

- ¾ Required model outputs essential to the project and therefore to be predicted by the model (Does the model predict the variables required by the project such as long-term sequence of flow?);

- ☐ Hydrologic processes that need to be modelled to estimate the desired outputs adequately (Is the model capable of simulating single-event or continuous processes?);
- ¾ Accessibility of input data (Can all the inputs required by the model be provided within the time and cost limits of the project?);
- ¾ Cost (Does the investment appear to be valuable for the objectives of the project?).

### **6.2.2 Reasons for Selecting SWAT Model**

The reasons for selecting SWAT model for this study are:

- ¾ The model simulates the major hydrological process in the catchment;
- ¾ Adequate literatures and well organised database;
- ¾ It is free and easily available for users;
- ¾ GIS interface;
- ¾ The model was applied for land use/land cover change impact assessment in different parts of the world, and

A major limitation to large area hydrologic modelling using SWAT is the spatial detail required to correctly simulate hydrological processes. Another limitation is data files can be difficult to manipulate and can contain a number of missing records. The model simulations can only be as accurate as the input data. The third limitation is that, the SWAT model does not simulate detailed event-based flood and sediment routing.

### **6.2.3 Model Description of SWAT 2012**

The SWAT is a river basin or watershed scale model developed and actively supported by the USDA (United States Department of Agriculture) - ARS (Agricultural Research Service) at the Grassland, Soil and Water Research Laboratory in Temple, Texas, USA (Arnold et al., 1998). The model is available in the public domain.

The model is a continuous time, semi-distributed, physically based model which operates on daily time step to predict the impact of land management practices on

water, sediment and agricultural chemical yields in large complex watersheds with varying soils, land use and management conditions over long periods of time (Neitsch et al., 2005; Gassman et al., 2007). SWAT uses Hydrological Response Units (HRUs) to describe spatial heterogeneity in terms of land use, soil types and slope within a watershed. In order to simulate hydrological processes in a watershed, SWAT divides the watershed into sub watersheds based upon drainage areas of the tributaries. The sub watersheds are further divided into smaller spatial modelling units known as HRUs, depending on land use/land cover, soil and slope characteristics. One of the main advantages of SWAT is that it can be used to model watersheds with less monitoring data. For simulation, SWAT needs digital elevation model (DEM), land use/land cover map, soil and climate data of the study area. These data are used as an input for the analysis of hydrological simulation of surface runoff and groundwater recharge. SWAT splits hydrological simulations of a watershed into two major phases: the land phase and the routing phase. The land phase of the hydrological cycle controls the amount of water, sediment, nutrient, and pesticide loadings to the main channel in each sub watershed. While the routing phase considers the movement of water, sediment and agricultural chemicals through the channel network to the watershed outlet.

In this study, the new version ArcSWAT2012 was used. It is an ArcGIS extension and is provided with a graphical user input interface. The SWAT model is embedded in ArcGIS that can integrate various readily available geospatial data to accurately represent the characteristics of the watershed. It is computationally efficient, uses readily available inputs and enables users to study long term impacts.

#### **6.2.4 Hydrological Component of SWAT**

Fig. 6.1 shows the various input/output components of the model simulations.

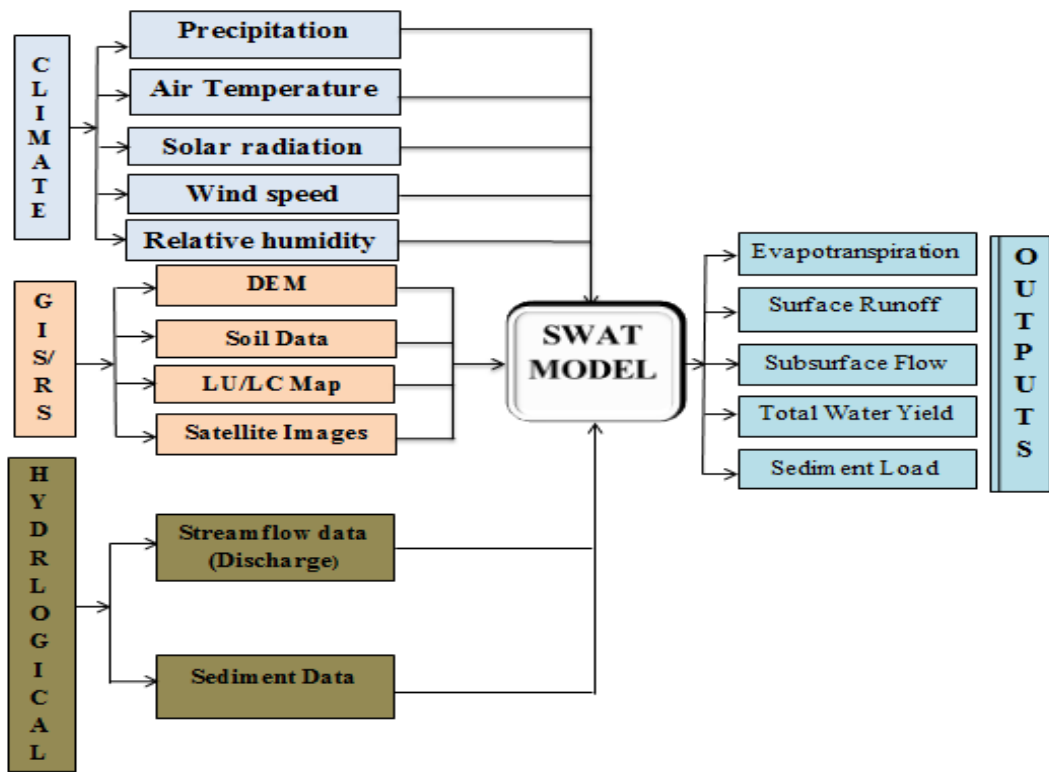


**Figure 6.1 Input and Output Components of the SWAT Model.**

Hydrological components simulated in land phase of the Hydrological cycle are canopy storage, infiltration, redistribution, evapotranspiration, lateral subsurface flow, surface runoff, ponds, tributary channels and return flow. SWAT simulates the hydrological cycle based on the water balance equation.

$$SW_t = SW_o + \sum_{i=1}^t R_{day} - Q_{surf} - E_a - W_{seep} + Q_{qw} \quad (6.1)$$

Where,  $SW_t$  is the final soil water content (mm),  $SW_o$  is the initial soil water content on day  $i$  (mm  $H_2O$ );  $t$  is the time (days),  $R_{day}$  is the amount of precipitation on day  $i$  (mm  $H_2O$ ),  $Q_{surf}$  is the amount of surface runoff on day  $i$  (mm),  $E_a$  is the amount of evapotranspiration on day  $i$  (mm  $H_2O$ ),  $W_{seep}$  is the amount of water entering the vadose zone from the soil profile on day  $i$  (mm  $H_2O$ ), and  $Q_{qw}$  is the amount of return flow on day  $i$  (mm  $H_2O$ ).

#### 6.2.4.1 Surface Runoff

Surface runoff occurs whenever the rate of precipitation exceeds the rate of infiltration. SWAT offers two methods for estimating surface runoff: the SCS curve number procedure (USDA-SCS, 1972) and the Green Ampt infiltration method (Green and Ampt, 1911). Due to the absence of sub-daily rainfall data where the Green and Ampt method demands, this was not chosen in this study. SWAT simulates surface runoff volumes and peak runoff rates for each HRU. Therefore, in this study the SCS curve number method was used to estimate surface runoff. The SCS curve number equation is:

$$Q_{surf} = \frac{R_{day} I_a^2}{R_{day} I_a S} \quad \text{if } R_{day} > I_a; \quad Q_{surf} = 0 \quad \text{otherwise} \quad (6.2)$$

Where,  $Q_{surf}$  is the accumulated direct runoff or rainfall excess (mm),  $R_{day}$  is the rainfall depth for the day (mm water),  $I_a$  is initial abstraction which includes surface storage, interception and infiltration prior to runoff (mm water) and  $S$  is the potential maximum retention parameter (mm water). Since  $S$  can vary between 0 and  $\infty$ , it is mapped to another variable called Curve Number (CN) using the transformation,

$$S = 25.4 \frac{100}{CN} - 10 \quad (6.3)$$

CN varies between 0 and 100 and its value is the function of LU/LC type, management practice, Antecedent Moisture Condition and soil hydrologic group.

The initial abstraction,  $I_a$ , is commonly approximated as  $0.2S$  and Eq. 6.2 becomes:

$$Q_{surf} = \frac{R_{day} 0.2S^2}{R_{day} 0.8S}, \quad \text{if } R_{day} > 0.2S; \quad Q_{surf} = 0 \quad \text{otherwise} \quad (6.4)$$

As a result of the changes in land surface features such as soils, land use, slope and management practices,  $S$  (or CN) varies spatially and it can also be affected temporally due to changes in AMC condition.



For the definition of soil hydrological groups, the model uses the U.S. Natural Resource Conservation Service (NRCS) classification. This defines a hydrological group as a group of soils having similar runoff potential under similar storm and land cover conditions. Thus, soils are classified in to four hydrologic groups (A, B, C, and D) based on infiltration which represent high, moderate, slow, and very slow infiltration rates, respectively.

#### 6.2.4.2 Sediment Component

In SWAT, erosion caused by rainfall and runoff is computed with the Modified Universal Soil Loss Equation (MUSLE) (Williams, 1975). MUSLE is a modified version of the Universal Soil Loss Equation (USLE) developed by Wischmeier and Smith (1965). It predicts average annual gross erosion as a function of rainfall energy. In MUSLE, the rainfall energy factor is replaced with a runoff factor which improves the sediment yield prediction and allows the equation to be applied to individual storm events. This improves sediment yield prediction because runoff is a function of antecedent moisture condition as well as rainfall energy.

$$Sed = 11.8 * Q_{surf} * q_{peak} * area_{hru}^{0.56} * K_{USLE} * C_{USLE} * P_{USLE} * LS_{USLE} * CFRG \quad (6.5)$$

Where  $Sed$  is the sediment yield on a given day (metric tons),  $Q_{surf}$  is the surface runoff volume (mm H<sub>2</sub>O/ha),  $q_{peak}$  is the peak runoff rate (m<sup>3</sup>/s),  $area_{hru}$  is the area of the HRU (ha),  $K_{USLE}$  is the soil erodibility factor (0.013 metric ton m<sup>2</sup> hr/(m<sup>3</sup>-metric ton cm)),  $C_{USLE}$  is the cover and management factor,  $P_{USLE}$  is the support practice factor,  $LS_{USLE}$  is the topographic factor and  $CFRG$  is the coarse fragment factor. The details of the USLE factors and the descriptions of the different model components can be found in (Arnold et al., 2012).

#### 6.2.4.3 Actual and Potential Evapotranspiration

ET<sub>a</sub> is the actual evapotranspiration (mm per unit time) from an area large enough that the heat and vapour fluxes are controlled by the evaporating power of the lower atmosphere and unaffected by upwind transitions where in the context of the complementary relationship, and techniques using the relationship, ET<sub>a</sub> includes

transpiration and evaporation from water bodies, soil and interception storage. The SWAT model computes  $ET_a$  as:

$$ET_a = \frac{\rho_a (R_n - G) U_a c_p (e_s - e_a)}{\rho_a \left[ 1 + \frac{r_s}{r_a} \right]} \quad (6.6)$$

Where  $R_n$  is the net radiation,  $G$  is the soil heat flux,  $(e_s - e_a)$  represents the vapour pressure deficit of the air,  $U_a$  is the mean air density at constant pressure,  $c_p$  is the specific heat of the air,  $\rho_a$  represents the slope of the saturation vapour pressure temperature relationship,  $J$  is the psychrometric constant, and  $r_s$  and  $r_a$  are the (bulk) surface and aerodynamic resistances.

Potential Evapotranspiration is a collective term that includes all processes by which water at the earth's surface is converted into water vapour. These are evaporation from the water bodies, soil and transpiration from the plants. Evaporation is the primary mechanism by which water is removed from a watershed. Therefore, Potential evapotranspiration (PET) is defined as the rate at which evapotranspiration would occur from a short green grass crop, uniformly covering the ground, disease free and of uniform height and never short of water (Penman, 1956). An accurate estimation of evapotranspiration is critical in the impact assessment of land use/land cover changes on water resources. There are many methods that are developed to estimate PET. SWAT provides three options for the calculation of PET: (1) Penman-Monteith (Penman and Monteith, 1965), (2) Priestley-Taylor (Priestley and Taylor, 1972), and (3) Hargreaves (Hargreaves and Samani, 1985) methods. These methods vary in terms of climate input data variables they require. Penman-Monteith method requires, air temperature, relative humidity, solar radiation and wind speed; Priestley-Taylor method requires solar radiation, air temperature and relative humidity; whereas Hargreaves method requires only air temperature. Based on the availability of meteorological data at the seven stations in the present study Penman-Monteith and Hargreaves methods have used to estimate evapotranspiration.

Penman-Monteith technique was selected for this study as the method is widely used and all climatic variables required by the model are available for three stations in and around the study catchment and the form of the equation is shown in Eq. (6.7).

$$ET_o = \frac{0.408 \left( \frac{R_n - G}{J} + \frac{900}{T + 273} u_2 (e_s - e_a) \right)}{J + 1 + 0.34 u_2} \quad (6.7)$$

Where,  $ET_o$  is reference evapotranspiration ( $\text{mm day}^{-1}$ ),

$R_n$  is net radiation at the crop surface ( $\text{MJ m}^{-2} \text{day}^{-1}$ ),

$G$  is soil heat flux density ( $\text{MJ m}^{-2} \text{day}^{-1}$ ),

$T$  is air temperature at 2 m height ( $^{\circ}\text{C}$ )

$u_2$  is wind speed at 2 m height ( $\text{m s}^{-1}$ )

$e_s$  is saturation vapour pressure (kPa)

$e_a$  is actual vapour pressure (kPa)

$e_s - e_a$  is saturation vapour pressure deficit (kPa)

$\hat{u}$  is slope of vapour pressure curve ( $\text{kPa } ^{\circ}\text{C}^{-1}$ ), and

$\gamma$  is psychrometric constant ( $\text{kPa } ^{\circ}\text{C}^{-1}$ )

The Hargreaves method was originally derived from eight years of cool season Alta fescue grass lysimeter data from Davis, California (Hargreaves, 1975). Several improvements were made to the original equation (Hargreaves and Samani, 1985) and same is used in SWAT and is given in Eq. (6.8).

$$E_o = 0.023 H_o (T_{max} - T_{min})^{\hat{u}} (T_{av} + 17.8) \quad (6.8)$$

Where,  $\lambda$  = Latent Heat of Vaporization ( $\text{MJd}^{-1}$ )

$E_o$  = Potential Evapotranspiration ( $\text{mm d}^{-1}$ )

$H_o$  = Extraterrestrial Radiation ( $\text{MJkg}^{-1}$ )

$T_{mx}$  = Maximum air temperature for given day ( $^{\circ}\text{C}$ )

$T_{mn}$  = Minimum air temperature for given day ( $^{\circ}\text{C}$ )

$T_{av}$  = Mean air temperature for given day ( $^{\circ}\text{C}$ )

#### 6.2.4.4 Water Movement in Soil

Water maintained in the soil profile after infiltration can flow under saturated or unsaturated conditions. In saturated soils, flow is driven by gravity and usually occurs in the downward direction. Unsaturated flow on the other hand, is caused by gradients arising due to adjacent areas of high and low water content and may occur in any directions. SWAT directly simulates saturated flow if the water content is more than the field capacity. The model records the water contents of different soil layers (1 to 10) but assumes that the water is uniformly distributed within a given layer. Unsaturated flow between layers is indirectly modelled with the depth distribution of plant water uptake and the depth distribution of soil water evaporation. SWAT allows water to percolate from one layer if the water content exceeds the field capacity for this layer. The amount of water that moves from one layer to the underlying layer is calculated using storage routing methodology. Water that percolates to the next layer is computed using Eq. (6.9).

$$W_{p,ly} = SW_{ly,excess} \left( 1 - \frac{Sat_{ly} - FC_{ly}}{Sat_{ly} - FC_{ly}} \right) \quad (6.9)$$

Where the travel time for percolation is unique for each layer and is calculated using Eq. (6.10).

$$TT_p = \frac{Sat_{ly} - FC_{ly}}{K_s} \quad (6.10)$$

Where  $W_{p,ly}$  is the amount of water percolating to the underlying soil layer on a given day (mm),  $SW_{ly,excess}$  is the drainable volume of water in the soil layer on a given day (mm),  $\Delta t$  is the length of the time step (hrs),  $TT_p$  is the travel time for percolation (hrs),  $Sat_{ly}$  is the amount of water in the soil layer when completely saturated (mm),  $FC_{ly}$  is the water content of the soil layer at field capacity (mm), and  $K_s$  is the saturated hydraulic conductivity for the layer ( $\text{mm} \cdot \text{hrs}^{-1}$ ).

Water that percolates out of the lowest soil layer enters the vadose zone (the unsaturated zone between the bottom of the soil profile and the top of the aquifer). SWAT also applies a multiplayer storage routing technique to partition drainable soil

water content for each layer into other components, which are lateral subsurface flow and percolation into the layer below.

#### 6.2.4.5 Ground Water Flow Estimation

To simulate ground water, SWAT partitions groundwater into two aquifer systems: shallow and deep. A shallow, unconfined aquifer which contributes return flow to streams within the watershed and a deep, confined aquifer which contributes return flow to streams outside the watershed (Arnold et al., 2012). In SWAT the water balance for a shallow aquifer is calculated with Eq. (6.11).

$$aq_{sh,i} = aq_{sh,i-1} + W_{rchrg} - Q_{gw} - W_{revap} - W_{deep} - W_{pump,sh} \quad (6.11)$$

Where,  $aq_{sh,i}$  is the amount of water stored in the shallow aquifer on day  $i$  (mm),  $aq_{sh,i-1}$  is the amount of water stored in the shallow aquifer on day  $i-1$  (mm),  $W_{rchrg}$  is the amount of recharge entering the aquifer on day  $i$  (mm),  $Q_{gw}$  is the ground water flow, or base flow, or return flow, into the main channel on day  $i$  (mm),  $W_{revap}$  is the amount of water moving in to the soil zone in response to water deficiencies on day  $i$  (mm),  $W_{deep}$  is the amount of water percolating from the shallow aquifer in to the deep aquifer on day  $i$  (mm), and  $W_{pump,sh}$  is the amount of water removed from the shallow aquifer by pumping on day  $i$  (mm).

#### 6.2.4.6 Flow Routing Phase

The second component of simulation of the hydrology of a watershed is the routing phase of the hydrologic cycle. It consists of movement of water, sediment and other constituents (e.g. nutrients, pesticides) in the stream network. Two options are available to route the flow in the channel network: (1) Variable storage and (2) Muskingum methods. The variable storage method uses a simple continuity equation in routing the storage volume, whereas the Muskingum routing method models the storage volume in a channel length as a combination of wedge and prism storages. In the latter method, when a flood wave advances into a reach segment, inflow exceeds outflow and a wedge of storage is produced. As the flood wave recedes or retreat, outflow exceeds inflow in the reach segment and a negative wedge is produced. In

addition to the wedge storage, the reach segment contains a prism of storage formed by a volume of constant cross-section along the reach length.

### **6.2.5 Data Acquisition and Preparation for SWAT Model**

Most often faced challenges in hydrological modelling are limitations in availability of quality and adequacy of data sets. Getting all hydrological variables at time-scales appropriate to catchment-scale processes is a difficult task. Yet even with these difficulties, such information is vital in order to understand catchment behaviour and response to hydrological events. Various data are required for this study which includes topographic data (DEM), Land use/land cover data, soil data, daily climatic data being, daily data of precipitation, maximum and minimum temperature, relative humidity, wind speed and solar radiation. Data used in this research was collected from various institutions and agencies while DEM and land cover satellite imagery data were obtained from the NASA website. Quality control was performed by use of graphical, statistical and ground-truthing methods.

### **6.2.6 SWAT Model Inputs**

The spatially distributed model used in the GIS platform needed for the ArcSWAT interface include the Digital Elevation Model (DEM), soil data, land use/land cover, weather data and stream network layers. Data on River discharge and sediment were also used for calibration of streamflow and prediction purposes.

#### **6.2.6.1 Digital Elevation Model (DEM)**

Topography is defined by DEM that describes the elevation of any point in a given area at a specific spatial resolution. A 30 m by 30m resolution ASTER Global Digital Elevation Model was obtained from dataset of the National Aeronautics and Space Administration (NASA) website. This data was projected to Transverse Mercator (UTM) on spheroid of Adindan UTM Zone 37 N and it was in raster format to fit in to the model requirement. The DEM was used to delineate the watershed using SWAT watershed delineator tools and to calculate the flow accumulation, analyse the drainage patterns of the land surface terrain. Sub-basin parameters such as slope

gradient, slope length of the terrain, and the stream network characteristics such as channel slope, length, and width was derived from the DEM.

### 6.2.6.2 Meteorological Data

SWAT requires daily meteorological data that could either be read from a measured data set or generated by a weather generator model. In this study, the weather variables were used for driving and analysing the hydrological changes and balances. The detail of the data used in the simulations is discussed in chapter 3 (section 3.6).

### 6.2.6.3 Soil Data

SWAT model requires different soil textural and physicochemical properties such as soil texture, available water content, hydraulic conductivity, bulk density and organic carbon content for different layers of each soil type (Table 6.1).

**Table 6.1: Soil Available Water and Hydraulic Conductivity.**

Major soil types	Soil Available Water (SOL_AWC) (mm/mm)	Hydraulic Conductivity (CH_K2)(mm/hr)
Leptosols	15	7.87
Vertisols	125	2.54
Cambisols	150	11.43
Luvisols	150	16.51
Calcisols	150	19.56
Arenosols	100	51.82
Alisols	150	15.75

These data were acquired from Soil and Terrain Database for North-Eastern Africa Food and Agriculture Organization of the United Nations, FAO (1998). Based on the geomorphology of Ethiopia at the scale of 1:50,000 topographic maps, major seven soil types were identified in the catchment: Leptosols, Vertisols, Cambisols, Luvisols, Calcisols, Arenosols and Alisols (Figure 6.2)

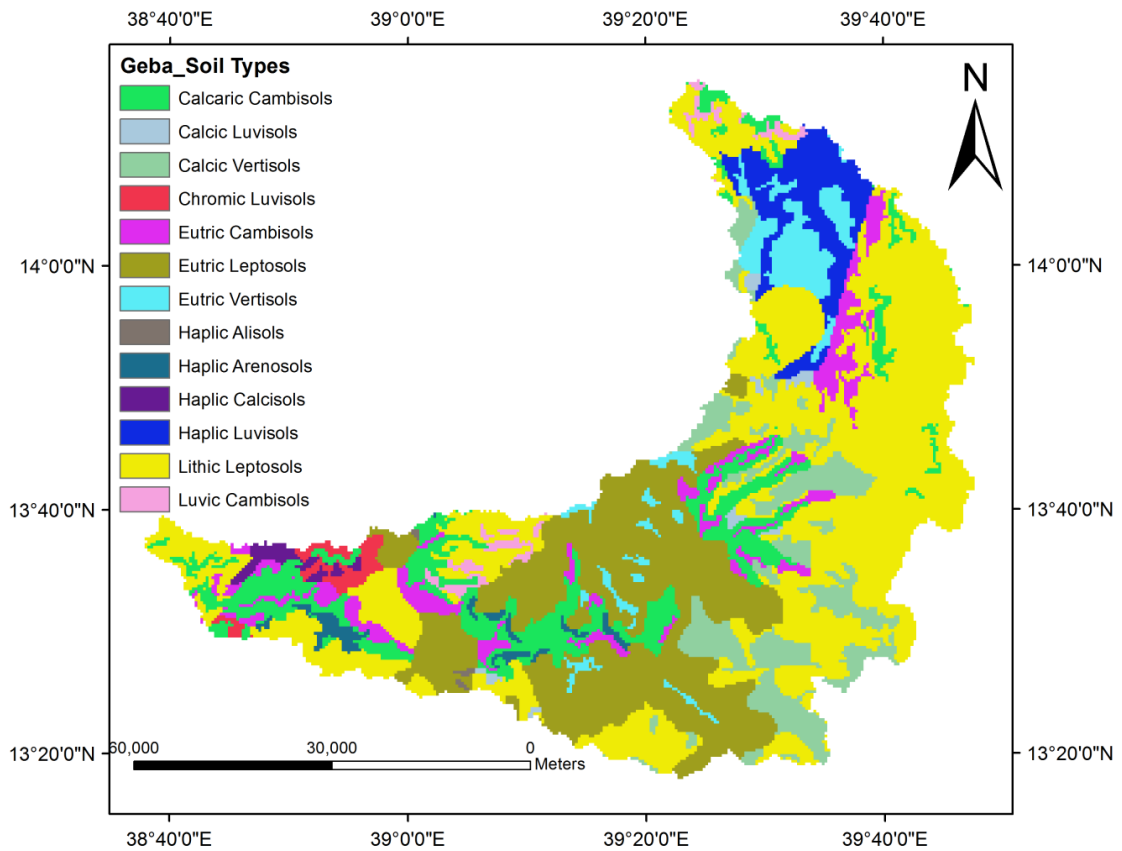


**Figure 6.2 Soil map of the Geba basin (FAO, 1998).**

#### **6.2.6.4 Land Use/Land Cover**

Satellite imagery was obtained from US Geological Survey, USA. For this study LANDSAT imagery (Landsat MSS, TM and ETM+) was chosen as it provides just the necessary detail required (high quality, moderate resolution) and at no cost. The detailed procedure adopted in producing land use/land cover map from remote sensing data is provided in Chapter 5 (Section 5.2).

#### **6.2.6.5 Hydrological Data**

Daily River discharge for the catchment's streamflow at Adikumtsi (gauge station) near Awegele was obtained from the department of hydrology Ministry Water, Irrigation and Energy (MoWIE) of Ethiopia. These daily River discharges at River gauging station were used for model calibration and validation. More details of this are provided in chapter 3 (section 3.6).



#### **6.2.6.6 Sediment data**

In this study daily sediment concentration data for the year 2008 to 2011 collected at Adikumtsi gauging station were used. It is important to understand that the sediment concentration data is accessible only for rainy season (i.e., July to September).

#### **6.2.7 SWAT Model Setup**

The model setup involved five steps: (1) data preparation, (2) sub-basin discretization, (3) HRU definition, (4) parameter sensitivity analysis, (5) calibration, validation and performance evaluation of the model.

The required spatial data sets were projected to Adindan UTM Zone 37 N, which is the Transverse Mercator projection parameters for Ethiopia, using ArcGIS® 10.1. The DEM was used to delineate the watershed and to analyze the drainage patterns of the land surface terrain. Digital stream network layer was imported and superimposed onto DEM to accurately delineate the location of the streams. The land use/land cover spatial data was reclassified into SWAT land cover. A user look up table was created that identifies the SWAT code for different categories of land use/land cover on the map as per the required format. The watershed delineation process include five major steps, DEM setup, stream definition, outlet and inlet definition, watershed outlets selection and definition and calculation of sub-basin parameters. After setting up of the model using the default parameter values, the default simulations of streamflow were carried out for the calibration period.

##### **6.2.7.1 Watershed Delineation**

The watershed and sub-watershed delineation was performed using 30 m by 30 m resolution DEM data using Arc SWAT model watershed delineation function. First, the SWAT project set up was created. The watershed delineation process consists of five major steps: DEM setup, stream definition, outlet and inlet definition, watershed outlets selection and definition and calculation of sub basin parameters. Once, the DEM setup was completed and the location of outlet was specified on DEM, the model automatically calculates the flow direction and flow accumulation. Subsequently, stream networks, sub-watersheds and topographic parameters were

calculated using appropriate tools. The stream definition and the size of sub basins were carefully determined by selecting threshold area or minimum drainage area required to form the origin of the streams. Using a threshold value suggested by the Arc SWAT interface, the Geba catchment was delineated in to 13 sub-watersheds having an estimated total area of 5137 km<sup>2</sup> (Figure 6.3).

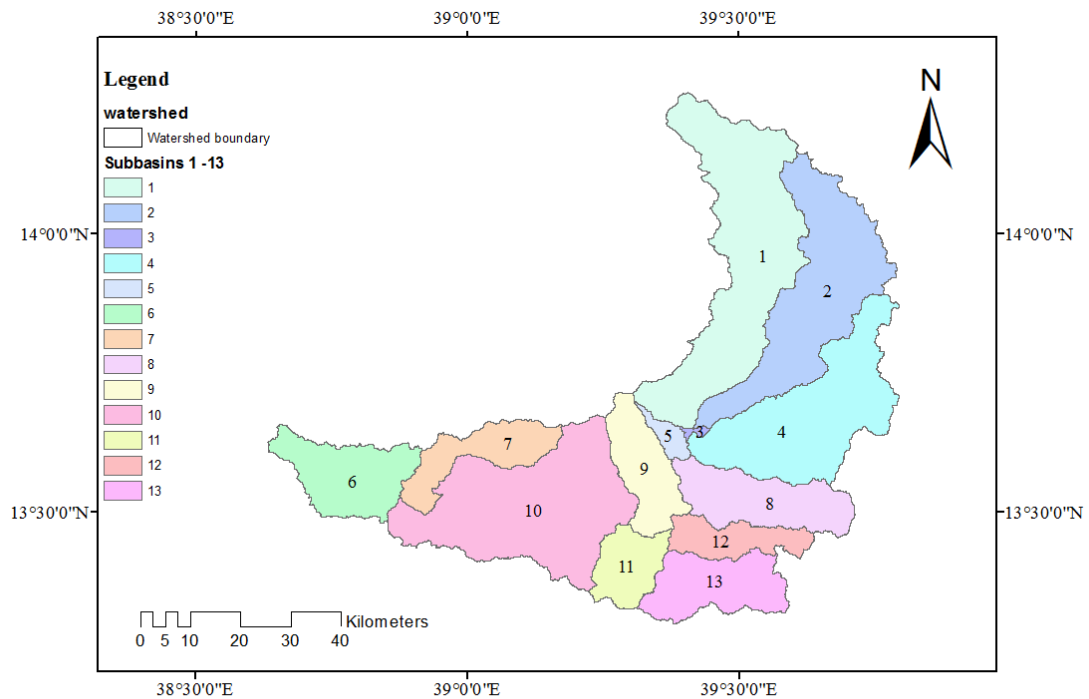


**Figure 6.3 Delineated sub-basins of the study area.**

During the watershed delineation process, the topographic parameters (elevation and slope) of the watershed and its sub-watersheds were also generated from the DEM data. Accordingly the elevation of the watershed ranges from 926 to 3301 meter above mean sea level, the highest elevation is at Mugulat Mountain around Adigrat and the lowest at the watershed outlet, called Chemoy. Slope classification was carried out based on the height range of DEM used during watershed delineation. The slope values of the watershed were reclassified in terms of Percentage area of the catchment into three classes (Table 6.2).

**Table 6.2: The slope classes of the Geba Catchment.**

Classes	Slope range	Area	
		Km <sup>2</sup>	%
Class1	0-8	1709.66	33.28
Class2	8-20	1804.15	35.12
Class3	>20	1622.77	31.59

#### **6.2.7.2 Hydrologic Response Units (HRU)**

The sub-watersheds were divided into HRUs by assigning the threshold values of land use/land cover, soil and slope percentage. In general the threshold level is used to eliminate minor land use/land covers in sub-basin, minor soil with in a land use/land cover area and minor slope classes with in a soil on specific land use/land cover area. Following minor elimination, the area of remaining land use/land covers, soils and slope classes are reapportioned so that 100 % of their respective areas are modelled by SWAT. Land use, soil and slope characterization was performed using commands from the HRU analysis menu on the Arc SWAT Toolbar. These tools allowed loading land use and soil maps which are in raster format in to the current project, evaluates slope characteristics and determining the land use/soil/slope class combinations in the delineated sub-watersheds. In the model, there are two options in defining HRU distribution: assign a single HRU to each sub-watershed or assign multiple HRUs to each sub-watershed based on a certain threshold values. The SWAT user's manual suggests that a 20 % land use threshold, 10 % soil threshold and 20 % slope threshold are adequate for most modelling application. However, Setegn et al. (2008) suggested that HRU definition with multiple options that account for 10 % land use, 20 % soil and 10 % slope threshold combination gives a better estimation of runoff and sediment components. In this study, HRU definition with multiple options that accounts for 10 % land use, 20 % soil and 10 % slope threshold combination was used. These threshold values indicated that land use which form at least 10 % of the sub watershed area and soils which form at least 20 % of the area within each of the selected land uses were considered in the HRU. Hence, the Geba catchment was

divided in to a total of 840 HRUs, each with a unique land use and soil combinations. The numbers of the HRUs within the sub-catchments are shown in Table 6.3.

**Table 6.3: HRU distribution across the sub-basins.**

<b>Sub-basin</b>	<b>Area (km<sup>2</sup>)</b>	<b>Number of HRUs</b>
1	967.95	102
2	730.03	69
3	7.9	27
4	693.26	63
5	45.63	24
6	326.13	87
7	237.21	117
8	342.2	45
9	252.8	63
10	881.64	105
11	181.21	54
12	171.08	36
13	299.54	48
<b>Total</b>	<b>5137</b>	<b>840</b>

### 6.2.7.3 Weather Generator

When there is lack of full and realistic long period of climatic data/missing data, weather generator generates data from the observed ones (Danuso, 2002). The Model requires daily values of all climatic variables from measured data or generated from values using monthly average daily data over a number of years. This study used measured data for all climatic variables. The weather data obtained for the stations in and around Geba catchment had missed records in some of the variables. These missed values were filled with the weather generator utility in the Arc SWAT Model from the values of weather generator parameters. Weather data of seven stations with continuous records were used as an input to determine the values of the weather generator parameters. Hence, for weather generator data definition, the weather

generator data file wgnstations.dbf was selected first. Subsequently, rainfall, temperature, relative humidity, solar radiation and wind speed data were selected and added to the model. The SWAT Model contains weather generator model called WXGEN (Shapley and Williams, 1990). It is used in SWAT model to generate climatic data or to fill missing data using monthly statistics which is calculated from existing daily data. From the values of weather generator parameters, the weather generator first separately generates precipitation for the day. Maximum temperature, minimum temperature, solar radiation and relative humidity are then generated. Lastly, the wind speed is generated independently.

#### 6.2.7.4 Sensitivity Analysis

Model calibration is commonly undertaken by changing the model parameters values; however SWAT model has large number of parameters. Understanding the parameters which are sensitive to advance the adjustment effectiveness is required. To categorize parameters that have significant impact on model predictions the Latin Hypercube testing according to One Factor at a Time (LH-OAT) technique was used and embedded in SWAT as an extension (Van Griensven et al., 2006). N Latin Hypercube test spots for N intervals was taken by the LH-OAT, and after that varying every LH test spot P times by way of varying individual parameters P once at a time. This technique functions through rings and every ring or loop begins with a point of Latin Hypercube. Holding the other inputs constant, a sensitivity directory S for every parameter for small change in  $e_i$  is computed using Eq .6.11.

$$S = \frac{M(e_1, \dots, e_i + \frac{e_i}{e_1}, \dots, e_p) - M(e_1, \dots, e_i, \dots, e_p)}{\frac{e_i}{e_1}} \quad (6.11)$$

Where S is sensitivity directory, M is the model output,  $e_i$  refers to the different model parameters, and  $\frac{e_i}{e_1}$  is the fraction by which the parameter  $e_i$  is varied (a pre described constant).

By averaging the fractional effects of every loop for the entire Latin Hypercube points, a final effect is computed. The final output can be ordered with the largest outcome being specified grade one and the smallest output being pre-arranged a position equal to the total number of parameters. Therefore, the most sensitive parameters can be recognized and the effect of every parameter on the model outcome can be understood. In this case, sensitivity analysis is important to identify and rank parameters that have significant impact on the specific model outputs of interest (Van Griensven et al., 2006). The daily and monthly average daily streamflow data of the watershed gauging station were used to compute the sensitivity of the streamflow parameters. In the sensitivity process, by entering the Arc SWAT interface sensitivity analysis window, first the SWAT simulation was specified for performing the sensitivity analysis and the location of the sub-basin where observed data was compared against simulated output. Then, selected parameters were entered for the sensitivity analysis with the default lower and upper parameter bounds. A total of 26 flow parameters were included for the analysis with default values as recommended by (Van Griensven et al., 2006). On completion of sensitivity analysis, the mean relative sensitivity (MRS) values of the parameters were used to rank the parameters, and their category of classification. The category of sensitivity was defined based on the classification criteria proposed by Lenhart et al. (2002) (Table 6.4).

**Table 6.4: SWAT parameters Sensitivity class.**

<b>Class</b>	<b>MRS</b>	<b>Sensitivity category</b>
I	$0.00 \leq \text{MRS} < 0.05$	Small to negligible
II	$0.05 \leq \text{MRS} < 0.20$	Medium
III	$0.2 \leq \text{MRS} < 1$	High
IV	$\text{MRS} > 1$	Very high

Accordingly, sensitivity analysis was performed for 22 parameters that may have the potential to influence Geba River flow (Table 6.5). The ranges of variation of these parameters are based on a listing provided in the SWAT2012 manual (Arnold et al., 2012) and are sampled by considering a uniform distribution.

**Table 6.5: Parameters and their ranges in sensitivity analysis of SWAT model.**

S.No	Parameters		Lower bound	Upper bound	Process
	Name	Description			
1	CN2	SCS runoff CN for moisture condition II	35	98	Runoff
2	SURLAG	Surface runoff lag coefficient	0	10	Runoff
3	SOL_AWC	Available water capacity of the soil layer(mm/mm soil)	0	1	Soil
4	SOL_K	Soil conductivity (mm/hrs)	0	100	Soil
5	SOL_Z	Soil depth	0	3000	Soil
6	EPCO	Plant evaporation compensation factor	0	1	Evaporation
7	ESCO	Soil evaporation compensation factor	0	1	Evaporation
8	SOL_ALB	Soil albedo	0	0.1	Evaporation
9	ALPHA_BF	Baseflow alpha factor (days)	0	1	Groundwater
10	GW_DELAY	Groundwater delay (days)	0	50	Groundwater
11	GW_REVAP	Groundwater revap coefficient	0.02	0.2	Groundwater
12	GWQMN	Threshold depth of water in the shallow aquifer required for return flow to occur(mm)	0	5000	Groundwater
13	RCHR_DP	Groundwater recharge to deep aquifer (fraction)	0	1	Groundwater
14	REVAPMN	Threshold depth of water in the shallow aquifer for revap to occur (mm)	0	500	Groundwater
15	SLOPE	Average slope steepness (m/m)	0.0001	0.6	Geomorphology
16	SLSUBBSN	Average slope length (m)	10	150	Geomorphology
17	CH_N1	Manning coefficient for tributary channel	0.008	30	Channel
18	CH_K1	hydraulic conductivity in tributary channel (mm/hrs)	0	150	Channel
19	CH_S1	Average slope of tributary channel (m/m)	0	10	Channel
20	CH_N2	Manning coefficient for main channel	0.008	0.3	Channel
21	CH_S2	Average slope of main channel (m/m)	0	10	Channel
22	CH_K2	hydraulic conductivity in main channel(mm/hrs)	0.01	150	Channel

## **6.2.8 Modelling of the Geba River Catchment**

### **6.2.8.1 Model Calibration, Validation, and Performance Evaluation**

Following the sensitivity analysis, model calibration was carried out to obtain optimum values for sensitive parameters. SWAT provides three options for calibration: (1) manual calibration, (2) auto-calibration, and (3) combination of these two methods. Firstly manual calibration was performed to fine tune some of the parameters where some model parameters were adjusted by manual calibration. In this procedure, parameter values were adjusted by changing one or two parameters at a time within the allowable ranges either by replacement of the initial value or addition or by multiplication of the initial value. Then, auto calibration procedure was applied. The calibration was done on monthly time steps using the average measured streamflow data of the Geba catchment. During the calibration step, the first three years were considered for model warm up in order to establish proper initial conditions and stabilize the model. Unlike other studies (Setegn et al., 2008; Setegn et al., 2010; Mango et al., 2011; Mengistu and Sorteberg, 2012; Shawul et al., 2013; Babar and Ramesh, 2015), where a single LU/LC map was utilised throughout the simulation period, a novel way of calibration is performed with multiple LU/LC maps in this study. To take into account impact of change in land cover, historical data available for the period 1973 to 2013 was divided in to 4 time steps. Calibration was performed separately for each of the time period. Say, from 1974 to 1979, 1984 to 1989, 1994 to 1999 and 2004 to 2009 for the 1973, 1987, 2000 and 2013 LU/LC maps, respectively.

Auto calibration was performed for sensitive flow parameters that produced medium, high and very high mean sensitivity index values. Arc SWAT includes a multi objective, automated calibration procedure that was developed by (Van Griensven et al., 2006). The calibration procedure is based on a Shuffled Complex Evolution Algorithm (SCE-UA) and a single objective function. The auto calibration tool in SWAT-CUP can be run in the Sequential Uncertainty Fitting (SUFI-2) with uncertainty analysis mode. For this study, the SUFI-2 option was selected (Abbaspour et al., 2007). This method was chosen for its applicability in both simple and complex



hydrological models. In this procedure, by entering the Arc SWAT interface Auto-Calibration window, first the SWAT simulation was specified for performing the auto-calibration and the location of the sub-basin, where observed data could be compared against simulated output. Then, the desired parameters for optimization, observed data file, and methods of calibration were selected. Hence, 12 flow parameters were considered in the calibration process. After the auto calibration runs completed, the model was run using the best parameter output values and the simulations were compared with observed streamflow data using model performance indicators.

Validation was also taken up to compare the model outputs with an independent data set without making further adjustment of the parameter values. The measured data of monthly average daily streamflow is used for validation of the model at the Geba River basin gauging station for an independent data set. Data were divided into time steps for the periods 1980-1983, 1990-1993, 2000-2003 and 2010-2013 for the 1973, 1987, 2000 and 2013 land use/land cover maps, respectively used. To ascertain the performance of the model across the simulation period four model performance statistics along with continuous and scatter plots were used. Performance statistics used being: (1) coefficient of determination ( $R^2$ ) (Eq. 6.12), (2) Nash and Sutcliffe simulation efficiency ( $E_{NS}$ ) (Eq. 6.13), (3) ratio of root mean square error to measured standard deviation (RSR) (Eq. 6.14) and (4) Percent bias (PBIAS) (Eq. 6.14). The coefficient determination ( $R^2$ ) describes the proportion the variance in measured data by the model. It is the magnitude of linear relationship between the observed and the simulated values.  $R^2$  ranges from 0 (which indicates the model is poor) to 1 (which indicates the model is good), with higher values indicating less error variance, and typical values greater than 0.6 are considered acceptable (Santhi et al., 2001). The Nash – Sutcliffe simulation efficiency ( $E_{NS}$ ) indicates that how well the plots (i.e., the goodness of fit) between the observed and the final best simulated data fits the 1:1 line (Nash and Sutcliffe, 1970).

$$R^2 = \frac{\sum_{i=1}^n (Q_{o,i} - \bar{Q}_o)(Q_{s,i} - \bar{Q}_s)}{\sqrt{\sum_{i=1}^n (Q_{o,i} - \bar{Q}_o)^2 \sum_{i=1}^n (Q_{s,i} - \bar{Q}_s)^2}} \quad (6.12)$$

$$E_{NS} = 1 - \frac{\sum_{i=1}^n (Q_{o,i} - \bar{Q}_o)(Q_{s,i} - \bar{Q}_s)}{\sum_{i=1}^n (Q_{o,i} - \bar{Q}_o)^2} \quad (6.13)$$

Where,  $Q_o$  observed discharge ( $m^3/s$ ),  $Q_s$  is simulated discharge ( $m^3/s$ ),  $\bar{Q}_o$  is the average observe discharge ( $m^3/s$ ) and  $\bar{Q}_s$  is the average simulated discharge ( $m^3/s$ ).

**RMSE-observations standard deviation ratio (RSR):** Root Mean Square Error (RMSE) is the error index statistics which is commonly used and it is generally accepted that the lower the RMSE the better the model performance (Chu and Shirmohammadi, 2004; Singh et al., 2004; Moriasi et al., 2007). RSR standardizes RMSE using the observations standard deviation, and it combines an error index (Moriasi et al. 2007). RSR is the ratio of the RMSE and standard deviation of measured data, and calculated using Eq. (6.14).

$$RSR = \frac{RMSE}{STDEV_{obs}} = \frac{\sqrt{\sum_{i=1}^n (Q_i^{obs} - Q_i^{sim})^2}}{\sqrt{\sum_{i=1}^n (Q_i^{obs} - Q_i^{mean})^2}} \quad (6.14)$$

RSR varies from the optimal value of 0, which indicates zero RMSE or residual variation and therefore perfect model simulation, to a large positive value. The lower RSR, lower is the RMSE and the better the model simulation performance.

**Percent bias (PBIAS):** the average tendency of the simulated data to be larger or smaller than their observed counterparts is measured by the Percent bias (PBIAS) (Gupta et al., 1999). The optimal value of PBIAS is 0.0, with low magnitude values indicating accurate model simulation. Positive values indicate model underestimation

bias, and negative values indicate model overestimation bias (Gupta et al., 1999). PBIAS is calculated with Eq. 6.15.

$$PBIAS = \frac{\sum_{i=1}^n Q_i^{obs} - \sum_{i=1}^n Q_i^{sim}}{\sum_{i=1}^n Q_i^{obs}} * 100 \quad (6.15)$$

## 6.3 Results and Discussion

### 6.3.1 Sensitivity Analysis and Parameter Estimation

Sensitivity analysis was performed on flow parameters of SWAT on monthly time steps with observed data. For this analysis, 22 parameters which influence hydrological processes within SWAT were considered. Figure (6.5) indicates the sensitivity ranks for each of these parameters. It can be seen that parameter CN is the most sensitive (rank number 1) and parameter Rchr\_Dp is the least sensitive one (rank number 22). Values of mean relative sensitivity (MRS) were calculated for each of these parameters and using the classification criteria presented in Table (6.4) they were assigned classes I to IV. All parameters falling in class I (small to negligible) were eliminated from further analysis. Accordingly, only 12 parameters falling in classes II (medium), III (high) and IV (very high) were considered and which are in common in run of the four LU/LC maps. These parameters along with their MRS values are listed in Table (6.6) starting with the most sensitive and ending with the least sensitive one. The result of the analysis indicates the most sensitive parameters are; Curve number (CN), Groundwater recession factor (ALPHA\_BF), Soil Available Water Capacity (SOL\_AWC), Soil Evaporation Compensation factor (ESCO), Threshold depth of water in the shallow aquifer required for return flow to occur (GWQMN), Threshold depth of water in the shallow aquifer for revap to occur (REVAPMN), hydraulic conductivity in main channel (CH\_K2), Manning coefficient for main channel, (CH\_N2), Saturated hydraulic conductivity (SOL\_K), are identified to be highly sensitive parameters. The other parameters such Groundwater revap coefficient (GW\_REVAP), Ground water delay (GW\_DELAY) and Soil depth (SOL\_Z) were identified as next important parameters and were retained rank 10 to

12, respectively. The remaining parameters were not considered during calibration process as the model simulation result was not sensitive to these parameters.

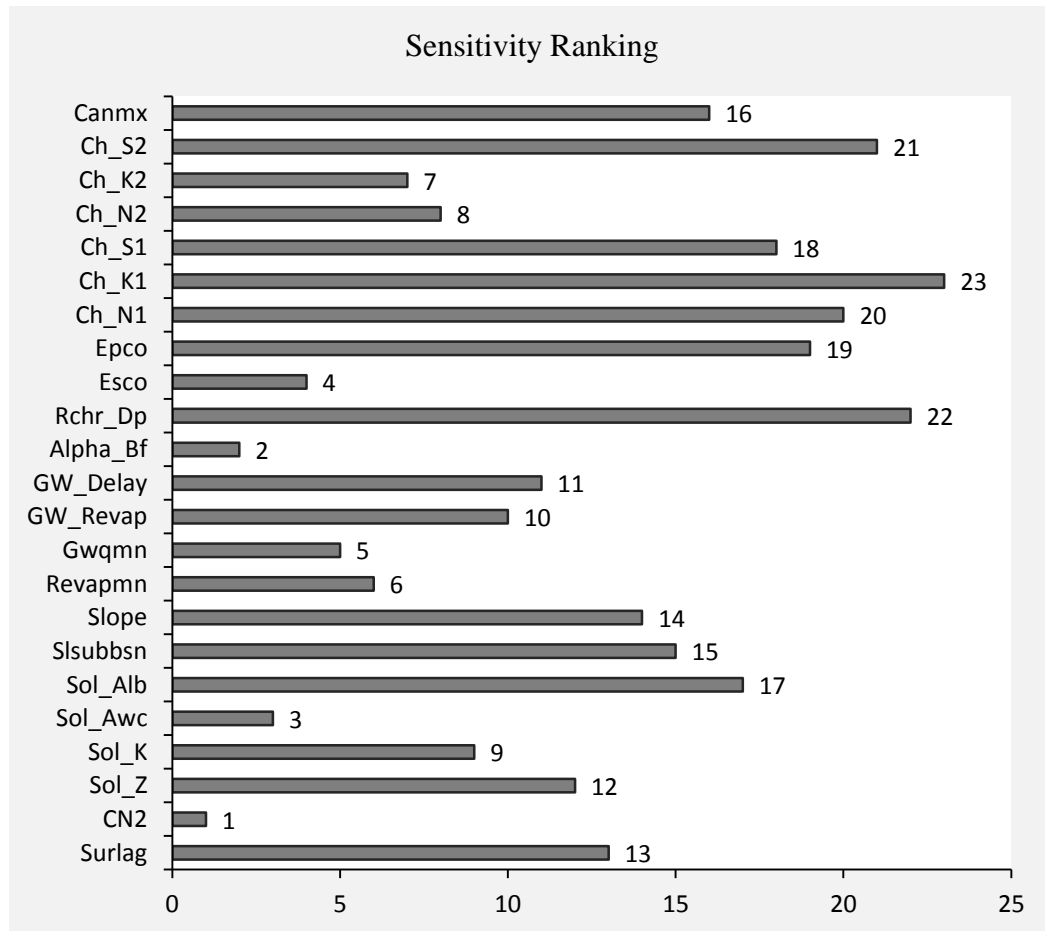


**Figure 6.5 Sensitivity ranking of 22 SWAT model parameters related to hydrological processes.**

**Table 6.6: SWAT most sensitive parameters and their MRS values.**

Sensitive Parameters	Description	Lower and		MRS	Category
		Upper	Rank		
CN2	SCS runoff CN for moisture condition II	± 0.25	1	2.67	V.H
ALPHA_BF	Baseflow alpha factor (days)	0-1	2	1.487	V.H
SOL_AWC	Available water capacity of the soil layer (mm/mm soil)	± 0.25	3	1.025	V.H
ESCO	Soil evaporation compensation factor	0-1	4	0.863	H
GWQMN	Threshold depth of water in the shallow aquifer required for return flow to occur (mm)	0-5000	5	0.51	H
REVAPMN	Threshold depth of water in the shallow aquifer for revap to occur (mm)	0-500	6	0.328	H
CH_K2	hydraulic conductivity in main channel (mm/hrs)	0-150	7	0.307	H
CH_N2	Manning coefficient for main channel	0-1	8	0.274	H
SOL_K	Soil conductivity (mm/hrs)	0-100	9	0.223	H
GW_REVAP	Groundwater revap coefficient	0.02-0.2	10	0.162	M
GW_DELAY	Groundwater delay (days)	0-50	11	0.147	M
SOL_Z	Soil depth	± 0.25	12	0.12	M

The 12 sensitive parameters (Table 6.6) are related to runoff, ground water, soil and channel components of the SWAT model. Interestingly, the parameters which have very high sensitivity CN2, ALPHA\_BF and SOL\_AWC influence runoff, groundwater and soil components respectively. CN2 determines the amount of rainfall that becomes runoff as well as the amount that infiltrates into soil profile. ALPHA\_BF is a direct index of ground water flow response to changes in recharges and affects dry season flows. SOL\_AWC being the maximum water holding capacity

of the soil profile determines the magnitude and timing of direct runoff and groundwater recharge components. The other parameters listed in Table (6.6) are also mostly related to the rate of water movement in the soil, groundwater and the river network. Overall, it appears that the most sensitive SWAT model parameters for the Geba basin are associated with the magnitude and timing of direct runoff and baseflow components of streamflow. These findings are in agreement with past studies undertaken in the Northern Highlands of Ethiopia (Setegn et al., 2008; Tesfahunegn et al., 2012; Ashenafi, 2014).

### **6.3.2 Model Calibration and Validation**

Simulation was initiated with the default parameter values. The streamflow hydrographs showed relatively weak matching between the simulated and observed values. This implies that, when SWAT model is applied in regions other than it was calibrated, it requires a fresh calibration. Model calibration is to improve the accuracy of model predictions was carried out. The sensitive flow parameters of SWAT which are already identified (Table 6.6) subjected to small changes to ensure a better match between observed and simulated streamflow. First, the most sensitive parameters were adjusted by manual calibration procedure based on the information available in literature. In this procedure, the values of the parameters were varied iteratively within the allowable ranges to increase the value of  $E_{NS}$  (Eq. 6.13). Then, auto calibration processes that significantly improved model efficiency was run using sensitive parameters that were identified during sensitivity analysis. Table 6.7 presents the final result of optimal model parameters achieved through calibration.

**Table 6.7: SWAT flow sensitive parameters and fitted values after calibration.**

Sensitive Parameters	Description	Lower and Upper bound	Final Fitted Value
CN2	SCS runoff CN for moisture condition II	±0.25	-0.143 <sup>r</sup>
ALPHA_BF	Baseflow alpha factor (days)	0-1	0.34 <sup>v</sup>
SOL_AWC	Available water capacity of the soil layer (mm/mm soil)	±0.25	-0.21 <sup>r</sup>
ESCO	Soil evaporation compensation factor	0-1	0.75 <sup>v</sup>
GWQMN	Threshold depth of water in the shallow aquifer required for return flow to occur (mm)	0-5000	321 <sup>v</sup>
REVAPMN	Threshold depth of water in the shallow aquifer for revap to occur (mm)	0-500	227 <sup>v</sup>
CH_K2	hydraulic conductivity in main channel (mm/hrs)	0-150	26.2 <sup>v</sup>
CH_N2	Manning coefficient for main channel	0-1	0.058 <sup>v</sup>
SOL_K	Soil conductivity (mm/hrs)	0-100	86.3 <sup>r</sup>
GW_REVAP	Groundwater revap coefficient	0.02-0.2	0.17 <sup>v</sup>
GW_DELAY	Groundwater delay (days)	0-50	20 <sup>v</sup>
SOL_Z	Soil depth	±0.25	0.24 <sup>r</sup>

<sup>r</sup> means relative change in the existing parameter where the current value is multiplied by  $1 + a$  given value).

<sup>v</sup> means the existing parameter value is to be replaced by the given value.

During the calibration step, the first three years were considered as model warm up period in order to establish proper initial conditions and to stabilize the model. Calibration was then performed for four time steps separately, i.e., from 1974 to 1979, 1984 to 1989, 1994 to 1999 and 2004 to 2009 for the 1973, 1987, 2000 and 2013 LU/LC map, respectively. To test the model's accuracy, goodness-of-fit measures were evaluated. Streamflow was calibrated first for average annual conditions followed by monthly and daily to fine-tune the calibration processes until model

simulation results were acceptable with values of  $R^2 > 0.6$ ,  $E_{NS} > 0.5$ ,  $RSR \leq 0.7$  and  $PBIAS \pm 25\%$  (Santhi et al., 2001; Moriasi et al., 2007).

Model performance during calibration for daily and monthly time steps were assessed quantitatively and qualitatively using; (i) performance indices (ii) times series plots and (iii) Scatter plots.

### 6.3.2.1 Daily and Monthly Streamflow Predictions

To begin the simulations SWAT model was run with a single static LU/LC (2000) map, mostly followed in many studies. The SWAT model was calibrated and validated using a single LU/LC map for the 1973-2013 time periods. The value of model performance indices obtained for daily and monthly streamflow predictions during the calibration and validation periods are shown in Table (6.8). It is found that the value of  $R^2$  was 0.63 and 0.68 for daily and monthly simulations for calibration period respectively and  $R^2$  value for validation period for daily and monthly simulations were 0.61 to 0.66 respectively. Similarly,  $E_{NS}$  value for daily and monthly simulations were 0.55 and 0.64 respectively for calibration period and 0.52 and 0.65 for daily and monthly time step simulations for the validation period. Though the values of  $R^2$  and  $E_{NS}$  fulfilled the minimum values recommended in the literature ( $R^2 > 0.6$ ,  $E_{NS} > 0.5$ ), one can say only they are satisfactory when compared with the model calibration and validation using multiple LU/LC maps (Table 6.9 and 6.10).

**Table 6.8: SWAT model performance evaluation for daily and monthly streamflow predictions using static LU/LC (2000) map.**

Model Performance Index	Calibration		Validation	
	1974-2000		2001-2013	
	daily	Monthly	daily	Monthly
$R^2$	0.63	0.68	0.61	0.66
$E_{NS}$	0.55	0.64	0.52	0.60
RSR	0.59	0.53	0.61	0.56
PBIAS	-17.75	-15.38	-20.11	-18.32



Values of the four model performance indices obtained for daily streamflow predictions during the calibration phase are listed in Table (6.9). As mentioned earlier the SWAT model was calibrated separately for four different historical periods using maps depicting LU/LC classes existing in the study area during the corresponding period. Measured and simulated flows, both for monthly and daily time steps had a favourable comparison during all the four time steps (Table 6.9, Figures 6.6). This is evident from values of  $R^2$  ranging from 0.89 to 0.94 for monthly simulations and for daily simulations  $R^2$  values ranged from 0.79 to 0.88. Correspondingly,  $E_{NS}$  values varied from 0.77 to 0.81 for monthly time step and 0.73 to 0.77 for daily simulations. While RSR values varied from 0.44 to 0.48 for monthly and 0.47 to 0.52 for daily simulations, PBIAS varied from -18.24 to -11.57 for daily and -14.21 to -10.66 for monthly calibration. Highest values of  $R^2$  and PBIAS were obtained for the 2000 LU/LC condition, and highest  $E_{NS}$  and RSR values resulted for the 1987 LU/LC condition (Table 6.10).

Overall we can say model performance is very good, consistently across calibration and validation in both daily and monthly predictions. These results are better than the earlier results published in this region where representative land covers were not utilised in the simulations (Setegn et al., 2008; Bertie et al., 2010; Tesfahunegn et al., 2012; Shawul et al., 2013). Though SWAT is not meant for peak flow estimation Hydrograph of observed and simulated flow indicated that the SWAT model is even capable of catching up the peaks and valleys of streamflow response.

The SWAT model derived streamflow volume estimation for high flow events is over estimated to some level for calibration period except between the years 1975 and 1977 in the 1973 LU/LC map and in 2006 in the 2013 LU/LC map (Figure 6.6). This may be due to the fact that: (i) usually measured high flows are erroneous compared to medium flows (ii) the spatial distribution of rainfall intensity spread over smaller area compared to low intense storms eventually catch of the rain gauge may not be representative (iii) SWAT model is not basically designed for flood modelling.

Figures 6.7 and 6.8 compare the daily and monthly simulated flows with observed daily and monthly flows. It is indicated that simulated flows are consistently more

than the observed ones for daily and monthly average daily flows. The daily and monthly average daily simulated streamflow values are plotted against the observed values and their distribution about 1:1. The simulated streamflow are distributed uniformly along the 1:1 line for both lower and higher values of observed streamflow during the calibration periods more for 2000 and 2013 LU/LC maps than 1973 and 1987 LU/LC maps. The statistical comparison between the observed monthly streamflow and best simulation result showed a good agreement.

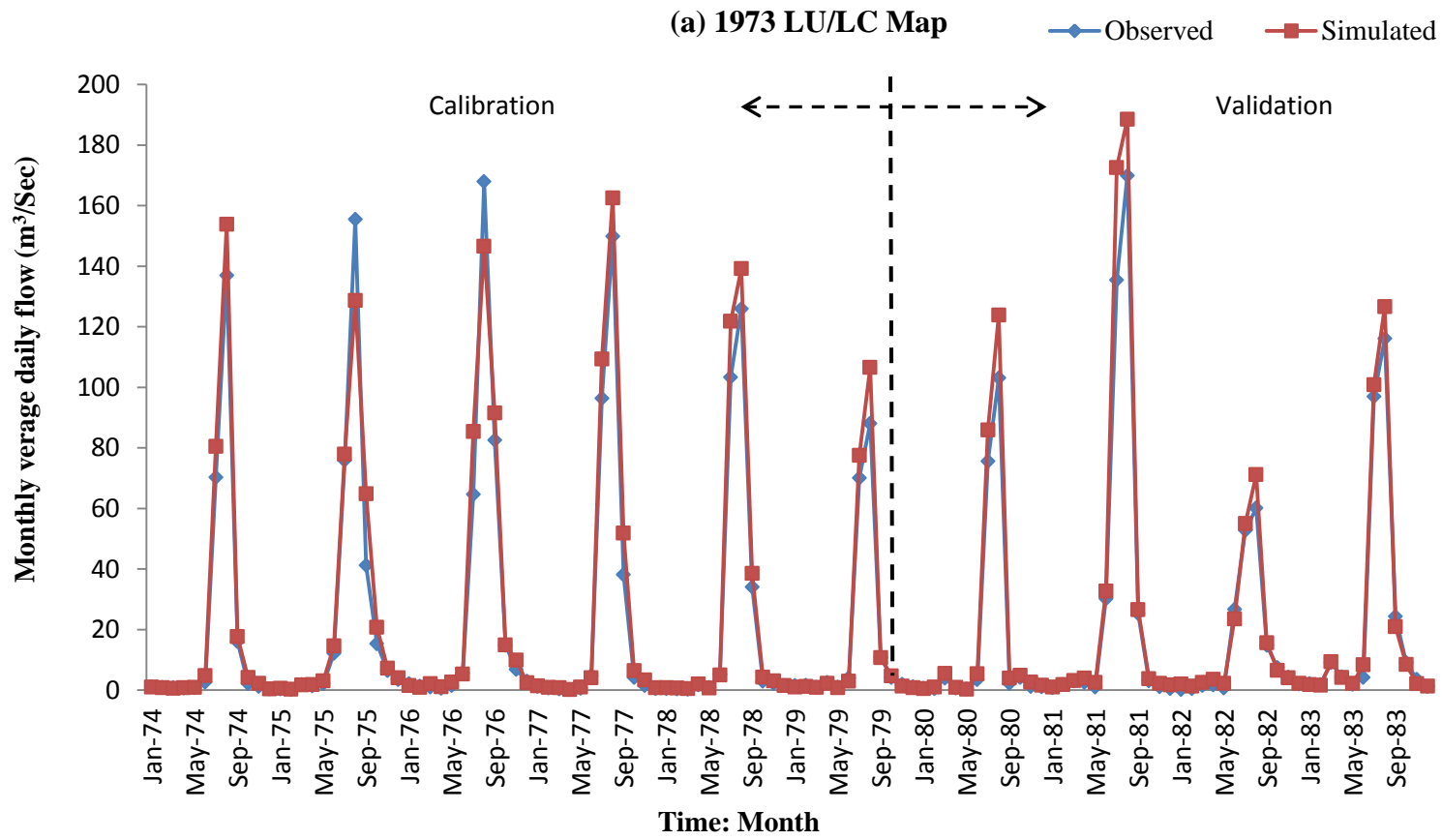
As simulations of multiple LU/LC maps carried out for calibration, the linear fit distribution also differs accordingly. In 1973 and 1987 LU/LC maps, the high flows were higher divergent than the low flows over the 1:1 fitting line. In 2000 and 2013 LU/LC maps though it shows over estimation, the simulations estimated the streamflow volume better remained more consistent compared to the other two LU/LC maps.

**Table 6.9: SWAT model performance evaluation for daily streamflow predictions.**

Model Performance Index	Calibration				Validation			
	1973 LU/LC	1987 LU/LC	2000 LU/LC	2013 LU/LC	1973 LU/LC	1987 LU/LC	2000 LU/LC	2013 LU/LC
	1974-1979	1984-1989	1994-1999	2004-2009	1980-1983	1990-1993	2000-2003	2010-2013
R <sup>2</sup>	0.84	0.86	0.88	0.79	0.77	0.86	0.91	0.87
E <sub>NS</sub>	0.75	0.77	0.75	0.73	0.7	0.77	0.78	0.79
RSR	0.51	0.47	0.49	0.52	0.55	0.49	0.43	0.46
PBIAS	-17.62	-16.79	-11.6	-18.24	-18.53	-14.82	-10.28	-16.10

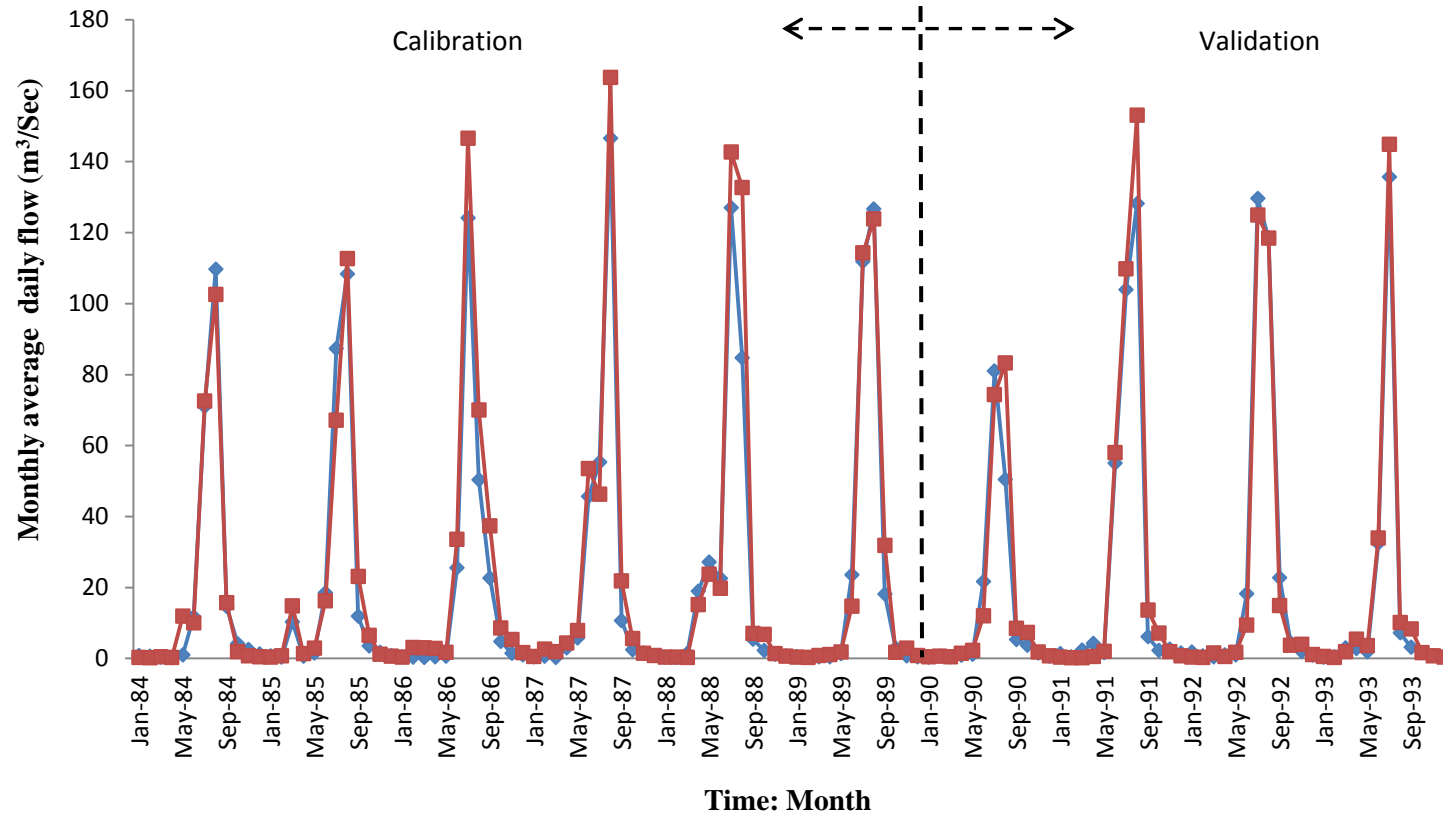
**Table 6.10: SWAT model performance evaluation for monthly streamflow predictions.**

Model Performance Index	Calibration				Validation			
	1973 LU/LC	1987 LU/LC	2000 LU/LC	2013 LU/LC	1973 LU/LC	1987 LU/LC	2000 LU/LC	2013 LU/LC
	1974-1979	1984-1989	1994-1999	2004-2009	1980-1983	1990-1993	2000-2003	2010-2013
R <sup>2</sup>	0.89	0.93	0.94	0.93	0.86	0.95	0.96	0.88
E <sub>NS</sub>	0.77	0.81	0.76	0.82	0.73	0.83	0.83	0.83
RSR	0.48	0.44	0.45	0.45	0.53	0.43	0.41	0.41
PBIAS	-12.28	-12.26	-10.66	-14.21	-13.17	-12.1	-10.31	-14.66

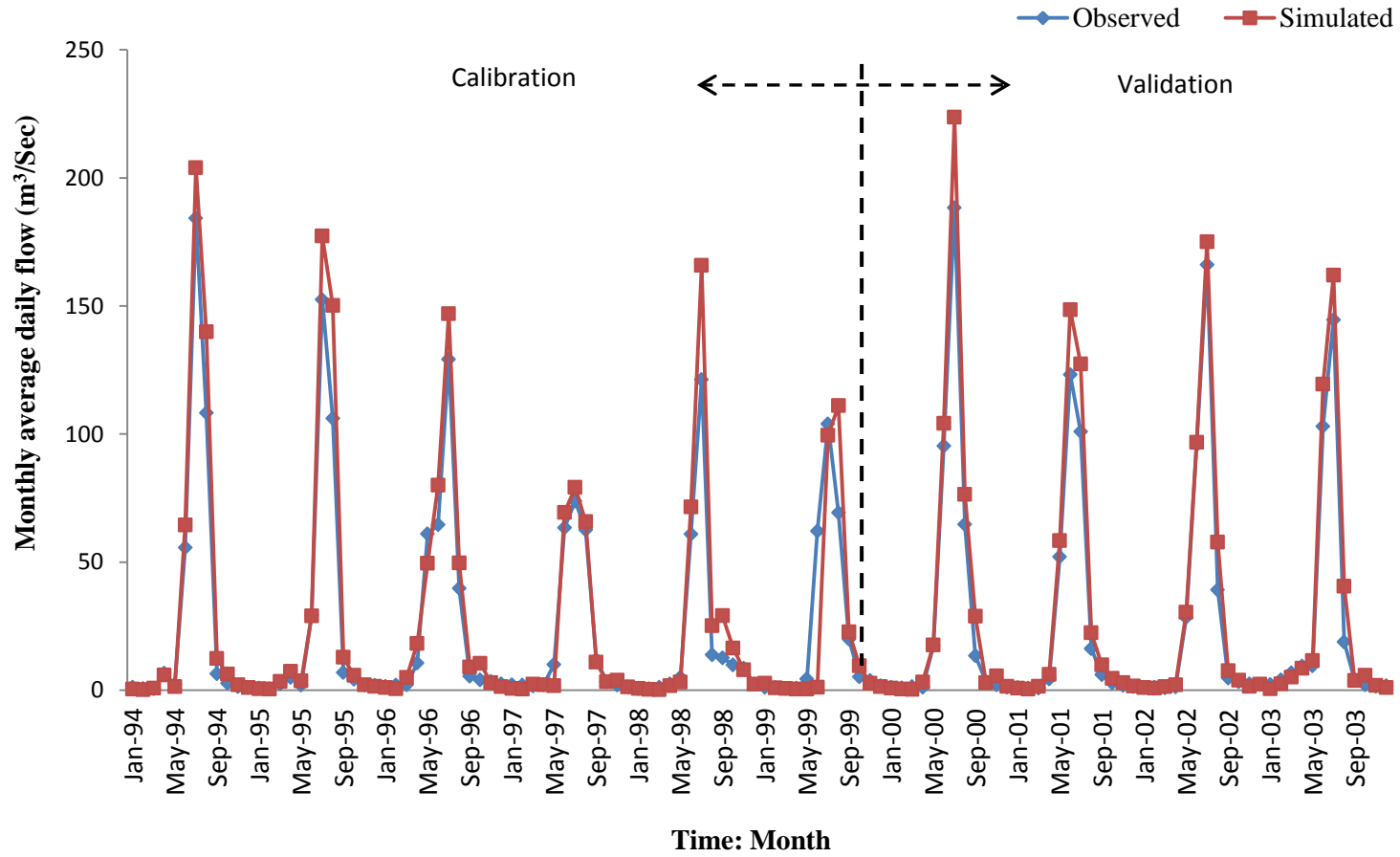


(b) 1987 LU/LC Map

—◆— Observed    —■— Simulated



(c) 2000 LU/LC Map



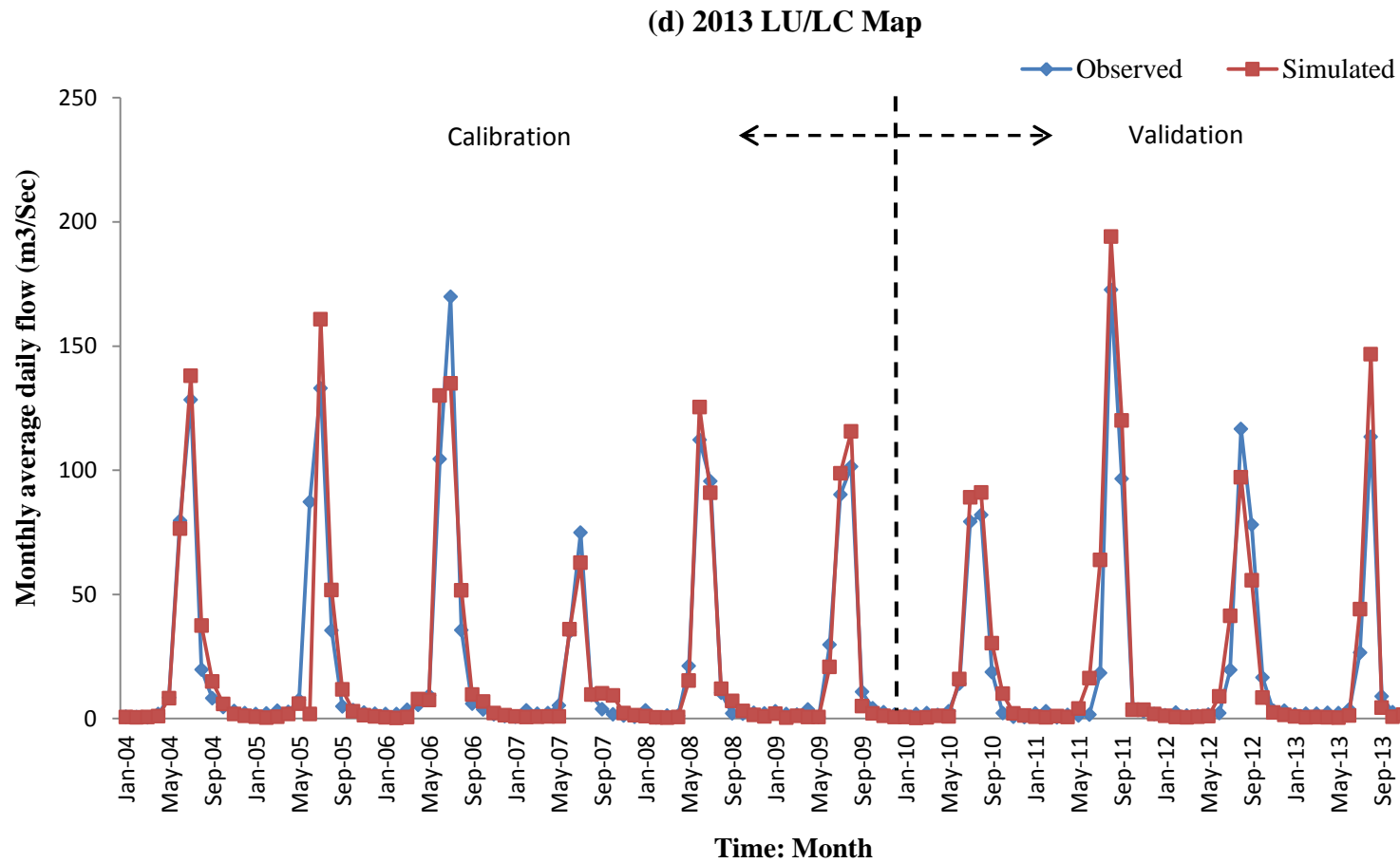


**Figure 6.6 Time series of observed and simulated monthly average daily streamflow for calibration and validation period for (a) 1973, (b) 1987, (c) 2000 and (d) 2013 LU/LC maps.**

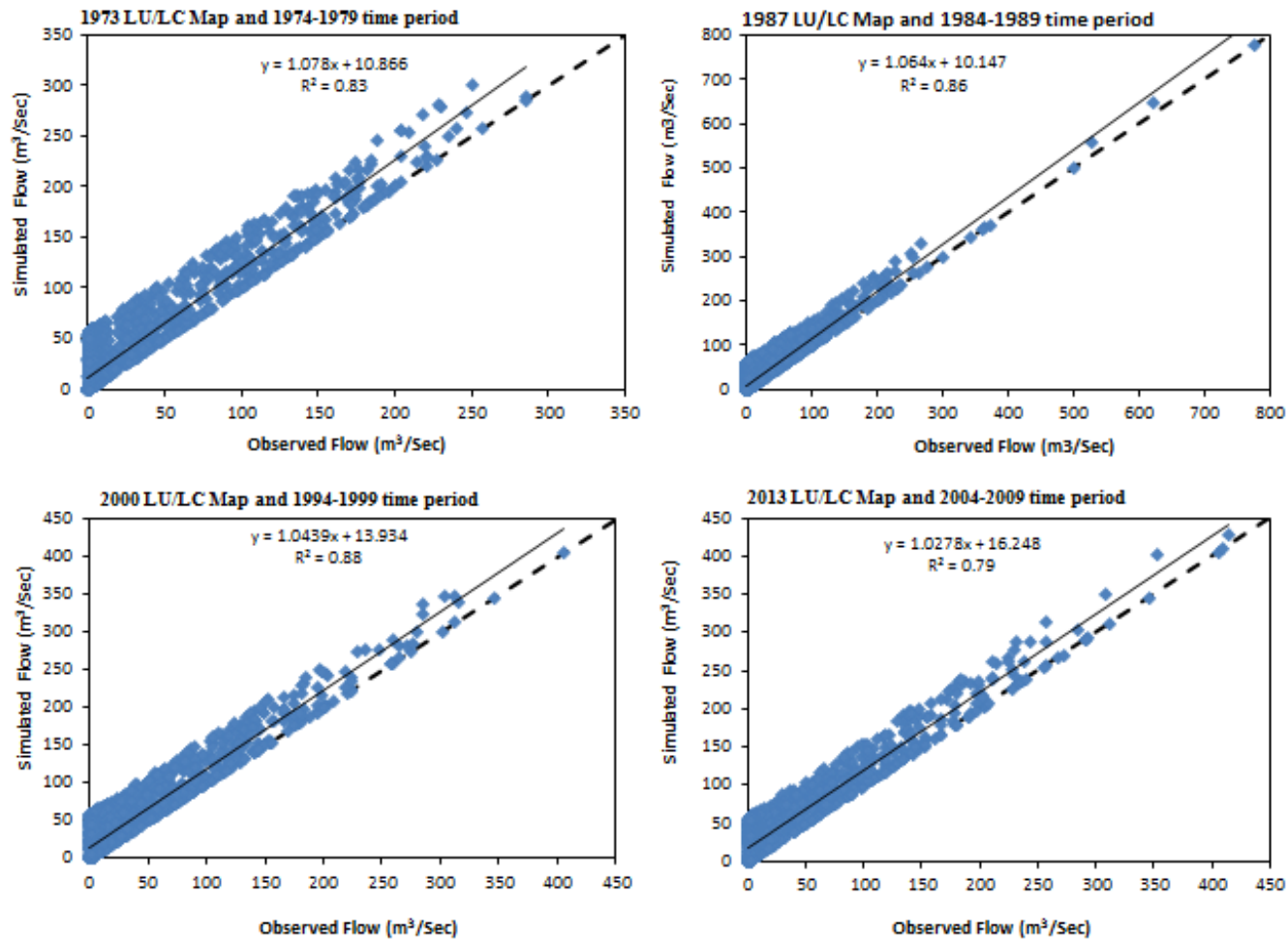


**Figure 6.7 Scatter plots of simulated and observed daily flow for calibration period.**



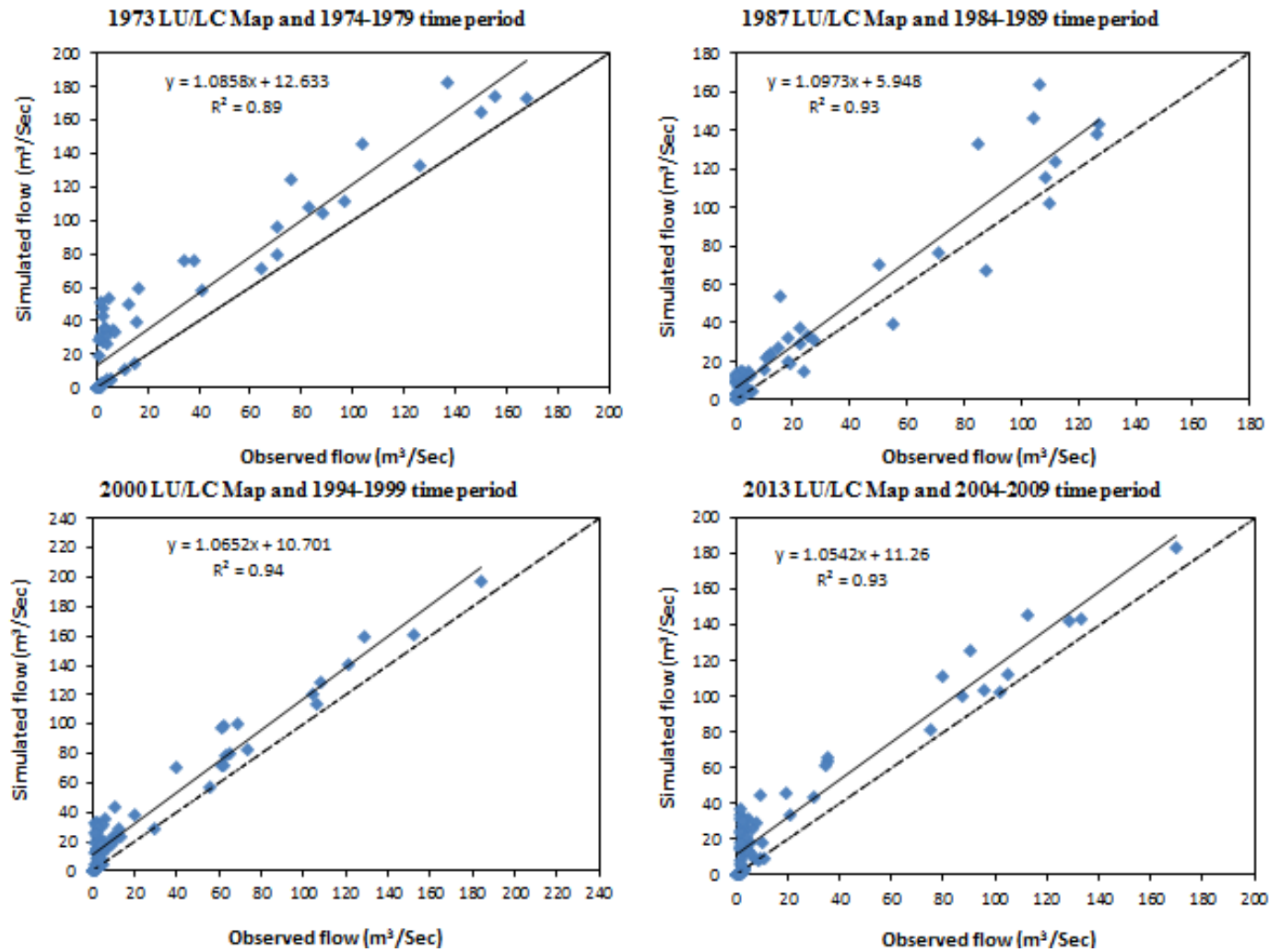


Figure 6.8 Scatter plots of simulated and observed monthly average daily flow for calibration period.

After the model is calibrated, validation of the model at the Geba River basin gauging station was performed for an independent data set on four time steps for the periods 1980-1983, 1990-1993, 2000-2003 and 2010-2013 for the 1973, 1987, 2000 and 2013 LU/LC map, respectively, which is different from the calibration periods without further adjustment of the calibrated parameters.

It was found that the model has strong predictive capability with  $R^2$ ,  $E_{NS}$ , RSR and PBIAS value ranging from 0.86 to 0.96, 0.73 to 0.83, 0.41 to 0.53 and -14.66 to -10.28 %, respectively for the monthly basis. In addition, for the daily values range from 0.77 to 0.91 for  $R^2$ , 0.7 to 0.79 for  $E_{NS}$ , 0.43 to 0.55 for RSR and -18.53 to -10.31 % . Statistical model efficiency criteria fulfilled the recommended requirement of  $R^2 > 0.6$  (Santhi et al., 2001), and  $E_{NS} > 0.5$ ,  $RSR \leq 0.7$  and  $PBIAS \pm 25$  % (Moriassi et al., 2007).

This showed the model parameters represent the processes occurring in the catchment to the best of their ability. The model validation outcomes both for daily and monthly streamflow (Figure 6.9 and Figure 6.10) showed a good fit between the measured and simulated values. The model performed well though the statistical model efficiency measures are high during the calibration process.

Figures 6.6 compares the monthly simulated observed flows that indicate simulated flows are always more than the observed ones except for the years 1992 and 2012 for the validation period for 1987 and 2013 LU/LC map, respectively. The monthly simulated streamflow values are plotted against the observed values and their distribution about 1:1. Validation of streamflow was carried out with multiple LU/LC maps as the calibration does. In all LU/LC maps, the simulations were above the fitting line, this showed over estimation of the simulated flow over the observed ones (Figure 6.9 and 6.10).

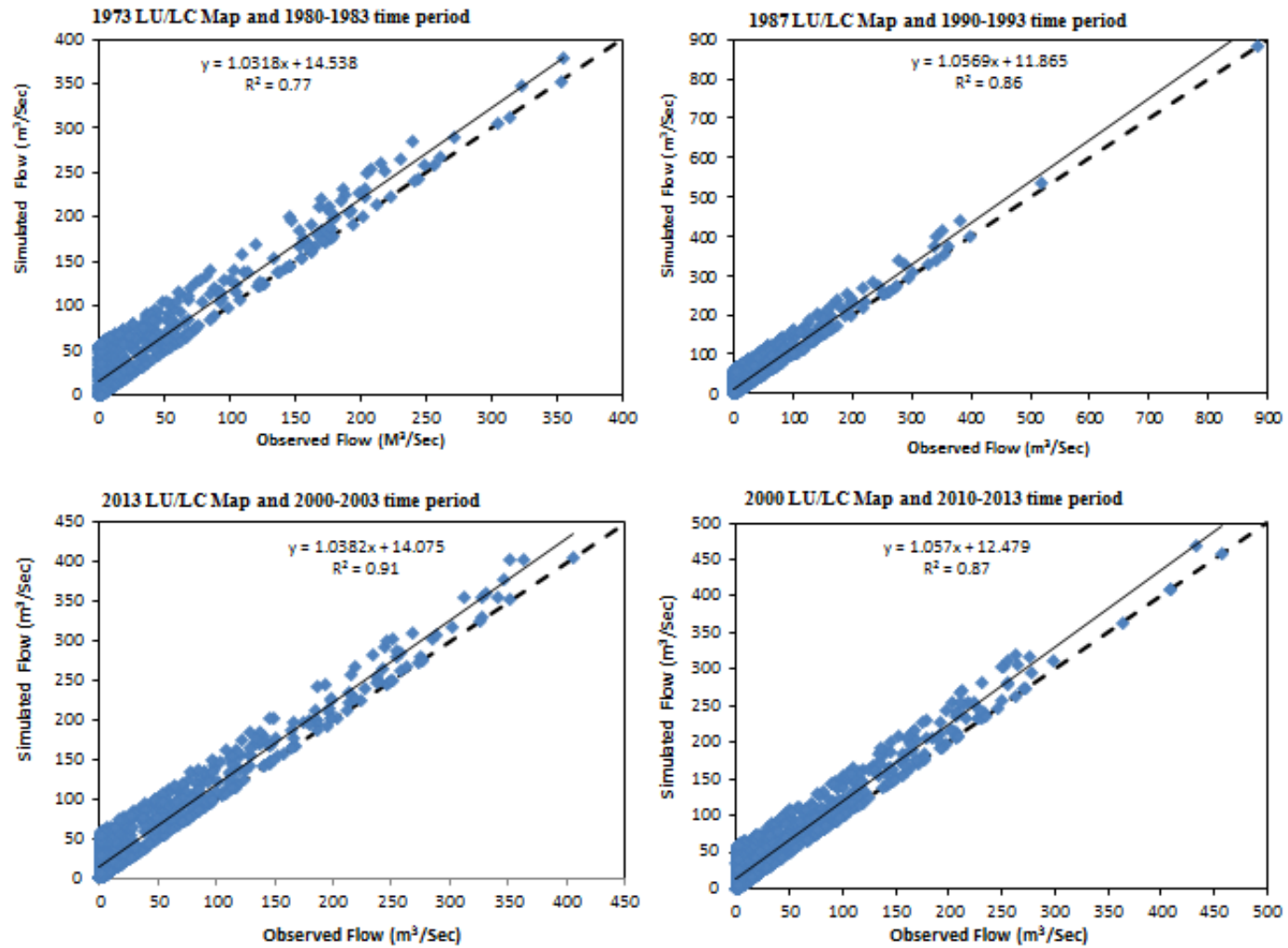


**Figure 6.9** Scatter plots of simulated and observed daily flow for validation period.

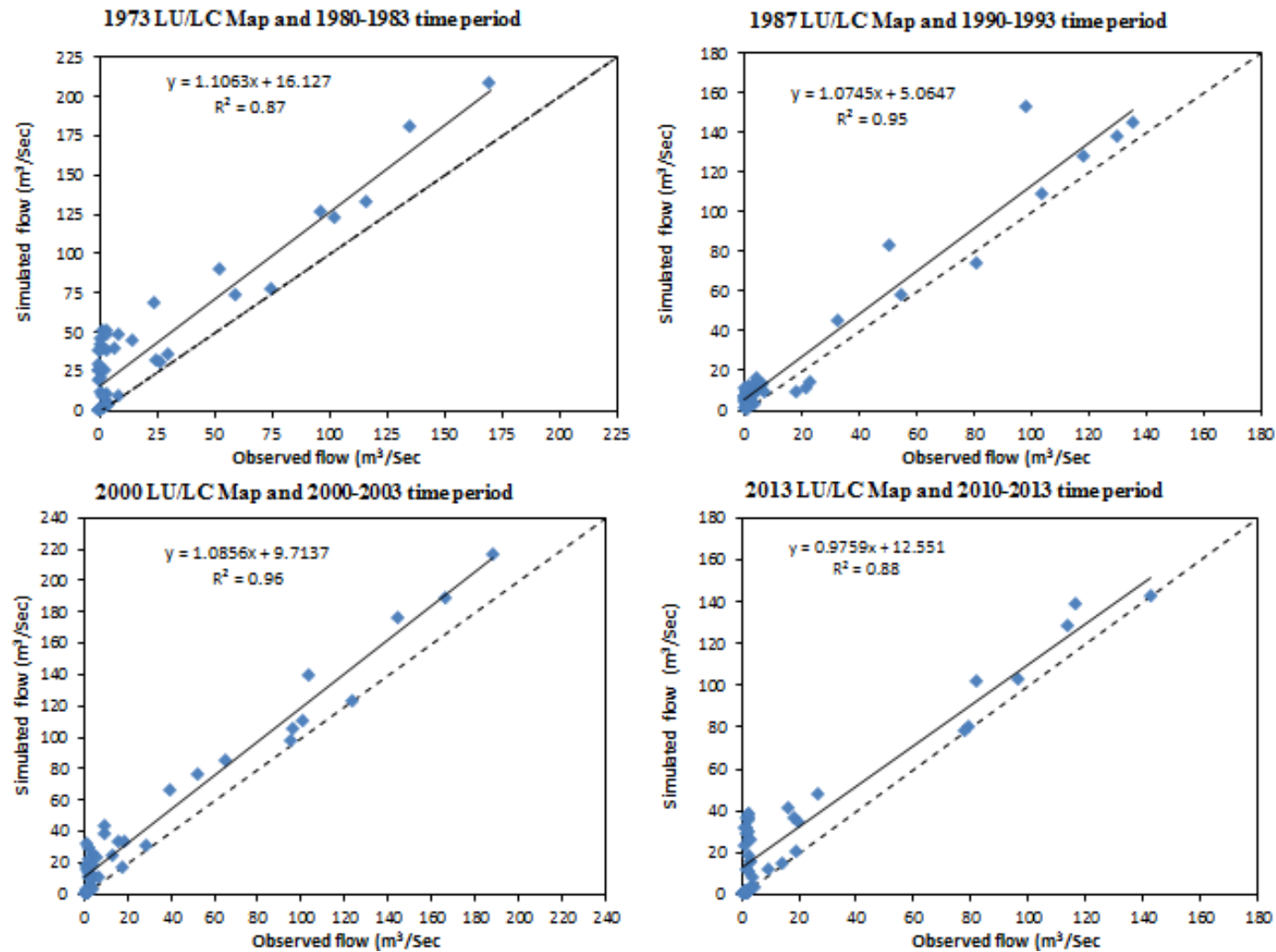


Figure 6.10 Scatter plots of simulated and observed monthly average daily flow for validation period.

The possibility of overestimating the streamflow may be due to the fact that, in such a complex terrain, rainfall is captured only through 7 gauges and the rainfall varies across the catchment from a minimum of 300 mm to a maximum of greater than 950 mm. This finding corroborates and is similar to other previous studies conducted in other parts of the region (Setegn et al., 2009, Ashenafi et al., 2014) where there is overestimation of flows by the SWAT model.

### **6.3.3 Water Balance Components**

The average water balance components for the Geba catchment were extracted from the outputs of the SWAT model. Annual average of the following water balance components were computed from the model output values: the total amount of rainfall (P), surface runoff (SURQ), lateral flow (LATQ), groundwater flow (GWQ), actual evapotranspiration (ET), potential evapotranspiration (PET) and the water yield from the watershed (WY) which includes the contribution from SURQ, LATQ and GWQ minus the transmission losses.

Table 6.11 presents the annual water balance components obtained from the SWAT model for the Geba catchment. Results revealed that evapotranspiration loss (ET) was 70.46 %, 72.67 %, 74 % and 73.8 % (or 535.5 mm, 560.3 mm, 643.7 mm and 513.2 mm) of rainfall (P) for 1973, 1987, 2000 and 2013 LU/LC maps, respectively. It appears that, though ET values are high, findings of this study corroborates and similar to other previous studies (Tewelde, 2009; Setegn, 2009; Afewerki, 2012; Ashenafi, 2014). The possible reason for this could be due to the fact that ET computation in the SWAT model framework is focused more on agricultural crops and therefore may not accurately simulated the process for deep-rooted forests and also since interception losses are not accounted for.

Annual water yields (WY) in the Geba catchment were in the range of 154 mm to 189 mm for the 1973 to 2013 time period which is 22 % and 24.8 % of the annual rainfall where higher water yields occurred in the 1973 LU/LC map where ET value was lower. It can be seen that the SWAT model predicted higher surface runoff (SURQ) in the 2000 LU/LC map, where there was higher deforestation than the other LU/LC maps. On the other hand, surface runoff (SURQ) was lower in the 2013 as integrated

watershed management approaches have been introduced in the catchment and in the region as well. However, a reversal scenario was noticed for ground water flow (GWQ). For annual periods, P must be equal to the sum of ET and WY. However, due to errors arising from a number of sources, this equality may not be satisfied, thereby resulting in a residual error. Accordingly, the annual water balance equation may be re-written as  $P = ET + WY + \text{Residual}$ . Values of Residual errors are shown in Table 6.9, from which it can be seen that for all the LU/LC maps considered the Residual error forms a relatively small percentage of the rainfall ( $< 5\%$ ). The benefits of integrated land resources management which initiated in the year 2000 is noticed in 2013 hydrologic simulation (Table 6.11).

**Table 6.11: Average annual water balance components derived from the SWAT model (all values are in mm of water).**

LU/LC Map	P	SURQ	LATQ	GWQ	WY	ET	PET	Residual
1973	760	88.5	54.45	46.12	189.07	535.5	1808.6	35.43
1987	771.3	97.07	42.34	39.12	178.53	560.3	1856	32.17
2000	870	118.85	34	31.91	184.76	643.5	2104.7	41.74
2013	695.5	87.65	30.62	36.5	154.77	513.2	1671.7	27.53

P, Rainfall; SURQ, Surface runoff contribution to streamflow; LATQ, Lateral flow contribution to streamflow; GWQ, Ground water flow; ET, Actual Evapotranspiration; PET, Potential Evapotranspiration; WY, Water Yield ( $WY = SURQ + LATQ + GWQ$ ); Residual =  $P - ET - WY$ .

#### **6.3.4 Model Calibration and Validation for Daily Sediment Simulations**

The SWAT sediment prediction model was calibrated using daily measured sediment data from 2008–2009 and validated for 2010 to 2011. It is important to understand that the sediment concentration data is accessible only for rainy season (i.e., July to September). The model performance of daily sediment prediction for calibration and validation time period is shown in Table 6.12.

For calibration period the simulated sediment concentration matched the observed with  $R^2$  value ranging from 0.87 to 0.89, the  $E_{NS}$  value varies from 0.78 to 0.81, the RSR values ranging from 0.43 to 0.47 and the PBIAS value varies from -16.04 to -10.72 % with highest  $R^2$  and  $E_{NS}$  for the 2013 land use/land cover condition, and highest RSR values for the 2000 land use/land cover condition (Table 6.12). On the other hand, the daily simulated sediment concentration showed good agreement to the observed which is verified by  $R^2$  with a value ranging 0.81 to 0.89,  $E_{NS}$  is 0.8, RSR value is 0.45 and PBIAS varying from -14.85 % to -10.18 % during validation period. Therefore, it is found that the performance of sediment simulation is very good for model calibration and validation as compared to the performance range model evaluation criterion ( $R^2 > 0.6$ ,  $E_{NS} > 0.5$ ,  $RSR \leq 0.70$  and  $PBIAS = \pm 55$  %) introduced by Santhi et al. (2001) and Moriasi et al. (2007).

Studies conducted in different parts of the country showed similar results so that the current study model performance comparable to the results reported by Steenhuis et al. (2009) who reported that the SWAT model showed a good match between measured and simulated sediment obtained  $E_{NS}$  is equal 0.75 for the calibration and  $E_{NS}$  is equal 0.69 for the validation periods, Bertie et al. (2011) reported calibration and validation periods with ( $E_{NS} = 0.88$ ,  $RSR = 0.35$ , and  $PBIAS = -0.05$  %) and ( $E_{NS} = 0.83$ ,  $RSR = 0.61$ , and  $PBIAS = -11$  %), respectively for the Blue Nile basin. Through modelling of the Lake Tana basin, Setegn et al, (2010) indicated that the sediment simulated with SWAT model were reasonable and accurate with  $R^2 = 0.86$ ,  $E_{NS} = 0.81$ ,  $RSR = 0.23$  and  $PBIAS = 28$  % for calibration and  $R^2 = 0.84$ ,  $E_{NS} = 0.79$ ,  $RSR = 0.29$  and  $PBIAS = 30$  % for validation periods.

**Table 6.12: Model Performance values for sediment during calibration and validation period for 2000 and 2013 LU/LC maps.**

Index	2000		2013	
	Calibration	Validation	Calibration	Validation
$R^2$	0.87	0.81	0.89	0.89
NSE	0.78	0.80	0.81	0.79
RSR	0.47	0.45	0.43	0.45
PBIAS	-16.04	-10.18	-10.72	-14.85

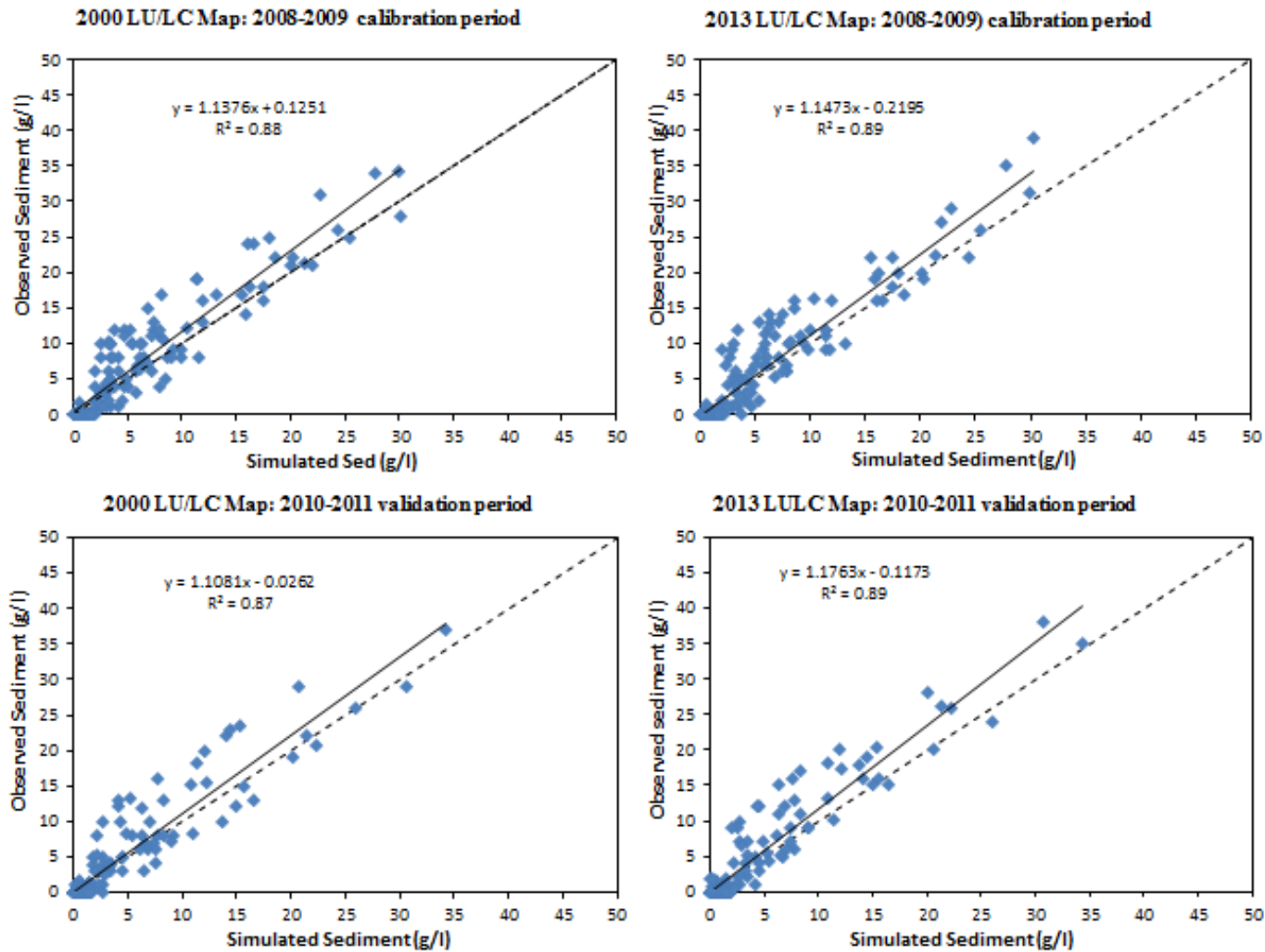
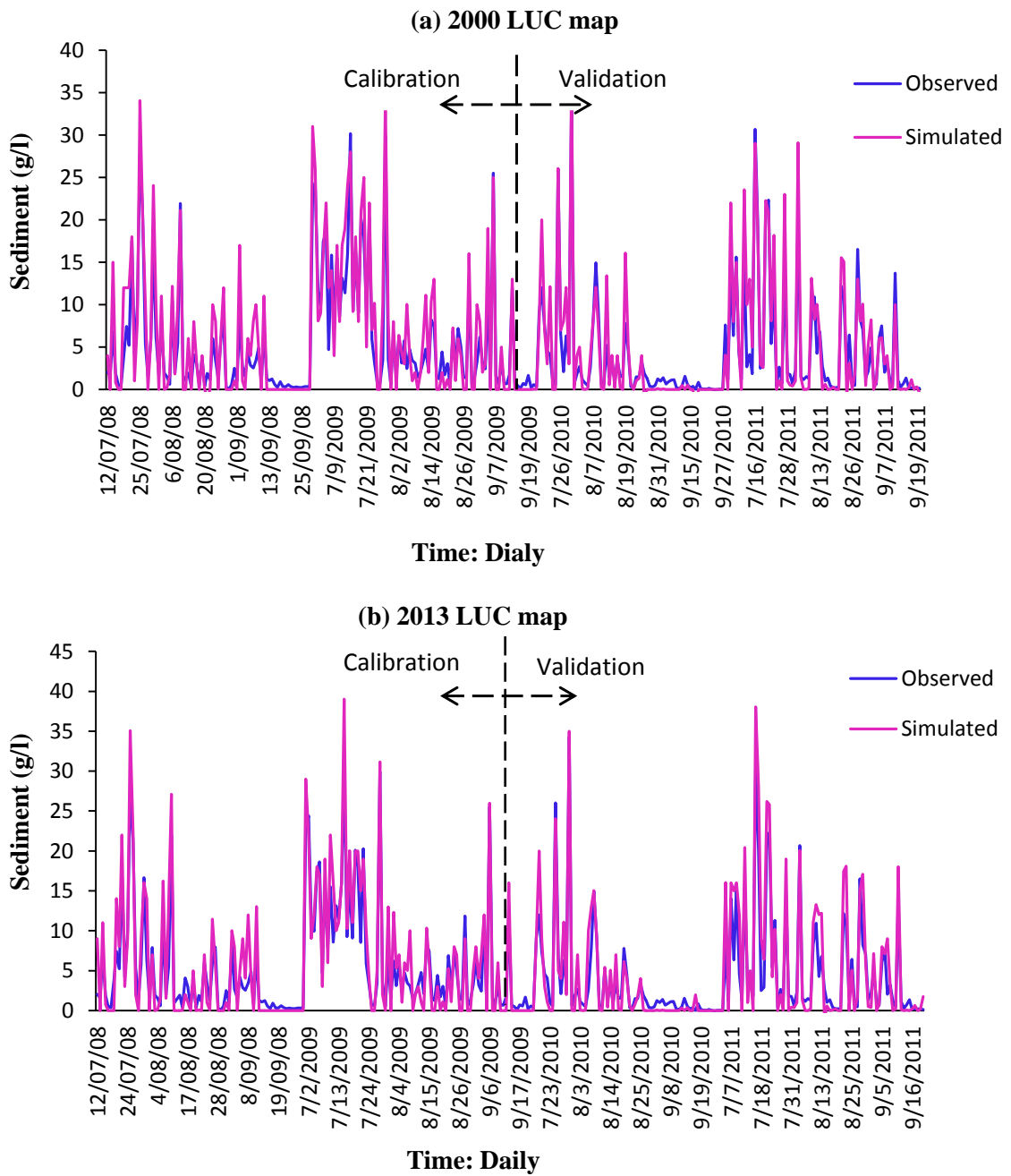


Figure 6.11 Scatter plot of observed and simulated sediment for calibration and validation period for 2000 and 2013 LU/LC map.



The final fitted values compare the monthly simulated with measured sediment yields. The monthly simulated sediment yield values are plotted against the measured values and their distribution about 1:1 (Figure 6.11). The simulated sediment yields are distributed uniformly along the linear distribution fitting line for both lower and higher values of measured sediment yields during the calibration and validation periods. The predictable sediment yield is a function of the surface runoff and peak rate of runoff and has direct relation with the rainfall and streamflow. Generally speaking the higher the rainfall the higher will be the surface runoff and the suspended sediment yield.

The daily sediment concentration comparisons between observed and simulated for calibration and validation period is shown in Figures 6.12. The model well simulated sediment concentration on the rising and the falling limbs of the sediment hydrograph during calibration and validation periods. Though, the sediment peak was well represented in all of the years, the model slightly overestimated the peaks for some days in the month of August in 2009 and August 2010 and 2011 for 2000 and 2013 land use/land cover conditions. Since the model also overestimated the streamflow, sediment overestimation is on the expected line. The possible reason may be inadequate representation of rainfall by seven gauges spread out in 5137 km<sup>2</sup> of catchment.



**Figure 6.11 Time series of observed and simulated daily sediment for Calibration and validation period for (a) 2000 and (b) 2013 LU/LC map.**

### 6.3.5 Demarcation of Soil Erosion Susceptibility

The soil erosion per unit area quantity is estimated using the MUSLE. Figure 6.12 shows the average annual soil erosion for the year 1973 to 2013. It is interesting to assess the spatial variability of soil erosion for the planning of integrated catchment

management. To effectively plan and apply suitable soil and water conservation methods, identification of most prone areas for soil erosion is very crucial. SWAT model annual sediment yield can be used to demarcate soil erosion susceptibility and can assist as a monitor to spatially detect the erosion exposed areas. The Geba catchment is spatially clustered into severe, moderate, low and very low soil erosion areas according to the annual sediment yield (Table 6.13). This ranking of soil erosion has been implemented for sediment studies in the highlands of Northern Ethiopia (Setegn et al., 2009).

**Table 6.13: Identification of soil erosion susceptible area.**

Erosion vulnerability	Sediment yield (ton/ha)
Severe	>30
Moderate	17 to 30
Low	9 to 17
Very low	< 9

The SWAT model could be used to assess the effect of soil conservation measures on sediment yield for the erosion susceptible areas. Figure 6.12 illustrates the comparative soil erosion susceptible areas in the Geba catchment. The sub-basins 6, 7 and 10 show severe soil erosion, in 2000 land use/land cover condition, whereas moderate erosion exhibited in sub-basins 2, 4, 6, 7 and 10 in all the LU/LC, and low erosion was observed in sub-basin 1, and very low erosion proneness was seen in sub-basins 3, 5, 8, 9, 11, 12, and 13 (Table 6.14). The sub-basins which showed greater susceptibility to soil erosion mostly lie in the south western and eastern parts of the study area. There are several causes for the variation in soil erosion in different sub-basins; these are several features of climate, topography, soil, land use/land cover conditions and anthropogenic activities.

It is very essential for this study to quantify the fractional contribution of each sub basin to the total sediment yield. The subsequent average annual loads of sediment producing from the respective sub-basins are presented in Table 6.13. As it is shown the sub-basins that contribute the highest quantity of sediment are located in the upper

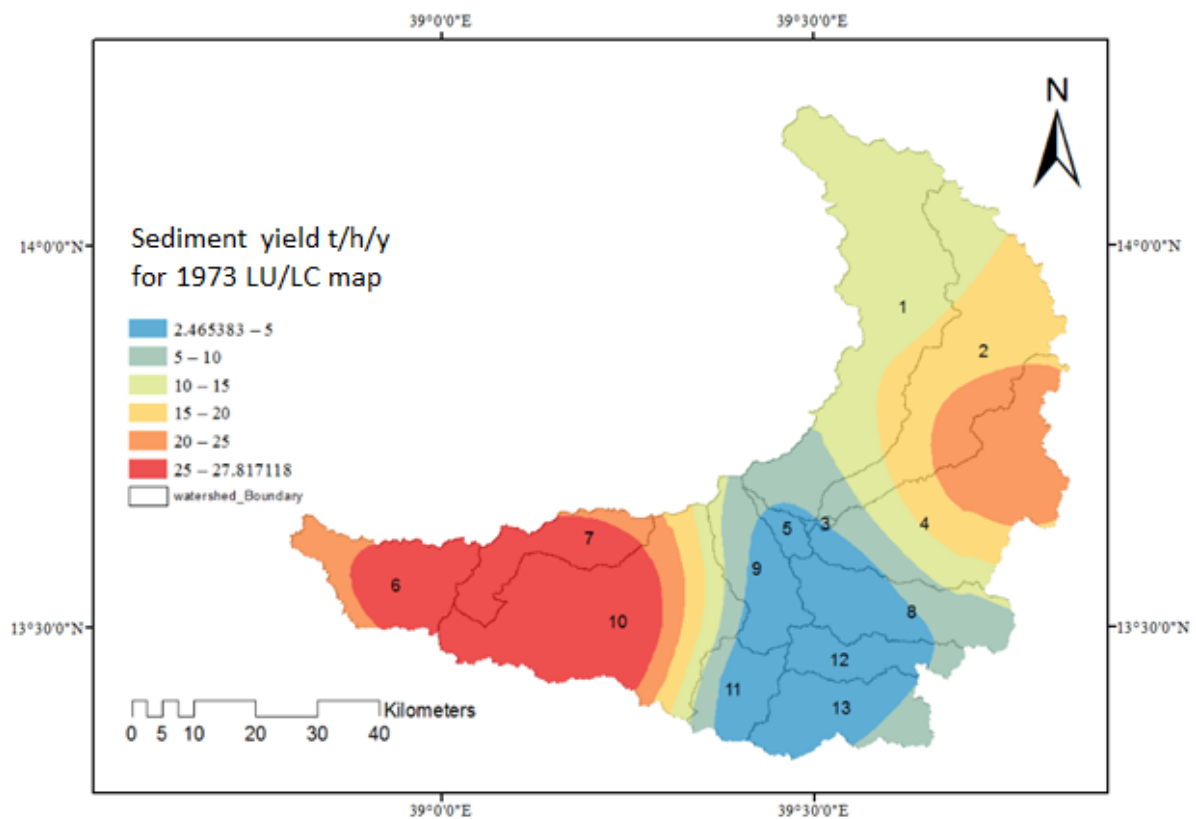
eastern and most downstream part of the catchment. This result is expected as relatively more rainfall is received by the upper eastern and most downstream regions initiating greater surface runoff, streamflow and soil erosion. Furthermore, the geographical settings and nearness of these areas with respect to confluence point increased the possibility to transport more loads.

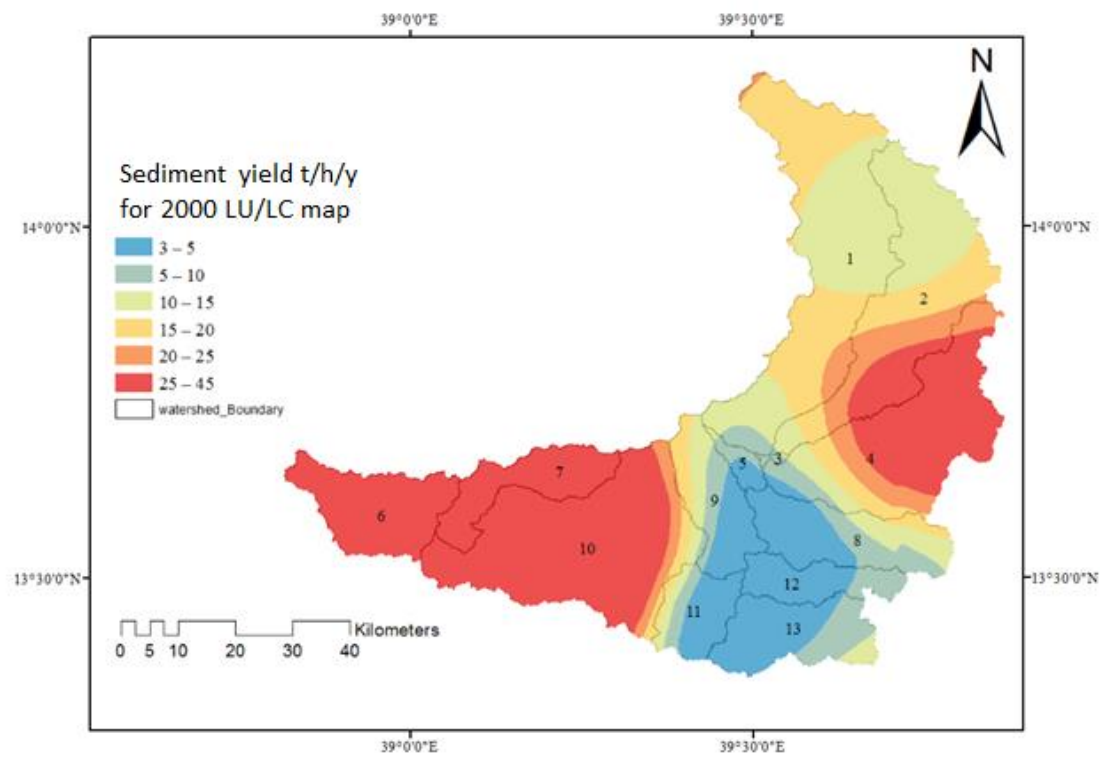
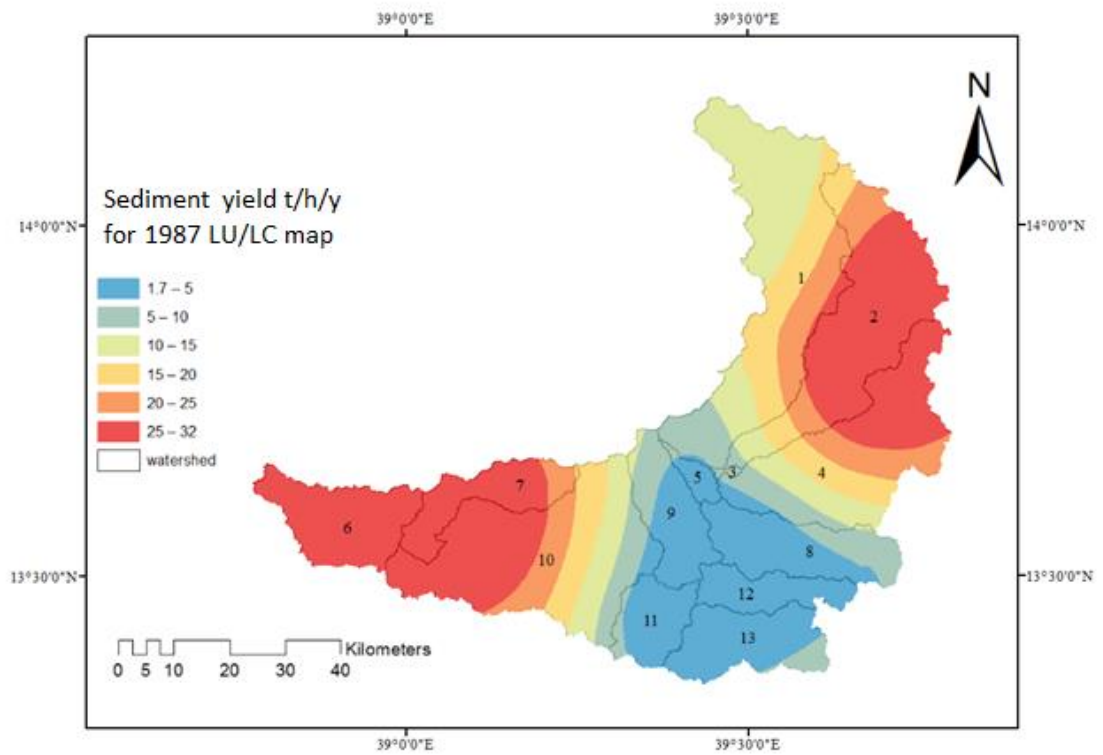
**Table 6.14: Sub-basin sediment yield of the simulation period.**

SUB	1973 Condition	Change	1987 Condition	Change	2000 Condition	2013 Condition	Change
1	11.39	1.14	12.53	3.01	15.54	12.87	-2.67
2	16.87	0.91	<b>17.78</b>	5.05	<b>22.83</b>	<b>18.83</b>	-4.00
3	4.69	1.62	6.31	2.33	8.64	6.62	-2.02
4	16.12	3.06	<b>19.18</b>	6.04	<b>25.22</b>	<b>21.37</b>	-3.85
5	1.69	0.78	2.47	1.24	3.71	2.65	-1.06
6	<b>24.08</b>	2.16	<b>26.24</b>	4.24	<b>30.48</b>	<b>28.21</b>	-2.27
7	<b>25.43</b>	2.21	<b>27.64</b>	3.70	<b>31.34</b>	<b>28.47</b>	-2.87
8	2.14	0.72	2.86	1.66	4.52	3.11	-1.41
9	3.26	0.82	4.08	1.36	5.44	4.18	-1.26
10	<b>21.6</b>	2.22	<b>23.82</b>	7.95	<b>31.77</b>	<b>24.62</b>	-7.15
11	1.76	1.21	2.97	0.27	3.24	3.13	-0.11
12	2.17	0.61	2.78	0.39	3.17	2.98	-0.19
13	1.98	0.64	2.62	0.68	3.3	2.66	-0.64
Average	<b>10.24</b>	1.39	<b>11.64</b>	2.92	<b>14.55</b>	<b>12.28</b>	-2.27

The average sediment yield at the outlet of the Geba catchment was estimated as 10.2, 11.6, 14.6 and 12.3 t ha<sup>-1</sup> yr<sup>-1</sup> for 1973, 1987, 2000 and 2013 land cover conditions, respectively. The results especially for the 2000 and 2013 land cover are approaching to 10.6 t ha<sup>-1</sup> yr<sup>-1</sup> estimate by Zenebe et al. (2013) and Vanmaercke et al. (2010). Moreover, specific sediment yield in ten different reservoirs located in and around the Geba basin studied by (Haregeweyne et al., 2005) and they projected an average annual sediment yield as 9.1 t ha<sup>-1</sup> yr<sup>-1</sup>. Afewerki (2012) also estimated 9.6 t ha<sup>-1</sup> yr<sup>-1</sup> using the WetSpa model which is close to the current study. However, running the model with different LU/LC map conditions provided very interesting results. The

anthropogenic effect has increased the total sediment yield by  $1.4 \text{ t ha}^{-1} \text{ yr}^{-1}$  and  $2.9 \text{ ha}^{-1} \text{ yr}^{-1}$  from 1973 to 1987 and from 1987 to 2000 land cover conditions which is equivalent to 14 % and 25 % increment, respectively where the highest sediment yield observed in sub-basins 2, 4, 6, 7 and 10. However, from 2000 to 2013 land cover conditions, the implementation of the integrated environmental rehabilitation in the region like biological conservation (plantation of trees) and physical soil and water conservation structures (soil and stone-bunds, terracing, water harvesting structures) has reduced the total sediment yield by  $2.3 \text{ t ha}^{-1} \text{ yr}^{-1}$  equivalent to 15.6 % reduction.





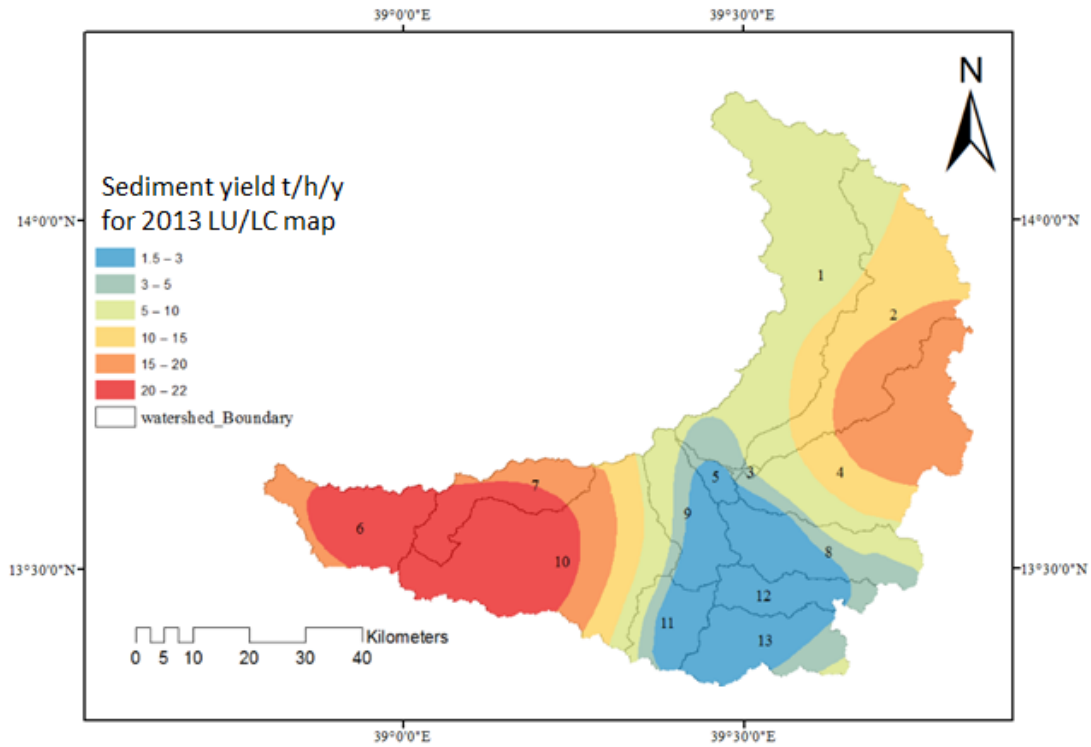


**Figure 6.12 Predicted annual net soil loss for the 1973, 1987, 2000 and 2013 LU/LC maps in the Geba catchment.**

## 6.4 Conclusion

The performance and applicability of SWAT model was successfully evaluated through sensitivity analysis, model calibration and validation, and reproducing streamflow. The study showed that surface and subsurface water model parameters are sensitive and have physical meaning, especially the CN2, ALPHA\_BF, SOL\_AWC, ESCO, GWQMN, REVAPMN, CH\_K2, CH\_N2 and SOL\_K were the most sensitive parameters with regard to streamflow prediction in the Geba River basin.

The  $R^2$  and  $E_{NS}$  for daily and monthly flow were very less (satisfactory) for the single static LU/LC (2000) map, mostly followed in many studies whereas greater than 0.75 during calibration and validation period for the multiple LU/LC maps. Model performance of the SWAT for simulating streamflow in the outlet of the Geba River basin was very good. The model has relatively high confidence and gives a very good

representation of the water balance and outflow hydrographs at the basin outlet. The model captured the dynamics of flow generation well, with surface runoff dominating during the rainy season and shallow aquifer contributing during the dry months. Therefore, SWAT model can be recommended for future studies to water yield/sediment yield of the basin.

Analysis of average annual water balance components simulated by the SWAT model indicated that evapotranspiration loss was 70 % to 74 % of rainfall for the Geba catchment. As a result the water yields (WY) as percentage of rainfall were low. Moreover, the SWAT model predicted higher surface runoff (SURQ) in the 2000 LU/LC map where there was higher deforestation, but lower in 2013 due the advancement of integrated watershed management approaches.

The model well simulated sediment concentration on the rising and the falling limbs of the sediment hydrograph during calibration and validation periods. Though, the sediment peak was well represented in all of the years, the model slightly overestimated the peaks for some days in the month of August in 2009, 2010 and 2011 for 2000 and 2013 land use/land cover conditions. Moreover, the average sediment yield at the outlet of the Geba catchment was estimated as 10.2, 11.6, 14.6 and 12.3 t ha<sup>-1</sup> yr<sup>-1</sup> for 1973, 1987, 2000 and 2013 land cover conditions, respectively which is high.

Erosion susceptibility map has been generated and extremely useful areas are more susceptible to erosion. Certain areas such as sub-basins 2, 4, 6, 7 and 10 are highly susceptible to erosion. Hence using the methodology adopted land use, water and watershed planners can take advantage of these maps for selecting appropriate soil and water conservation measures for sustainable land resources management.





# HYDROLOGICAL IMPACTS TO CHANGES IN LAND USE/LAND COVER AND CLIMATE VARIABILITY

## 7.1 Introduction

Evaluating effects of LU/LC changes and variation of climate on surface hydrological process is crucial for sustainable water resources management and environmental renewal. LU/LC and climate are the leading factors that directly control hydrological processes of the catchment. For instance, variations in LU/LC can bring about changes in flood magnitude, subsurface flow and mean annual and seasonal discharge (Legesse et al., 2003; Bewket and Sterk, 2005; Descheemaeker et al., 2006; Nyssen et al., 2009; Zenebe et al., 2013). Variation of climate can alter the flow routing time, high flows and volume (Laurance, 1998; Prowse et al., 2006; Taye et al., 2013; Taye and Willems, 2013). Therefore, differentiating impact of changes in LU/LC from the corresponding variations in climate poses a specific challenge (Setegn et al., 2011; Chawla and Mujumdar, 2015).

A number of techniques were established to appraise the hydrological impacts of changes in environmental settings, which generally fall into the following clusters: paired catchments method, time sequence study (statistical method) and hydrological modelling. Paired catchments method is challenging to be applied to medium and large catchments though it is often considered as an important technique to substitute for variation of climate in small trial watersheds. Periodical sequences assessment is a numerical technique which is simple to understand, however it investigates only hydrological impacts of environmental variation merely due to deficiencies of physical performance. Therefore, this is essential to exercise wide-ranging and physically based means to acquire information to the level of best from scarce existing data. To hypothesize and examine the interactions among LU/LC, climate, water resources management and human activities, hydrological models make available an outline to have reliable interactions (Jothityangkoon et al., 2001). Moreover, the distributed hydrological models have significant use since they make a

correlation between model parameters with physically apparent land surface features (Legesse et al., 2003).

There have been several studies to understand hydrological response to changes in LU/LC and other environmental changes. The magnitudes to which changes in LU/LC and climate variability affect the hydrological processes differ at various spatio-temporal scales. Spatially, LU/LC effects on high flows were normally most prominent at small scales, for example on an area of hillslope (Tollan, 2002; Nyssen et al., 2010; Girmay et al., 2010; Mahmoud and Alazba, 2015). Conversely, the impact of changes in LU/LC on the yearly water balance was comparatively insignificant overall watersheds attributable to worthwhile impacts in a complex watershed (Fohrer et al., 2001; Setegn et al., 2008). Temporally, the immediate effects of changes in LU/LC and variability of climate may perhaps frequently be recognized on maximum streamflow rate, whereas the continuing influences are further evident on the average-yearly streamflow (Brown et al., 2005; Hurni et al., 2005; Bewket and Sterk 2005; Prowse et al., 2006; Brath et al., 2006; Legesse et al., 2010). Changes in the combined effects in LU/LC and variations of climate need to be studied. The output of such study is useful to provide information to water planners, managers and decision-makers to encourage environmental rehabilitation specifically afforestation, sustainable water resources development and watershed management. To our knowledge there is limited literature on isolating the effects of LU/LC and Climate variability on the hydrological responses. The objective of this chapter is to quantify separately the influence of LU/LC and climate on the hydrological responses. Accordingly, the focus of this chapter was to:

- (i) Quantify and analyse the impacts of future land use scenarios (hypothetical) on surface hydrological processes namely surface/ subsurface flow, available soil water contents and potential evapotranspiration.
- (ii) Quantify and analyse the impacts of variability of climate on surface hydrological processes in the Geba basin Northern highlands of Ethiopia.

## **7.2 Methodology**

### **7.2.1 Land Use Land Cover Scenarios Development**

The development of strategies for water resource planning and management and the assessment of impacts of potential environmental change are often guided by the analysis of multiple future scenarios.

The sensitivity of the Geba River catchment hydrological system to future land use/land cover changes were analysed using SWAT model, by formulating a range of land use/land cover change scenarios. As a first test, two extreme limiting scenarios were considered - maximum deforestation and complete afforestation. The modelling process was carried out to assess influences on the dynamics of runoff components and total water yield in response to these bounding conditions. Most likely changes to land use/land cover are conversion from shrub land and forest to agriculture in a land degradation (pessimistic) scenario, and conversion from agricultural land to shrub land and forest in a land restoration (optimistic) scenario. Changes to all three of these land use/land cover types have influences on catchment hydrology. Urbanisation and water body equally affects hydrological processes. However, it was excluded from scenario analysis, as it constitutes a small fraction of the total area, and in the region, still a small area of change.

In the second stage scenario modelling, a range of scenarios were considered, in which fractional changes were made to these three land cover classes for the pessimistic and optimistic trends. These sensitivity analyses were aimed at providing insights on the behaviour of the model, and at generating possible scenarios for guiding land use policy and development strategies.

Each scenario was created by changing patches of selected land use/land cover type one into target land use/land cover type two. Land cover classifications derived from the 2013 Landsat image were used as the baseline. The type two LU/LC were defined by assigning changed areas to the baseline classification, selected randomly by

computer simulation within the selected land cover type, and spread evenly over the catchment under study. The total area affected in each scenario was an assigned proportion of the original area of land use/land cover type one.

Scenarios were developed for changes in the original areas of shrub land and forestry in increments of 10 %, 20 %, and 40 %. Scenario runs were conducted for these incremental steps separately for each of the two types of LU/LC, for degradation and restoration scenarios. Combined scenarios were run for the restoration scenario only, in which agricultural land reverts to shrub land and forest, each changed by the medium and maximum increments (20 % and 40 %) to evaluate combined effects on the hydrology. Description of the scenarios is provided in the sections to follow.

#### **7.2.1.1 Existing State (Baseline Scenario)**

For existing state a baseline scenario, year 2013 land use/land cover map was used. Compared to the 2000 land use/land cover map, the following gross changes are noted in the 2013 land use/land cover map: Forests are slightly increased within the catchment in favour of transitional woodland-shrub; there is transformation of barren land and rangeland into agricultural land, shrub lands and forest. The hydrological model was run with the 2013 land use/land cover map unchanged, and the 1989 climatic data set. (Note that the streamflow data for 2002 was unusable. Therefore, it was not possible to carry out a full validation of the SWAT model using 2002 climatic records and the 2002 land cover classification. The SWAT model, validated using the 1989 land cover image and earlier catchment streamflow, was used instead.)

#### **7.2.1.2 Land Degradation Scenario**

The second scenario, termed land degradation, represents an unfavourable scenario, including accelerated LU/LC changes with extensive deforestation. In this case, significant fractions of forest and shrub land areas are transformed in to the category agricultural land generic, which includes subsistence agricultural areas, bare soil and rangeland areas. There is a significant decrease in the area of the shrub lands because of

the increased use of land for agriculture to produce food and consumption of fuel wood for the growing population. Although this scenario may imply increasing built-up areas, as a fraction of the catchment this change is minor and so the size of the built-up area remains somehow constant. Two different extents of deforestation; forest and shrub land respectively were tested as shown in Table 7.1, indicating a range of increasingly pessimistic scenarios up to 2040.

### **7.2.1.3 Land Restoration Scenario**

The third scenario, termed land restoration, represents of the creation of a green environment through management and re-forestation. This scenario involves the rehabilitation of potentially vulnerable areas (subsistence agricultural land, rangeland and bare land) in to forest and shrub lands. Different extents of forestation were investigated, as shown in Table 7.2, indicating an optimal scenario up to 2040.

**Table 7.1: Characteristics of 2013 LU/LC data and deforestation scenarios.**

Scenario		Baseline	S1	S2	S3	S4	S5	S6
LU/LC		Bounding Scenario	RNGB converted to AGRL			FRST converted to AGRL		
LU/LC Type	Description	LU/LC 2013	10%	20%	40%	10%	20%	40%
AGRL	Area (Km <sup>2</sup> )	2196.10	2349.8	2503.63	2811.17	2214.12	2232.14	2268.19
	%	42.75	745.74	48.74	54.72	43.10	43.45	44.15
RNGB	Area (Km <sup>2</sup> )	1537.67	1383.9	1230.14	922.60	1537.67	1537.67	1537.67
	%	29.94	26.95	23.95	17.97	29.94	29.94	29.94
FRST	Area (Km <sup>2</sup> )	180.22	180.22	180.22	180.22	162.20	144.18	108.13
	%	3.51	3.51	3.51	3.51	3.16	2.81	2.11
Land categories not changed significantly in scenario analysis								
Urban	Area (Km <sup>2</sup> )	144.35	144.35	144.35	144.35	144.35	144.35	144.35
	%	2.81	2.81	2.81	2.81	2.81	2.81	2.81
Water	Area (Km <sup>2</sup> )	22.73	22.73	22.73	22.73	22.73	22.73	22.73
	%	0.44	0.44	0.44	0.44	0.44	0.44	0.44

**Table 7.2: Characteristics of simulated LU/LC afforestation scenarios.**

Scenario		Baseline	S7	S8	S9	S10	S11	S12
LU/LC		Bounding Scenario	AGRL converted to RNGB		AGR converted to FRST		AGRL converted to both RNGB and FRST	
LU/LC Type	Description	LU/LC 2013	20%	40%	20%	40%	20%	40%
AGRL	Area(Km <sup>2</sup> ) %	2196.10	1756.88	1317.66	1756.88	1317.66	1317.66	439.22
		42.75	34.20	25.65	34.20	25.65	25.65	8.55
RNGB	Area(Km <sup>2</sup> ) %	1537.67	1976.89	2416.11	1537.67	1537.67	1537.67	2416.11
		29.94	38.49	47.04	29.94	29.94	29.94	47.04
FRST	Area(Km <sup>2</sup> ) %	180.22 3.51	180.22	180.22	619.44	1058.66	619.44	1058.66
			3.51	3.51	12.06	20.61	12.06	20.61
Land categories not changed significantly in scenario analysis								
Urban	Area(Km <sup>2</sup> ) %	144.35 2.81	144.35	144.35	144.35	144.35	144.35	144.35
			2.81	2.81	2.81	2.81	2.81	2.81
Water	Area(Km <sup>2</sup> ) %	22.73	22.73	22.73	22.73	22.73	22.73	22.73
		0.44	0.44	0.44	0.44	0.44	0.44	0.44



Complete and comparative changes in annual values of surface flow, baseflow and total water yield were calculated for each scenario. Average annual and monthly outflows simulated at the catchment outlet for the various change scenarios were then compared to the baseline case.

### **7.2.2 Hydrological Impact of Changes in LU/LC and Climate Variability**

To evaluate the hydrological impact due to the LU/LC changes and climate variability, one factor at a time approach was applied i.e., holding other factors constant while changing of one factor at a time (Van Griensven et al., 2006). The meteorological data of four time-steps of 1974–1983 and 1984–1993, and 1994–2003 and 2004–2013 were chosen, and every time-step comprised one LU/LC map. LU/LC map of 1973, 1987, 2000 and 2013 have taken to characterize LU/LC forms of 1970s and 1980s, 1990s and 2000s for the four time-steps, respectively. The SWAT model was run for all of the four combinations of two time-steps and four LU/LC maps having four scenarios for each phase. Each of the phases consists of four simulations and altogether there were 12 SWAT model simulations for the catchment. The impact of changes in LU/LC and variation of climate were enumerated through associating the outputs of SWAT model for the four conditions with three phases shown below:

#### **Phase I**

- S1: 1973 LU/LC map and 1974–1983 climate.
- S2: 1987 LU/LC map and 1974–1983 climate.
- S3: 1973 LU/LC map and 1984–1993 climate.
- S4: 1987 LU/LC map and 1984–1993 climate.

#### **Phase II**

- S1: 1987 LU/LC map and 1984–1993 climate.
- S2: 2000 LU/LC map and 1984–1993 climate.
- S3: 1987 LU/LC map and 1994–2003 climate.
- S4: 2000 LU/LC map and 1994–2003 climate.

### **Phase III**

S1: 2000 LU/LC map and 1994–2003 climate.

S2: 2013 LU/LC and map 1994–2003 climate.

S3: 2000 LU/LC and map 2004–2013 climate.

S4: 2013 LU/LC and map 2004–2013 climate

## **7.3 Results and Discussion**

### **7.3.1 Scenario Analysis for LU/LC Changes**

In terms of scenario generation, as a first test approach, two extreme limiting scenarios were considered: total deforestation and total restoration. The modelling process was carried out to assess influences on run-off components and total water yield in response to these bounding conditions. Hypothetical LU/LC of different magnitude was considered for simulation while holding the most recent climatic conditions. One is changed to the other LU/LC, the other LU/LC remain constant. Most likely changes to land cover are conversion from shrub land and forest to agriculture in a land degradation scenario, and conversion from agricultural land to shrub land and forest in a land restoration scenario. Changes to all three of these land cover types have influences on catchment hydrology. Urbanisation equally affects hydrological processes. However, it was excluded from scenario analysis, as it constitutes a small fraction of the total area, and in the Northern part of the country, still a small area of change.

Simulations were performed using three scenarios, which were compared to the baseline case. The baseline case was taken as the simulation using measured climate (2004-2013) and the 2013 land use/land cover image. The scenarios are the case of bounding scenarios (which were used to test the sensitivity of SWAT in simulating changes in land use/land cover characteristics), land degradation and land restoration. The hydrological responses at the outlet thus simulated were compared to the baseline case in terms of average annual catchment streamflow, surface runoff and baseflow.

### 7.3.1.1 Bounding Scenarios

Changes in land use/land cover cause changes in curve number, the internal model parameter that determines the partitioning of rainfall into surface flow and percolation. Evaluation of model sensitivity, through the trial of extreme land use/land cover scenarios, revealed the maximum degree and patterns of interaction between changes in land use land cover and modelled hydrological responses.

The results of the two extreme scenarios are compared to the baseline case (Table 7.3). Maximum deforestation of the entire land surface of the catchment generated a total water yield of 190.93 mm y<sup>-1</sup>, compared to 154.77 mm y<sup>-1</sup> for the reference scenario. In the case of total deforestation, there is increase in surface flow of 108.2 mm y<sup>-1</sup> compared to 87.65 mm y<sup>-1</sup>, and a decrease in baseflow of 50.3 mm y<sup>-1</sup> in comparison with 65.6 mm y<sup>-1</sup> for the reference scenario. Barren areas have a strong effect by promoting rapid runoff and thereby reducing percolation. Ground water storage is reduced and surface direct evaporation enhanced.

For complete afforestation, total water yield reduced to 108.3 mm y<sup>-1</sup>. In the case of total land use/land cover change to forest, there is a decrease in surface flow from 87.65 mm y<sup>-1</sup> to 61.35 mm y<sup>-1</sup> and increase in baseflow from 65.60 mm y<sup>-1</sup> 85.65 mm y<sup>-1</sup>. Forests absorb most of the rainfall hence there is increased interception, percolation and evapotranspiration, rather than prompt streamflow.

Results of this sensitivity analysis showed the maximum changes that could be expected from extreme changes in LU/LC, and hence bounding conditions for the further scenario modelling. The model behaves as expected, with barren land increasing prompt runoff and reducing percolation, and conversely reducing runoff and total yield for full afforestation.

**Table 7.3: Simulation results from bounding cases scenarios.**

Conditions	Total water yield (mm)	Surface flow (mm)	Baseflow (mm)
2013 Land cover	154.77	87.65	65.6
Complete change to barren soil	190.93	108.2	50.3
Complete change to vegetation cover	108.3	61.35	85.27

### 7.3.1.2 Land Degradation Scenario

Simulation runs were performed using land use/land cover from scenarios termed land degradation, which represents an unfavourable scenario with accelerated land use/land cover change with extensive deforestation. Table 7.4 lists the annual values of catchment streamflow, baseflow and surface flow for each case as simulated from the land degradation scenarios.

Decreasing land under shrub land and forest cover, differences in total annual catchment streamflow, baseflow and surface flow were observed. Under the existing land cover (reference scenario, 2013), the annual catchment streamflow observed was 154.77 mm, with baseflow making up to 43.4 % and the remaining 56.6 % from surface flow. In terms of absolute mean annual changes between the reference state and the scenarios, decreasing forest areas by different magnitudes increases surface flow and decreases baseflow and total water yield at the outlet.

A 40 % decrease in the shrub lands increases total water yield from 154.77 mm  $y^{-1}$  to 162.64 mm  $y^{-1}$ . With a 10 % decrease in shrub lands, baseflow remains at 65.6 mm  $y^{-1}$  while surface flow was 88.63 mm  $y^{-1}$  with minor difference from the reference scenario at 87.65 mm  $y^{-1}$ .

**Table 7.4: Simulation results from land degradation scenarios.**

Scenario	Land cover change	Total water yield (mm)	% Change	Surface flow (mm)	% Change	Baseflow (mm)	% Change
	2013 Baseline case	154.77		87.65		65.6	
1	10% from RNGB to AGRL	154.23	-0.35	88.63	1.12	65.6	0
2	20% from RNGB to AGRL	158.41	-0.23	97.18	10.87	61.23	-6.66
3	40% from RNGB to AGRL	162.64	7.73	102.53	16.98	60.11	-8.37
4	10% from FRST to AGRL	152.67	-1.36	88.85	1.37	63.82	-2.71
5	20% from FRST to AGRL	153.81	-0.62	91.48	4.37	61.33	-6.51
6	40% from FRST to AGRL	154.68	-0.06	93.04	6.15	61.64	-6.04

However, decreasing shrub lands by 20 % produces an increase in total water yield and surface flow but a decrease in baseflow. Total water yield increased from 154.77 mm y<sup>-1</sup> to 157.41 mm y<sup>-1</sup> while surface flow increased from 87.65 mm y<sup>-1</sup> to 97.18 mm y<sup>-1</sup>. A 4.37 mm y<sup>-1</sup> decrease in baseflow has been observed once shrub land was decreased by 20 %. The conversion of shrub lands into subsistence agriculture does not cause considerable changes in the macro scale basin. The reason for this may be the similarity of the characteristics of both land use/land cover forms under tropical natural conditions. Shrub land vegetation has scattered trees and is deciduous during the dry season. Thus, a considerable amount of land is exposed, similar to subsistence agricultural land.

A 40 % decrease in forest yielded total water yield of 154.68 mm y<sup>-1</sup>, not as such different from the reference scenario. Slight decreases in baseflow ranging from 61.64 mm y<sup>-1</sup> to 63.82 mm y<sup>-1</sup> have been observed with an increase in the magnitude of deforestation. For example, a 10 % decrease in forest results in a decrease in baseflow from 65.6 mm a<sup>-1</sup> to 63.82 mm y<sup>-1</sup>, while a 40 % decrease in forest produces a decrease in baseflow 61.64 mm y<sup>-1</sup>. Surface flows were observed to be increasing as forestland is reduced. For example, a 40 % decrease in forest increases surface flow from 87.65 mm y<sup>-1</sup> to 93.04 mm y<sup>-1</sup>.

The relative effect of shrub land and forest reduction (expressed as percentages) on the annual water balance is compared to that of subsistence agriculture. The 10 % decrease in forest reduces total water yield by 1.36 %, whereas a 20 % reduction of forest leads to a decline of water yield by 0.62 %. Overall, the strongest relative impact can be observed in the amount of surface runoff. Decreasing land under shrub land cover by 20 % increases surface flow by 10.87 % while decreasing forest by 40% increases surface flow by 6.15 %. This is due to the increase in land under subsistence farming. The absence of trees and shrubs implies a minimum in surface evapotranspiration and, consequently, a maximum in runoff. The soil is less protected against raindrop impact under agriculture since after harvesting and shortly after sowing, when the plants do not cover the soil completely.

### 7.3.1.3 Land Restoration Scenario

Simulation runs were also performed for land cover scenarios termed land restoration, which represents the creation of a green environment through management and replantation. Table 7.5 lists the annual volumes of catchment streamflow, baseflow and surface flow for each scenario as simulated from land restoration scenarios. The restoration of subsistence agricultural land into shrub land and forest leads to changes in the water balance.

A 40 % increase in forest increases total water yield from 154.77 mm y<sup>-1</sup> to 157.12 mm y<sup>-1</sup>. However, the proportion of water infiltrating increases from 65.6 mm y<sup>-1</sup> to 86.21 mm a<sup>-1</sup> while surface flow decreased from 87.65 mm y<sup>-1</sup> to 70.91 mm y<sup>-1</sup>. Slight increases in baseflow have been observed with a 20 % increase in forest, when baseflow increases from 65.6 mm y<sup>-1</sup> to 72.7 mm y<sup>-1</sup>. Surface flows were observed to decrease as shrub land expands. For example, a 40 % increase in shrub land, results in a drop in total water yield from 154.77 mm y<sup>-1</sup> to 132.27 mm y<sup>-1</sup>. This reduction is associated with an increase in baseflow from 65.6 mm y<sup>-1</sup> to 78.47 mm y<sup>-1</sup>. Increasing the areas of forest and shrub land decreases water yield, surface flow and increases baseflow. For instance, an increase of 20 % decreases total water yield to 145.86 mm y<sup>-1</sup> while an increase 40 % decreases water yield to 136.61 mm y<sup>-1</sup> compared to 154.77 mm y<sup>-1</sup> from the reference scenario. The reduction of the mean annual flow results in a decreasing surface flow during the rainy season with a simultaneous increase in baseflow.

**Table 7.5 Simulation results obtained from land restoration scenarios.**

Scenario	Land cover change	Total water yield (mm)	% Change	Surface flow (mm)	% Change	Baseflow (mm)	% Change
	2013 Baseline case	154.77		87.65		65.6	
7	20% to RNGB	146.62	-5.27	75.32	-14.07	71.3	8.67
8	40% to RNGB	132.27	-14.54	53.8	-38.62	78.47	19.62
9	20% to FRST	155.81	0.61	83.11	-5.2	72.7	10.82
10	40% to FRST	157.12	1.52	70.91	-19.1	86.21	31.42
11	20% to both RNGB and FRST	145.86	-5.76	72.42	-17.38	73.44	12
12	40% to both RNGB and FRST	136.61	-11.73	52.47	-40.14	84.14	28.26



Increasing woodland (both shrub land and forest) has a profound effect on the annual water balance when compared to the reference scenario (Table 7.5). The 20 % increase in the forest increases total water yield by 0.61 % whereas an additional 20 % increase of forest leads to an increase in water yields by 1.52 %. This could be due to the small amount of land initially under forest.

Generally, the strongest relative impact can be observed in the amount of surface flow. Increasing land under shrub land cover by 40 % decreases surface flow by 38.62 %, while increasing the shrub land by 20 % decreases surface flow by 14.07 %. Differences in surface flow and baseflow were also observed with increases of both forest and shrub lands by 40 % and 20 % respectively. Reductions in surface flow of 40.14 % and 17.38 % were observed respectively. This is due to the decrease in land under subsistence farming. Baseflow increases and surface flow decreases are due to the higher interception of shrub and forests lands in comparison to other cereal crops. Observational and experimental studies have established that forests consume more water during evapotranspiration than any other forms of land cover (Tamene et al., 2008). Large reductions of the river discharge and therefore a considerable increase of water retention in the catchment would occur only in the case of afforestation of large areas. Therefore, depending on the magnitude of percentage change in forest cover, afforestation would decrease average and dry-season streamflow.

### **7.3.2 Hydrological Impact of LU/LC Changes and Climate Variability**

#### **7.3.2.1 Impact on Runoff**

Total streamflow is composed of surface runoff and baseflow (lateral flow and shallow ground water discharge to streams). Comparisons were also carried out to evaluate differences in surface flow and baseflow from different land use/land cover types classified from the 1973, 1987, 2000 and 2013 land use/land cover data sets. Between 1973 and 2013, dominant land cover changes were observed in sub-basins 2, 4, 6, 7 and 10. Table 7.6 and 7.7 showed differences in surface runoff, baseflow and the percentage changes.

**Table 7.6: Simulated surface runoff volumes for the 1973-2013 land use/land cover scenarios.**

SUB	1973 Condition		1987 Condition		2000 Condition	2013 Condition	
	Runoff Volume Yield	% Change from 1987 Condition	Runoff Volume Yield	% Change from 2000 Condition	Runoff Volume Yield	Runoff Volume Yield	% Change from 2000 Condition
1	87.56	5.52	92.40	18.54	109.52	95.89	-12.45
2	82.62	14.62	94.69	33.52	126.44	94.03	-25.63
3	70.52	7.51	75.81	26.02	95.54	86.11	-9.87
4	102.03	17.94	120.34	15.25	138.70	112.09	-19.19
5	46.01	5.52	48.55	23.15	59.79	58.79	-1.68
6	178.05	8.93	193.95	12.91	218.99	211.30	-3.52
7	176.72	7.25	189.53	21.14	229.58	217.63	-5.21
8	51.66	3.21	53.32	27.67	68.07	58.67	-13.80
9	53.71	4.09	55.91	20.94	67.62	61.71	-8.74
10	173.69	13.05	196.35	21.54	238.64	204.75	-14.20
11	45.17	10.77	50.03	30.61	65.35	61.42	-6.01
12	44.80	11.08	49.76	37.28	68.31	57.46	-15.89
13	38.00	8.60	41.27	41.72	58.49	50.56	-13.55
Total	1150.54	118.09	1261.91	330.29	1545.04	1139.45	-149.74
Ave.	88.50	9.08	97.07	25.41	118.85	87.65	-11.52

The highest annual surface runoff of (102, 178, 176.7 and 173.7 mm), (120.3, 194, 190.5 and 196.4 mm), (138.7, 219, 229.6 and 238.6 mm), and (112.1, 211.3, 217.6 and 204.6 mm) for the 1973, 1987, 2000 and 2013 land use/land cover map were generated from sub-basins 4, 6, 7 and 10, respectively (Table 7.6). The land cover in these sub-basins had changed to subsistence agriculture and barren area from 1973 to 2000. Thus, surface runoff increased by (18, 9, 7 and 13 %,.) and (15, 13, 21 and 21.5 %) from sub-basins 4, 6, 7 and 10 in 1987 and 2000 land use/land cover conditions, respectively. On the contrary the surface runoff decreased by (19, 3.5, 5 and 14 %) in 2013 LU/LC. Furthermore, baseflow decreased by (23, 10.7 and 5.6) and (21.7, 19.5 and 15.7 %) for sub-basins 4, 6, 7 and 10, in 1987 and 2000, respectively, while in 2013 the baseflow increased by 18, 15.8 and 8 % for sub-basins 4, 6, 7 and 10, respectively (Table 7.7). Agricultural land is characterised by scattered green grass crop lands, used for communal grazing during the dry season. At the onset of the rainy season, most of these fields are bare soils that have been prepared for planting, or denuded by grazing. Most of the runoff generated in the cultivated and rangelands constitute storm flow, especially at the beginning of the rainy season between June and till the second week of July.

**Table 7.7: Simulated baseflow from 1973 to 2013 land use/land cover conditions.**

SUB	1973 Condition		1987 Condition		2000 Condition	2013 Condition	
	Runoff Volume Yield	% Change from 1987 Condition	Runoff Volume Yield	% Change from 2000 Condition	Runoff Volume Yield	Runoff Volume Yield	% Change from 2000 Condition
1	47.14	-8.12	43.31	-16.46	36.19	39.28	8.56
2	44.88	-11.11	39.89	-15.53	33.70	37.40	10.98
3	31.72	-22.14	24.70	-32.97	16.55	22.27	34.52
4	48.01	-19.14	38.82	-18.35	31.70	40.01	26.22
5	17.40	2.28	17.80	-28.00	12.81	14.50	13.16
6	89.45	-23.04	68.84	-21.70	53.90	63.71	18.20
7	85.38	-10.69	76.25	-19.47	61.41	71.15	15.86
8	33.92	-15.53	28.65	-11.95	25.22	26.70	5.87
9	32.45	-20.52	25.79	-14.80	21.97	25.55	16.28
10	81.85	-5.60	77.27	-15.71	65.13	70.49	8.24
11	24.91	-26.24	18.37	-15.48	15.53	17.66	13.75
12	33.09	-19.75	26.55	-15.21	22.52	24.58	9.15
13	29.30	-24.02	22.26	-18.10	18.23	21.21	16.36
Total	599.50	-203.62	508.50	-243.73	414.86	474.51	197.15
Ava	46.12	-15.66	39.12	-18.75	31.91	36.50	15.17

Similar observations have been noted in most of the sub-basins where LU/LC has changed from shrub land (RNGB), forest (FRST) and rangeland (RNGE) to agricultural land (AGRL) and Barren land (BARR) from 1973 to 2000, whereas from 2000 to 2013 dominant land use has changed from Barren land and rangeland to agricultural land, shrub lands and other land uses. Under the simulated conditions of a fixed climatic scenario, with only the measured land use/land cover changes inserted, simulated baseflow decreased in all the sub-basins in 1987 to 2000 land cover condition compared to the baseline of 1973. While, the baseflow is increased by an average of 14 % in 2013 land use/land cover condition. The high variability between sub-basins indicates the need to segment catchments into these smaller units, to understand the full extent of land cover changes. Generally large portions of the shrub and forest areas had cleared from 1973 to 2000. This is due to expansion of agricultural land for food production and fuel wood, and the majority of subsistence farmers in the region practiced traditional methods of cultivation. From 2000 to 2013 different physical and biological soil and water conservation activities have been extensively practised. Therefore, the land cover has changed to some extent positively.

The mean yearly predicted runoff by the SWAT model under various LU/LC and climate has shown in Table 7.8. Rather than the observed data the predicted outcomes were used for the comparison of the hydrological impacts for all the four hypothetical circumstances. Comparing with scenario 1 (S1), predicted runoff in scenario (S4) of phase I and II increased by 9.26 mm and 14.71 mm, respectively, while decreased in phase III by 3.65 mm, this indicated the joint effects of changes in LU/LC and the variation of climate. The difference between scenario (S1) and scenario (S2) specified the effect of changes in LU/LC between the two stages. Changes of the LU/LC increased runoff in phase I and II by 6.35 and 7.4 mm and declined by 2.85 mm in phase III, which accounted for 68.59 %, 50.1 % and 78.16 % of the total change (9.26), (14.71) and (-3.65) for the respective phases, respectively (Table 7.8). The difference between scenario (S1) and scenario (S3) specified the effect of the climate disparity. Climate disparity increased runoff by 3.4 mm and 2.7 mm in phase I and II and declined by 1.3 mm in phase III, which accounted 36.6 % and 18.3 %, increment

of the total runoff for phase I and II, and 35.3 % reduction in the third phase. The outcomes LU/LC change and climate variability during 1970s, 1980s, and 1990s increased runoff, however during 2000s runoff was declined slightly but the contribution of LU/LC changes were slightly larger than the variability of climate (Table 7.8). It should be known that the aggregation of the observed runoff increment triggered by the variability of climate and LU/LC change together (6.67 mm), (12.04) were to some extent lesser than the predicted joint effect of scenario 4 (S4) (9.26 mm) and (14.71 mm) for the first two phases, respectively, as a result of the interactions concerning the variation of climate and changes in LU/LC signified in the SWAT model.

#### **7.3.2.2 Impact on Available Soil Water and Potential Evapotranspiration**

According to the four conditions predicted by SWAT model for potential evapotranspiration (PET) and available soil water contents outcomes presented in Table 7.9.

Results indicated that both changes in LU/LC and climate inconsistency declined available soil water contents, and the percentage shares were 50.68 % and 29.06 % and 56.1 %, and 34.57 % for the LU/LC change and climate inconsistency in phase I and II, respectively. However, there is an increase by 76.25 % and 46.13 % in phase III. The joint impacts of changes in LU/LC and variations of climate scenario (S4) increased PET by 14.55 mm and 16.46 mm for phase I and II. While, LU/LC and climate inconsistency reduced PET by 11.33 mm and 7.39 mm, reporting for 81.68% and 53.31 % of the whole joint impact of 13.87 mm, respectively for phase III (Table 7.9). In the case of phase III the results indicated that LU/LC and variation of climate increased available soil water content, and the percentage share were 76.25 % and 46.13 %, in the order. The combined impact of these factors S4 of phase III declined the potential evapotranspiration by 13.87 mm.

**Table 7.8: Predicted average annual runoff volume under various LU/LC and climatic conditions.**

Scenarios	LU/LC	Climate	Measured (mm)	Simulated (mm)	Simulated change (mm)	Percent, %
Phase I						
S1	1973	1974-1983	138.03	134.62	-	-
S2	1987	1974-1983	-	140.97	6.35	68.59
S3	1973	1984-1993	-	138.01	3.39	36.62
S4	1987	1984-1993	144.70	143.88	9.26	100.00
Phase II						
S1	1987	1984-1993	144.70	143.88	-	-
S2	2000	1984-1993	-	151.28	7.40	50.31
S3	1987	1994-2003	-	146.57	2.69	18.30
S4	2000	1994-2003	156.74	158.59	14.71	100.00
Phase III						
S1	2000	1994-2003	156.74	158.59	-	-
S2	2013	1994-2003	-	155.74	-2.85	-78.16
S3	2000	2004-2013	-	157.30	-1.29	-35.25
S4	2013	2004-2013	151.67	154.94	-3.65	-100.00

**Table 7.9 Predicted average annual soil water and PET under different LU/LC and climatic conditions.**

Scenarios	LU	Climate	Rainfall (mm)	Soil Water			Potential Evapotranspiration		
				Simulated (mm)	Change (mm)	Percent, %	Simulated (mm)	Change (mm)	Percent, %
Phase I									
S1	1973	1974-1983	604.87	171.75	-	-	1566.71	-	-
S2	1987	1973-1983	604.87	166.17	-5.58	-50.68	1576.22	9.52	65.40
S3	1973	1984-1993	643.12	168.56	-3.20	-29.06	1571.24	4.53	31.13
S4	1987	1984-1993	643.12	160.74	-11.01	-100.00	1581.26	14.55	100.00
Phase II									
S1	1987	1984-1993	643.12	160.74	-	-	1578.26	-	-
S2	2000	1984-1993	643.12	153.42	-7.32	-56.10	1590.14	11.88	72.20
S3	1987	1994-2003	708.11	156.23	-4.51	-34.57	1585.37	7.11	43.22
S4	2000	1994-2003	708.11	147.69	-13.05	-100.00	1594.71	16.46	100.00
Phase III									
S5	2000	1994-2003	708.11	150.65	-	-	1594.71	-	-
S6	2013	1994-2003	708.11	157.61	6.96	76.25	1583.38	-11.33	-81.68
S7	2000	2004-2013	576.12	154.86	4.21	46.13	1587.32	-7.39	-53.31
S8	2013	2004-2013	576.12	159.78	9.13	100.00	1580.84	-13.87	-100.00



Generally shrub land and forest produced minimum runoff depths and available soil water contents however more evapotranspiration than other LU/LC types. Such conditions were realistic merely when the plant canopy cover of the shrub land and forest were above a definite limit. Consequently, the transformation of forest and shrub land to agricultural land and other LU/LC types in the Geba catchment during 1973–2000 increased runoff and evapotranspiration in the high cover of green grass crop whereas available soil water content is reduced. Moreover, from 2000 onwards results showed runoff and evapotranspiration decreased, but available soil water content showed increasing tendency. Furthermore the impacts of LU/LC and variation of climate in the study area was a key reason, which had a tendency to be slightly cooler during 2000–2013 and plainly directed to decrease in runoff and evapotranspiration (Tables 7.8 and 7.9). According to the joint impacts of changes in LU/LC and climate variations, hydrological circumstance of the Geba catchment altered prominently, and various factors had various consequences on the hydrological condition and water resources as well. Changes in LU/LC played a more pronounced role than climate discrepancy in influencing surface hydrology in the study watershed. Consequently, when planning for environmental rehabilitation and water resources management, LU/LC change and variation of climate ought to be considered in assessing the appropriate conservation measures and judicious use of water resources.

In the second approach, a variety of parameters were considered, in which each parameter was varied while holding the other parameters constant to see the hydrological impacts of isolated and combined of LU/LC and climate variability. Moreover, multiple classes can be changed more realistic scenario in this approach than the first scenario where one class changed at a time. Care was taken when varying the parameters to make sure that the impact has realized. Hence, the second approach takes the advantage over the conventional approach by considering different parameters.

## 7.4 Conclusions

It is verified that SWAT model is a worthwhile tool for evaluating the effects of environmental changes comprising LU/LC and climate changes in the Geba catchment. The coefficient of determination ( $R^2$ ), Nash–Sutcliffe model efficiency ( $E_{NS}$ ), ratio of root mean square error to measured standard deviation (RSR) and Percent bias (PBIAS) for monthly and daily flow signified that the performance of SWAT in the Geba watershed was very good. During 1973–2000 about 10.83 % of the catchment area was transformed largely from shrub, forest and rangeland mainly to agriculture and barren land, and climate showed warmer and dry. Furthermore, during 2000–2013 around 18.37 % of the total catchment area was changed from barren land and rangeland to agricultural land, shrub land and urban area, and climate changed to slightly cooler.

The combined impacts of these fluctuations increased runoff, and potential evapotranspiration, while decreased available soil water contents during 1973 to 2000 and vice versa during 2000 to 2013 time period. Both LU/LC and climate change increased runoff and PET (percentage contributions were 68.6 % and 36.6 % for phase I and 50.3 % and 18.3 % for phase II for runoff, and (65.4 % and 31.13 %) and (72.2 % and 43.2 %) for phase I and II for PET, respectively), while in phase III runoff and PET decreased by (78.16 % and 35.25 %), and (81.68 % and 53.31 %), respectively. However, soil water decreased in phase I and II by (50.68 % and 29.06 %), and (56.1 % and 34.57 %), while increase by 76.5 % and 46.13 % for phase III. Generally, surface hydrology was influenced by the changes in LU/LC more significantly than that of climate variation in the Geba catchment during 1973–2013 time periods. As a result, the effect of change in climate should be separated when assessing the hydrological responses of LU/LC in the study area.

Changes in LU/LC influenced the hydrology to some extent in this study, possibly because the degree of the LU/LC change was comparatively higher. Nevertheless, with substantial changes in LU/LC forms and plant cover in other areas of the region, the impact of LU/LC change warrants more attention when appraising the impacts of plant restoration on hydrological processes, ecosystems and water resources.

The next chapter give concluding remarks and recommendations, and forwarding scope of the future research work.

## CHAPTER 8

### CONCLUSIONS

#### 8.1 Introduction

To evaluate the impact assessment of changes in LU/LC, conservation measures, and climate variability on the hydrological responses, the SWAT model has been used in the Geba catchment, Northern highlands of Ethiopia. The results include statistical and trend analysis of hydro-meteorological data, water balance statistics, land use/land cover change assessment, calibration and validation, performance evaluation of the model and sediment dynamics. This chapter summarizes the important findings of this study to advance the field of physically based hydrological modelling and impact assessment of LU/LC and climate change for the management of water resources in general and Geba basin, Northern Ethiopia in particular. It also discusses some of the limitations of the SWAT model, and also forwarded important recommendations and scope for further research.

#### 8.2 Conclusions

##### 8.2.1 Historical Trends of Hydro-Meteorological Analysis

This study examined that, there are substantial spatial changes in mean annual, seasonal and trends of historical (1971-2013) rainfall recorded at 7 stations in semi-arid areas of the Geba River basin, Northern Ethiopia. Seasonal rainfall inconsistency is higher throughout Bega and Belg seasons in the most of the stations. In contrast, Kiremt rainfall variability which directly distresses agricultural production is less variable over stations in the study area.

1. Larger part of the Geba catchment has recorded decrease in rainfall though the upper part of the basin receives relatively less rainfall than the lower part of the catchment. This could be the main cause for the frequent drought and crop failures in the area.

2. Most of climate stations analysed for Geba River basin showed decreasing trends in the number of consecutive dry days (CDD) index. In contrast, increasing trends were detected for the number of consecutive wet days (CWD), but no trend was identified over majority of the climate stations. In terms of PRCPTOP, the annual total rainfall during wet days, four stations showed a decreasing trend and three stations showed increasing trends. Furthermore, decreasing trends were noticed in the extreme rainfall indices, R10mm and R20mm and 25mm, in most of the stations except Abiadi and Wukro.
3. For the monthly maximum 1-day (Rx1day) and 5-day (Rx5day) rainfall index, a mix of decreasing and increasing trends was detected in the stations of the River basin. The annual total rainfall when daily rainfall exceeds 90, 95 or 99 % threshold index, R90p/R95p/R99p, an increasing trends seen in most of the stations and mostly positive trends were observed for R90p. Like other indices, the rainfall intensity index, SDII, showed decreasing trends in stations Adigudem, Hawzien, Mek'ele and Senkata and increasing trends in Abiadi, Adigrat and Wukro.
4. Even though, there is an increase or decrease trend in the extreme rainfall trend analysis, majority of the stations did not show statistically significant change over time in the 1971–2013 time period, except Abiadi station which showed statistically significant increasing trend for most of the extreme rainfall indices (PRCPTOT, R10 mm, R20 mm, R25 mm, P90p, P95p, P99p, SDII, RX1D and RX5D) at the 95 % confidence level. In general, the findings in this study are in agreement with other studies that examined changes in rainfall in East Africa.
5. Furthermore, the analysis of monthly and daily minimum and maximum temperature records have shown a mix of decreasing and increasing trend for the study period. In general, the findings showed that a slightly decrease in the monthly temperature occurred in the 1971 to 2013 time period. Daily maximum temperature revealed a rising trend at three stations; out of these two of them were statistically significant (increase of 0.053 °C per decade). A decreasing trend in daily maximum temperature was noted in the remaining four stations,

but the trend was statistically significant only at two stations (decrease of 0.084 °C per decade).

6. Trend analysis of annual and rainy season streamflow showed decreasing trend having a Sen's slope magnitude -0.341 and -0.001 mm per year, respectively but not statistically significant.
7. The average monthly PET showed increasing trend mainly caused by a significant increase in maximum air temperature and wind speed during the study period.
8. There are local factors for the variability of rainfall in the region that can be attributed to local topography (orographic processes) and proximity to sources of moist air and seasonal air mass movements. The decrease in rainfall in the catchment, coupled with higher evapotranspiration occasioned by temperature increases in this region, could lead to decrease in observed streamflow at the outlet gauge station. Therefore, temporal variability of seasonal and annual rainfall may affect the agricultural crop production and future water availability in the undulating topography of the region. Finally results of this study contribute to climate change research in the region and provide inputs for better planning towards adapting to changing climate.

### **8.2.2 Land Use/Land Cover Change Assessment**

Understanding interactions between hydrological responses and associated changes in land use/land cover and climate variability is imperative in the Geba catchment with increasing anthropological activities. These interferences can be attained by assimilating land use planning and water resources management. Consequently, a widespread valuation of the spatio-temporal scattering of impacts on the hydrological processes due to changes in land use/land cover are essential to resolve current challenges and avoid probable catastrophes in the future water resources development and management . Outcomes of this research can be applied to advance land use planning and management at national level to attain sustainable water utilization in the Geba river basin.

1. It is evident that land use/land cover changes have occurred between 1973 and 2013. Seven land use/land cover classes, comprising agriculture, range, shrub, barren, forests, built-up (urban) areas and water bodies, were mapped for the Geba catchment, with overall accuracy of 87.1%, 80.2 % and 82.5 % for 1973 to 1987, 1987 to 2000, and 2000 to 2013 land cover map, respectively. The land use/land cover maps produced have well-matched digital presentations; therefore they can be used simply to a variety of future GIS applications. Additional themes can be combined as more resource evidence develops accessible, or as new management demands are recognized.
2. LU/LC change analysis exhibited shrub land, rangeland, and forest dramatically decreased from 38 %, 21.88 % and 4.19 % to 23.38 %, 16.54 % and 1.61 %, respectively, the main driving factors attributed to firewood, and clearing for subsistence agricultural intensifications from 1973 to 2000 time period. In contrast, shrub land and forest increased from 23.38 % and 1.61 % to 29.94 % and 3.51 % for 2000 to 2013 time period respectively. The agricultural area consistently increased over the years from 27.39 % to 42.75 % during the study period. These land use/land cover conversions have caused land degradation in different sub-basins of the Geba catchment and have hindered with biodiversity and ecosystems. Moreover, these practices have been diminishing the overall quality and quantity of water resources.

### **8.2.3 Calibration, Validation and Performance Evaluation of SWAT Model**

Hydrological response to changes in LU/LC is important within catchments of large rivers. The SWAT hydrological model was used in this study, to simulate streamflow, sediment dynamics and water balance of the Geba River catchment. Moreover, this hydrological model was used to appraise impacts of LU/LC changes and climate variability on hydrological processes. The performance and applicability of SWAT model was successfully evaluated through sensitivity analysis, model calibration and validation, and reproducing streamflow. Model calibration was performed using digital elevation model, soil and land use/land cover data, and 6 years of observed daily climatic variables for each land use/land cover maps.

1. The study showed that surface and subsurface flow model parameters are sensitive and have physical meaning, especially the CN2, ALPHA\_BF, SOL\_AWC, ESCO, GWQMN, REVAPMN, CH\_K2, CH\_N2 and SOL\_K were the most sensitive parameters with regard to streamflow prediction.
2. The  $R^2$  and  $E_{NS}$  for daily and monthly flow were very less (satisfactory) for the single static LU/LC (2000) map, mostly followed in many studies whereas greater than 0.75 during calibration and validation period for the multiple LU/LC maps. Model performance of the SWAT for simulating streamflow in the outlet of the Geba River basin was very good. The model has relatively high confidence and gives a very good representation of the water balance and outflow hydrographs at the basin outlet. The model captured the dynamics of flow generation well, with surface runoff dominating during the rainy season and shallow aquifer contributing during the dry months. Therefore, SWAT model can be recommended for future studies to water yield/sediment yield of the basin.
3. Though calibration and validation results of the SWAT model showed simulated monthly and daily flows were in reasonable agreement with measured values, the SWAT model derived simulation streamflow volume over estimated for calibration period consistently except between the years 1975 and 1977 in the 1973 LU/LC map, and in 2006 in the 2013 LU/LC map which showed the observed flow is over estimated. The same holds true for validation period except for the years 1992 and 2012 for 1987 and 2013 LU/LC map, respectively. The possible reason may be the spatial distribution of rainfall intensity spread over smaller area compared to low intense storms eventually catch of the rain gauge may not be representative.
4. Changes in water balance components were identified from the study due to deforestation and restoration of natural resources in the Geba catchment. The SWAT model predicted higher surface runoff (SURQ) in the 2000 LU/LC map where there was higher deforestation, but lower in 2013 due the advancement of integrated watershed management approaches. Moreover, analysis of average annual water balance components simulated by the SWAT model indicated that



evapotranspiration loss was 70 % to 74 % of rainfall for the Geba catchment. Though ET appeared high, the values are within the range of other previous studies conducted in arid and semi-arid regions. As a result the water yields (WY) as percentage of rainfall were low.

5. With a limited data set the model well simulated sediment concentration consistently on the rising and the falling limbs of the sediment hydrograph during calibration and validation periods. Though, the sediment peak was well represented in all of the years, the model slightly overestimated the peaks for some days in the month of August in 2009, 2010 and 2011 for 2000 and 2013 land use/land cover conditions. Average sediment yield at the outlet of the Geba catchment was estimated as 10.2, 11.6, 14.6 and 12.3 t ha<sup>-1</sup> yr<sup>-1</sup> for 1973, 1987, 2000 and 2013 land cover conditions, respectively which is high. The possible reason for the decreased sediment yield in 2013 LU/LC is successive physical soil and water conservation activities along with afforestation initiated after the year 2000.
6. Erosion susceptibility map has been generated and extremely useful areas are more susceptible to erosion. Sub-basins 2, 4, 6, 7 and 10 are highly susceptible to erosion. Hence using the methodology adopted land use, water and watershed planners can take advantage of these maps for selecting appropriate soil and water conservation measures for sustainable land resources management.

#### **8.2.4 LU/LC and Climate Variability Impact Assessment on the Hydrology of the Geba Catchment**

In the present study, the impacts of hypothetical LU/LC change characteristics upon the hydrological processes that rainfall undertakes on distributing to the land surface were also investigated. Flow parameters discussed - surface flow, baseflow and streamflow are affected by the land cover condition. The results of the analysis have emphasized the understanding of surface and baseflow flow in response to endorsed decrease in woodlands.

1. In the hypothetical scenario where the shrub lands were reduced by 20 % showed average annual increment of total water yield however reduced baseflow. The total water yield increased from 154.77 mm y<sup>-1</sup> to 158.41 mm y<sup>-1</sup> and surface flow increased from 87.65 mm y<sup>-1</sup> to 97.18 mm y<sup>-1</sup>. Subsequently, seasonal variations in river discharge have been associated with decreased infiltration during the wet season, which can affect the streamflow during the dry season by obstructing ground water recharge.
2. Impact assessment of afforestation on flow variability has revealed that land covered with forest decreases surface flow and increases ground water recharge. In a scenario of increasing shrub lands and forested areas, catchment streamflow reduced from 154.77 mm y<sup>-1</sup> to 145.86 mm y<sup>-1</sup> for a 20 % shrub lands and forest area raised, and to 136.61 mm y<sup>-1</sup> for a 40 % shrub lands and forest area increase.
3. Hydrological processes are an integrated indicator of catchment conditions, and changes in LU/LC may affect the overall health and functioning of a catchment. Understanding of spatio-temporal changes and trends in streamflow and the proportion of surface flow and baseflow are critical for directing efforts in managing LU/LC and improving agricultural practices. This study has integrated LU/LC and water resources management which comprises harmonizing the reliability of landscape and hydrological characteristics to achieve sustainable long-term management of water resources. This approach enhances understanding of the on-going LU/LC changes, processes and possibly predicts future trends in the Geba catchment as well as in the region. Within such an approach, proper policies of water resources, water demand management, water availability for small-scale irrigation and sustainable agricultural practices can then be developed.
4. The changes in LU/LC over the period 1973-2000 have been significant and have contributed to a considerable increase in runoff, while a decrease in the 2000 - 2013 time period. It should be noted that the aggregation of the observed runoff decrement triggered by the variability of climate and LU/LC change together (6.67 mm), (12.04) were to some extent lesser than the predicted combined effect of scenario 4 (S4) (9.26 mm) and (14.71 mm) for the first two phases, respectively

as a result of the interactions concerning the variation of climate and changes in LU/LC signified in the SWAT model.

5. Individual LU/LC change, climate variability and the combined effect in the study increased surface runoff and ET considerably while decreased base flows and soil water till 2000 LU/LC map and a reversal trend was noticed in 2013. Hydrological impacts of changes in LU/LC and climate variability are somehow challenging to distinguish in case of large river basins that have a diversity of LU/LC types. However, in this study the results shown the difference was clearly distinguished where LU/LC change for the considered period influenced hydrological processes more significantly and strongly than the climate variability. Furthermore, spatio-temporal rainfall variations may exist across decades.

### **8.3 Contributions from this Research**

1. The condition of natural resources particularly water resources in the Geba catchment, Northern Ethiopia, as shown from the study has been under great pressure due to rapid population growth, poor agricultural practices, deforestation, rapid changes in land cover and climate variability over the last four decades. This research has contributed to narrowing an important knowledge gap, by making a land use planning and sustainable water resources management relationship in a quantifiable way. It is important to combine landscape change analyses with hydrological parameters for enhanced understanding of the processes of LU/LC change and hydrological variables. This provides an appropriate solution for designing strategy interventions targeted at reducing the adverse effects of LU/LC change and climate variability on hydrological processes. Such improvements are required to address issues relating to sustainable water resources management and food security in the region. It also supports decision makers, and land use and water resource planners to enhance water supply and demand, and to advocate for sound land use practices, while confirming environmental sustainability.

2. This study has contributed to the sustainability of water resources management by providing evidences of strong linkages between the isolated and combined effects of LU/LC and climate variability on streamflow, evapotranspiration and soil water responses. The application of modern tools of remote sensing combined with advanced numerical hydrological models (such as SWAT) have been established to be in developing tools for monitoring and managing LU/LC and hydrological processes in data scarce regions.
3. For multiple LU/LC images in a dynamic environment the model has calibrated and validated specifically using streamflow and sediment for all the respective LU/LC images unlike other studies. Hence, the results from this study are particularly relevant for Ethiopia in formulating, implementing and monitoring strategies for sustainable development. These results provide a platform to select variables and identify practical interactions in dynamic and process-based hydrological models.

#### **8.4 Recommendations**

To predict the quantity and quality of water resources, changes in land use/land cover and change detection assessment, climate variability studies, and evaluating their hydrological impacts are very important.

1. To model the Geba catchment missing of discharge and sediment records and inadequate number of gauging stations became the most thoughtful restrictions. If this condition continues it will be more challenging for further studies, hence there need for rapid quality control to predict long-term hydrological and climatic data records in government agencies and other stakeholders. Ensuring appropriate efforts to combine LU/LC data and hydrological variables avoid the limitations identified in the current application; some of the significances for coming annotations and investigation are defined. With such enhancements, it is estimated, that future studies could provide a dynamic hydrological model that could be applied with better confidence in planning and decision-making activities.

2. Shortages of reliable and continuous hydro-meteorological data troubled hydrological modelling efforts in the study area. The study suggests the requirement to increase number of measurements and provide more measuring gauging stations for example, in the outlets of each sub-basin to improve long term streamflow and sediment data collection in the study region for hydrological modelling. It is essential to search more advanced automatic recording instruments at gauging stations to reduce unrealistic and unacceptable data. Furthermore, to fulfil national demands streamflow and sediment data acquired from stream gauges must be reliable, recorded using standard procedures and up-to-date technologies, and check through quality control techniques. Hydro-meteorological gauge stations should be necessary to register about the site, stations, and station variables in the database and preserve basic metadata. The data have to experience several stages of quality control investigation to identify doubtful values once the metadata has been arranged in the required format for every station. Therefore, values identified as unacceptable (e.g. constantly identical values or typically high variations) are discard from the data sets prior to dissemination to stakeholders.
3. For real management of data sets, reliable and efficient measurements of hydro-meteorological data must be controlled by experienced and qualified professional. This study recommends higher institutions and departments responsible for water resources and meteorology must have a memorandum of understanding for long-term partnership. The purpose of this teamwork is to provide opportunities to trained professional and increase the quality of data to satisfy different stakeholders which are demanding some specific data set.
4. Worldwide several river basins are regarded as inadequate measurements of key hydrological parameters such as precipitation, especially in east Africa, including Ethiopia. Hence, for streamflow and other hydrological variables prediction of precise rainfall data for the river basin is very essential. As a result, this study suggests use of spatially distributed rainfall from other sources such as meteorological satellites may generate an improvement over the data-scarce areas. Radar-sensed rainfall can be expected to have better spatial accuracy than a

sparse network of rain-gauge stations. The interaction of changes in LU/LC and climate variability become vital for long-term studies to evaluate the impacts associated to hydrologic processes. For this reason, future effort on the impact of changes in LU/LC would be stretched considering climate change in to account, its alteration of hydrological processes and the response on LU/LC changes.

5. In this study it is recommended to increase the distribution of water all over the Geba catchment in the dry and wet seasons through conservation and regeneration of the natural vegetation as well as active management strategies. Organized and more intense agricultural extension training and awareness on sustainable land management to minimise soil loss is required for rural societies; because the soil quality reduction due to existing subsistence agricultural practices has an inference for the sustainability of the landscape and water resources. Appropriate land management practices must be applied to recover degraded landscapes through different biological (e.g. grass strips along the contours, mulching and crop residues management, vegetative fencing, area closure, agroforestry practices and overall afforestation), and physical soil and water conservation activities (e.g. bench terracing, hillside terraces, hillside terraces with trenches, level soil and stone bunds), and water harvesting structures. These play an important role and expected to significantly increase baseflow and decrease storm flow events. Therefore, environmental rehabilitation and management planning should obviously deal with safeguard of natural resources on steeply sloping parts of the landscape.
6. The population of Ethiopia is growing at about 3 % every year and it is estimated that 85 % in the rural areas depend on rain fed subsistence agriculture and natural resources for their livelihoods. This study recommends launching assessment of opportunities of other economic activities in the area. Such activities could be mineral exploration, small-scale rural business adventures and a general industrialisation to decrease overdependence on subsistence agriculture. Moreover, Small-scale irrigation projects should be encouraged especially in areas where water is available. Facilities for water harvesting for dry season

farming must be provided to the communities, while decreasing surface runoff, and limitless expansion of natural resources.

#### **8.4 Perspectives for Future Studies**

1. For the purpose of comparing catchment characteristics and impact assessment, it is essential to search the performance of other hydrologic models. In Ethiopia, particularly in the Northern highlands very little effort has been done on distributed hydrologic modelling and much less related to impact assessments of LU/LC changes and climate variability on hydrological response and sustainable water resources management.
2. To make climate change scenarios for the hydrological modelling and applications, climate evidences at a higher spatio-temporal resolution is necessary. More research on climate impact assessment can support to give a solution for such activities by appraising the value added by downscaling climate information to discover the downscaled climate change projections.
3. It is comprehensible that the rainfall and baseflow relationship is an area of research where further investigation is required as their association could not be established in the current study.

#### **8.6 SWAT Model Limitation**

In SWAT models, HRUs are not spatially located as sub-basins do. This poses some difficulty in finding a balance between creating HRUs and sub-basins that will give enough spatial information in a detail manner for the proposed application. Therefore, provided that landscape position is considered into account, an adjustment to SWAT in this respect will necessitate comprising interaction among HRUs.

## REFERENCES

- f* Abbaspour, K.C., Yang, J., Maximov, I., Siber, R., Bogner, K., Mieleitner, J., Zobrist, J., Srinivasan, R. (2007). “Modelling hydrology and water quality in the pre-alpine/alpineThur watershed using SWAT.” *Journal of Hydrology*, 333:413-430
- f* Abtew, W., Melesse, M.A., Dessalegn, T. (2009). “Spatial, inter and intra-annual variability of the Upper Blue Nile Basin rainfall.” *Hydrologic Processes* 23(21), 3075–3082
- ☐ Afewerki, H.G. (2012). “Modelling of Hydrological Processes in the Geba River Basin, Ethiopia, PhD Thesis.” *Vrije Universiteit Brussel, Brussels, Belgium*, 304pp.
- f* Agarwal, C., Green, G. M., Grove, J. M., Evans, T.P. and Schweik C.M. (2002). “A review and assessment of land-use change models - Dynamics of space, time, and human choice.” 84p. *USDA, Forest Service, North-eastern Research Station, General Technical Report NE-297*.
- f* Akintug, B. and Rasmussen, P.F. (2005). “A Markov switching model for annual hydrologic time series.” *Water resources research*, 41 (9): W09424.
- f* Alexander, L. V., Zhang, X., Peterson, T. C., Caesar, J., Gleason, B., Klein Tank, A. M. G., Haylock, M., Collins, D., Trewin, B., Rahimzadeh, F., Tagipour, A., Rupa Kumar, K., Revadekar, J., Griffiths, G., Vincent, L., Stephenson, D. B., Burn, J., Aguilar, E., Brunet, M., Taylor, M., New, M., Zhai, P., Rusticucci, M., and Vazquez-Aguirre, J. L., (2006). “Global observed changes in daily climate extremes of temperature and rainfall.” *Journal of Geophysical Research*, Vol. 111, D05109.



- ☒ Allen, R.G., Pereira, L. S., Raes, D., Smith, M. (1998). “Crop evapotranspiration, Guidelines for computing crop water requirements.” *FAO Irrigation and Drainage Paper 56*, FAO, Rome.
- f Angassa, A. and Oba, G. (2007). “Relating long-term rainfall variability to cattle population dynamics in communal rangelands and a government ranch in southern Ethiopia.” *Agricultural Systems*, 94, 715-725.
- f Arnell, N.W. and Reynard, N.S. (1996). “The effects of climate change due to global warming on river flows in Great Britain.” *Journal of Hydrology*, 183 (3-4): 397-424.
- f Arnold, J.G., Kiniry, J.R., Srinivasan, R., Williams, J.R., Haney, E.B. and Neitsch, S.L. (2012). “Soil and Water Assessment Tool: User’s manual, version 2012.”
- f Arnold, J.G., Srinivasan, R., Muttiah, R.S. and Williams, J.R. (1998). “Large area hydrologic modelling and assessment Part 1: Model development.” *Journal of American Water Resources Association*, 34 (1), 73-89.
- ☒ Ashenafi, A.A. (2014). “Modelling Hydrological Responses to Changes in Land Cover and Climate in Geba River Basin, Northern Ethiopia.” PhD thesis, *Freie Universität Berlin*, PP-187.
- f Awulachew, S. B., Yilma, A. D., Loulseged, M., Loiskandl, W., Ayana, M., Alamirew, T. (2007). “Water Resources and Irrigation Development in Ethiopia.” *Colombo, Sri Lanka: International Water Management Institute, (Working Paper 123)*, 78 pp.
- f Babar, S. and Ramesh, H. (2015). “Runoff Response to LU/LC–Land Cover Change over the Nethravathi River Basin, India.” *Journal of Hydrologic Engineering*, 20(10): 05015002. DOI: 10.1061/(ASCE) HE.1943-5584.0001177

- ☒ Babar, S.F. Ramesh, H. (2013). “Analysis of south west monsoon rainfall trend using statistical techniques over Nethravathi basin.” *International Journal of Advanced Technology in Civil Engineering*, 2: 130-136.
- f Baumgartner, M.F. and Apel. G.M. (1996). “Remote sensing and geographic information Systems.” *Hydrological Science Journal*, 41 (4): 593-608.
- ☒ Belay T. (2002). “Land cover/use changes in the Derekolli catchment of the South Welo Zone of Amhara Region, Ethiopia.” *Eastern Africa Social Science Research Review*, 18 (1): 1-20.
- f Betrie, G. D. Mohamed, Y. A., van Griensven A., and Srinivasan, R. (2011). “Sediment management modelling in the Blue Nile Basin.” *Hydrology and earth system sciences*, 15, 807–818.
- f Beven, K.J. (2001). “Rainfall-Runoff modelling” The Primer, John Wiley and Sons Ltd, England.
- f Bewket, W. (2003). “Towards integrated watershed management in highland Ethiopia: the Chemoga watershed case study.” *PhD thesis, Wageningen University and Research Centre*, ISBN 90-5808-870-7.
- f Bewket, W. and Sterk, G. (2005). “Dynamics in land cover and its effect on stream flow in the Chemoga watershed, Blue Nile basin, Ethiopia.” *Hydrologic Process*, DOI: 10.1002/hyp.5542.
- f Bewket, W., Conway, D. (2007). “A note on the temporal and spatial variability of rainfall in the drought-prone Amhara region of Ethiopia.” *International Journal of Climatology*, 27: 1467–1477.
- f Brath, A., Montanari, A., Moretti, G. (2006). “Assessing the effect on flood frequency of LU/LC change via hydrological simulation (with uncertainty).” *Journal of Hydrology*, 324 (1–4), 141–153.

- ▣ Bryan, E., Ringler, C., Okoba, B., Roncoli, C., Silvestri, S., and Herrero, M. (2013). “Adapting agriculture to climate change in Kenya: Household strategies and determinants.” *Journal of Environmental Management*, 114: 26-35.
- f Brown, A.E., Zhang, L., McMahon T.A., Western, A.W. and Vertessy, R.A. (2005). “A review of paired catchment studies for determining changes in water yield resulting from alterations in vegetation.” *Journal of Hydrology*, 310: 28–61.
- f Camberlin, P. and Philippon, N. (2002). “The East African March–May Rainy Season: Associated Atmospheric Dynamics and Predictability over the 1968–97 Period.” *Journal of climate*, 15: 1002-1019.
- f Central Statistical Agency of Ethiopia (CSA) (2008). “Statistical Abstract of Ethiopia national census 2007, Central Statistical Agency, Addis Ababa: Ethiopia.”
- f Chang, K. (2008). “Introduction to Geographic Information system.” 4th ed. *McGraw-Hill, New Delhi*, 468pp.
- f Cheung, W., Senay, G., Singh, A. (2008). “Trends and spatial distribution of annual and seasonal rainfall in Ethiopia.” *International Journal of Climatology*, 28: 1723–1734.
- f Chow, V.T., Maidment, D.R. and Mays, L.W. (1988). “Applied Hydrology.” *McGraw-Hill, New York*, 498pp.
- f Chu, T.W. and Shirmohammadi, A. (2004). “Evaluation of the SWAT Model’s Hydrology Component in the Piedmont Physiographic Region of Maryland.” *Transactions of the ASAE*, 47 (4): 1057-1073.
- f Congalton and Green (1991). “A Review of Assessing the Accuracy of Classifications of Remotely Sensed Data.” *Remote Sensing of Environment*, 37, 35-46.

- f* Conway, D., and Schipper, E. (2011). “Adaptation to climate change in Africa: Challenges and opportunities identified from Ethiopia.” *Global Environmental Change*, 21:227-237.
- f* Conway, D., Mould, C., Bewket, W. (2004). “Over one century of rainfall and temperature observations in Addis Ababa, Ethiopia.” *International Journal of Climatology*, 24: 77–91.
- f* Conway, D. (2000). “Some aspects of climate variability in the north east Ethiopian Highlands-Wollo and Tigray.” *SINET Ethiop Journal of Science*, 23:139–161
- f* Collier, P., Conway, G., and Venables, T. (2008). “Climate Change and Africa.” *Oxford Review of Economic Policy* 24, 337-353.
- f* Cunderlik, J. (2003). “Hydrological model selection for CFCAS project, Assessment of water resource risk and vulnerability to change in climate condition University of Western Ontario.
- ☐ Daniel E.B., Camp, J.V., LeBoeuf, E.J., Penrod, J.R., Dobbins, J.P. and Abkowitz, M.D. (2011). “Watershed Modelling and its Applications: A State-of-the-Art Review.” *The Open Hydrology Journal*, 5, 26-50.
- f* Deressa, T.T., Hassan, R.M., Ringler, C. (2011). “Perception of and adaptation to climate change by farmers in the Nile basin of Ethiopia.” *J. Agric. Sci.*, 149: 23-31.
- f* Danuso, F. (2002). “Climak: A Stochastic Model for weather Data Generation.” *Italian Journal of Agronomy* 6 (1): 57-7, 67-68pp.
- f* Descheemaeker, K., Nyssen, J., Poesen, J., Raes, D., Mitiku, Haile, Muys, B., Deckers, S. (2006b). “Runoff on slopes with restoring vegetation: a case study from the Tigray highlands, Ethiopia.” *Journal of Hydrology* 331 (1–2), 219–241.

- f* De Sherbinin, A. (2002). “A CIESIN Thematic Guide to Land Land-Use and Land Land- Cover Change (LUCC).” *Center for International Earth Science Information Network (CIESIN) Columbia University Palisades, NY, USA.*
- f* Drapela, K. and Drapelova, I. (2011). “Application of Mann-Kendall test and the Sen’s slope estimates for trend detection in deposition data from Bílý Kříž (Beskydy Mts., the Czech Republic) 1997–2010.” *Beskydy Mendel University in Brno*, 4 (2), 133–146.
- f* Easton, Z. M., Fuka, D. R., White, M. T., Collick, E. D., Biruk A. S., Ashagre, B., McCartney, M., Awulachew, S. B., Ahmed, A. A., and Steenhuis, T. S. (2010). “A multiple basin SWAT model analysis of runoff and sedimentation in the Blue Nile, Ethiopia.” *Hydrology and earth system sciences*, 14, 1827–1841.
- f* Elfert, S., Bormann, H. (2010). “Simulated impact of past and possible future land use changes on the hydrological response of the Northern German lowland ‘Hunte’ catchment.” *Journal of Hydrology*, 383, 245–255.
- f* ENMA (2007). “Climate change national adaptation programme of action (NAPA) of Ethiopia, National meteorological Agency.” Ethiopia.
- f* Food and Agriculture Organisation (2005). “Land Cover Classification System: Classification concepts and User manual.” *FAO, Rome*, 190 pp.
- f* FAO. (2002). “Major Soils of the World. Land and Water Digital Media Series.” *Food and Agricultural Organization of the United Nations, Rome*, CD-ROM.
- f* FAO (1998). “The Soil and Terrain Database for northeaster Africa (CD-ROM).” *FAO, Rome Field Document 2*, AG: DP/ETH/781003, Addis Ababa, Ethiopia.
- f* Fohrer, N., Haverkamp, S. and Frede, H.-G. (2005). “Assessment of the effects of land use patterns on hydrologic landscape functions: development of sustainable

- land use concepts for low mountain range areas.” *Hydrological Processes*, 19, 659–672.
- f* Fohrer, N., Moller D., Steiner, N. (2002). “An interdisciplinary modelling approach to evaluate the effects of land use change”. *Physics and Chemistry of the Earth*. 27: pp.655-662.
- f* Fohrer, N., Haverkamp, S., Eckhardt, K. and Frede, H.G. (2001). “Hydrologic response to land use changes on the catchment scale.” *Physics and Chemistry of the Earth*, 26 (7-8): pp.577-582.
- f* Fontaine, T.A., Klassen, J.F., Cruickshank, T.S. and Hotchkiss, R.H. (2001). “Hydrological response to climate change in the Black Hills of South Dakota, USA.” *Hydrological Sciences. Journal*, 46(1): 27-40
- f* Fortin, V., Perreault L. and Salas, J.D. (2004). “Retrospective analysis and forecasting of streamflows using a shifting level model.” *Journal of Hydrology*, 296(1-4):135-163.
- f* Friedrich, J.K, Griensven, A.V, Uhlenbrook, S, SirakTekleab, Teferi, E. (2012). “The Effects of Land use Change on Hydrological Responses in the Choke Mountain Range Ethiopia: A new Approach Addressing Land Use Dynamics in the Model SWAT.” *International Environmental Modelling and Software Society (iEMSs)*, <http://www.iemss.org/sites/iemss2012/proceedings.html>.
- f* Garg, S.K. (2005). “Irrigation Engineering and Hydraulic Structures.” *Hindustan Offset Press, Naraina, Delhi*, ISBN: 8174090479.
- f* Gassman, P. W., Reyes, M., Green, C. H. and Arnold, J. G. (2007). “The Soil and Water Assessment Tool: Historical development, applications, and future directions.” *Trans. ASABE* 50 (4): 1211- 1250.

- ☐ Gebrehiwot, T., Van der Veen, A. (2013). “Assessing the evidence of climate variability of rainfall in Northern part of Ethiopia. *Journal of Development Agricultural Economics*, 5(3): 104-119.
- f Gete, Z. and Hurni, H. (2001). “Implications of Land use/cover dynamics for mountain resource degradation in the northwestern Ethiopian highlands.” *Mountain Research and Development*, 21: 184-191.
- f Gilbert, R.O. (1987). “Statistical Methods for Environmental Pollution Monitoring.” *John Wiley and Sons, New York, ISBN: 9780471288787*, pp: 336.
- f Girmay, G., Singh B.R., Dick Ø. (2010). “Land-use changes and their impacts on soil degradation and surface runoff of two catchments of Northern Ethiopia.” *Acta Agriculturae Scandinavica, Section B-Soil and Plant Science*, 60:3, 211-226, DOI: 10.1080/09064710902821741.
- f Girmay K. (2003). “GIS based analysis of land use and land cover, land degradation and population changes: A study of Boru Metero area of south Wello, Amhara Region.” *MA Thesis, Department of Geography, Addis Ababa University*. 110 pp.
- f Gizawchew, A. (1995). “Soil erosion assessment: Approaches magnitude of the problem and issues on policy and strategy development (Region 3).” *Paper presented at the Workshop on Regional Natural Resources Management Potentials and Constraints, Bahir Dar, Ethiopia*, 9 pp.
- f Global Land cover facility (2013). “land cover imagery, edited”
- ☐ Global Water Partnership (2005). “Sustainable management of water resources, edited.
- f Green, W.H. and Ampt, G.A. (1911). “Studies on soil physics, 1: The flow of air and water through soils. *Journal of Agricultural Sciences*, 4: 11-24.

- f Gregor, M., Schütt, B. and Förch, G. (2004). “Land use/land cover changes in the Lakes Abaya-Chamo Basin South Ethiopia since 1981- a remote sensing based analysis.” *1<sup>st</sup> Ethiopia Proceedings Sedimentary Studies in Tropics and subtropics*, ISBN 3-932604-14-8, Siegen, Germany.
- f Govender, M. and Everson, C.S. (2005). “Modelling streamflow from two small South African experimental catchments using the SWAT model.” *Hydrological Processes*. 19(3): 683-692.
- f Grunwald, S. and Norton, L. D. (2000). “Calibration and validation of a non-point source pollution model.” *Agricultural Water Management*, 45, 17–39.
- f Guo, H., Hu, Q. and Jiang, T. (2008). “Annual and seasonal streamflow responses to climate and land-cover changes in the Poyang Lake basin, China.” *Journal of Hydrology*, 355, 106– 122.
- f Gupta, H., Sorooshian, S., Yapo, P. (1999). “Status of automatic calibration for hydrologic models: Comparison with multilevel expert calibration.” *Journal of Hydrologic Engineering*, 4, 135–143, 1999.
- ▣ Hadda, M.S. and Sandhu, B.S. (2001). “Evaluation of Erosivity Factor of USLE for Predicting Soil Loss from Individual Storm in Watersheds in Sub montane Punjab.” *Journal of Soil Conservation, India*, Vol. 29, pp. 69 – 72
- f Hadgu, K.M. (2008). “Temporal and spatial changes in land use patterns and biodiversity in relation to farm productivity at multiple scales in Tigray, Ethiopia.” *PhD Thesis Wageningen University, Wageningen, the Netherlands*, pp. 184.
- f Hagdu, G., Tesfaye, K., Mamo, G., Kassa, B. (2013) “Trend and Variability of ainfall in Tigray, Northern Ethiopia: Anaylsis of Meteorological data and Farmers’ Perception.” *Academic Journal of Agricultural Research* 1(6):88-100.



- f Haregeweyn, N., Poesen, J., Nyssen, J., Verstraeten, G., de Vente, J., Govers, G., Deckers, J., Moeyersons, J. (2005). "Specific sediment yield in Tigray – Northern Ethiopia: assessment and semi-quantitative modelling." *Geomorphology* 69: 315–331.
- f Haregeweyn, N. and Yohannes, F. (2003). "Testing and evaluation of the agricultural non-point source pollution model (AGNPS) on Augucho catchment, western Hararghe, Ethiopia." *Agricultural Ecosystem and Environment*, 99, 201–212.
- f Hargreaves, G.H., Samani, Z.A. (1985). "Estimating potential evapotranspiration." *Journal of the Irrigation and Drainage Division, ASCE*, 108 (3): 225-230.
- f Hargreaves, G.H. (1975). "Moisture availability and crop production." *ASAE*, 18, 980-984.
- f Hengsdijk, H., Meijerink, G., and Mosugu, M. (2005). "Modelling the effect of three soil and water conservation practices in Tigray, Ethiopia." *Agricultural Ecosystem and Environment*, 105, 29–40.
- f Herweg, K. and Stillhardt, B. (1999). "The variability of soil erosion in the highlands of Ethiopia and Eritrea." Research report 42, *Centre for Development and Environment, University of Berne*.
- f Hirsch, R.M., Slack, J.R. and Smith, R.A. (1982). "Techniques of trend analysis for monthly water quality data." *Water Resources Research* 18(1):107-121.
- f Huang, M.B. and Zhang L. (2004). "Hydrological responses to conservation practices in a catchment of the Loess Plateau, China." *Hydrological Processes* 18:1885–1898.
- f Hudson, N.W. (1995). "Soil Conservation." *Batsford: London*, 391 pp.

- f* Hulme, M., Doherty, R., Ngara, T., New, M., Lister, D. (2001). “African climate change: 1900-2100.” *Climate Research*, 17: 145-168.
- f* Hurni, H., Tato, K., Zeleke, G. (2005). “The implications of changes in population, LU/LC, and land management for surface runoff in the upper Nile basinarea of Ethiopia.” *Mountain Research and Development*, 25 (2), 147–154.
- f* Hurni, H. (1993). “Land degradation, famines and resource scenarios in Ethiopia.” In: *World Soil Erosion and Conservation*, edited by: Pimentel, D., Cambridge University Press, Cambridge.
- f* Hurni, H. (1990). “Degradation and conservation of the soil resources in the Ethiopian highlands.” In: *African Mountains and Highlands: Problems and Perspectives* pp. 51-64, (Messerli, B. and Hurni, H. eds.). Marceline, Missouri (USA).
- f* Hurni, H. (1988). “Degradation and conservation of the resources in the Ethiopian highlands.” *Mountain Research and Development*, 8: 123-130.
- f* IPCC, (2013). “Summary for Policymakers. In: *Climate Change 2013: The Physical Science Basis. Contribution of Working Group I to the Fifth Assessment Report of the Intergovernmental Panel on Climate Change* [Stocker, T.F., D. Qin, G.-K. Plattner, M. Tignor, S.K. Allen, J. Boschung, A. Nauels, Y. Xia, V. Bex and P.M. Midgley (eds.)].” *Cambridge University Press, Cambridge, United Kingdom and New York, NY, USA*, pp. 1–30, doi:10.1017/CBO9781107415324.004.
- f* IPCC (2012). “Managing the Risks of Extreme Events and Disasters to Advance Climate Change Adaptation, edited by: Field,C. B., Barros, V., Stocker, T. F., and Dahe, Q.” *Cambridge University Press, Cambridge, UK and New York, USA*, 582 pp.

- ☐ IPCC, 2007b: Climate Change. (2007). “Impacts, Adaptation, and Vulnerability - Contribution of Working Group II to the Third Assessment Report of the Intergovernmental Panel on Climate Change, edited by M. L. Parry et al.” *Cambridge Univ. Press, Cambridge, U. K.*
- f IPCC, 2001: Climate Change (2001). “The Scientific Basis. Contribution of Working Group I to the Third Assessment Report of the Intergovernmental Panel on Climate Change [Houghton, J.T., et al. (eds.).]” *Cambridge University Press, Cambridge, United Kingdom and New York, NY, USA.*
- f Jensen, J.R. (2005). “Introductory digital image processing: A remote sensing perspective.” *Prentice Hall, USA, USA.*
- f Jha, M., Pan, Z., Takle, E.S., and Gu, R. (2004). “Impacts of climate change on stream flow in the Upper Mississippi River Basin: A regional climate model perspective.” *Journal of Geophysical Research*, 109, D09105, doi: 10.1029/2003JD003686.
- f Jothityangkoon, C., Sivapalan, M., Farmer, D.L. (2001). “Process controls of water balance variability in a large semi-arid catchment: downward approach to hydrological model development.” *Journal of Hydrology* 254, 174–198.
- f Kendall, M.G. (1975). “Rank Correlation Methods.” 4<sup>th</sup> ed. *Charles Griffin, London*, ISBN: 0195205723.
- f Kepner, W.G., Semmens, D.J., Bassett, S.D., Mouat, D.A. and Goodrich, D.C. (2004). “Scenario Analysis for the San Pedro River, Analyzing Hydrological Consequences of a Future Environment.” *Environmental Monitoring and Assessment*, 94: 115–127.
- f Kinh'Uyu, S.M., Ogallo, L.A., Anyamba, E.K. (2000). “Recent trends of minimum and maximum surface temperatures over eastern Africa.” *Journal of Climatology*, 13: 1-11.

- ☐ Kiros G, Shetty A, Nandagiri L (2015a) Performance Evaluation of SWAT Model for Land use/land cover Changes in Semi-arid Climatic Conditions: A Review. *Hydrology Current Research* 6, 216-223. doi:10.4172/2157-7587.1000216.
- f Korecha, D. and Barnston, A. G. (2007). “Predictability of June–September Rainfall in Ethiopia.” *Monthly Weather Review*, 135: 628–650.
- f Kundzewicz, Z. W. and Robson, A. J. (2004). “Change detection in hydrological records—a review of the methodology.” *Hydrological Sciences Journal* 49 (1), 7–19.
- f Lacy, G. (1930). “Stable Channel in Alluvium.” *Journal Engineering*, Vo. 129, pp. 29-36.
- f Lal, R., Ahmadi, M. and Bajracharya, R.M. (2000). “Erosional impacts on soil properties and corn yield on Alfisols in central Ohio.” *Land Degradation Development*, 11: 575–585.
- f Lambin, E.F., Geist, H.J. and Lepers, E. (2003). “Dynamics of land use/cove change in tropical regions.” *Annu. Rev. Environ. Resour*, 2003. 28:205–41.
- f Lenhart, T., Eckhardt, K., Fohrer, N., Frede, H.G. (2002). “Comparison of two different approaches of sensitivity analysis.” *Physics and Chemistry of the Earth* 27: 645-654.
- f Laurance, W.F. (1998). “A crisis in the making: responses of Amazonian forests to land use and climate change, *Trends in Ecology & Evolution*.” 13(10): 411–415.
- f Legesse1, D., Abiye, T.A., Vallet-Coulomb, C., Abate, H. (2010) “Runoff sensitivity to climate and land cover changes: Meki River, Ethiopia.” *hydrology and earth system sciences*, 14, 2277–2287.

- ☐ Legesse, D., Vallet-Coulomb, C. and Gasse, F. (2003). “Hydrological response of a catchment to climate and land use changes in Tropical Africa: case study South Central Ethiopia.” *Journal of Hydrology*, 275, 67–85.
- f Li, Z., Liu W., Zhang, X. and Zheng, F. (2009). “Impacts of land use change and climate variability on hydrology in an agricultural catchment on the Loess Plateau of China.” *Journal of Hydrology*, 377, 35–42.
- f Lillesand, T.M., Kiefer, R.W., Chipman, J.W. (2004). “Remote sensing and image interpretation.” 5<sup>th</sup> ed., *John Wiley and Sons, USA*.
- f Lin, Y. P., Hong, N.M., Wu P. J., Wu C. F. and Verburg, P.H. (2007). “Impacts of land use change scenarios on hydrology and land use patterns in the Wu-Tu watershed in Northern Taiwan.” *Landscape and Urban Planning*, 80, 111–126.
- f Li, Q., Cai, T., Yu, M., Lu, G., Xie, W., and Bai, X. (2013a). “Investigation into the impacts of LU/LC changes on runoff generation characteristics in the Upper Huaihe River basin, China.” *Journal of Hydrologic Engineering*, 10.1061/(ASCE) HE.1943-5584.0000489, 1464–1470.
- f Li, Q., Yu, X., Xin, Z., and Sun, Y. (2013b). “Modelling the effects of climate change and human activities on the hydrological processes in a semiarid watershed of Loess Plateau.” *Journal of Hydrologic Engineering*, 10.1061/(ASCE) HE.1943-5584.0000629, 401–412.
- f Liu, X., Ren , L., Yuan , F., Singh, V. P., Fang , X., Yu, Z. and Zhang, W. (2009). “Quantifying the effect of LU/LC and land cover changes on green water and blue water in Northern part of China.” *hydrology and earth system sciences*, 13(6), 735–747.
- f Maidment, D. R. (1993). “Handbook of hydrology.” McGraw-Hall, New York.

- ☐ Mahmoud SH, Alazba, A.A. (2015). “Hydrological Response to Land Cover Changes and Human Activities in Arid Regions Using a Geographic Information System and Remote Sensing.” *PLoS ONE* 10(4): e0125805. doi:10.1371/journal.pone.0125805.
- f Mango, L.M., Melesse, A.M., McClain, M.E., Gann, D. and Setegn, S. G. (2011). “Land use and climate change impacts on the hydrology of the Mara River Basin.” *hydrology and earth system sciences*, 15, 2245–2258.
- f Mao, D. and Cherkauer, K.A. (2009). “Impacts of land-use change on hydrologic responses in the Great Lakes region.” *Journal of Hydrology*, 374, 71–82.
- f Mann, H.B. (1945). “Non-parametric test against trend.” *Econometrica*, 13: 245-259.
- f Mather, P. M. (1993). *Computer processing of remotely sensed images*, 352 pp., John Wiley.
- f Mekuria, A.D. (2005). “Forest conversion-soil degradation-farmer’s perception nexus: Implication for sustainable land use in the southwest of Ethiopia.” *Ecological and Development Series No.26, PhD Thesis University of Bonn*.
- f Mengistu, D. T., and Sorteberg, A. (2012). “Sensitivity of SWAT simulated runoffs to climatic changes within the eastern Nile River basin.” *hydrology and earth system sciences*, 16(2), 391–407.
- f Mengistu, T.K. (2009). *Watershed Hydrological Responses to Changes in Land Use and Land Cover, and Management Practices at Hare Watershed, Ethiopia.* PhD thesis, Universität Siegen Fakultät Bauingenieurwesen Research Institute for water and Environment.

- ☐ Mersha, E. (1999). “Annual rainfall and potential evapotranspiration in Ethiopia.” *Ethiopian Journal of Natural Resources* 1(2): 137-154. *Meteorology* 24: 1388-1391.
- f Mersha, E. (2003). “Agro-climatic belts of Ethiopia: Potentials and constraints.” In: M. Engida (Ed). *Proceedings National Sensitization Workshop on Agro-meteorology and GIS, Ethiopian*
- f Meze-Hausken, E. (2004). “Contrasting climate variability and meteorological drought with perceived drought and climate change in Northern Ethiopia.” *Climate Research* 27: 19–31.
- f Mikos, M., Jost, D. and Petkovsek, G. (2006). “Rainfall and Runoff Erosivity in the Alpine Climate of North Slovenia: A Comparison of Different Estimation Methods.” *Journal of Hydrological Sciences, IAHS*, Vol. 51, pp. 115 - 126.
- f Moglen, G.E., Eltahir, E.A.B. and Bras, R.L. (1998). “On the sensitivity of drainage density to climate change.” *Water Resources Research*, 34: 855-862.
- f Mohammed, H., Yohannes, F., and Zeleke, G. (2004). “Validation of agricultural non-point source (AGNPS) pollution model in Kori watershed, South Wollo, Ethiopia.” *International Journal Applied Earth Observation* 6, 97–109.
- f Mondal, A., Kundu, S., Mukhopadhyay, A. (2012). “Rainfall trend analysis by Mann-Kendall test: A case study of North-Eastern part of Cuttack district, Orissa.” *International journal geology earth environmental sciences*, 2: 70-78.
- f Moriasi, D. N., Arnold, J. G., Van Liew, M. W., Bingner, R. L., Harmel, R. D., and Veith, T. L. (2007). “Model evaluation guidelines for systematic quantification of accuracy in watershed simulations.” *T. ASABE*, 50, 885–900.

- ☐ Motiee, H. and McBean, E. (2009). “An Assessment of Long Term Trends in Hydrologic Components and Implications for Water Levels in Lake Superior.” *Hydrology Research*, 40.6, 564-579.
- f MoWE (2001). “Initial National Communication of Ethiopia to the United Nations Framework Convention on Climate Change.” Report 127pp.
- f MoWE (2010). “Surface water resources of Ethiopia, Ministry of Water and Energy” ([www.mowr.gov.et](http://www.mowr.gov.et)) visited on December 15, 2013, at 12:21 AM.
- f MoWR (2002). “Ethiopian Water Sector Strategy.” *MoWR, Addis Ababa, Ethiopia*.
- f Moyo, M., Mvumi, B.M., Kunzekweguta, M., Mazvimavi, K., Craufurd, P., Dorward, P. (2012). “Farmer perceptions on climate change and variability in semi-arid Zimbabwe in relation to climatology evidence.” *Africa Crop Science Journal*, 20: 317-335.
- f Mwangi, M.N, Desanker, P.V. (2007). “Changing climate, disrupted livelihoods: The case of vulnerability of nomadic maasai pastoralism to recurrent droughts in Kajiado district, Kenya.” <http://adsabs.harvard.edu/abs/2007AGUFMGC12A.02M>.
- f Nash, J. E. and Sutcliff, J. V. (1970). “River flow forecasting through conceptual models, part I – a discussion of principles.” *Journal of Hydrology*, 10, 282–290.
- f Neitsch, S.L., Arnold, J.G., Kiniry, J.R. and Williams, J.R. (2005). “Soil and Water Assessment Tool: *Theoretical Documentation, version 2005*.
- f Nicholson, S.E. (2000). “The nature of rainfall variability over Africa on time scale of decades to millenia.” *Global Planet Change*, 26: 137-158.
- f Nyong, A. Niang-Diop, I. (2006). “Impacts of Climate Change in the Tropics: The African Experience.” In: *Avoiding Dangerous Climate Change*, Schellnhuber, H.J.



and W.P. Cramer (Eds.). *Cambridge University Press, Cambridge*, ISBN: 9780521864718.

- f* Nyssen, J., Clymans, W., Descheemaeker, K., Poesen, J., Vandecasteele, I., Vanmaercke, M., Walraevens, K. (2010). “Impact of soil and water conservation measures on catchment hydrological response – A case in north Ethiopia.” *Hydrological Processes*, 24, 1880–1895.
- f* Nyssen, J., Clymans, W., Poesen, J., Vandecasteele, I., De Baets, S., Haregeweyn, N., Deckers, J. (2009a). “How soil conservation affects the catchment sediment budget – A comprehensive study in the north Ethiopian highlands.” *Earth Surface Processes and Landforms*, 34, 1216–1233.
- f* Nyssen, J., Poesen, J., Mitiku, H., Moeyersons, J., Deckers, J., Hurni, H. (2009b). “Effects of LU/LC and land cover on sheet and rill erosion rates in the Tigray highlands, Ethiopia.” *Zeitschrift fur Geomorphologie*, N. F., 53, 171–197.
- f* Nyssen, J., Poesen, J., Moeyersons, J., Haile, M. and Deckers, J. (2007). “Dynamics of soil erosion rates and controlling factors in the Northern Ethiopian Highlands towards a sediment budget. *Earth Surface Processes and Landforms*, DOI: 10.1002/esp.1569.
- f* Nyssen J., Vandenreyken H., Poesen J., Moeyersons J., Deckers J., Haile M., Salles C. and Govers G. (2005). “Rainfall erosivity and variability in the Northern Ethiopian Highlands.” *Journal of Hydrology*, 311(1-4): 172-187.
- f* Nyssen J., Poesen J., Moeyersons J., Deckers S., Haile M. and Lang A. (2004). “Human impact on the environment in the Ethiopian and Eritrean highlands—a state of the art.” *Earth-Science Reviews*, 64: 273–320.
- f* Opiyo, F., Nyangito, M., Wasonga, OV., and Omendi, P. (2014). Trend Analysis of Rainfall and Temperature in Arid Environment of Turkana, Kenya. *Environment Research Journal* 8(2): 30-43.

- f Omondi, P.A.O., Awange, J.L., Forootan, E., Ogallo L.A., Barakiza R. (2013). “Changes in temperature and precipitation extremes over the Greater Horn of Africa region from 1961 to 2010.” *International Journal of Climatology*, 34: 1262-1277.
- f Pikounis M., Varanou, E., Baltas, E., Dassaklis, A. and Mimikou, M. (2003). “Application of the SWAT model in the Pinios river Basin under different land-use scenarios.” *Global Nest: the International Journal*, 5(2): 71-79.
- f Penman, H.L. (1956). “Evaporation: An introductory survey.” *Netherlands Journal of Agricultural Science* 4:7-29.
- f Penman, H.L., Monteith, J.L. (1965). “Evaporation and the environment. p. 205-234. In The state and movement of water in living organisms.” 19<sup>th</sup> *Symposia of the Society for Experimental Biology*. Cambridge Univ. Press, London, U.K.
- f Peterson, T. C., Folland, C., Gruza, G., Hogg, W., Mokssit, A., Plummer, N. (2001). “Report on the activities of the working group on climate change detection and related rapporteurs 1998–2001.” *Report WCDMP-47, WMOTD 1071, Geneva, Switzerland*, 143 pp.
- f Priestley, C.H.B., Taylor, R.J. (1972). “On the assessment of surface heat flux and evaporation using large-scale parameters.” *Mon. Weather Rev.* 100:81-92.
- f Prowse, T.D., Beltaos, S. Gardner, J. T., Gibson, J. J., Granger, R. J. , Leconte, R., Peters, D. L., Pietroniro, A., Romolo L. A., Toth B. (2006). “Climate change, flow regulation and land-use effects on the hydrology of the Peace-Athabasca-Slave system; findings from the Northern rivers ecosystem initiative.” *Environmental Monitoring and Assessment* 113, 167–197.
- f Raes, D., Willems, P. Baguidi, G.F. (2006). “RAINBOW – a software package for analyzing data and testing the homogeneity of historical data sets.” *Proceedings of*

the 4<sup>th</sup> International Conference on Watershed Hydrology and Water Quality Management, January 2006.

- f Renard, K.G., Simanton, J.R., Osborn, H.B. (1974). "Applicability of the Universal Soil Loss Equation to Semi-Arid Rangeland Conditions in the Southwest." *Proc. A WRS and Arizona Academy of Science, Arizona*.
- f Roberts, G. (1998). "The effects of possible future climate change on evaporation losses from four contrasting UK water catchment areas." *Hydrological Processes*, 12: 727-739.
- f Saleh, A., Arnold, J.G., Gassman, P.W., Hauck, L.M., Rosenthal, W.D. Williams, J.R. and McFarland, A.M.S. (2000). "Application of SWAT for the Upper North Bosque River Watershed." *Trans. ASAE* 43(5):1077-87.
- f Santhi, C., Arnold, J.G., Williams, J.R., Dugas, W.A., R. Srinivasan, and Hauck, L.M. (2001). "Validation of the SWAT model on a large river basin with point and nonpoint sources." *Journal of the American Water Resources Association* 37(5): 1169-1188.
- f Schulze, R.E. (2000). "Hydrological responses to land use and climate change: a southern African perspective." *Ambio*, 29 (1): 12–22.
- f Schulze, R.E. (1998). "Hydrological Modelling: Concepts and Practice." *International Institute of Infrastructural, Hydraulic and Environmental Engineering, Delft, Netherlands*.
- f Schreck, C.J, Semazzi, F.H. (2004). "Variability of the recent climate of eastern Africa." *International Journal of Climatology* 24: 681-701.
- f Sefton, C.E.M. and Boorman, D.B. (1997). "A regional investigation of climate change impacts on UK streamflow." *Journal of Hydrology*, 195: 26-44.

- ☐ Seleshi Y, Camberlin P (2006). “Recent changes in dry spell and extreme rainfall events in Ethiopia.” *Theoretical Application of Climatology* 83:181–191.
- f Seleshi, Y. and Zanke, U. (2004). “Recent changes in rainfall and rainy days in Ethiopia.” *International Journal Climatology*, 24: 973-983.
- f Sen, P.K. (1968). “Estimate of the regression coefficient based on Kendall's tau.” *Journal of American Statistical Association*, 63, pp. 1379-1389.
- f Setegn, S. G., Rayner, D., Melesse, A. M., Dargahi, B. and Srinivasan R. (2011). “Impact of climate change on the hydro-climatology of Lake Tana Basin, Ethiopia.” *Water Resource Research*, 47, W04511.
- f Setegn, S., Dargahi, B., Srinivasan, R., and Melesse, A. (2010). “Modelling of sediment yield from Anjeni-gauged watershed, Ethiopia using SWAT model.” *Journal of American Water Resources Association*, 46, 514–526.
- f Setegn, S. G., Srinivasan, R., Melesse, A. M. and Dargahi, B. (2010). “SWAT model application and prediction uncertainty analysis in the Lake Tana Basin, Ethiopia.” *Wiley InterScience, Hydrologic Process*, 24: 357-367.
- f Setegn, S.G, Srinivasan, R. Dargahi, B. Melesse, A.M. (2009). “Spatial delineation of soil erosion vulnerability in the Lake Tana Basin, Ethiopia.” *Hydrologic Processes*, 23:3738-3750.
- f Setegn, S.G., Srinivasan, R. and Dargahi, B. (2008). “Hydrological Modelling in the Lake Tana Basin, Ethiopia Using SWAT Model.” *The Open Hydrology Journal*, 2:49-62.
- f Shang H, Yan J, Gebremichael M, Ayalew, S.M. (2011) “Trend analysis of extreme precipitation in the north-western highlands of Ethiopia with a case study of Debre Markos.” *Hydrological Earth System Science* 15 (6):1937–1944.

- ☐ Sharpley, A.N. and Williams, J.R., eds. (1990). “EPIC - Erosion/Productivity Impact Calculator: 1. Model Documentation.” *U.S. Department of Agriculture Technical Bulletin* No. 1768. 235.
- f Shawul, A. A., Alamirew, T. and Dinka, M. O. (2013). “Calibration and validation of SWAT model and estimation of water balance components of Shaya mountainous watershed, Southeastern Ethiopia.” *hydrology and earth system sciences*, 10, 13955–13978.
- f Shibu D., Rieger, W. and Strauss, P. (2003). “Assessment of gully erosion in eastern Ethiopia using photogrammetric techniques.” *Catena* 50: 273– 291.
- f Singh, J., Knapp, H.V., Demissie, M. (2005). “Hydrologic Modelling of the Iroquois River Watershed Using HSPF and SWAT.” *Journal of the American Water Resources Association* 41(2):343- 360.
- ☐ Singh, V.P., and Woolhiser, D.A. (2002). “Mathematical modelling of watershed hydrology.” *Journal of Hydrologic Engineering*, 7(4): 270-292.
- f Skole, D.L. (1994). “Data on global land-cover change: Acquisition, assessment, and analysis.” In Meyer, W. B. & Turner B. L. II (Eds) *Changes in land use/cove: A global perspective: Cambridge University Press*, 437-471.
- f Smith, D.D and Whitt, D.M. (1948). “Evaluating Soil Losses from Field Areas.” *Journal of Agricultural Engineering*, 29, 394 - 396.
- f Solomon, A. (2005). “Land-use and land-cover change in headstream of Abay watershed, blue Nile basin, Ethiopia.” *M.Sc. Thesis, Addis Ababa University*.
- f Srinivasan, R. and J.G. Arnold. (1994). “Integration of a basin-scale water quality model with GIS.” *Water Resources Bulletin* (30)3:453-462.
- f Steenhuis, T., Collick, A., Easton, Z., Leggesse, E., Bayabil, H., White, E., Awulachew, S., Adgo, E., and Ahmed, A. (2009). “Predicting discharge and

- sediment for the Abay (Blue Nile) with a simple model.” *Hydrological Process*, 23, 3728–3737.
- f* Sveinsson, O.G.B., Salas, J.D., Boes, D.C and Pielke Sr, R.A. (2003). “Modelling the dynamics of long term variability of hydroclimatic processes.” *Journal of Hydrometeorology*, 4 (3):489-505.
- f* Swain, A. (1997). “Ethiopia, the Sudan, and Egypt: the Nile River dispute.” *J. Mod. Afr. Stud.*, 35, 675–694.
- f* Tabari, H. Taye, M.T, Willem, P. (2015) “Statistical assessment of rainfall trends in the upper Blue Nile River basin.” *Stochastic Environmental Research and Risk Assessment* 29:1751–1761.
- f* Tabari, H. Hosseinzadeh, T.P. (2011) “Temporal variability of rainfall over Iran: 1966–2005.” *Journal of Hydrology* 396:313–320.
- f* Tamene, L, Vlek, P.L.G. (2008). “Soil erosion studies in Northern Ethiopia.” In: Braimoh AK, Vlek PLG (eds) Land use and soil resources, *Springer Science 7 Business Media B.V. Dordrecht, The Netherlands* p73-100.
- f* Tamene, L., Park, S., Dikau, R., and Vlek, P. (2006). “Analysis of factors determining sediment yield variability in the highlands of Northern Ethiopia.” *Geomorphology*, 76, 76–91.
- f* Taye , G., Poesen , J., Wesemael, BV., Vanmaercke , M., Tekla , D., Deckers , J., Goosse , T., Maetens, W., Nyssen , J., Hallet,V., Haregeweyn, N. (2013). “Effects of LU/LC, slope gradient, and soil and water conservation structures on runoff and soil loss in semi-arid Northern Ethiopia.” *Physical Geography*, 34:3, 236-259.
- f* Taye, M.T., Willems, P. (2013). “Influence of downscaling methods in projecting climate change impact on hydrological extremes of upper Blue Nile basin.” *hydrology and earth system sciences*, 10, 7857–7896.

- f Taye, M.T., Ntegeka, V., Ogiramoi, N.P., Willems, P. (2011). “Assessment of climate change impact on hydrological extremes in two source regions of the Nile River Basin.” *hydrology and earth system sciences*, 15 (1), 209–222.
- f Tesemma ZK, Mohamed YA, Steenhuis TS (2010) Trends in rainfall and runoff in the Blue Nile Basin: 1964–2003. *Hydrologic Process* 24:3747–3758.
- ▣ Tesfahunegn, G., Tamene, L., Vlek, L.G. (2012). “Modelling soil erosion by water using SWAT in Northern Ethiopia.” *East African Journal of Science and Technology*, 2(1):1- 28.
- f Tewolde, T.G. (2009). “Regional groundwater flow modelling of the Geba basin, Northern Ethiopia, PhD Thesis.” *VUB, Belgium*, 274pp.
- f Thiel, H. (1950). “A rank-invariant method of linear and polynomial analysis, part 3.” *Nederlandse Akademie van Wetenschappen, Proceedings*, 53: 1397–1412.
- f Tilahun, K. (2006). “The characterisation of rainfall in the arid and semi-arid regions of Ethiopia.” *Water SA*, 32(3): 429-436.
- f Tollan, A. (2002). “Land use/land cover change and floods: what do we need most research or management?” *Water Science and Technology* 45, 183–190.
- f UNECA. (2011). “Climate change and water in Africa: Analysis of knowledge gaps and needs United Nations Economic Commission for Africa (UNECA).” *African climate policy centre, working paper no 4*. 14pp.
- f USDA-SCS (United States Department of Agriculture Soil Conservation Service) (1972). “National Engineering Handbook.” *Section 4 Hydrology*, Chapters 4-10.
- f Van Doren, C.A. and Bartelli, L.J. (1956). “A Method for Forecasting Soil Losses.” *Journal of Agricultural Engineering*, Vol. 37, pp. 335 - 341.

- ☐ Van Griensven A., Ndomba, P., Yalew, S. and Kilonzo, F. (2012). “Critical review of SWAT applications in the upper Nile basin countries.” *hydrology and earth system sciences*, 16, 3371–3381.
- f Van Griensven, A., Meixner, T., Grunwald, S., Bishop, T., Diluzio, M., Srinivasan, R. (2006). “A global sensitivity analysis tool for the parameters of multi-variable catchment models.” *Journal of Hydrology* 324 (1–4), 10–23.
- f Van Liew, M.W. and Garbrecht, J. (2001). “Sensitivity of hydrologic response of an experimental watershed to changes in annual precipitation amounts.” 2001 ASAE Annual International Meeting, July 30-August 1, 2001, Sacramento, CA. Paper No. 01-2001, ASAE, 2950 Niles Rd., St. Joseph, MI.
- f Vanmaercke M., Zenebe A., Poesen J., Nyssen J., Verstraeten G., Deckers J. (2010). “Sediment dynamics and the role of flash floods in sediment export from medium-sized catchments: a case study from the semi-arid tropical highlands in Northern Ethiopia.” *Journal of Soils and Sediments*, 10: 611-627.
- f Varanou, E., Gkouvatsou, E. Baltas, E. and Mimikou, M. (2002). “Quantity and quality integrated catchment modelling under climate change with use of soil and water assessment tool model.” *Journal of Hydrologic Engineering* 7(3): 228-244.
- f Victor D.G. and Ausubel, J.H. (2000). “Restoring the forests.” *Foreign Aff.* 79(6):127–144.
- f Wang, H., Chen, Y. and Chen, Z. (2013). “Spatial distribution and temporal trends of mean rainfall and extremes in the arid region, northwest of China, during 1960-2010.” *Hydrologic Process* 27:1807–1818.
- f Wagesho, N., Goel N.K., Jain, M.K. (2013). “Temporal and spatial variability of annual and seasonal rainfall over Ethiopia.” *Hydrological Science Journal*, 58: 354-373.



- ☐ Williams J.R. (1995). Chapter 25: The EPIC model. In: V.P. Singh (eds.), *Computer models of Watershed hydrology, Water resources Publications, Highlands Ranch, CO*. pp. 909-1000.
- f Williams, G.P. (1989). “Sediment Concentration versus Water Discharge during Single Hydrologic Events in Rivers.” *Journal of Hydrology*, Vol. 111, pp. 89 - 106.
- f Williams, J.R. (1975). “Sediment Yield Prediction with Universal Equation Using Runoff Energy Factor, in Present and Prospective Technology for Predicting Sediment Yield and Sources.” *USDA ARS, S-40*, pp. 244 - 252.
- f Wischmeier, W.H., Smith, D.D. (1965). “Predicting Rainfall-Erosion Losses from Cropland East of the Rocky Mountains - Guide for Selection of Practices for Soil and Water Conservation.” *USDA Handbook No.282*.
- f Wubishet T., Stephanie W., William C., Constance W. (2015). “Assessing the Impact of Land-Use Land-Cover Change on Stream Water and Sediment Yields at a Watershed Level Using SWAT”. *Open Journal of Modern Hydrology*, 5, 68-85
- f Zenebe, A., Vanmaercke, M., Poesen, J., Verstraeten, G., Haregeweyn, N., Haile M., Amare, K., Deckers, J., Nyssen J. (2013). “Spatial and temporal variability of river flows in the degraded semi-arid tropical mountains of Northern Ethiopia.” *Zeitschrift für Geomorphologie* 57,2: 143–169.
- f Zenebe, A.A. (2009). “Assessment of spatial and temporal variability of River discharge, sediment yield and sediment-fixed nutrient export in Geba River catchment, Northern Ethiopia.” [3K'7KHV LV:8/HXYHQSS](https://doi.org/10.1007/s11365-009-9188-8) .
- f Zhan, C., Xu Z., Ye, A. and Su, H. (2011). “LUCC and its impact on run-off yield in the Bai River catchment upstream of the Miyun Reservoir basin.” *Journal of Plant Ecology* 4(1–2), 61–66.

## APPENDIX

**Table 1: Annual Rainfall of the study area for all the stations**

Year	Abiadi	Adigudem	Mekelle	Adigrat	Hawzien	Senkata	Wukro	Sum	Mean
1971	885	366.5	433.7	334.9	404.1	422.7	361.8	3208.7	458.39
1972	1192.3	563.5	565.2	358.5	529.7	498	447.8	4155	593.57
1973	866.3	466.2	476.16	451.5	602.4	397.1	334.4	3594.06	513.44
1974	820.1	467.7	518.6	652.9	360	279.6	601.3	3700.2	528.60
1975	926.7	713.4	770.9	874.7	706.5	618.9	625	5236.1	748.01
1976	668.6	396.7	532	511.6	623.1	561.4	1423.9	4717.3	673.90
1977	923.5	348.9	669.8	624.5	656	915.1	845.3	4983.1	711.87
1978	782.1	215	438.9	614.5	451.3	1465.8	157.1	4124.7	589.24
1979	399.7	631.3	373.8	719.4	412.3	1166	617.1	4319.6	617.09
1980	649.2	688.6	712.6	442.7	502.1	448.9	742.4	4186.5	598.07
1981	573.6	566	618.11	786.9	686.9	596.4	1736.2	5564.11	794.87
1982	441.5	120.1	588.61	498.4	473.8	473.8	344.1	2940.31	420.04
1983	530.5	502.5	706.3	462.7	596.2	576.2	344	3718.4	531.20
1984	328.9	722.6	303.5	428.1	585	562	497.6	3427.7	489.67
1985	541.6	274.6	536.1	664.3	873.14	748.62	585.3	4223.66	603.38
1986	657.2	1152.6	413.7	731	1421.74	1317.53	557.6	6251.37	893.05
1987	597.4	251	737.7	333.4	1165.49	1038.27	480	4603.26	657.61
1988	592.3	556.8	915.1	488.8	748.07	653.28	574	4528.35	646.91
1989	964.2	672.3	532.8	564.2	348	386.7	453.7	3921.9	560.27
1990	1097.3	795.4	663.6	565.5	398.9	446.2	509	4475.9	639.41
1991	741	573.3	621.4	512.8	556.6	345.8	771.3	4122.2	588.89
1992	836.7	510.8	564.7	542.4	428.3	586.1	304.8	3773.8	539.11
1993	551.2	433.9	721.9	753.3	546.1	578.9	491.5	4076.8	582.40
1994	663.3	658	658.4	770.2	517.9	748.8	612.7	4629.3	661.33
1995	1031.2	582.4	692.4	636	502	357.9	486.4	4288.3	612.61
1996	1193.1	433.4	586.31	741.4	512.5	451	927.8	4845.51	692.22
1997	572.5	415.1	552.34	680.9	488.6	395.6	352.4	3457.44	493.92
1998	2212	1103.5	747.6	664.3	594.6	589.4	796.2	6707.6	958.23
1999	950	553.9	717.1	313	580.4	518.4	533.42	4166.22	595.17
2000	726.2	481.5	455.9	422.3	768.5	562.7	984	4401.1	628.73
2001	1059	624.1	646	556.5	890.8	859.4	1112.227	5748.027	821.15
2002	520.7	287.8	456.7	572.2	433.3	405.2	654.2	3330.1	475.73
2003	985.2	417.4	526.8	548.2	395.2	471.9	471.4	3816.1	545.16
2004	1375.4	241.2	390	438.9	367.7	603.1	482	3898.3	556.90
2005	853.1	343.8	599.3	497.9	448	509.9	493.2	3745.2	535.03
2006	1143	630	755.2	716.5	750.5	642	674.3	5311.5	758.79
2007	1304.3	584.6	619.3	671.7	523.1	564	757.81	5024.81	717.83
2008	1051.1	283.2	286.9	487.6	340.5	563.3	502.5	3515.1	502.16
2009	677.74	381.6	416.8	372.4	440.3	306.7	370.3	2965.84	423.69
2010	975.7	459.3	630.3	574.9	568	651.6	692.1	4551.9	650.27
2011	1793.7	427.9	530.8	573.9	500.3	615.1	683.9	5125.6	732.23
2012	1420.5	638.7	512	532.7	644.2	549	646.6	4943.7	706.24
2013	759.15	533.3	454.6	196.1	249.3	375	375	2942.45	420.35
<b>Mean</b>	<b>879.86</b>	<b>513.27</b>	<b>573.25</b>	<b>555.46</b>	<b>571.89</b>	<b>600.54</b>	<b>614.27</b>		
<b>Std</b>	<b>365.79</b>	<b>205.77</b>	<b>134.86</b>	<b>146.00</b>	<b>215.82</b>	<b>253.22</b>	<b>290.56</b>		
<b>CV</b>	<b>41.57</b>	<b>40.09</b>	<b>23.52</b>	<b>26.28</b>	<b>37.74</b>	<b>42.16</b>	<b>47.30</b>		

**Table 2: Average Monthly Minimum Temperature of the Geba River Basin from 1971- 2013.**

Month	Abiadi	Adigudem	Mek'ele	Adigrat	Hawzien	Senkata	Wukro
	Ave. Tmin	Ave. Tmin	Ave. Tmin	Ave. Tmin	Ave. Tmin	Ave. Tmin	Ave. Tmin
Jan	11.35	8.94	9.27	6.56	9.28	8.65	9.83
Feb	12.17	9.71	10.11	7.29	10.3	9.59	11.04
Mar	13.65	10.99	11.49	8.88	11.65	11.31	12.49
Apr	15.01	12	12.9	10.04	12.88	12.72	13.88
May	15.03	12.19	13.4	10.59	13.21	12.86	14.04
Jun	14	12.28	13.07	11.14	12.93	12.59	13.52
Jul	13.26	11.59	13.32	10.66	12.4	12.23	13.12
Aug	13.46	11.52	12.51	10.37	12.48	12.27	12.8
Sep	13.06	10.71	11.27	8.82	11.46	11.05	11.98
Oct	12.87	10.1	10.68	8.13	10.66	10.74	11.44
Nov	12.04	9.64	10.13	7.64	10.32	9.95	10.86
Dec	11.44	8.7	9.13	6.81	9.35	8.81	10.05

**Table 3: Average Monthly Maximum Temperature of the Geba River Basin from 1971- 2013.**

Month	Abiadi	Adigudem	Adigrat	Hawzien	Mekelle	Senkata	Wukro
	Ave. Tmax	Ave. Tmax	Ave. Tmax	Ave. Tmax	Ave. Tmax	Ave. Tmax	Ave. Tmax
Jan	26.89	26.3	23.59	24.82	24.55	24.06	26.32
Feb	27.81	27.14	24.88	26.08	25.8	25.32	27.17
Mar	28.55	27.83	25.25	26.44	26.42	25.09	27.35
Apr	29.35	28.69	25.52	26.96	26.89	25.33	27.94
May	29.4	28.85	25.51	27.41	27.72	26.14	28.29
Jun	28.76	28.23	25.18	26.63	27.36	25.67	28.42
Jul	25.61	25.54	22.68	23.57	23.72	22.84	26.46
Aug	25.27	24.97	22.68	23.28	23.16	22.59	25.96
Sep	26.72	26.31	24.24	24.81	25.19	23.84	27
Oct	26.87	26.84	23.98	24.97	24.8	23.52	26.83
Nov	26.35	26.56	23.66	24.67	24.1	23.35	26.01
Dec	26.27	25.98	23.49	24.51	23.74	23.52	25.95

**Table 4: Soil Type in Geba River Basin after Reclassification.**

S.No.	FAO Soil Name	Code used in SWAT	Area (ha)	% of Watershed Area
1	Haplic Alisols	GBALH	6941.32	1.351
2	Haplic Arenosols	GBARH	15530.84	3.024
3	Haplic Calcisols	GBCLH	8012.27	1.560
4	Luvic Cambisols	GBCML	26021.07	5.066
5	Calcaric Cambisols	GBCMC	59225.94	11.530
6	Eutric Cambisols	GBCME	2747.74	0.535
7	Eutric Leptosols	GBLPE	114123.64	22.218
8	Lithic Leptosols	GBLPQ	163512.66	31.833
9	Haplic Luvisols	GBLVH	29602.91	5.763
10	Calcic Luvisols	GBLVK	7811.43	1.521
11	Chromic Luvisols	GBLVX	10102.95	1.967
12	Eutric Vertisols	GBVRE	27310.21	5.317
13	Calcic Vertisols	GBVRK	42715.22	8.316

**Table 5: Weather Generator (WGEN\_USER) for all the stations in the Geba River Basin.**

Weather Station: Abiadi			Month									
Patameters	Jan	Feb	Mar	Apr	May	Jun	Jul	Aug	Sep	Oct	Nov	Dec
TMPMX	26.89	27.81	28.55	29.35	29.40	28.76	25.61	25.27	26.72	26.87	26.35	26.27
TMSTDMX	1.36	1.06	1.23	1.38	1.35	1.71	1.49	1.32	1.30	1.06	0.99	1.26
TMPMN	11.35	12.17	13.65	15.01	15.03	14.00	13.26	13.46	13.06	12.87	12.04	11.44
TMSTDMN	1.67	1.62	1.77	1.77	1.91	1.42	1.13	1.20	1.19	1.41	1.38	1.91
PCPMM	0.05	0.05	0.39	0.53	1.17	3.80	8.46	10.45	3.36	0.74	0.33	0.03
PCPSTD	0.22	0.14	1.37	1.95	3.15	6.89	10.84	12.58	6.87	2.53	1.18	0.16
PCPSKW	17.98	18.13	7.80	8.45	5.80	2.79	1.96	2.07	7.36	8.66	21.22	34.16
PR_W1	0.01	0.01	0.01	0.01	0.03	0.23	0.13	0.10	0.10	0.01	0.07	0.01
PR_W2	0.01	0.01	0.01	0.01	0.01	0.27	0.61	0.65	0.07	0.01	0.03	0.01
PCPD	0.21	0.26	1.35	2.19	4.16	10.88	18.53	20.02	8.72	2.12	0.70	0.14
RAINHHMX	15	17.6	30	40	64.3	66.5	80	90.8	150	67	116	32.6
SOLARAV												
DEWPT	9.35	10.19	11.68	13.07	13.08	12.02	11.30	11.49	11.07	10.87	10.04	9.52
WNDAY												

Weather Station: Adigudem		Month										
Patameters	Jan	Feb	Mar	Apr	May	Jun	Jul	Aug	Sep	Oct	Nov	Dec
TMPMX	26.30	27.14	27.83	28.69	28.85	28.23	25.54	24.97	26.31	26.84	26.56	25.98
TMSTDMX	1.94	1.09	1.17	1.20	1.32	1.60	1.44	1.19	1.19	0.92	1.01	1.07
TMPMN	8.94	9.71	10.99	12.00	12.19	12.28	11.59	11.52	10.71	10.10	9.64	8.70
TMSTDMN	1.27	1.29	1.48	1.18	1.24	2.08	1.25	1.38	0.98	1.18	1.68	1.22
PCPMM	0.03	0.06	0.23	0.57	0.51	1.46	5.52	6.68	1.45	0.10	0.06	0.03
PCPSTD	0.16	0.23	1.00	1.77	1.84	3.27	7.83	8.89	4.27	0.41	0.27	0.16
PCPSKW	15.58	11.51	12.44	6.35	8.38	3.97	3.79	2.76	17.15	19.54	18.99	19.62
PR_W1	0.01	0.01	0.01	0.52	0.13	0.17	0.23	0.16	0.17	0.01	0.01	0.01
PR_W2	0.01	0.01	0.01	0.01	0.01	0.20	0.48	0.58	0.03	0.01	0.01	0.01
PCPD	0.26	0.47	1.12	2.72	2.07	5.93	17.79	17.98	4.21	0.49	0.33	0.19
RAINHHMX	8.60	9.30	32.70	30.40	45.90	40.00	126.60	97.20	205.00	30.20	20.40	10.50
SOLARAV												
DEWPT	7.04	7.81	9.05	10.06	10.25	10.36	9.64	9.60	8.81	8.24	7.75	6.79
WNDVAV												

Weather Station: Adigrat		Month										
Patameters	Jan	Feb	Mar	Apr	May	Jun	Jul	Aug	Sep	Oct	Nov	Dec
TMPMX	23.59	24.88	25.25	25.52	25.51	25.18	22.68	22.68	24.24	23.98	23.66	23.49
TMSTDMX	1.17	1.35	1.25	1.21	1.28	1.47	1.39	1.24	1.03	0.98	1.07	1.05
TMPMN	6.56	7.29	8.88	10.04	10.59	11.14	10.66	10.37	8.82	8.13	7.64	6.81
TMSTDMN	1.41	1.53	1.67	1.28	1.18	1.94	1.33	1.37	1.42	1.25	1.50	1.58
PCPMM	0.35	0.32	1.10	2.13	1.37	1.36	5.27	4.53	0.54	0.59	0.61	0.20
PCPSTD	1.24	1.21	3.17	4.63	3.99	3.55	8.56	7.93	1.94	1.93	1.79	0.70
PCPSKW	9.15	11.03	7.78	3.65	6.23	5.33	3.86	3.57	7.99	7.69	8.22	12.65
PR_W1	0.01	0.01	0.13	0.07	0.19	0.17	0.19	0.19	0.01	0.03	0.01	0.01
PR_W2	0.01	0.01	0.03	0.03	0.16	0.13	0.26	0.19	0.01	0.06	0.01	0.01
PCPD	1.26	1.42	4.44	7.42	14.28	5.98	17.14	15.40	3.02	1.95	2.47	1.16
RAINHHMX	35.60	40.90	77.40	46.20	78.00	44.70	118.80	86.00	37.00	41.30	43.30	35.40
SOLARAV	22.40	22.27	20.57	20.95	19.40	16.12	11.97	11.84	16.46	20.43	21.85	22.00
DEWPT	4.71	5.44	7.01	8.16	8.69	9.22	8.69	8.41	6.91	6.25	5.78	4.96
WNDVAV	1.24	1.49	1.60	1.72	1.73	1.94	1.66	1.43	1.40	1.43	1.27	1.21

Weather Station: Hawzen		Month										
Patameters	Jan	Feb	Mar	Apr	May	Jun	Jul	Aug	Sep	Oct	Nov	Dec
TMPMX	24.82	26.08	26.44	26.96	27.41	26.63	23.57	23.28	24.81	24.97	24.67	24.51
TMSTDMX	1.02	1.03	1.03	1.00	1.05	1.39	1.20	1.04	1.08	0.84	0.93	0.86
TMPMN	9.28	10.30	11.65	12.88	13.21	12.93	12.40	12.48	11.46	10.66	10.32	9.35
TMSTDMN	1.21	1.56	1.37	1.20	1.01	1.00	0.99	1.01	1.17	1.18	1.16	1.27
PCPMM	0.10	0.24	0.86	1.84	1.34	2.06	5.77	6.37	1.02	0.51	0.33	0.10
PCPSTD	0.45	0.67	2.43	4.00	3.43	4.47	8.62	9.77	2.80	1.85	1.15	0.41
PCPSKW	13.95	7.81	6.31	5.74	6.04	4.55	3.31	3.46	5.76	11.78	17.51	14.85
PR_W1	0.01	0.01	0.01	0.01	0.16	0.17	0.19	0.23	0.13	0.03	0.01	0.01
PR_W2	0.01	0.01	0.90	0.01	0.16	0.17	0.19	0.23	0.13	0.03	0.01	0.01
PCPD	0.44	1.14	3.19	5.30	4.09	8.02	17.70	16.14	3.42	1.63	1.09	0.58
RAINHHMX	21.40	18.00	42.70	79.30	63.10	57.90	102.30	121.00	47.10	73.80	78.40	22.60
SOLARAV												
DEWPT	6.83	7.83	9.29	10.54	10.83	10.57	10.15	10.20	9.12	8.29	7.96	7.00
WNDVAV												

Weather Station: Mekelle			Month									
Parameters	Jan	Feb	Mar	Apr	May	Jun	Jul	Aug	Sep	Oct	Nov	Dec
TMPMX	24.55	25.80	26.42	26.89	27.72	27.36	23.72	23.16	25.19	24.80	24.10	23.74
TMSTDMX	1.51	1.51	1.33	1.24	1.34	1.71	1.54	1.34	2.12	0.97	1.02	1.26
TMPMN	9.27	10.11	11.49	12.90	13.40	13.07	13.32	12.51	11.27	10.68	10.13	9.13
TMSTD MN	1.35	1.46	1.47	1.42	1.35	1.40	5.71	1.22	1.23	1.36	1.36	1.46
PCPMM	0.07	0.26	0.77	1.20	0.96	1.56	6.17	6.32	0.83	0.15	0.17	0.03
PCPSTD	0.28	0.96	2.71	3.42	3.21	3.38	8.66	9.36	2.43	0.66	0.73	0.16
PCPSKW	11.33	12.83	6.89	7.23	8.35	4.27	2.93	3.04	5.67	17.46	16.57	21.85
PR_W1	0.01	0.01	0.13	0.07	0.23	0.17	0.19	0.13	0.13	0.01	0.01	0.01
PR_W2	0.01	0.01	0.03	0.07	0.06	0.10	0.35	0.58	0.07	0.01	0.01	0.01
PCPD	0.81	1.26	3.63	4.98	3.44	9.07	20.47	20.23	5.19	0.84	0.86	0.44
RAINHHMX	9.80	38.80	43.30	74.90	70.20	34.40	95.40	118.50	37.10	41.10	42.00	11.90
SOLARAV	22.33	23.11	21.10	21.89	22.07	16.04	12.10	12.53	18.05	22.42	22.95	22.87
DEWPT	7.40	8.23	9.59	11.07	11.52	11.16	11.39	10.59	9.37	8.81	8.21	7.24
WND AV	2.33	2.80	2.81	2.70	2.18	1.73	1.61	1.38	1.54	2.17	2.36	2.35

Weather Station: Sinkata			Month									
Parameters	Jan	Feb	Mar	Apr	May	Jun	Jul	Aug	Sep	Oct	Nov	Dec
TMPMX	24.06	25.32	25.09	25.33	26.14	25.67	22.84	22.59	23.84	23.52	23.35	23.52
TMSTDMX	1.07	1.17	1.15	1.10	1.23	1.45	1.31	1.23	1.03	0.96	1.00	1.01
TMPMN	8.65	9.59	11.31	12.72	12.86	12.59	12.23	12.27	11.05	10.74	9.95	8.81
TMSTD MN	1.55	1.51	1.57	1.33	1.24	1.36	1.08	1.11	1.32	1.45	1.41	1.56
PCPMM	0.12	0.46	1.08	1.90	1.37	2.29	6.14	6.30	1.26	0.43	0.38	0.23
PCPSTD	0.51	1.43	2.96	4.11	3.34	4.70	9.75	10.56	2.92	1.44	1.10	0.80
PCPSKW	12.16	7.68	6.43	5.61	6.24	4.32	3.24	3.73	6.40	7.91	7.88	10.52
PR_W1	0.01	0.01	0.01	0.03	0.03	0.17	0.23	0.19	0.07	0.03	0.03	0.06
PR_W2	0.01	0.01	0.01	0.01	0.01	0.01	0.13	0.19	0.07	0.01	0.01	0.06
PCPD	0.77	1.91	4.44	5.35	4.56	7.81	17.12	15.00	4.12	1.63	1.33	1.00
RAINHHMX	18.80	38.00	50.60	79.30	63.10	57.90	79.30	126.20	72.20	36.00	28.30	28.40
SOLARAV	23.06	23.33	21.37	21.06	20.02	15.37	11.16	11.63	17.30	21.80	23.20	23.10
DEWPT	6.77	7.70	9.40	10.88	10.96	10.65	10.28	10.33	9.12	8.83	8.03	6.92
WND AV	1.50	1.84	1.96	2.13	2.06	1.70	1.41	1.39	1.55	1.61	1.52	1.67

Weather Station: Wukro			Month									
Parameters	Jan	Feb	Mar	Apr	May	Jun	Jul	Aug	Sep	Oct	Nov	Dec
TMPMX	26.32	27.17	27.35	27.94	28.29	28.42	26.46	25.96	27.00	26.83	26.01	25.95
TMSTDMX	1.65	1.62	1.57	2.24	1.38	1.76	1.63	1.39	1.28	1.25	1.26	1.31
TMPMN	9.83	11.04	12.49	13.88	14.04	13.52	13.12	12.80	11.98	11.44	10.86	10.05
TMSTD MN	1.57	1.49	1.62	1.56	1.55	1.42	1.53	1.10	1.38	1.52	1.61	1.50
PCPMM	0.03	0.15	0.62	0.92	0.96	1.59	6.48	7.10	1.38	0.30	0.26	0.07
PCPSTD	0.13	0.64	1.95	2.85	2.94	3.84	9.91	12.02	3.60	1.06	0.75	0.27
PCPSKW	16.27	16.45	9.78	7.28	6.19	6.27	3.94	4.57	6.76	8.76	12.24	10.95
PR_W1	0.03	0.01	0.13	0.07	0.16	0.13	0.23	0.23	0.10	0.01	0.03	0.01
PR_W2	0.01	0.01	0.03	0.01	0.03	0.10	0.13	0.10	0.03	0.01	0.01	0.01
PCPD	0.35	0.56	2.40	3.60	3.44	6.12	17.16	15.12	4.93	1.07	0.84	0.51
RAINHHMX	7.60	36.20	64.30	60.50	42.00	81.30	131.70	205.00	79.30	28.20	41.80	11.80
SOLARAV												
DEWPT	7.95	9.13	10.54	12.03	12.17	11.61	11.14	10.82	10.06	9.55	8.97	8.16
WND AV												



## **PUBLICATIONS**

### **International Journal Papers**

1. **Kiros, G.**, Shetty A, Nandagiri L (2016). “Analysis of Variability and Trends in Rainfall over Northern Ethiopia.” *Arabian Journal of Geosciences*, 9(6): 1-12. (DOI: 10.1007/s12517-016-2471-1).
2. **Kiros, G.**, Shetty, A., Nandagiri L. (2015). “Performance Evaluation of SWAT Model for Land use/land cover Changes in Semi-arid Climatic Conditions: A Review.” *Hydrology Current Research* 6: 216-223. DOI: 10.4172/2157-7587.1000216.
3. **Kiros, G.**, Shetty, A., Nandagiri L. (2016). “Extreme Rainfall Signatures under Changing Climate in Semi-arid Northern Highlands of Ethiopia.” *Arabian Journal of Geosciences (AJGS)*, (Under Review).
4. **Kiros, G.**, Shetty, A., Nandagiri L. (2016). “Hydrological Responses to Changes in Land Use/Land Cover (LU/LC) and Variability of Climate in Northern Ethiopia. (Under Review).

### **International Conferences Papers**

1. Kiros, G., Shetty, A., Nandagiri L. (2015). “Trend Analysis of Temperature Time Series in Geba River Basin, Northern Ethiopia.” *HYDRO 2015 INTERNATIONAL: 20<sup>th</sup> International Conference on Hydraulics, Water Resources and River Engineering*, 17-19 December, 2015 IIT Roorkee, India.
2. Kiros, G., Shetty, A., Nandagiri L. (2016). “Variability and Trends Analysis of Precipitation over Time Using Mann-Kendall Test, Northern Ethiopia.” *International Water Conference 2016 Water Resources in Arid Areas: The Way Forward*, March 13-16, 2016 Muscat, Oman.





## RESUME

**Name:** Gebremedhin **Kiros** Hailu

**Date of Birth:** 27-05-1984

**Address:** Aksum University, Shire campus  
Department of Soil Resources and Watershed  
Management: P. O. Box -314, Shire Endasselassie,  
Tigray, Ethiopia



### **Contact Details**

Dept.: +251-034-444-4899

Mobile: +251-096-743-7525

+251-091-180-3268

Fax: +251-034-444-4898

E-mail: [k.gebremedhin@yahoo.com](mailto:k.gebremedhin@yahoo.com)/ [kiros1999@gmail.com](mailto:kiros1999@gmail.com)

### **Professional Education**

**x PhD, Hydraulics and Water Resources Engineering**

Thesis title: 'Assessment of Hydrological Impacts of Land Cover Changes and Climate Variability in the Geba Catchment, Ethiopia'

Department of Applied Mechanics and Hydraulics

National Institute of Technology Karnataka Surathkal Mangalore, India, 2013-2016

**x Master of Science in Tropical Land Resources Management**

Mekelle University, Ethiopia, 2011.

**x Bachelor of Science in Land Resources Management and Environmental Protection (Specialization: Soil and Water Conservation)**

Mekelle University, Ethiopia, 2006.

### **Publications**

**x International Journal: 2; Under Review: 2**

**x International Conferences: 2**